2013

An investigation of the mechanism(s) of hyperoxia-induced cilial epithelial loss in mammalian bronchial tissue

Abd Al-Sahib, Hanady

An investigation of the mechanism(s) of hyperoxia-induced cilial epithelial loss in mammalian bronchial tissue

by

Hanady S. Abd Al-Sahib

A thesis submitted to the Plymouth University in
partial fulfilment for the degree of

DOCTOR OF PHILOSOPHY

School of Biomedical and Biological Sciences

Faculty of Science and Technology

August 2013

Copyright Statement

An investigation of the mechanism(s) of hyperoxia-induced cilial epithelial loss in mammalian bronchial tissue

Hanady S. Abd Al-Sahib

Abstract

Hyperoxia is an essential aid to life support in patients with severe respiratory failure. However, it is recognised as a contributor to the pathological consequences of oxidative stress including oxidative tissue damage, inflammation and cell death resulting in acute or chronic lung injury. The specific mechanisms behind this type of injury are still not completely understood. This study was undertaken with two main aims. Firstly, to evaluate the adverse effects of hyperoxia on the ciliary coverage using a novel large animal model. For the first time, an *in vitro* bronchus bovine tissue culture model was developed and used to quantify ciliary coverage loss over time. The protection role of antioxidant supplementation with α-tocopherol and ascorbate was also investigated. Secondly, the importance of the tight junction protein ZO-1 in hyperoxia-induced monolayer permeability was investigated using a human bronchial cell line (16HBE14o-) and the potential inflammation effects on bronchial tightness. Additionally studies were carried out in order to find out if antioxidant vitamin treatment can protect against or reduce these effects.

Scanning electronic microscopy indicated that hyperoxia caused a time dependent decline ($t_{½}$ = 3.4 d compared to 37.1 d under normoxia) in ciliary coverage ($P < 0.0001$). This was associated with an increase in the number of sloughed cells, many apparently intact, into the medium ($p < 0.05$). Several biochemical parameters were assessed to obtain evidence of oxidative stress

caused by hyperoxia in this model including tissue damage (lactate dehydrogenase, LDH, in the medium), lipid peroxidation (thiobarbituric acid reactive substances, TBARS), DNA damage (comet assay used for the first time with primary bronchus culture), protein oxidation (OxyBlot kit) and antioxidant status (total glutathione). Antioxidant vitamins had a significant protective effect on the hyperoxia-induced reduction in percentage ciliary coverage ($P < 0.05$). Moreover, an increase in the bronchial permeability was shown characterised by a significant decrease ($P < 0.05$) in transepithelial electrical resistance (TER) under hyperoxic conditions. The reduction of ZO-1 associated fluorescence ($P < 0.01$) is in compatible with the downregulation of ZO-1 expression assessed by RT-PCR. Levels of the pro-inflammatory cytokines IL-8, IL-6 and TNF-α concentration in the medium, as measured by ELISA, increased significantly ($P < 0.001$) under hyperoxia, and this was accompanied with a marked increase in the cytokine expression. However, the antioxidant vitamins E and C, partially reduced the impact effects of hyperoxia, both individually and in combination, whilst increases in ZO-1 expression and fluorescence intensity ($P < 0.05$), as well as the suppression of cytokine secretion and gene expression was modest. Use of these vitamins was not enough to reduce the epithelial permeability significantly compared to normoxia.

The data implies that hyperoxia-induced damage to cultured bovine bronchial epithelium and the denudation of cilia over time with increased permeability was due, at least in part, to the decline in TJ protein expression and associated fluorescence intensity. The antioxidant vitamins vitamin E and C had partial protective effects against hyperoxia damage. However, additional studies are called for in order to further understand the possible associations between oxidative stress and inflammation caused by hyperoxia and tight junction

proteins, also response to treatment with antioxidant individually or in combination.

Table of Contents

List of Tables

Chapter 1

Chapter 5

List of Figures

Chapter 1

Chapter 2

Chapter 3

Chapter 4

Chapter 5

Acknowledgements

First of all I would like to acknowledge my government, Ministry of higher education and scientific Research/Republic of Iraq, for believing in me and providing me with this scholarship and all the funding and support that has come with it.

Next, I would like to express my sincere thanks to the following people, without whose kind support, advice and assistance this thesis would not have got off the ground successfully. Dr John Moody for being my Director of Studies, providing me with invaluable guidance, moral support and practical training throughout my study.

Professor Robert Sneyd, Dr Roy Moate and Dr Peter Macnaughton for being my supervisors and who have given me time and logistic supportive whenever I have needed it.

Special thanks goes to Professor Waleed Al-Murrani for being himself and being vital supportive and helpful at all times.

My gratitude goes to the following staff in Plymouth University for their practical help and support: Peter Russel for carrying out the lung supplements from the abattoir, Dr Wondwossen Abate Woldie, Dr Paul Waines, the guys in the electronic microscopy centre- Peter Bond and Glen Harper- you have been good company.

Finally, my heartfelt thanks go to my family, my mum who has given so much unconditional love and encouragement throughout my life even in her difficult moments and my sisters for their love which, without my family life would be meaningless. I also extend my thanks to all my friends for their ongoing support. And to everyone who has made me feel welcome and in getting me to this point in a small or large way. A **big** thanks.

Author's Declaration

At no time during the registration for the degree of Doctor of Philosophy has the author been registered for any other University award without prior agreement of the Graduate Committee. This study was financed with the aid of Ministry of higher education and scientific Research/Republic of Iraq. Relevant scientific seminars and conferences were attended at which work was presented and papers have been prepared for publication:

Publications

(please refer to Appendix I for the full manuscripts)

1- Al-Shmgani, H. S., Moate, R. M., Sneyd, J. R., Macnaughton, P. D. & Moody, A. J. 2012. Hyperoxia-induced ciliary loss and oxidative damage in an *in vitro* bovine model: the protective role of antioxidant vitamins E and C. *Biochemical and Biophysical Research Communications,* 429**,** 191-196.

2- Al-Shmgani, H. S., Moate, R. M., Sneyd, J. R., Macnaughton, P. D. & Moody, A. J. 2013.Effects of hyperoxia on permeability of 16HBE14o- cell monolayers: the protective role of antioxidant vitamins E and C.*FEPS Journal*, doi: 10.1111/febs.12413.

Poster presentations

(please refer to Appendix II for the published abstract)

1- Hyperoxia mediates barrier permeability dysfunction in 16HBE140- cells: the protective role of antioxidant vitamins E and C. ERS annual congress, Austria, Vienna, August 2012. *Lung injury and repair: reactive oxygen species and beyond.* Poster number 3772.

2- Hyperoxia mediates barrier permeability dysfunction in 16HBE140- cells. Postgraduate society annual conference in Plymouth University, Plymouth, UK, March 2012.

3- Investigation of the mechanism(s) of oxygen-induced ciliated epithelial loss in bovine bronchus tissue. Injury and repair mechanisms in chronic airway diseases conference, UK, London, April 2011.
4- Investigation of the mechanism(s) of oxygen-induced ciliated epithelial loss in bovine bronchus tissue. Analysis of free radical, radical modifications and redox signaling meeting, Birmingham, UK, April 2011.
5- Hyperoxia-induced ciliated epithelial loss in bovine bronchus tissue: antioxidant vitamins E and C protection. Centre for Research in Translational Biomedicin research day, Plymouth, UK, April 2011.Winner of best poster prize.
6- Hyperoxia effects on bronchus ciliated epithelium. Postgraduate society annual conference in Plymouth University, Plymouth, UK, June 2011.

Oral presentations

1- Hyperoxia: lung cell life or death. Plymouth University, Plymouth, UK, January 2013.
2- Hyperoxia-induced ciliated epithelial loss in bovine bronchus tissue: the protective role of non- enzymatic antioxidant vitamins E and C. Postgraduate society annual conference in Plymouth University, Plymouth University, Plymouth, UK, June 2012. Winner of best presentation prize.
3- The impact of hyperoxia on ciliated cells in the mammalian respiratory tract. Plymouth University, Plymouth, UK, March 2010.

Word count (chapters 1-6 inclusive): 31,326

Signed:

Date:

List of Abbreviations

AJ	adherens junction
ANOVA	analysis of variance
AP-1	activator protein-1
APS	ammonium persulphate
BCA	bicinchoninic acid
BM	basement membrane
BSA	bovine serum albumin
CAT	catalase
cDNA	complimentary DNA
DDRC	diving diseases research centre
DMEM	Dulbecco's modified Eagle's medium
DMSO	dimethyl sulphoxide
DNP	dinitrophenylhydrazones
DNPH	2,4-dinitrophenylhydrazine
DTNB	5,5'-dithiobis-(2-nitrobenzoic acid)
EDTA	ethylenediaminetetraacetic acid
ELISA	enzyme-linked immunosorbent assay
FBS	fetal bovine serum
$FeCl_3$	ferric chloride
GAPDH	glyceraldehyde-3-phosphate dehydrogenase
GPx	glutathione peroxidase
GSH	Glutathione (reduced)
GSSG	glutathione disulfide (oxidised)
GTP	guanosine-5'-triphosphate
H_2O_2	hydrogen peroxide
HBSS	Hank’s balanced salt solution
HDL	high density lipoprotein
HGF	hepatocyte growth factor
HIF1-α	hypoxia-inducible factor 1-α
$HO^{\cdot}$	hydroxyl radical
HRP	horseradish peroxidase
IFN-γ	interferon gamma

IL	Interleukin
KGF	keratinocyte Growth Factor
LDH	lactic Dehydrogenase
LDL	low density lipoprotein
LMP	low-melting agarose
LSD	Fisher's least significant difference
MAGUK	membrane-associated guanylate kinases
MAPKs	mitogen activated protein kinases
MDA	malondialdehyde
MEM	minimum Essential Media
M-MLV	Moloney Murine Leukaemia virus
MMPs	matrix MetalloProteinases
NaCl	sodium chloride
NAD^+	nicotinamide adenine dinucleotide
NADPH	nicotinamide Adenine Dinucleotide Phosphate
NaOH	sodium hydroxide
NF-κB	nuclear factor kappa B
$NO^{\bullet}$	nitric oxide
$O_2^{\bullet-}$	superoxide
$OONO^-$	peroxynitrite
PBS	phosphate buffered saline
PEG	Polyethylene glycol
PNEC	pulmonary neuroendocrine cells
PO_2	partial pressure of oxygen
PVDF	polyvinylidene difluoride
ROS	reactive oxygen species
RT	reverse transcription
RT-PCR	real time polymerase chain reaction
SCGE	alkaline single-cell gel electrophoresis
SDS	sodium dodecyl sulphate
SDS-PAGE	sodium dodecyl sulphate polyacrylamide gel electrophoresis
SEM	scanning Electronic Microscopy
SOD	superoxide dismutase
STAT	signal transducer and activators of transcription

SVCT	Sodium- dependent vitamin C transporter
TBARS	thiobarbituric Acid Reactive Substances
TEM	transmission Electronic Microscopy
TER	transepithelial resistance
TGF	transforming growth factor
TJ	tight junction
TMB	tetramethylbenzidine
TNF-α	tumour Necrosis Factor- alpha
ZO-1	Zona-occludins protein 1

Dedication

I dedicated this thesis

In the loving memory of my

Father, who taught me how to hold the pen and draw the words without regrets.

Sister, 15 years and i can't stop the tears falling down my face.

I was and will always love you and miss you.

Mather, to your endless love, inspiration and support throughout my life.

Lovely sisters, in my heart all the time.

Hanady

Chapter 1: General introduction

and literature review

1.1 General introduction

There is undoubtedly a beneficial therapeutic use of hyperoxia for critically ill patients with acute respiratory failure (Snider and Rinaldo, 1980). However, it is also well documented that hyperoxia can have adverse impacts resulting in acute or chronic lung injury (Altemeier and Sinclair, 2007). Hyperoxia causes damage in different organs, e.g. the nervous system and lungs. Ciliary epithelial tissue covers a large area of the respiratory tract surface and is particularly susceptible to exogenous oxidants because of its position as a first line of defence against pathogens. Damage caused by hyperoxia is characterised by oedema, epithelial and endothelial barrier disruption, mucociliary dysfunction, inflammation and cell death (Slutsky, 1999).

There are several mechanisms which have been suggested by which hyperoxia can lead to lung epithelial cell damage and death. First is the excessive generation and accumulation of reactive oxygen species (ROS) including superoxide ($O_2^{\bullet-}$), hydrogen peroxide (H_2O_2) and hydroxyl radical ($HO^{\bullet}$), leading to oxidant/antioxidant imbalance, oxidative stress and consequently oxidative damage. Oxidative damage to proteins, lipids and DNA are potential end points of ROS-induced cell injury. Secondly, hyperoxia activates a pro-inflammatory mediator response, by which respiratory cells increase the secretion of inflammatory cytokines and chemo attractants that, *in vivo*, lead to recruitment of leukocytes such as neutrophils and monocytes. The accumulation of these leukocytes is an additional source of ROS, thus, the connection between inflammatory mediators and ROS is a critical component of a cycle that triggers or exacerbates lung cell damage. A third mechanism is the activation of

signaling pathways leading to cell death. Previous studies have clarified the interaction of many factors in regulated epithelial cell death induced by hyperoxia. It has been shown that members of the mitogen-activated protein kinase (MAPK) family (ERK1/2, JNK1/2 and p38) are associated with pulmonary epithelial cell death and inflammation following exposure to hyperoxia (Zhang et al., 2003). Hyperoxia has been found to alter the expression of different members of the Bcl-2 family of proteins resulting in an imbalance between pro-apoptotic, e.g. Bax and Bad, and antiapoptotic (for example Bcl-2 and Bcl-Kl) proteins (Zaher et al., 2007). Also hyperoxia induces the activation of other transcription factors such as nuclear factor-kappa B (NF-κB), signal transducers and activators of transcription (STAT) and Activator protein-1 (AP-1) (Lee and Choi, 2003). Thus, cell death induced by hyperoxia involves activation of a network of signal transduction pathways (Figure 1.1, overleaf).

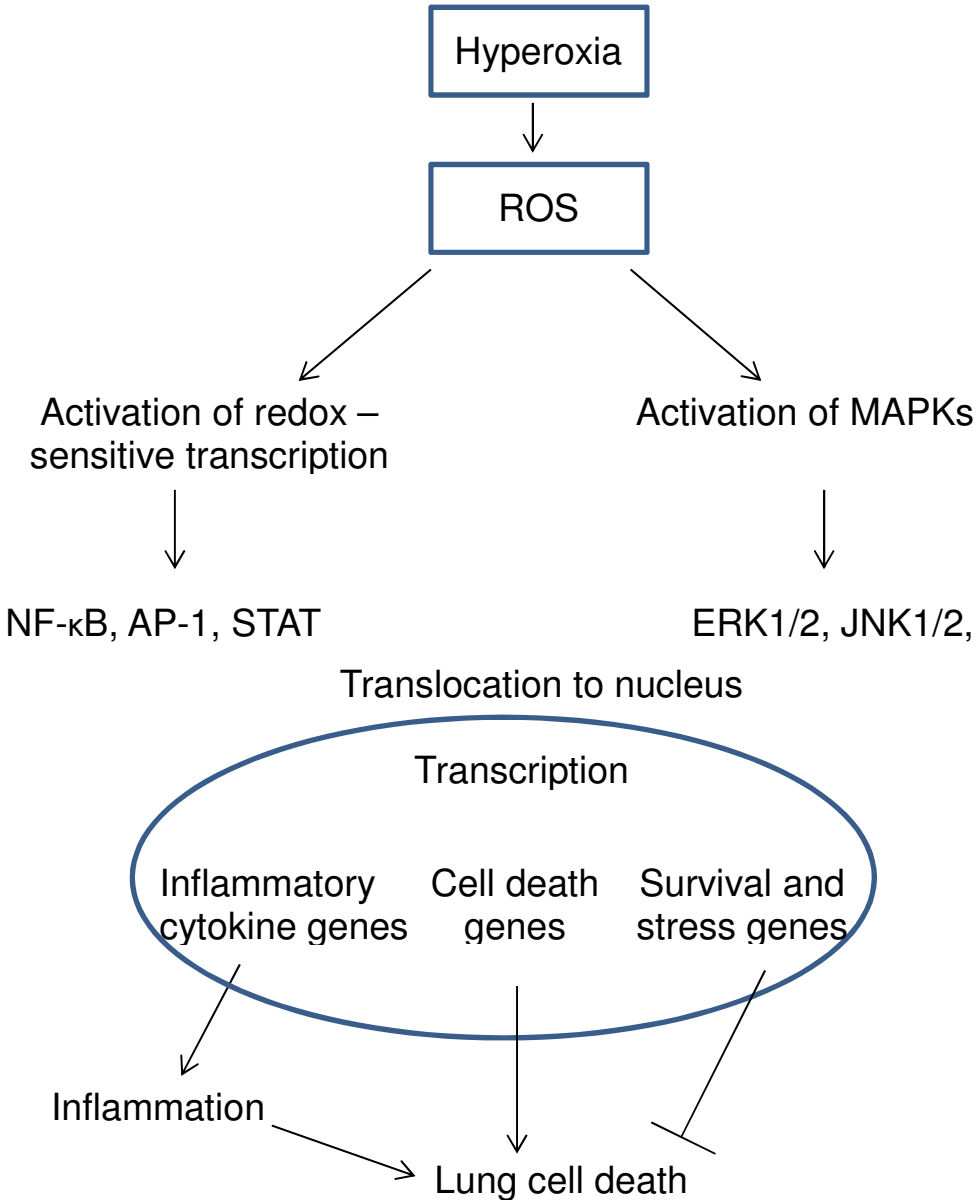

Figure 1.1 Potential mechanisms and pathways involved in hyperoxia-induced pulmonary epithelial cell death.

To control the adverse impacts of ROS, the body has a well-developed antioxidant system, which includes both endogenous enzymatic and non-enzymatic components (Bakan et al., 2003) (Figure 1.2, below).

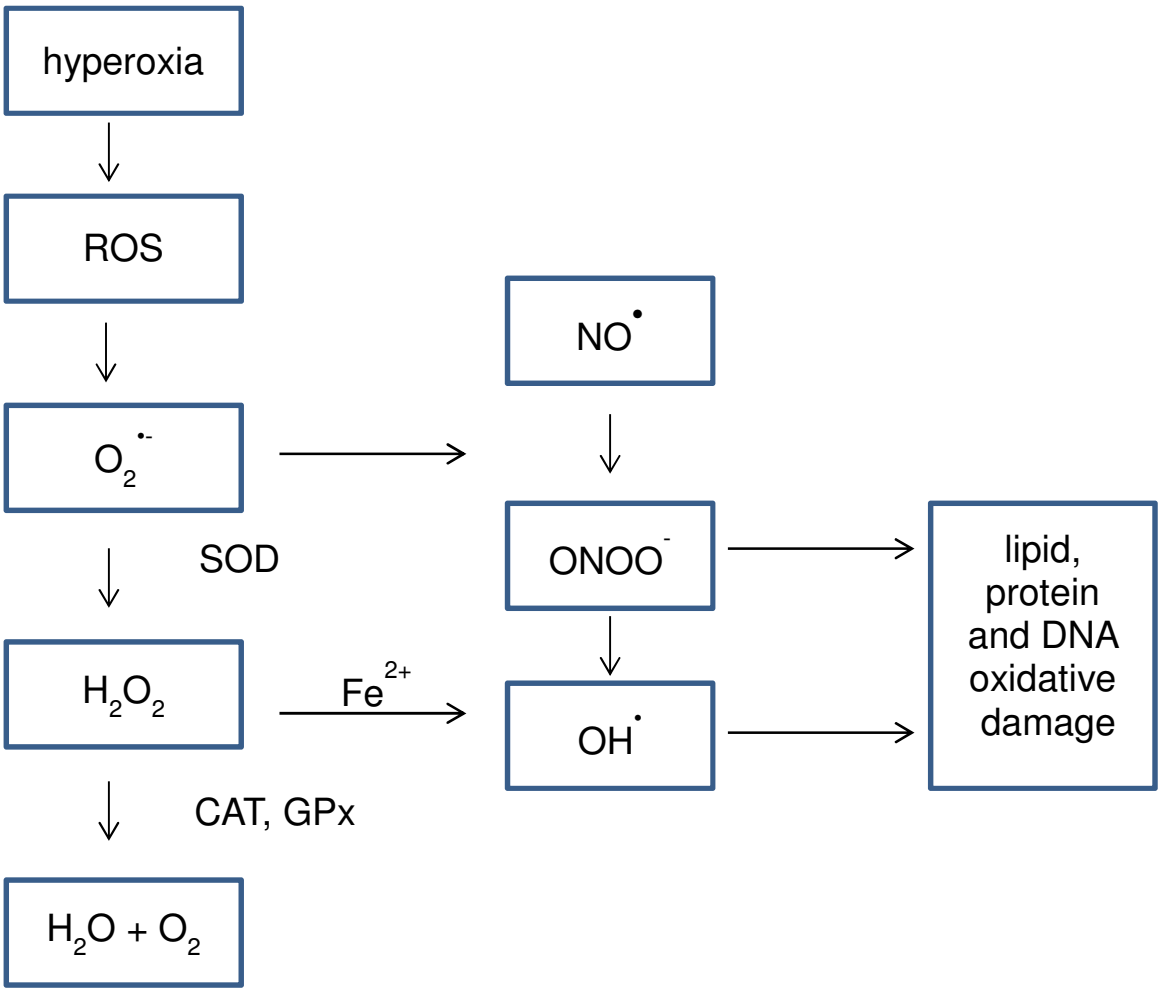

Figure 1.2 The generation of reactive oxygen species (ROS) during hyperoxia and the protective role of enzymatic antioxidants. Different enzymatic antioxidants are used by the cell to reduce oxidative damage including superoxide dismutase (SOD), catalase (CAT) and glutathione peroxidase (GPx). Increased production of ROS may overwhelm the antioxidant capacity leading to oxidative damage of lipids, proteins and DNA**.**

However, an imbalance between ROS production and antioxidant capacity leads to oxidative stress in cells (Powell et al., 2005). Antioxidants act at different levels and by different mechanisms (Hamid et al., 2010). As the airway epithelium is the first surface in direct contact with outer environmental stimuli including hyperoxia it has developed different defense mechanisms to ensure its protection. One of the most important functions is mucociliary clearance which is dependent on cilia function, mucus and periciliary fluid, in which debris and insoluble components adhere to the sticky upper mucus layer, and are removed toward the oropharynx by active cilia immersed in a watery periciliary layer containing a range of antioxidants such as glutathione, superoxide dismutase (SOD) and catalase. The periciliary layer also contains ascorbate, α-tocopherol, urate, albumin and transferrin (Cross et al., 1994). The antioxidant distribution in the periciliary layer has been found to vary along the different regions of the respiratory tract. On one hand, higher urate levels are found where the periciliary layer is thicker and, on the other hand, ascorbate and glutathione are at higher concentrations where this layer is thinner (Van der Vliet and Cross, 2000). It has also been shown that pulmonary epithelial cells respond to different oxidants by the selective induction of antioxidants (Shull et al., 1991). The protective role of antioxidants as scavengers of ROS is well known, but as reducing agents (e.g. vitamins C and E) antioxidants can also alter the redox potential, which in turn changes the cellular redox state (Brash and Havre, 2002). The redox state regulates the activity of a variety of transcription factors (Sun and Oberley, 1996), by which cell apoptosis is regulated, thus the use of antioxidants has been assessed as an approach to reduce tissue oxidative damage (Figure 1.3, overleaf).

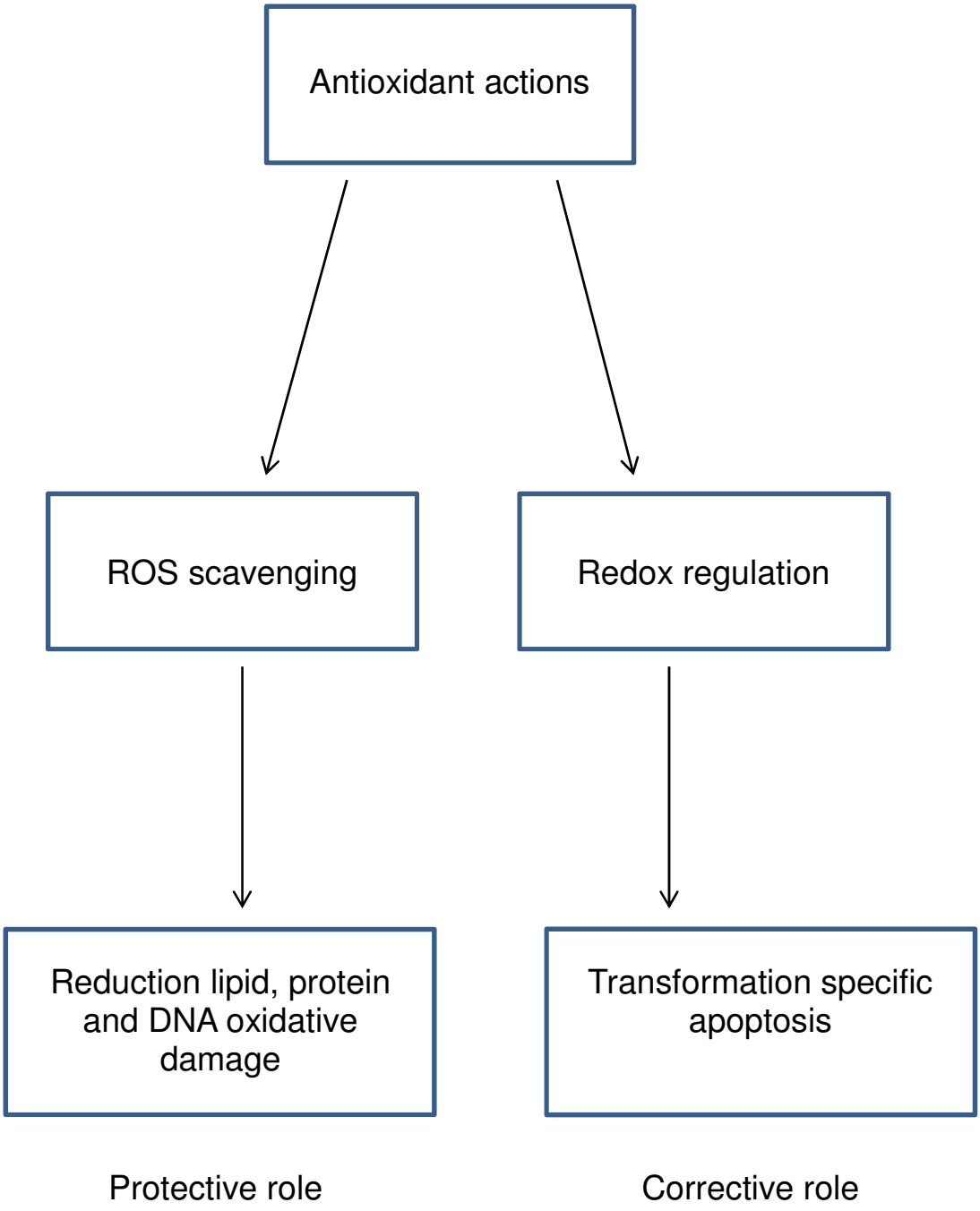

Figure 1.3 The protective and corrective functions of antioxidants in cells. Adapted from Brash and Havre (2001).

1.2 Literature review

1.2.1 Anatomical structure of the respiratory tract

The respiratory tract can be divided into the upper and lower respiratory tract. The upper tract consists of the nostrils, nasal cavities, pharynx, epiglottis, and the larynx, while the lower tract contains the trachea, bronchi, bronchioles and the lungs. Inside the lung lobes the bronchial tubes divide into smaller bronchi and then into bronchioles which end with alveoli (air sacs) that are the site of gas exchange (Cormack, 1998) (Figure 1.4, overleaf).

The tissue in the respiratory tract is organized into four main layers. The first layer is the mucosa, which is divided into the epithelium and the lamina propria. The latter is a thin, vascular (i.e. supplied with blood vessels) layer of connective tissue. Beneath the lamina propria is the submucosa, which is a layer of loose connective tissue; sub-mucosal mixed (serous and mucous) glands are found in this layer (Cormack, 1998). The third layer contains cartilage, the shape of which ranges from small irregular plates in the bronchi to C-shapes in the trachea (Cormack, 1998). Cartilage is not seen in bronchi with a diameter less than 1 mm (Erlandsen and Magney, 1992). Finally, there is a fourth layer, where the tubes from the trachea through to the alveolar ducts are surrounded by a sheet of smooth muscle fibres. In this layer, contraction of these fibres reduces the diameter of the conducting tubules, and thus the air flow is regulated during exhalation (Junqueira et al., 1989).

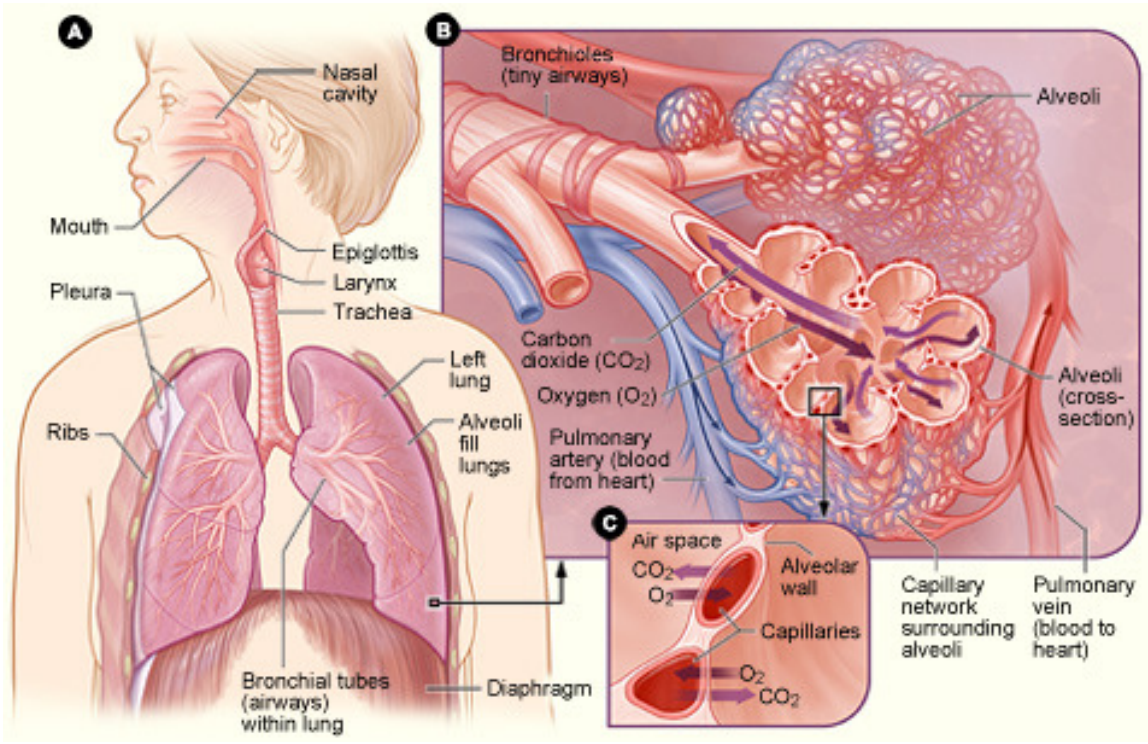

Figure 1.4 Schematic diagram illustrating the upper and lower respiratory tract (A), bronchioles, alveoli and pulmonary net capillaries (B), gas exchange between capillaries endothelium and alveolar wall (C). Taken from Lounge (2009).

.

Most of the respiratory tract is lined by ciliated pseudostratified columnar epithelium which is a single layer consisting of different cell types (Junqueira et al., 1989). Human bronchial epithelial cells have been found to be involved in many biological functions including mucociliary clearance, release of cytokines/growth factors, and modulation of inflammatory cell activation/differentiation. The epithelium also regulates the smooth muscle cell function through the production of bronchoactive mediators (van der Velden et al., 1998).

1.2.2 Histology of the airway epithelium

The respiratory tract is lined with different epithelial cell types that function to guarantee lung homeostasis and preserve barrier integrity and function (Figure 1.5, page 13). The lungs are constantly exposed to microbial pathogens and particles that are usually cleared by a robust defence system via mucociliary clearance, fluid secretion and antimicrobial molecules, in addition to the actions of the innate immune system (Tompkins et al., 2009). These epithelial cells are categorised depending on where they are found in the respiratory tree.

1.2.2.1 Basal cells

The basal cells lie on the basement membrane but do not extend to the lumen of the airway. These cells are known to be involved in many actions including their subsequent differentiation into other epithelial cells types (i.e. ciliated and secretor cells) (Moran and Rowley, 1988). Basal cells are important in epithelial

integrity because they anchor the epithelial cells to the basement membrane via hemidesmosomes. It has been found that they are the only cell type in the pulmonary epithelium which forms hemidesmosome junctions with the basement membrane (Green and Jones, 1996). Basal cells therefore have a unique role in attaching the columnar epithelial cell (1.2.2.2) to the basal lamina; columnar cells are attached to the basal cells via desmosome junctions; failure of the desmosomes results in columnar cells detaching and sloughing (Evans et al., 2001). Further, basal cells may play an antioxidant role in protecting against oxidative stress via the expression of extracellular SOD. Multidrug resistance-protein transmembrane transporter (transport lipophilic substrates out of cancer cells) has been found localised in basal and ciliated bronchial epithelial cells (Brechot et al., 1998); in addition to their involvement in differentiation and proliferation through the binding of growth factors to basal cell receptors (Evans et al. 2001).

1.2.2.2 Columnar ciliated cells

Columnar ciliated cells represent more than 80% of the airway epithelial cells (Knight and Holgate, 2003). Their main function is mucus transport via the covering of cilia. The involvement of ciliated cells in epithelial repair is controversial. Overall, ciliated cells are considered not to contribute to respiratory tissue repair as they are terminally differentiated (Rawlins and Hogan, 2008). However, ciliated cells have been found to play a potential role in differentiation in the injured airway (Lawson et al., 2002). For example, the spreading of flattened cells which then underwent morphological changes to

form Clara cells (Section 1.2.2.3) and ciliated cells was present after injury by naphthalene in order to maintain integrity of the epithelium (Park et al., 2006).

1.2.2.3 Secretory cells

Cells, known as mucus goblet cells, are present in large airways (trachea and bronchi) and are the main source of secreted mucus which acts as a coating protective liquid and also moistens the air. In small airways (bronchioles) Clara cells have been observed; Clara cells are believed to secrete proteins that protect the epithelium against oxidative pollutants and inflammation (Junqueira and Carneiro, 2005). Surfactant apoproteins and leukoprotease inhibitor have been found to be released from these cells (DeWater et al. 1986), and they can also differentiate into other small airway epithelial cells (Park et al., 2006).

Serous-like cells are another type of granular cell, and such cells have been found in the submucosal layer in rodents and the bronchiole airways of human lung. It is believed that these cells secrete water to the upper surface of epithelium to maintain water/ mucus balance (Rogers et al., 1993).

1.2.2.4 Alveolar cells

Alveoli are lined by two types of cells. The first (Type I) are squamous epithelium cells, which cover about 95% of the airway alveolar surface (where blood-gas exchange occurs). These cells are important in maintaining alveolar epithelium homeostasis (Berthiaume et al., 2006). The second type (Type II) is cuboidal epithelial cells which represent only about 7% of the alveolar surface

area (Hazinski, 2002). These cells have been found to be involved in two important functions that maintain normal lung function and structure. Firstly, they function as progenitors for Type I cells (especially after lung injury) and secondly, they have a role in pulmonary surfactant synthesis and production (Andreeva et al., 2007). In addition, these cells participate in gas exchange, immune response and phagocytosis of apoptotic Type I cells (Fehrenbach, 2001).

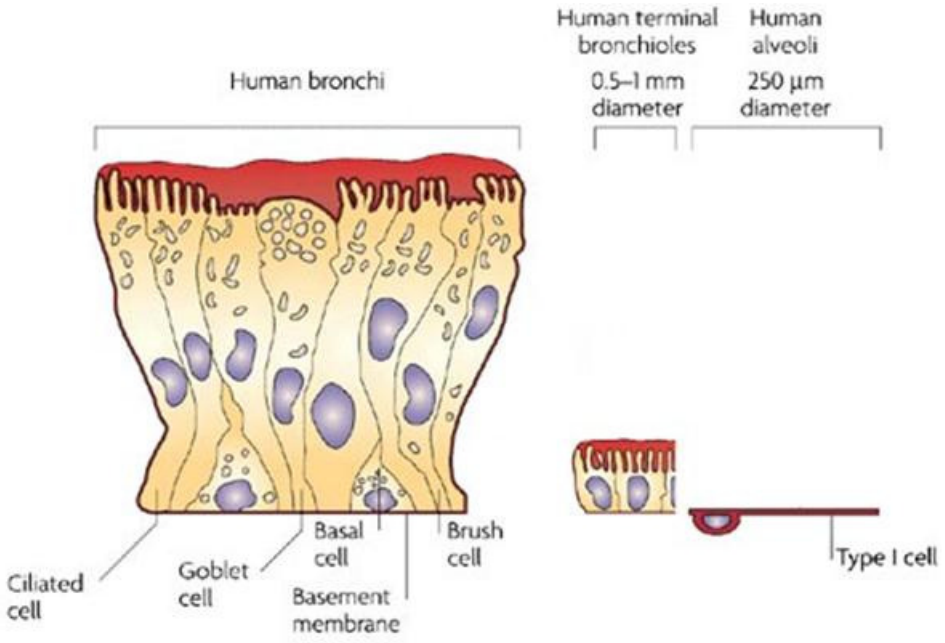

Figure 1.5 Airway epithelium in cross section showing the different types of pulmonary cells in pseudostratified ciliated epithelial tissue. Adapted from Patton and Byron (2007).

1.2.2.5 Pulmonary neuroendocrine cells (PNEC)

In addition to the main, cells ciliated columnar, secreted and basal cells mentioned earlier, bronchial branches and bronchioles have specific cells called pulmonary neuroendocrine cells (PNEC). These cells are present either as individual cells or groups of 80-100 cells called neuroepithelial bodies (Weichselbaum et al., 2005). These cells contain granules and are supplied with cholinergic nerve endings. Consequently, they act as chemoreceptors that respond to changes in gas composition within the airway and also contribute to the reparative process of airway epithelial cell renewal after injury (Junqueira and Carneiro, 2005).

1.2.2.6 Basement membrane (BM)

The epithelial basement membrane (BM), is a thin layer (50-100 nm) mainly consisting of Type IV collagen, laminin (non-collagenous glycoprotein), nidogen (also known as entactin) glycoprotein and perlecan proteoglycan, in addition to other minor components such as fibronectin, agrin and osteonectin (LeBleu et al., 2007). The BM provides structural support by holding the epithelial cells together, serving also as a boundary between the epithelium and mesenchyme, its pores facilitating the migration of inflammatory cells into the epithelium (Howat et al., 2001).

1.2.2.7 Cilia structure

Cilia are hair-like extensions from the surface of the columnar epithelial cells. They move with a wave motion (known as a metachronal wave) to propel mucus and particles toward the throat (Moran and Rowley, 1988). The ciliary beat cycle has two active parts, the effective or power stroke where the cilium fully extends and moves through an arc perpendicular to the cell surface, and the recovery or preparatory stroke where the cilium swings near the cell surface (Sleigh et al., 1988). The basal body of each cilium is attached to the cytoplasmic microtubules via lateral basal foot and short striated rootlets which together provide anchorage (Sleigh and Silvester, 1983). The effective strokes of all cilia in the cell have a common orientation because all of the basal feet in each cell are oriented in the same direction (Holley and Afzelius, 1986). Therefore, studies of the basal feet of the central microtubules are commonly used to determine cilia orientation (Rautiainen et al., 1986). The normal length of cilia is about 5-7 µm in large airways and 2-3 µm in small airways, with a diameter about 0.25-0.33 µm; this normal length is essential for mucociliary transport (Rautiainen et al., 1990). Each cilium contains an axoneme (Figure 1.6), a cylindrical structure built from a (9 + 2) arrangement of microtubules (Figure 1.6, page 17). Each doublet has a complete A-subfibre (13 protofilaments) associated with an incomplete B-subfibre (11 protofilaments) (Wanner et al., 1996). The cilial apical region, which is known as the ciliary crown, has a highly specialized structure, consisting of single A-subfibres instead of the nine outer doublets microtubules. This allows it to be narrower and stiffer, resulting in better clearance of mucus (Kubo et al., 2008). Three types of boundary link the microtubules together. These are:

1. Radial spokes: connecting the peripheral microtubules specifically the A subfibres to the central microtubules.
2. Nexin: a highly elastic protein connecting the adjacent peripheral microtubules.
3. Dynein: a motor protein connecting subfibre A with subfibre B between two adjacent microtubules (Lodish et al., 2000). Dynein is an arm-like structure affixed to the A subfibre. There are two dynein arms, the outer arm with a periodicity of 24 nm, and the inner dynein arm with a periodicity of 96 nm (Reed et al., 2000). Ciliary motility is a result of tubule sliding caused by changes in the dynein arms and cyclical attachment between adjacent microtubules (Rutland et al., 1983).

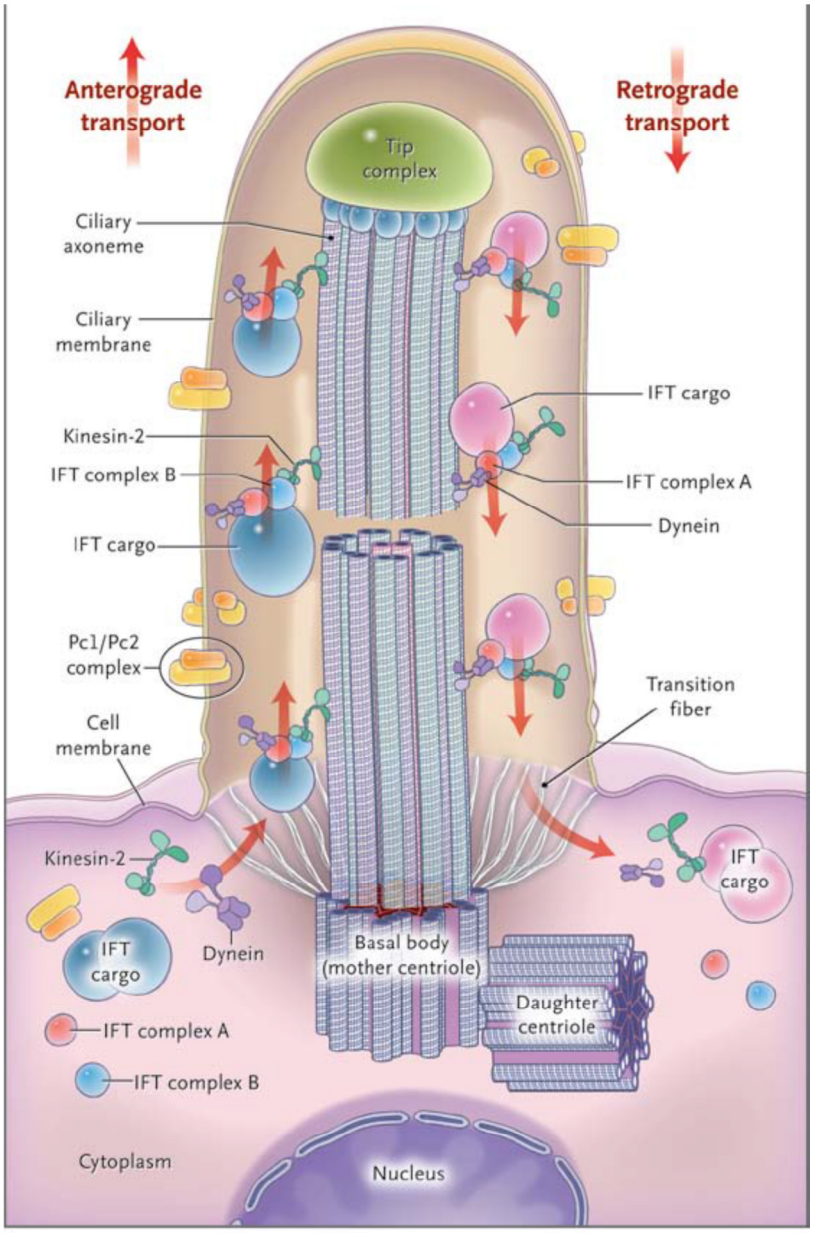

Figure 1.6 Structure of a cilium showing the arrangement of microtubules in the 9+2 axoneme.Transport of molecules in/out of the cilium is also shown. Taken from Hildebrandt et al. (2011) with permission.

1.2.2.8 Cilia malformation

Ciliary abnormalities can be categorised into three main groups: central axoneme defects, peripheral axoneme defects, and membrane disarrangements. In healthy individuals, between 3 and 5% of cilia have abnormal structure because of the exposure of the epithelial surface to various factors in the external environment. However, the mucociliary clearance function as a whole is not affected. In contrast, increased (> 5%) cilia microtubule abnormality has been associated with decreased cilia beat frequency, impacts on mucociliary clearance and increased cilia disorientation (Wisseman et al., 1981). For example, Wilson et al. (1987) reported that more than 70% of patients with viral cold infections had cilia defects. Such infections can also lead to loss of ciliated cells and increased mucus production which, as a consequence, affects mucociliary clearance. Scanning electronic microscopy (SEM) studies have demonstrated the effects of elevated oxygen on cilia morphology and action. For example, in hamster tracheal culture, it has been shown that exposure to 40% oxygen does not impact on cilia structure whilst at 60% exposure there was a significant decline in cilia action and at 95% exposure severe damage was observed (Barnes et al., 1983). Konradova et al. (2003) reported a slight ciliary pathology associated with exposure of rabbit trachea to oxygen levels of 35-37% for 4 days. This included cilia membrane swelling and the appearance of small vacuoles in the shafts of cilia, with this damage being more commonly associated with goblet cells than with ciliated cells. However, exposure to high oxygen concentrations (90%) for a short time (2 h) has been found to induce severe pathological modification to tracheal ciliated epithelium (Konradova et al., 1988).

1.2.3 Airway epithelial functions

The airway epithelium has developed many functions to ensure protection against different external stimuli. These include mechanical clearance of the mucus; homeostasis of ion and water transport; antioxidants; antimicrobial agents and cellular barrier function, through the junctions between epithelial cells (Puchelle et al., 2006). More detailed explanations of these functions are given in Section 1.2.3.1 (below).

1.2.3.1 Barrier and adhesion functions

As the epithelium is the first point of contact with foreign particles and microbial pathogens, including toxic chemicals and gases, viruses and bacteria, this makes it vulnerable to injury. However, epithelial cells have developed an adhesive mechanism to regulate and preserve tissue functions. This protection is facilitated through the integrity of the epithelium as a physical barrier, the secretion of mediators and ciliary function resulting in effective mucocilliary clearance. It has been found that bronchus epithelium produces several antibacterial agents such as lactoferrin and lysozyme, antioxidants such as SOD, catalase and components of the glutathione cycle, and antiproteases such as metalloprotease and leukoprotease inhibitors (van der Velden et al., 1998).

Cell junctions, including cell-cell junctions and cell-matrix junctions, are essential for tissue integrity and function (Shasby, 2007), and are summarized in Figure 1.7 (page 21). Cell-cell junctions are classified into four groups; gap,

tight, adherens and desmosome junctions. Cell-matrix junctions consist of two groups, hemidesmosomes and focal adhesions (Flamme and Kowalczyk, 2008). Gap junctions consist of channels 1.5-2 nm in diameter, and permit the passage of molecules and ions between adjacent cells (Sherwood, 2005). Tight junctions use the protein families occludin and claudin as linkage proteins. They have two important functions. Firstly, they regulate the transport and diffusion of molecules and ions between cells. Secondly, they prevent the movement of integral membrane proteins (Morin, 2005). Adherens junctions and desmosomes use cadherin as the linkage protein (Flamme and Kowalczyk, 2008), and their function is to hold cells tightly together. Hemidesmosomes are patches that anchor the epithelial cells to the basement membrane (known also as attachment plaques). These attachment plaques contain integrins (Alberts et al., 2002). Components of focal adhesion complexes such as integrins, focal adhesion kinase, paxillin and talin provide a structural basis for anchoring the cells to their surroundings (Romer et al., 2006). By using freeze-fracture electron microscopy the network of connections in human bronchial epithelial tight junctions was studied by Matsumura and Setoguti (1989). Image comparisons between the numbers of connecting strands between epithelial cells showed that there is a large number, about 7-11, of parallel strands between neighbouring ciliated cells, while there are only 2-4 strands between neighbouring goblet cells.

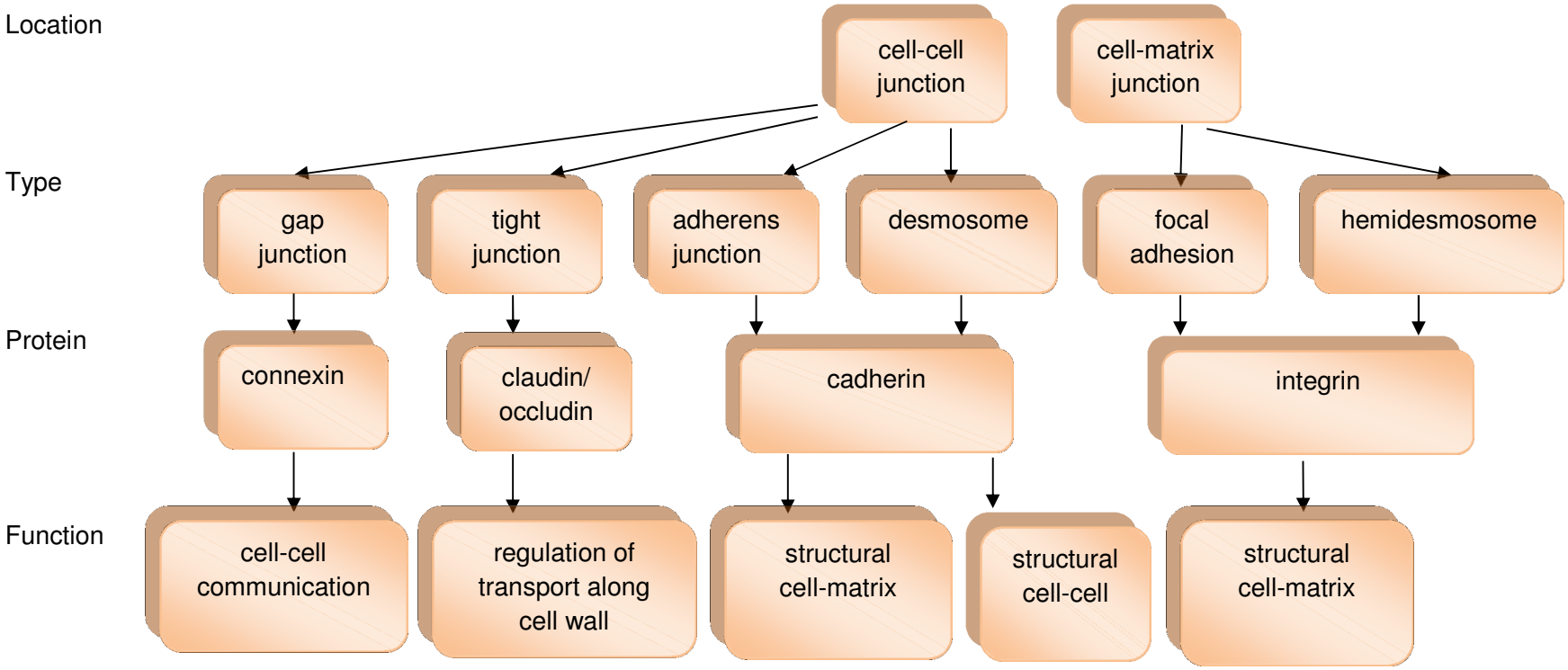

Figure 1.7 Types of cell junctions and proteins (Schneeberger and Lynch, 1992, and Silverthorn, 2009).

1.2.3.2 Cellular defence mechanisms

1.2.3.2.1 Mucociliary clearance

One of the essential mechanisms of defence against pathogens in the respiratory tract is mucociliary clearance (Rautiainen et al., 1992), which depends on ciliary function, mucus properties and periciliary fluid (Stannard and O'Callaghan, 2006). In addition to its role in trapping inhaled pathogens and removing them from the tracheobronchial tree it plays a protective role through the compounds contained in periciliary layer such as antioxidants and antibacterial agents (e.g. lysozyme, opsonins and lactoferrin; van der Velden et al., 1998).

The periciliary liquid layer and mucus are transported along the airway surfaces in one direction via ciliary action (Matsui et al., 1998). It has been reported that patients with chronic mucopurulent sinusitis have slow mucociliary clearance as a result of ciliary disorientation (Rayner et al., 1995). Ciliary disorientation has also been noticed in primary ciliary dyskinesia patients, due to ciliary movement failure as a result of the absence of dynein arms (Rutman et al., 1993). Konradova et al. (2003) has reported that after exposing rabbits to hyperoxia the number of stimulated goblet cells increased significantly and rapid mucus discharge occurred due to acceleration in the mechanism of secretion, after which the overstimulated goblet cells degenerated and sloughed off. Moreover, the number of cilia was decreased with the subsequent impairment of self-cleaning ability (Konradova et al., 1988).

1.2.3.2.2 Antioxidant-based defence mechanisms

The respiratory epithelium is covered with a thin layer of fluid which is about 1-10 µm in thickness, consisting of an upper layer (the mucus), and an aqueous lower layer (periciliary liquid), both of which have antioxidant functions (Table 1.1, overleaf). Halliwell and Gutteridge (1999) have defined an antioxidant as "any substance that when present at a low concentration compared with those of an oxidisable substrate significantly delays or prevents the oxidation of that substrate". Antioxidants can be categorised as either non-enzymatic or enzymatic. The former include some vitamins and low molecular weight compounds (e.g. thiols), while the latter consist of SOD, catalase and glutathione peroxidase (Wright et al., 1994). Respiratory epithelial cells can produce antioxidant enzymes such as glutathione peroxidase and SOD. Both lipid and water-soluble antioxidant vitamins provide defence against lipid peroxidation, aqueous free radicals and ROS, respectively (Tasinato et al., 1995, Mojon et al., 1994). The antioxidant concentration has been found to differ in the bronchioalveolar fluid and the plasma and this is summarized in Table 1.2 (overleaf).

Table 1.1 Antioxidants present in the respiratory epithelium

Enzymes and metal binding proteins	Low molecular weight antioxidants
Glutathione peroxidase	α-tocopherols
EC-SOD	ascorbate
lactoferrin	L-cysteine
ceruloplasmin	urate
transferrin	reduced glutathione

Table 1.2 Comparison of some antioxidant concentrations in plasma and bronchoalveolar lavage fluid (van der Vliet et al., 1999)

Antioxidant	Concentration in plasma (μM)	Concentration in bronchoalveolar lavage (μM)
ascorbate	~67	~400
α-tocopherol	~16	~0.7
glutathione	~1	~109
urate	~387	~207

1.2.3.2.2.1 Vitamin C

Vitamin C, also known as L-ascorbic acid/ascorbate, was first isolated in 1928 by Dr Albert Szent-Gyorgyi (Ranek et al., 2011). The majority of mammalian species can produce ascorbate from glucose, with the exception of humans, primates and guinea pigs, all of whom lack the L-gulono-γ-lactone oxidase enzyme, which catalyses ascorbate synthesis in the liver (Nishikimi et al., 1988). Moreover, a deficiency state, commonly referred to as 'scurvy' when clinically expressed, appears when humans do not consume substantial amounts of vitamin C in their diets.

The predominant form of vitamin C present in solutions when the pH < 4 is ascorbic acid but the predominant form at physiological pH is ascorbate. Ascorbate is a six carbon lactone, and as a reducing agent (Rumsey and Levine, 1998) it donates two electrons from the double bond between the second and third carbons. Vitamin C is considered as a free radical scavenger (Padayatty et al., 2003), as potentially harmful free radicals are reduced and replaced by a less reactive one. Upon loss of the first electron, the ascorbyl radical or semidehydroascorbate is formed. This is a relatively unreactive free radical with a half-life of 6-20 minutes. With the loss of the second electron dehydroascorbate is formed. Both forms can be reduced to ascorbate via different enzyme pathways and using reducing agents such as NADH or GSH; dehydroascorbate can also undergo irreversible oxidation to 2,3-diketogulonate which is further oxidised to xylonate, lyxonate and oxalate (Rumsey and Levine 1998) (Figure 1.8, overleaf).

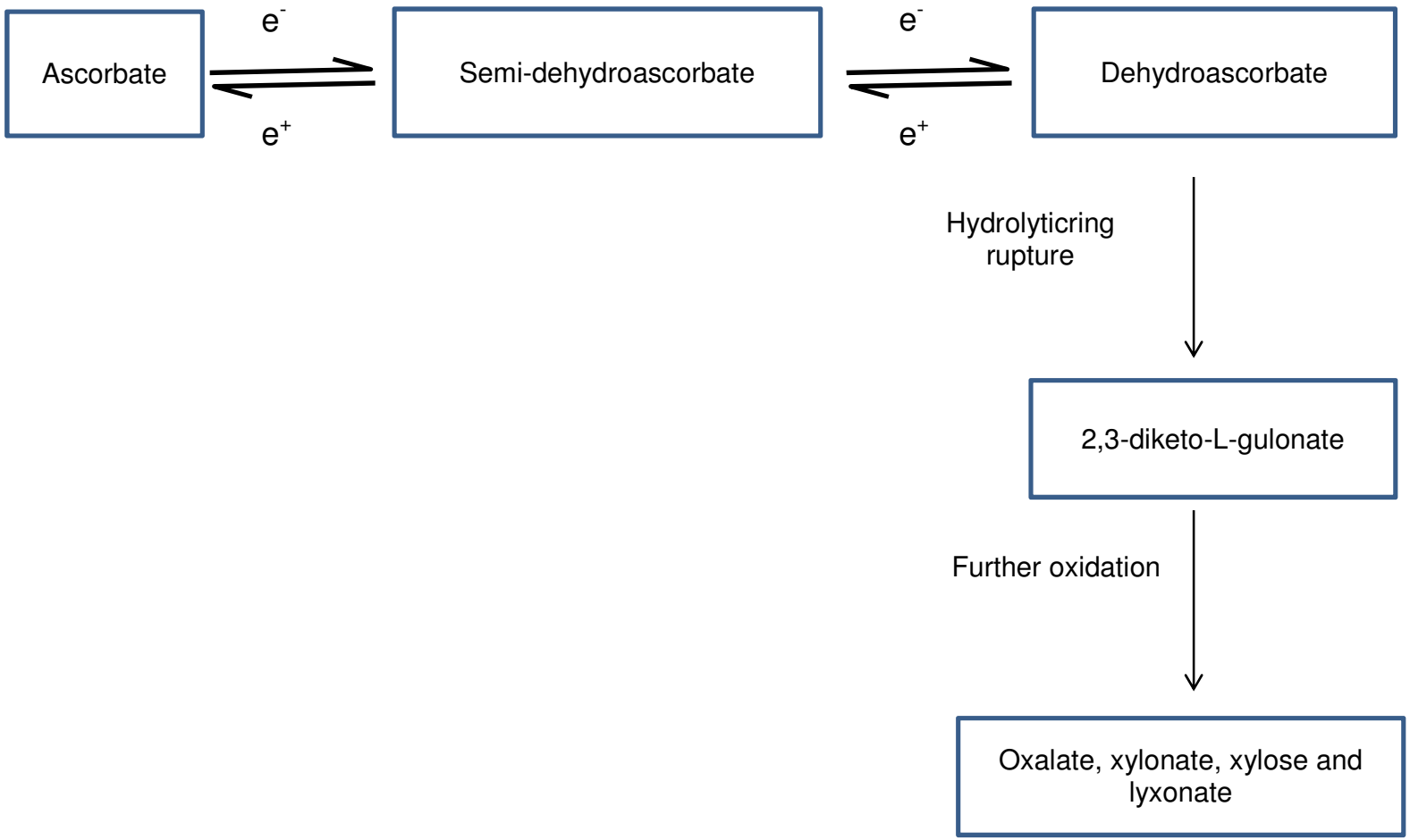

Figure 1.8 Biochemistry of ascorbate and its derivatives.the reversible loss of two electrons (-e) produce dehydroascorbat. With the irreversible oxidation of dehydroascorbate, oxalate is formed.

Due to its reducing ability, vitamin C acts as a scavenger of ROS and non-radicals compounds (such as nitrosating compounds, hypochlorous acid, and ozone). It also acts as a reducing agent for the tocopheroxyl radical which is formed when a free radical reacts with α-tocopherol. Hence, there is a synergistic action between ascorbate and α-tocopherol, whereby vitamin C reduces α-tocopherol back to its active form (Carr and Frei, 1999a). Ascorbate is involved in many biological activities and has been found to have a protective role in lung conditions associated with oxidative stress; for example lower concentrations of ascorbate have been found in plasma and leucocytes of asthmatic patients (Romieu, 2005).

Ascorbate is delivered to tissues after absorption of both the ascorbate and dehydroascorbate forms in the proximal intestine via a sodium-dependent system (Rumsey and Levine 1998). Most dehydroascorbate is immediately reduced to ascorbate via glutathione and enzymatic reduction; therefore, ascorbate is the available form used intracellularly (Rose, 1988). Dehydroascorbate can be transported into cells via glucose transporter isoforms 1 and 3, but under normal physiological conditions, with the presence of high glucose concentrations, the uptake of vitamin C does not depend on this mechanism. However, cells can take up 10 fold higher levels of ascorbate under oxidative conditions than normal. There are two forms of sodium-dependent ascorbate transporter; SVCT1 and SVCT2 which vary in their tissue distribution; SVCT1 can be found in epithelial tissue whereas SVCT2 is present in more metabolically active tissue, e.g. brain and eye (Tsukaguchi et al., 1999).

The concentration of vitamin C in the plasma is dose dependent; scurvy, a clinical expression of vitamin C deficiency, develops when the plasma concentration is < 4

µM. With a dose of 30 mg d^{-1} the normal plasma concentration is 7 µM in men and 12 µM in women and this can rise to approximately 60 µM when the dose is increased to 100 mg d^{-1}. At doses of about 400 mg d^{-1} a steady state is reached where the plasma is entirely saturated (Padayatty et al. 2003). The concentration in humans is determined by gastrointestinal absorption, tissue distribution, excretion and metabolism (Rumsey and Levine 1998). In the tissue the concentration varies, with the highest concentrations observed in the adrenal and pituitary glands to liver, spleen, kidney, and the lowest concentrations in the heart and muscles (Iqbal et al., 2004).

1.2.3.2.2.2 Vitamin E

Vitamin E was first discovered as an essential nutrient for reproduction in rat by Evans and Bishop in 1922, then described in 1950s by Klaus Schwarz as antioxidant and located within the cellular antioxidant system (Brigelius-Flohe and Traber, 1999). The majority of alveolar surfactant is made up of polyunsaturated fatty acids and cholesterol; vitamin E is found to have important role in the protection of this against lipid peroxidation, thus it plays an important role in protecting against lung injury. Vitamin E has eight lipophilic forms categorised into two groups, the tocopherols and tocotrienols, each of which has four forms, but the predominant form in the plasma is α-tocopherol. In humans, the α-tocopherol transfer protein in the liver has difficultly recognising the other types (β,γ, δ-tocopherols and tocotrienols) and they are not converted to α-tocopherol by humans (Brigelius-Flohe and Traber 1999).

Vitamin E in all its forms is absorbed in the proximal intestinal cells and secreted in chylomicrons after entering the circulatory system and transported to the liver with other lipid particles. Only α-tocopherol passes through the liver and appears in the plasma, and is further distributed to the tissues via lipoproteins. Through cytochrome P450-dependent processes α-tocopherol is degraded into tocopherol-CEHC and excreted out of the body via the urine (Traber and Sies, 1996) (Figure 1.9, overleaf).

Vitamin E is considered to be a scavenger of peroxyl radicals that are generated in the oxidation of fatty acids, their reaction with which then produces the tocopheroxyl radical. This in turn is reduced by a hydrogen donor (e.g. ascorbate or retinol) to its active, reduced form again. Type II alveolar cells supplement the surfactant with vitamin E; high density lipoprotein (HDL) is the main source of the vitamin for these cells (Kolleck et al., 1999). The uptake of the vitamin from HDL is regulated by three high density lipid specific receptors: (a) scavenger receptor BI, (b) high density lipid binding protein-2 and (c) membrane dipeptidase, in addition to the cooperative role of the peripheral membrane proteins cubilin and megalin (Kolleck et al., 2002). As a lipid-soluble factor vitamin E has a tendency to concentrate in the cell membranes after it is taken up by cells. The concentration of the vitamin in the plasma is about 27 µM and can only increase up to a maximum of about 80 µM despite increasing dosage up to 1320 mg d^{-1} (Dimitrov et al., 1991).

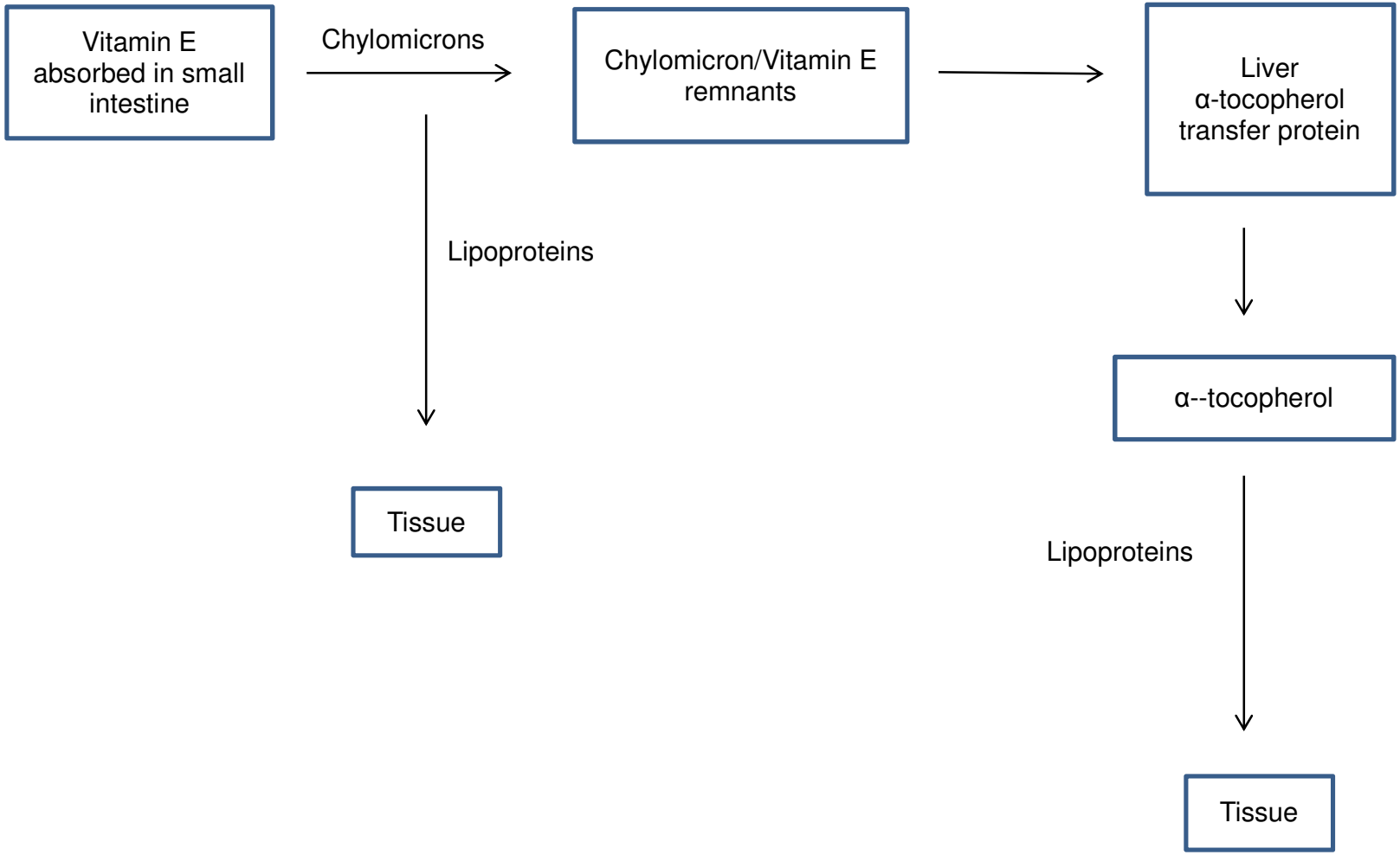

Figure 1.9 Schematic overview of the mechanism of vitamin E absorption and transport in human body.

1.2.3.3 Epithelial inflammatory functions

A range of mediators are produced and released as a response to epithelial injury and damage such as cytokines, chemokines, arachidonic acid metabolites and growth factors (Velden and Versnel 1998). The interaction between the micro-organisms and inflammatory cells in the surface liquids prevents them passing through the epithelial cell barrier (Warner et al., 1998).

1.2.3.4 Role of epithelium in remodelling after injury

After an injury or wound, epithelial tissue intervenes in a series of consecutive processes of repair and regeneration, including active mitosis, spreading of the basal cells near the wound area, migration, proliferation and then progressive redifferentiation with the emergence of preciliated cells, and ciliogenesis with complete regeneration of the pseudostratified epithelium (Puchelle et al., 2006). A study by Zahm (1997) has shown that the most important step in the wound repair process is the spreading and migration of cells in the denuded airway epithelium and that the peak of cell proliferation is 48 h after injury after which the mitotic activity subsides when wound closure is completed. Many molecular factors contribute to these remodelling processes such as epidermal and fibroblast growth factors including TGF-α, KGF and HGF; cytokines including IL-β1, 2, 4, and 13; extracellular matrix metalloproteinases e.g. MMP-2, MMP-7 and MMP-9; cytoskeletal structures; and matrix materials such as collagen and fibronectin (Figure 1.10, page 33). Several signaling pathways are involved in the regulation of

this complex process e.g. MAPK, STAT3 and Rho-GTPases (Crosby and Waters, 2010).

After recovery from hyperoxia-induced injury, proliferation of Type II and non-ciliated cells increases in the lung (Yee et al., 2006). Studies refute the concept that ciliated and Type I alveolar cells are terminally differentiated cells and do not contribute to proliferation in the lung (Evans et al., 1986). Park et al. (2006) showed that ciliated cells have remarkable plasticity during the redifferentitation process in bronchiolar epithelium when rapidly undergoing squamous metaplasia and transdifferentiation into cuboidal then to columnar cells (ciliated and non-ciliated). Moreover, Coraux et al. (2005) found that MMP-9 and -7 expression increased in the stage of well-differentiated surface epithelium while IL-8 expression decreased at this stage but its maximal expression occurred in step one of regeneration when the cells adhered and migrated. Furthermore, an *in vitro* study by Lechapt-Zalcman et al. (2006) demonstrated the role of transforming growth factor-β1 (TGF-β1) in enhancing the airway epithelial repair by increasing MMP-2 secretion from epithelial cells.

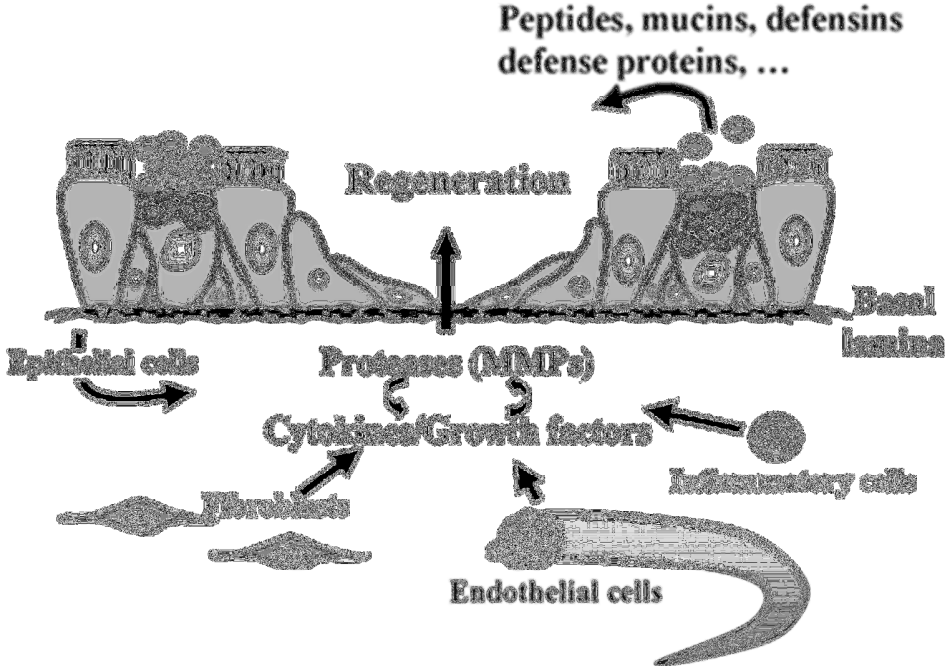

Figure 1.10 Cellular and molecular factors involved in the repair and regeneration of the airway epithelium. Based on Puchelle et al. (2006) with permission.

1.2.4 ROS production and its role in the respiratory tract

The reduction of oxygen molecules generates a more reactive group of free radicals and molecules known as reactive oxygen species (ROS). ROS are regarded as the key factors behind the oxidative stress and damage associated with hyperoxia. Superoxide anions ($O_2^{\bullet-}$) are the first radicals formed in the reduction of O_2. Once $O_2^{\bullet-}$ is produced, a cascade of further ROS production may occur with more reduction. $O_2^{\bullet-}$ then spontaneously dismutates to O_2 and hydrogen peroxide (H_2O_2). Furthered reduction of H_2O_2 forms hydroxyl radicals ($HO^{\bullet}$) which are very reactive molecules formed through both Haber-Weiss and Fenton-like reactions in the presence of metal ions (Figure 1.11, page 35). In addition, $O_2^{\bullet-}$ can react with nitric oxide (NO) to produce a highly reactive peroxynitrite ($OONO^-$) (Trachootham et al., 2008), as shown below:

$$NO + O_2^{\bullet-} \rightarrow OONO^-$$

There are several enzymatic and non-enzymatic potential sources of ROS in cells. The mitochondrial electron transport system is considered as a major non-enzymatic site of ROS production, with cytochromes P450 constituting another potential source. The most important enzymatic producer is NADPH oxidase which can be found in a variety of cell types such as neutrophils, fibroblasts, endothelial cells, chondrocytes and mesenchymal cells (Hancock et al., 2001).

Non-enzymatic	$O_2 + e^- \rightarrow O_2^{\bullet -}$
Enzymatic	$2O_2 + NADPH \rightarrow 2\ O_2^{\bullet -} + NADP^+ + H^+$
Superoxide dismutase	$O_2^{\bullet -} + 2\ H^+ \rightarrow H_2O_2 + O_2$
Fenton/Haber-Weiss chemistry	$H_2O_2 + Fe^{2+} \rightarrow Fe^{3+} + HO^- + OH^{\bullet}$

Figure 1.11 Cascade formation of ROS in living cells

There is a robust antioxidant defence system by which ROS are controlled. When the level of ROS exceeds the capacity of the defence system, oxidative damage can result in lipid, proteins and DNA (Turi et al., 2002). Once oxidative stress occurs, redox-sensitive transcription factors including nuclear factor kappa B (NF-κB), activator protein-1 (AP-1) and mitogen-activated protein kinases (MAPKs) are activated as a response, which in turn promote up-regulation of pro-inflammatory cytokines.

1.2.5 Hyperoxia

Hyperoxia is simply defined as exposure of tissues to partial pressures of oxygen (PO_2) greater than normal (approximately 21 kPa (160 mmHg) during normal breathing) (Dean et al., 2004). Normally, the partial pressure of the inspired oxygen in the lung alveoli is lower than normal air at atmospheric pressure because of

humidification of the air in the upper airway, the uptake of O_2 by tissues and the diffusion of CO_2. Thus, the normoxia in the alveoli is about 14 kPa (107 mmHg). Medically, hyperoxia therapy supplementation is essential whenever tissue oxygenation is decreased (PO_2 < 8 kPa, < 60 mmHg at sea level). The oxygen fraction of the supplied air can range from 25%-100% depending on the patient‘s condition in comparison with the normal fraction which is 21% (Bellomo et al., 2011). In the US it has been estimated that about 800,000 patients receive therapeutic oxygen with a cost of 1.8 billion dollars every year (Kim et al., 2008). The prolonged use of hyperoxia leads to an increased epithelial PO_2 with the potential for oxidative stress and damage. Lung tissue is the first target of oxygen toxicity as the lungs are the first organ that encounter the high oxygen levels whilst tissues of other organs receive almost normal oxygen partial pressures due to the tissue haemoglobin-oxygen buffering system (oxygen toxicity occurs in the tissue when the oxygen fraction > 60%) (Mach et al., 2011, Zhou et al., 2007).

Humans encounter relative hyperoxia as neonates following birth. There is a change from an intrauterine alveolar PO_2 of 3-4 kPa to 13-14 kPa; the body usually copes with this change by up-regulating the lung antioxidant defence system (Ochoa et al., 2003). Premature babies unprepared for this transformation can exhibit sensitivity to the oxidative stress with the possibility of developing pulmonary diseases such as intraventricular haemorrhaging and bronchopulmonary dysplasia (Kelly, 1993). Jean et al. (2013) demonstrated the increased expression of more than 150 genes in mice at two hours *postpartum*, controlling intracellular activities such as transcriptional regulation, differentiation, antioxidant and apoptosis. The activation of transcription factors are regulated as a

response to PO_2 change during the birth transition, with increased HIF-1α levels and NF-κB activation having previously been reported (D'angio and Finkelstein, 2000, Haddad, 2002a).

1.2.5.1 Pathological effects of hyperoxia in the respiratory tract

Pathological changes in airway tissue have been reported to occur associated with prolonged exposure to high concentrations of oxygen which may lead to acute or chronic lung injury (Zaher et al., 2007). Pulmonary oedema due to increased pulmonary microvascular permeability, fibrin deposition and impairment of surfactant production were also demonstrated with prolonged exposure (Mach et al. 2011). Alveolar endothelial and epithelial cells are highly vulnerable to hyperoxia-induced damage, which is characterised by alteration in the airspace function and structure, surfactant disruption and an influx of inflammatory cells (Clerch and Massaro, 1993).

Hyperoxia-induced lung injury may be due to enhanced generation of ROS (Dean et al., 2004) and/or activation of redox transcription factors such as NF-κB (Zaher et al., 2007). Lipid peroxidation in cells, protein leakage into the alveolar spaces, alteration of amino acids in structural and functional proteins, alteration of cellular metabolism, DNA strand breakage, reduction in ciliary activity and reduction in bronchial mucus transport velocity are all potential consequences of ROS-induced damage (Dedhia and Banks, 1994, Wright et al., 1994, Olive, 1998, Ahmed et al., 2003) (Figure 1.12, overleaf). In addition, increased expression of pro-inflammatory cytokines such as IL-6, IL-8 and TNF-α occurs as a response to exposure to

hyperoxia (Barazzone and White, 2000). This supports the concept that the interaction between ROS and inflammatory processes augments lung injury.

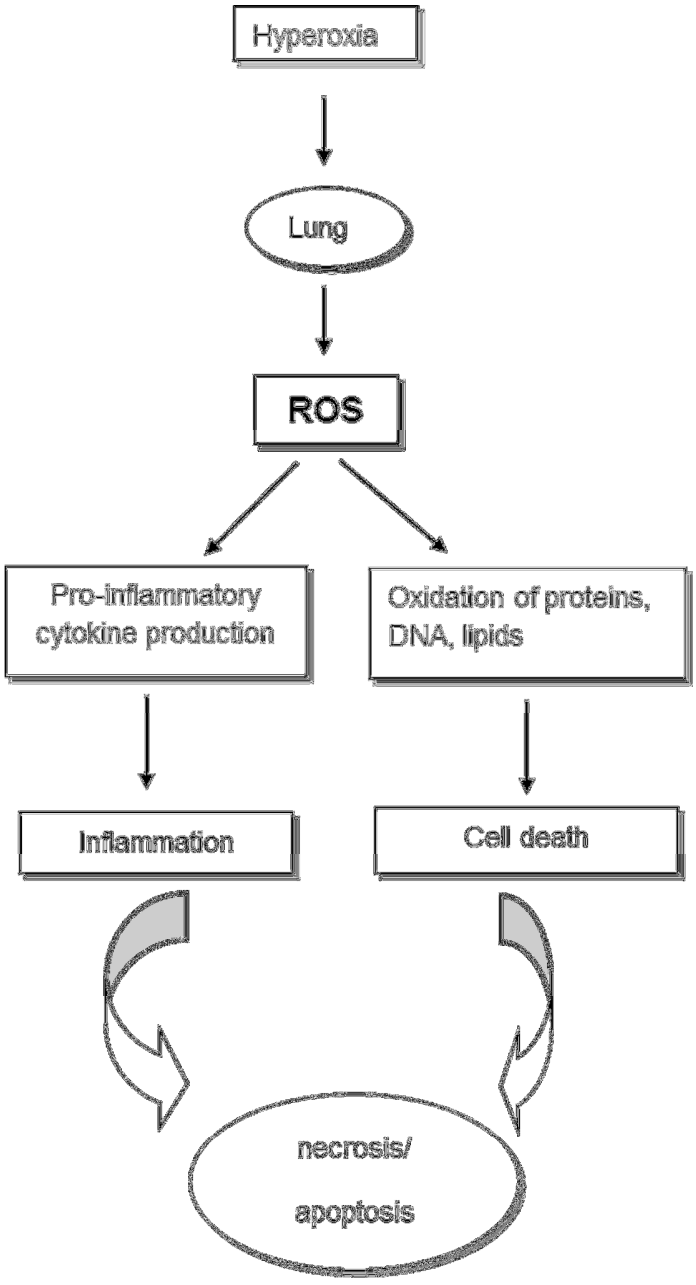

Figure 1.12 ROS-dependent cell death pathways. Hyperoxia-induced imbalance between ROS production/antioxidant defence results in oxidation of macromolecules and activation of redox-sensitive transcription factors leading to production of inflammatory mediators and activation of cellular death pathways.

1.2.5.2 Hyperoxia-induced airway epithelial cell death

The airway epithelium is essential in maintaining the pulmonary integrity and function. Hyperoxia has been shown to induce cell death in capillary endothelium and pulmonary epithelium (Mantell and Lee, 2000). Using several animal models and cell culture studies it has been shown that both necrosis, where the cells undergo plasma membrane disruption and nuclear swelling, and , apoptosis, where the cells undergo nuclear and cytoplasmic condensation, are characteristic of hyperoxic cell injury. Indeed, hyperoxia-induced cell death in airway epithelium shows morphological features characteristic of both necrosis and apoptosis. For example, a study by Barazzone et al. (1998) using mice exposed to 100% O_2 found that condensed chromatin and disrupted plasma membrane both occurred in dying endothelial and epithelial cells. Also, Wang et al. (2003) highlighted the involvement of apoptotic genes in hyperoxia-induced epithelial cell necrosis and found increased activation of the pro-apoptotic proteins Bid and Bax in A549 human cells. The activation of caspases (e.g. caspases 9 and 3) has been shown to increase in murine transformed lung epithelial cells exposed to hyperoxia (Zhang et al., 2003). Many factors are involved in regulating cell death pathways. Activation of Bcl-2, an anti-apoptotic protein, has been found to play an important role in attenuating hyperoxia-induced lung epithelial cell death (Barazzone and White 2000). Studies demonstrated that the activation of ERK/MAPK and phosphatidylinostitol 3-kinase-Akt (PI-3-K–Akt) (both are signaling survival pathways) are delay lung epithelial cells death induced by hyperoxia (Buckley et al.,

1999, Lua et al., 2001). Moreover, *in vivo* and *in vitro* studies have indicated the protective role of haem oxygenase (HO1) against hyperoxia (Lee et al., 1996).

1.2.5.3. Hyperoxia-induced inflammation

The oxidative stress caused by hyperoxia may also provoke an inflammatory mediator response. ROS production induces secretion of cytokines and other chemoattractants by pulmonary cells, and stimulates macrophage, monocyte, mast cell and neutrophil recruitment and accumulation in the lungs leading to further ROS production (Mach et al. 2011). Alveolar macrophages contribute to the initiation of neutrophil arrival by the secretion of neutrophil chemokines such as IL-8. Neutrophils have been found to play an essential role in the initial stages of lung inflammation, further stimulating the increase in neutrophil chemokines that provide autocrine signaling and enhancing oxidative stress by releasing more extracellular free radicals via NADPH oxidase activity and protease secretion (Min et al., 2012, Thorley and Tetley, 2007).

1.2.5.4 Effects of hyperoxia on cell adhesion

Matrix metalloproteinases (MMPs) are proteins that are found in the extracellular matrix, and are secreted from immune cells (Nagase et al., 2006). MMPs have direct role in the remodelling and differentiation of airway epithelial cells after injury (Coraux et al., 2008). Many studies have explored the role of these proteins in the pathological and histological changes in which occur as a result of acute lung injury

after exposure to high concentrations of oxygen (Gushima et al., 2001), such as study by Kohno et al. (2004) who observed an increase in the active form of MMP-2, as well as an increase in the activities of collagenase and gelatinase in the bronchoalveolar lavage fluid (BAL) in hyperoxia-exposed rats. Chetty et al. (2008) investigated levels of MMP-2 and MMP-9 in neonatal mouse lung and found significant increases in the mesenchyme and alveolar epithelium. In asthma, MMP-9 directly targets tight and adherens junction leading to structural and functional alteration, resulting in detachment cells and death of the airway epithelial cells (Vermeer et al., 2009).

In addition, cell junctions can be affected indirectly by hyperoxia through the effects of cytokines. Acute lung inflammation is associated with increased production of tumour necrosis factor alpha (TNF-α) which may lead to structural and functional alterations in pulmonary tight junctions in mice (Mazzon and Cuzzocrea, 2007). Also, bronchial epithelial cell apoptosis and loss of cadherin-mediated intercellular adhesion in asthma are associated with secretion of interferon gamma (IFN-γ) and TNF-α (Trautmann et al., 2005). Expression of the gene for intercellular adhesion molecule-1 (which is localised at the junctions between endothelial cells and plays and an important role in controlling the transendothelial movement of leukocytes) increased with hyperoxia in human pulmonary endothelial and neutrophil cells (Suzuki et al., 1997).

1.2.6 Antioxidant treatments to protect against lung oxidative damage

In view of the widely-held belief that supplementation or activation of antioxidants might reduce the oxidative stress which accompanies a variety of lung diseases, several *in vivo* and *in vitro* studies have investigated the protective role of antioxidants in this regard. A study by Jyonouchi (1998) suggested a protective role of antioxidant vitamins E and C in small airway epithelial cells against hyperoxia-induced cell proliferation suppression and apoptosis. Jacobson et al. (1990) found that increasing tissue antioxidant (vitamin E and butylated hydroxyanisole) levels and antioxidant enzymes (combination of polyethylene glycol (PEG)-SOD and PEG-catalase), can prevent some hyperoxia- induced pulmonary injuries such as alveolar-capillary permeability and lung weight increase. This result was similar to that reported by Gurtner et al. (1985), in which pre-treatment with vitamin E or butylated hydroxyanisole (BHA) prevented the loss of vascular reactivity in isolated rabbit lungs. Transgenic mice which overexpress intracellular antioxidant enzymes (Cu/Zn-SOD and Mn-SOD) are significantly protected against oxygen toxicity (White et al., 1991, Wispe et al., 1992). Moreover, Sussana et al. (2009) suggested that activation of nuclear erythroid 2 p45 related factor (a redox transcription factor that regulates genes for several antioxidant factors) can protect mice during chronic exposure to cigarette smoke-induced oxidative stress.

1.2.7 Oxidative stress biomarkers

Oxidative stress is simply defined as a condition of imbalance between antioxidants and pro-oxidants e.g. ROS with excess pro-oxidants levels leading to cell damage (Betteridge, 2000). In biochemistry the measurement of products formed as a consequence of oxidative stress is often used, as the detection of oxidants may be difficult because of their short life. Some biomarkers of oxidative stress are described below.

1.2.7.1 Lipid peroxidation

Lipid peroxidation refers to ROS-induced damage to a fatty acid (L-H). ROS are reactive enough to abstract a hydrogen atom from a methylene carbon in the hydrocarbon tail. As hydrogen has a single electron, its removal leaves the carbon atom with an unpaired electron (lipid radical). A lipid peroxyl radical ($L^{\bullet}$) results from the reaction of the latter with O_2. Peroxyl radicals are capable of abstracting hydrogen atoms from neighbouring fatty acids leading to propagation of lipid peroxidation, as well as attacking membrane proteins and reacting with another peroxyl radicals (Halliwell and Chirico, 1993) (Figure 1.13, page 45). The length of the peroxidation chain reaction depends on several factors including the concentration of oxygen, the ratio of proteins to lipids in the membrane and the presence of chain-breaking antioxidants (e.g. α-tocopherol). For example, poly-unsaturated fatty acids are vulnerable to hydroxyl radicals leading to the development of lipid peroxidation by which several products such as aldehydes

and epoxides are produced (Janero, 1990). In contrast, monounsaturated and saturated fatty acids are more resistant to free radical damage. Lipid peroxidation can lead to disruption of membrane function, including increased permeability, decreased fluidity and inactivation of membrane enzymes (Gutteridge and Halliwell, 1990). Malondialdehyde (MDA) is considered to be the major product of lipid peroxidation (Marnett, 2002). MDA can react with free amine groups on proteins resulting in possible modification of the protein's properties (Palmieri and Sblendorio, 2007). MDA has been widely used as a marker of oxidative stress in the lung studies including levels in bronchoalveolar lavage, plasma and tissue. The easiest and most widespread assay for measuring the MDA is the thiobarbituric acid reactive substances (TBARS) assay, which is based on the reaction of two TBA molecules with one MDA molecule, resulting in ketoaldehyde formation.

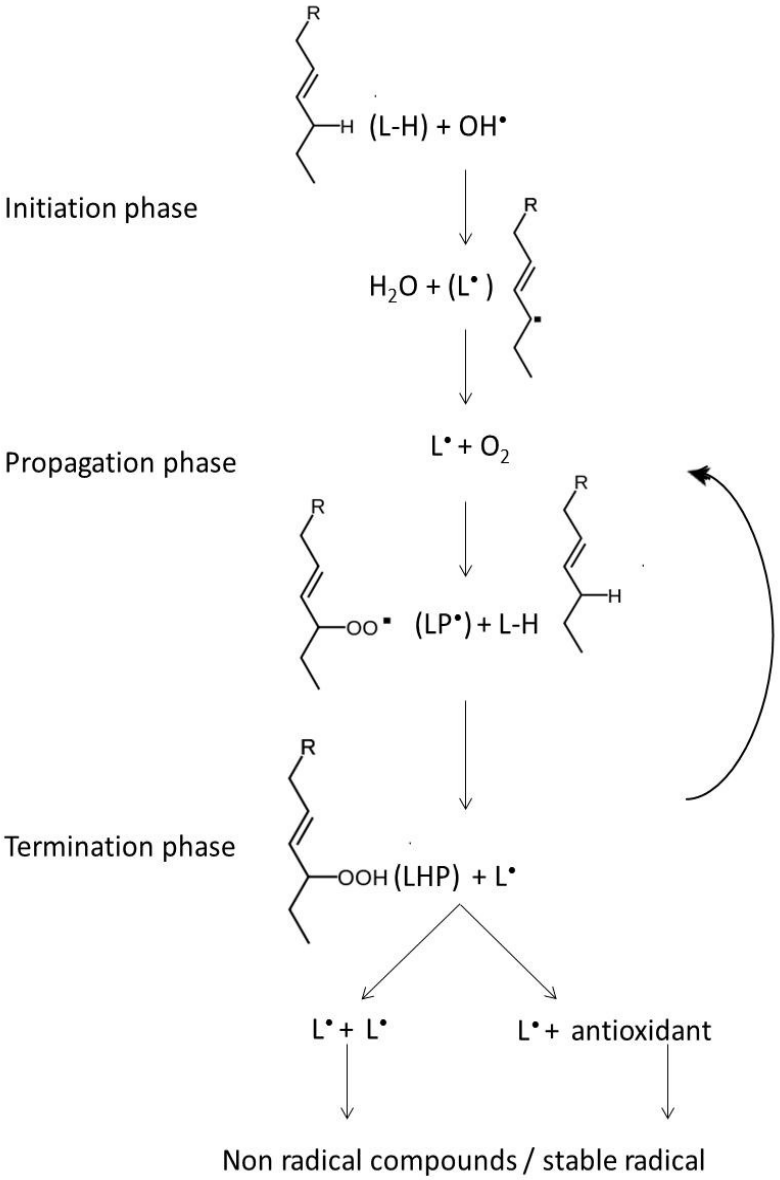

Figure 1.13 The three phases of lipid peroxidation start with the *initiation* phase. Here, the unsaturated fatty acid (L-H) is attacked by ROS (e.g. hydroxyl radical) resulting in a lipid radical ($L^{\bullet}$) and water. By addition of O_2 to the lipid radical, the second, *propagation* phase is initiated, in which lipid a peroxyl radical ($LP^{\bullet}$) is formed, which is able to attack another fatty acid to give rise to lipid hydroperoxide (LHP) and a lipid radical. One initial peroxidation event can trigger a chain reaction. In the *termination* phase, lipid radicals can react with other lipid radicals or with an antioxidant to form non-radical compounds or stable radicals.

1.2.7.2 Total glutathione

Glutathione is a tripeptide, and is also known as γ-glutamylcysteinylglycine. It is one of the most important biological antioxidants, and is involved in many biological activities including the synthesis of DNA and proteins, and the regulation of enzyme activities (Meister, 1981). Glutathione exists in two forms; reduced glutathione (GSH) and oxidized glutathione (GSSG). Two enzymes are involved in the synthesis of GSH; γ- glutamylcysteinyl synthetase, which catalyzes the conjugation of glutamate and cysteine to form γ-GluCys, and glutathione synthetase which catalyzes the reaction of γ-GluCys with glycine to form GSH. Glutathione peroxidase (GPx) catalyzes the oxidation of two molecules of GSH by H_2O_2 to produce GSSG, thereby detoxifying H_2O_2 to water. GPx can also use organic peroxides (e.g. produced in lipid peroxidation) as substrates. GSSG is reduced again by NADPH in a reaction catalysed by glutathione reductase, resulting in two GSH molecules for reuse (Figure 1.14, overleaf). The ratio of GSH:GSSG is normally high with GSH > 90% and is an indicator of cellular redox homeostasis. Measurement of increased GSSG levels is therefore useful as a marker of oxidative stress and high levels of GSSG have been implicated in cell death, differentiation and proliferation (Schafer and Buettner, 2001).

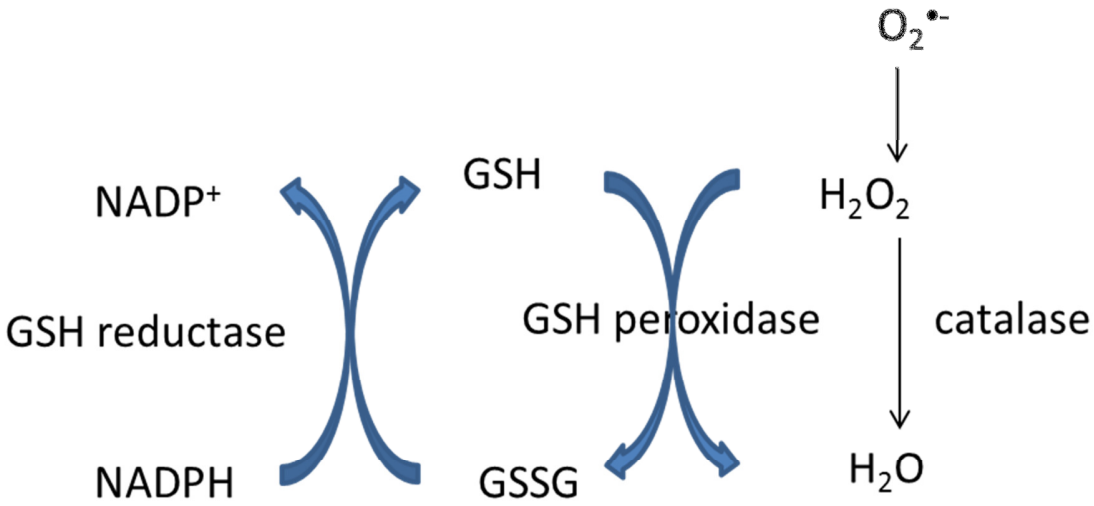

Figure 1.14 The glutathione cycle and its function in the removal of hydrogen peroxide (H_2O_2), one of the ROS produced in cells. The cycle involves the conversion of reduced glutathione (GSH) to oxidised glutathione (GSSG) catalysed by glutathione peroxidase. GSSG is reduced in the presence of glutathione reductase and using reduced nicotinamide adenine dinucleotide phosphate (NADPH) as electron donor; GSH and $NADP^+$ are formed.

In addition, GSH can act as a direct scavenger of ROS, and it can inactivate lipid peroxides and aldehydes via the glutathione-S-transferases, leading to irreversible glutathione oxidation (Townsend and Tew, 2003). In addition, reports support the idea of a synergistic interaction between GSH and ascorbate in animal and human cells. Both water-soluble antioxidants have been found to spare each other (reversibly resources each other); in glutathione-deficient animals, high levels of ascorbate protect the animals from tissue damage (Meister, 1994). Similarly, guinea pigs, which are ascorbate-deficient show a delay in the onset of scurvy when the animals are supplied with high levels of glutathione ester (Martensson et al., 1993). Studies on the correlation of glutathione (reduced and disulphide), ascorbate and α-tocopherol in human lymphocytes have shown a direct correlation between ascorbate and glutathione concentration (Lenton et al., 2000).

1.2.7.3 Protein oxidation

Proteins are significant targets for oxidants, and this may result in irreversible modification. ROS may oxidize the side chains of specific amino acids including lysine, arginine, tyrosine, threonine, proline and tryptophan leading to carbonyl groups formation. In addition, aldehyde compounds produced by lipid peroxidation such as MAD and 4-hydroxynonenal can react with proteins leading to carbonyl groups production (Berlett and Stadtman, 1997). These carbonyl groups have been used as an indicator of oxidative stress in the lung. The carbonyl groups can be derivatized by 2,4-dinitrophenylhydrazine (2,4-DNPH) to produce 2,4-dinitrophenyl group, a product which can be detected by a specific antibody (Levine et al., 2000),

followed by ELISA or western blotting to provide a qualitative and quantitative oxidised protein measurement (Aldred and Griffiths, 2004).

1.2.7.4 DNA strand breaks

Base modification and strand breakage in DNA is considered to be an indicator of oxidative stress. Base modification and strand breakage can occur due to reactions with $HO^{\bullet}$, in which purines and pyrimidines are modified, thus leading to backbone fragmentation and DNA single strand breakage (Breen and Murphy, 1995). Hydrogen peroxide will also cause strand breakage, possibly via Fenton chemistry involving metal ions bound to the DNA (Stohs and Bagchi, 1995)

The comet assay has been used as a sensitive method for assessing single cell DNA damage. The assay is based on the movement of negatively charged DNA embedded in an agarose gel, formed on a microscope slide and subjected to an electric current. The benefits of this assay are that is sensitive enough to detect low level of DNA damage, economical (low-cost), and can provide information on strand breakage using low numbers of single cells (50-100 cells/slide) (Tice et al., 2000). Different tail parameters are calculable by commercial software to evaluate the DNA damage (e.g. Komet 5.0 image analysis software). These include olive tail moment (tail mean intensity – head mean intensity) × %DNA in the tail), tail extent moment (tail length × %DNA in the tail) and the percentage tail DNA (tail intensity/total comet intensity (tail + head)). The most reliable of these is the percentage tail DNA as it is considered the most representative and easy to conceptualise (Kumaravel and Jha, 2006).

1.2.8 Hypotheses

1- Hyperoxia causes oxidative damage that leads to hyperoxia-induced ciliary denudation which is associated with sloughing of the epithelial cells.
2- Hyperoxia-induced epithelial cell loss is due to weakening of the tight junctions.
3- The antioxidant vitamins, C (ascorbate) and E (α-tocopherol), can protect against the effects of hyperoxia on ciliated epithelial cells.

1.2.8.1 Research objectives

The specific objectives for this project were:

1- to establish a large animal tissue culture model to investigate the effects of hyperoxia on ciliary coverage (Chapter 3).
2- to establish a primary cell culture model to detect damage induced by hyperoxia on ciliated epithelium (Chapter 3).
3- to determine ciliary abundance through the development of image analysis methods by using the scanning electronic microscope (SEM) under normal and hyperoxic conditions (Chapter 3).
4- to determine the protective role of the vitamins (α-tocopherol and ascorbate) on ciliary coverage (Chapter 3) and on reduction of epithelial permeability and inflammation induced by hyperoxia (Chapter 5).

5- to investigate oxidative damage in tissue through the detection of lipid peroxidation; detection of carbonyl modification of proteins; DNA strand breakage; and leakage of LDH activity to detected the damage, and to detect oxidative stress in the tissue based on the levels of total glutathione (Chapter 4).

6- to determine the effects of hyperoxia on the tight junction protein zona occludins 1 (ZO-1) by using immunohistochemistry assay and quantification of gene expression (Chapter 5).

7- to characterise the effects of hyperoxia on the inflammatory process by analysing the levels of the cytokines IL-6, IL-8 and TNF-α cytokines and the levels of expression of the genes for these cytokines (Chapter 5).

8- to evaluate whether antioxidant vitamin supplementation could reduce hyperoxia-induced inflammation (Chapter 5).

Chapter 2: General materials and methods

2.1 General consumables

All media and cell culture associated reagents were purchased from Invitrogen (GIBCO, UK) or Lonza (Slough, UK). Transwell inserts and well plates were obtained from Becton Dickinson (NJ, USA). All other reagents and chemicals were obtained from Sigma Aldrich (Poole, UK) and Fisher Scientific Ltd (Loughborough, UK), unless otherwise stated. Gas mixes were supplied by Plymouth Hyperbaric Medical Centre (DDRC, Plymouth, Devon, UK).

2.2 Primary cultures

2.2.1 Sample collection and dissection

Samples of fresh bovine lung were collected from a local abattoir (near Newton Abbot, Devon, UK) and transported to the laboratory at Plymouth University for immediate processing. The time between death of animal and the start of processing was less than an hour. Secondary bronchi (approx. 25 mm in diameter) were dissected from the lung using a sharp kitchen knife and washed with cell culture grade phosphate buffered saline (PBS) to remove mucus and blood. Tissue was then rinsed with Dulbecco's modified Eagle's medium (DMEM) with 10% Fetal

Bovine Serum (FBS), containing 1% antibiotic and antimycotic (containing 10,000 U ml^{-1} penicillin G, 10 mg ml^{-1} streptomycin and 25 µg ml^{-1} amphotericin B).

2.2.2 Preparation of collagen-coated culture supports

Bovine type I collagen (Invitrogen, UK) to be used for coating culture supports was prepared according to the manufacturer's instructions. Firstly, the collagen was dissolved in 0.02 M acetic acid in a volume dependent on the surface area to be coated at a final level of 10 µg cm^{-2}. After this, the 1 ml of solution was applied to either Petri dishes (30 mm) or Transwell inserts and incubated for 1 h at room temperature, followed by three washes with PBS after aspiration of the excess solution. Type I collagen is a key component of the basement membrane *in vivo*, and *in vitro* encourages cells to grow, differentiate and spread in a way that mimics *in vivo* conditions (Fiedler et al., 1991). Coated materials were either used immediately or kept at 4 °C until use within a few days.

2.2.3 Primary bovine bronchial cell culture

Primary bronchial bovine cell culture was carried out as described by Wyatt et al. (2003). After dissection and preparation of the samples as described in Section 2.2.1, all bronchus segments (2 cm^2) were incubated overnight in 0.1% bacterial protease (Sigma P8811, from *Streptomyces griseus*) in minimum essential medium (MEM) at 4 °C. The following day the bronchus samples were rinsed several times

with Dulbecco's modified Eagle's medium (DMEM) with 10% FBS. The washes were collected in a 50 ml centrifuge tube and left at room temperature for 5-10 min by which time almost all the detached epithelial cells that had lined the lumen had settled to the bottom as a pellet. The pellet was then re-suspended in fresh medium and the cells counted as described in Section 2.2.4. Cells were then cultured on collagen-coated Petri dishes (Section 2.2.2) in 1:1 LHC-9/RPMI medium. Petri dishes were then incubated at 37 ℃, under 5% CO_2. Monolayers of cells were obtained after 3 days.

2.2.4 Cell counting and viability

Cell density was determined before each experiment as follows. Cells were collected from adherent monolayer by trypsinization; firstly, the monolayer of cells was washed twice with cell grad solution (e.g. PBS, Hank's balanced salt solution HBSS). A solution of 0.05% trypsin containing 0.5 mM EDTA was then added for 5 min to release the cells with gentle agitation at 37 ℃ to help the cells detach. Following this, 5 ml of medium containing FBS was added to neutralize the trypsin and the mixture was centrifuged at 130 *g* for 5 min (Denley BR40, west Sussex, UK). Cells were collected as a pellet and re-suspended in culture medium in a 50 ml centrifuge tube. A small sample of suspension (50 µl) was then placed in a 1.5 ml centrifuge tube and 50 µl of 10% Trypan blue stain to assess cell viability was added, gently mixed by pipetting and transferred to a Neubauer haemocytometer. The cells were immediately counted (within 5 min) using a light microscope (Olympus BH 2, Olympus, Japan) using the ×20 objective. The mean of the cell

count from four large squares (each measuring 1 mm x 1 mm x 0.1 mm) at each corner was calculated. The cell density was calculated thus:

$$\text{Total cell count (cell ml}^{-1}) = \text{mean number of counted } /2 \times 10000$$

and the cellular viability percentage was calculated thus:

$$\text{Cell viability (\%)} = \text{numberof unstained cells / total number of cells } \times 100$$

2.2.5 Bovine tissue culture

Large tissue samples, including the lining of the ciliated epithelium together with the underlying cartilage, were first dissected as described in Section 2.2.1. Then duplicate samples (3-4 mm^2), i.e. samples taken from the same region of bronchus, were dissected out using sterile (autoclaved) scissors. Bronchial samples were cultured as described by Rankin et al. (2007) with slight modifications. Each matching pair of bronchus samples was placed with the ciliated surface uppermost within 12 well-plate cell culture membrane inserts (Transwell inserts, 3.0 µm, high-density membrane). This technique was used to avoid the suppression of ciliated cells in culture over time (Clark et al., 1995). The growth medium consisted of a 1:1 mixture of LHC-9 and RPMI 1640, supplemented with 1% antibiotic/ antimycotic solution (see Section 2.2.1). This medium was chosen as it has proven effective for bronchial epithelial culture in the past (Lechner and LaVeck, 1985). Medium (100 µl) was carefully pipetted around the samples ensuring that the epithelial surface was not covered, and an additional 1 ml of medium was placed in the culture well below,

supplying the tissue nutrients by capillary action and diffusion through the membrane support.

2.2.6 Exposure to hyperoxia

The cultured cells or tissue in plates as described in Sections 2.2.3 and 2.2.5 were exposed to the required oxygen concentration as follows. The plates were placed within custom-made airtight polypropylene boxes (5 l) prepared at Plymouth Hyperbaric Medical Centre (DDRC, Plymouth, UK). The boxes were flooded with gas mixes, which were either normoxic (21% O_2, 5% CO_2 and 74% N_2) or hyperoxic (95% O_2, 5% CO_2) (Figure 2.1, overleaf). The boxes were then placed in an incubator at 37 ℃. The humidity level in the boxes was maintained using tissue moistened with 20 ml sterilized PBS placed in the box. The medium was changed daily in order to maintain the structure and function of the ciliated cells (Jackson et al., 1996).

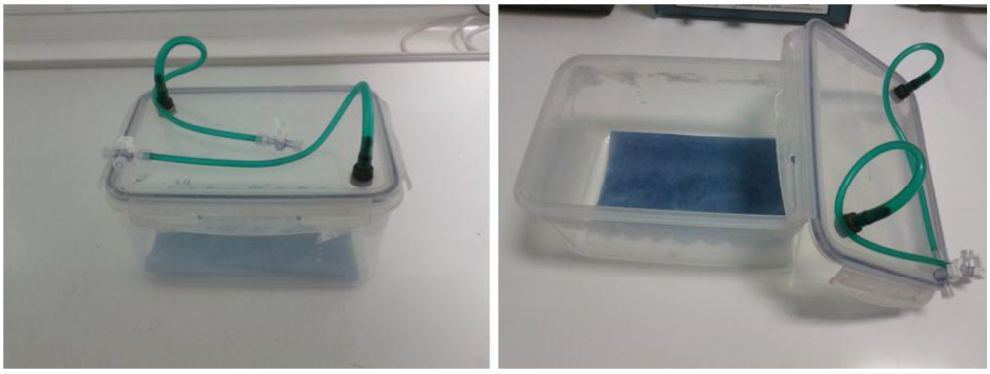

Figure 2.1 Boxes used in the experiments to provide the normoxic and hyperoxic culture conditions.

2.2.7 Co-culture with antioxidant vitamins

The protective role of antioxidants against loss of ciliary coverage induced by hyperoxia in bovine bronchial epithelium was investigated. α-tocopherol (Vitamin E), L-ascorbate (vitamin C) and a combination of the both vitamins were used. Bronchial tissue samples were prepared and cultured as described in sections 2.2.1 and 2.2.6, and supplemented with medium containing either α-tocopherol or ascorbate. Six experimental conditions were used. Samples were exposed to normoxia (21% O_2) as a control; hyperoxia (95% O_2); hyperoxia with 10^{-7} M α-tocopherol; hyperoxia with either 10^{-6} M or 10^{-7} M ascorbate and hyperoxia with a combination of α-tocopherol and ascorbate at 10^{-7} M and 10^{-6} M, respectively. The stock vitamin solutions were prepared as described by Jyonouchi et al. (1998);

briefly, α-tocopherol was dissolved in an ethanol, methanol and isopropanol mixture (19:1:1, respectively) at 10^{-3} M and then diluted to give the final concentration (10^{-7} M) within the culture medium. Ascorbate was dissolved in PBS at 10^{-3} M and diluted within the culture medium to give final concentrations of 10^{-6} M and 10^{-7} M. Samples were maintained in culture with the media and gas changed daily.

2.3 Scanning electron microscopy (SEM) and image analysis

Samples were cultured, exposed to gas and supplemented with vitamin as described in Sections 2.2.3, 2.2.6 and 2.2.7 and immediately processed for scanning electron microscopy (SEM). Following protocol described by Blanchard et al. (1992) samples were gently washed several times with PBS to remove any associated particles from the medium, before being fixed in 2.5% glutaraldehyde (Agar Scientific, Essex, UK, R1102) in 0.1 M sodium cacodylate buffer pH 7.2 (Agar Scientific, R1012). All samples were subsequently rinsed in 0.1 M sodium cacodylate three times for 15 minutes each, followed by dehydration in an ascending ethanol dehydration series of 30% (in water), 50%, 70%, 90% and 100% for 15 minutes each with two 100% changes. Samples were then critical point dried using a critical point dryer (Emitech K850, Quorum Technologies, Kent, UK), mounted on sample stubs and sputter coated in gold (nominal thickness 10 nm) using an Emitech K550 sputter coater (Quorum Technologies, UK). Sample

observation was carried out using a JEOL 5600 SEM operated at 15 kV. There were some problems with the initial images, i.e. there was heavy mucus covering the ciliated epithelial surface and commonly observed problem was the presence of star-like artefacts covering the ciliated surface (Figure 2.2, overleaf). This problem was solved by further washing of culture samples during dissection (Section 2.2.1) and additional washes (5×) with cell culture grade PBS of each sample before fixing with glutaraldehyde.

For each sample, any areas of mechanical damage were avoided and ten contiguous images were acquired at ×2500 magnification. A quantitative analysis of cilia coverage was carried out using ImageJ image analysis software (http://rsbweb.nih.gov/ij/). The methodology was based on counting cilia-containing squares using a grid system. The quantitative assessment of cilia coverage (%) was carried out blind using the following steps. The images were first converted into 8-bit format, and the cropping tool was used to remove any text generated by the microscope, e.g. the scale bar. After this the image analysis steps were performed. Firstly, the Plugins option was chosen, and the Analyze option employed to apply a grid of (settings: grid type, lines; area per point, 0.21 in^2). The cell counter plugin was then used to count squares containing cilia and the percentage ciliary coverage was calculated as:

$$\%\ \text{cilia coverage} = (\text{number of ciliated squares})/(\text{total number of squares}) \times 100$$

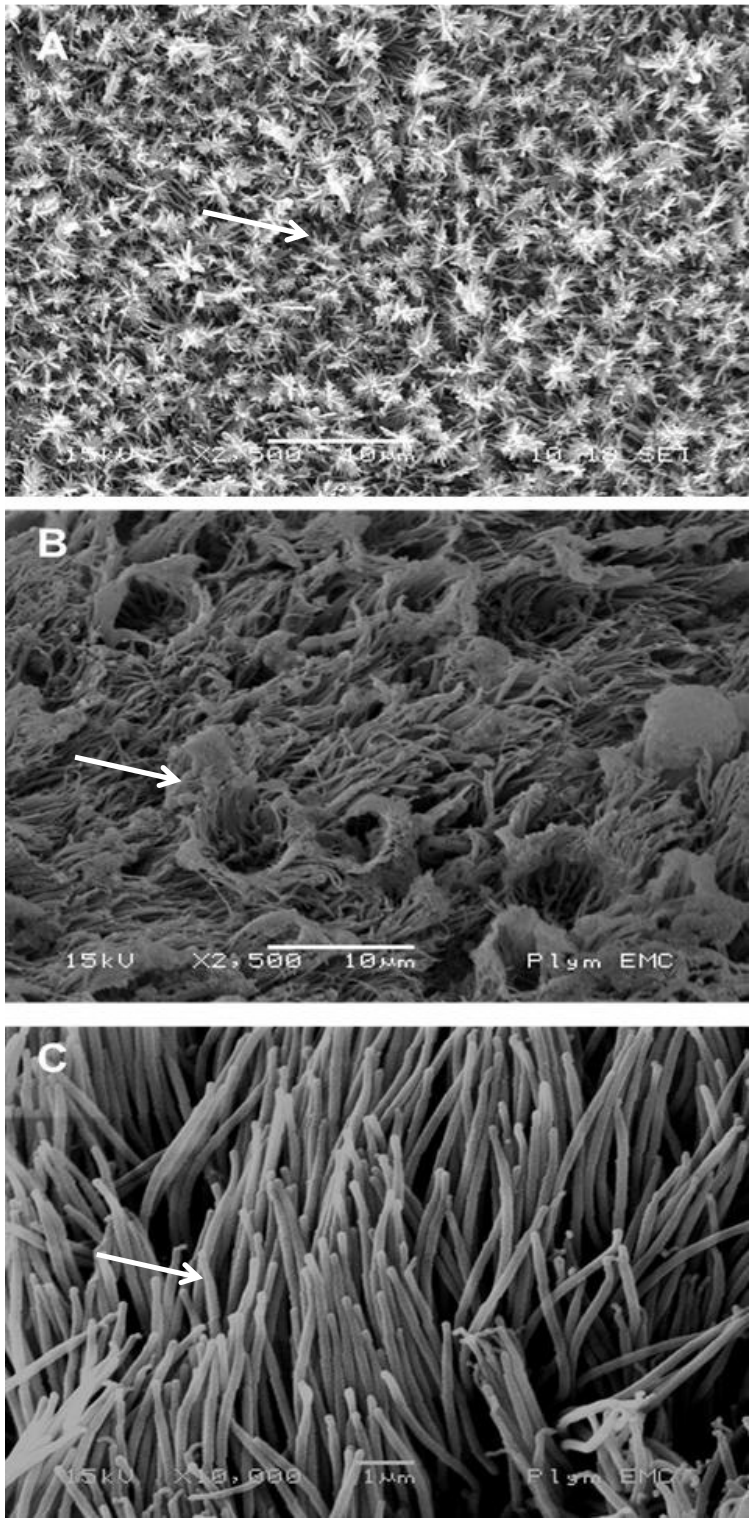

Figure 2.2 SEM images of bovine epithelial bronchus tissue culture (A) showing the star-like artefacts which might have been salt crystals or other particles from the medium, (B) the mucus and (C) an example of an artefact-free image.

Chapter 3: Hyperoxia-induced ciliary coverage loss in bovine bronchus tissue culture

3.1 Introduction

Oxygen therapy is a life-saving emergency treatment for patients that have experienced severe respiratory failure. However, the beneficial use of inspired high fractions of oxygen may lead to significant levels of oxidative stress particularly to the pulmonary epithelium. There is no defined concentration of inspired elevated oxygen that is considered to be safe for patients; the lowest oxygen fraction which provides adequate delivery is the best to be used. There are four main clinical symptoms of oxygen toxicity; absorption atelectasis, tracheobronchitis, bronchopulmonary dysplasia and acute respiratory distress syndrome (Sharma et al., 2008). Many critical care patients suffer from reduced cilia beat frequency, mucus clearance and ciliary loss, which may be related to the retention of secretion and the development of pneumonia (Konrad et al., 1995).

A range of *in vitro* mammalian models has been used to investigate the effects of hyperoxia on the ciliogenesis and mucociliary clearance, including the use of small animals as well as human tissue culture (Konradova et al., 1988, Kay et al., 2002, Rankin et al., 2007). There are several disadvantages with these models. For example, as a consequence of metabolic scaling, the basal metabolic rate is much higher in small animals than in humans (Bergen and Phillips, 2005), and the distribution of cilia in the small mammal trachea may be discontinuous i.e. cilia occur in bands (Rankin et al., 2007). Furthermore, the human airway epithelium is characterised by pseudostratified ciliated columnar epithelia tissue as described in Chapter One, whereas the proximal airway epithelium of small mammals is only

one or two cells thick resting on a very sparse network of basal cells (Rock and Hogan, 2011). Moreover, it has been demonstrated that small animals such as rats are not a good alternative model to the human airway with respect to studying the airway permeability; using freeze-fracture electron microscopy, it has been shown that there is a quantitative difference between the two in terms of the structural characteristics of the tight junctions, where it is less deep, with fewer strand interconnections in the rat tracheal epithelium compared to human tissue (Godfrey et al., 1994). Finally, there are noticeable differences between large and small animals in the width of the epithelium; these differences raise the possibility that key mechanisms and anatomy may also differ between species (Plopper and Hyde, 2008).

Although the use of human tissue samples is possible, these samples are more difficult to obtain. For example, bronchial samples can be obtained after surgical intervention (e.g. removal of lung tumours), but these are potentially contaminated with cancer cells (Rankin et al., 2007). Another possibility is the use of post mortem material, but again this is difficult to obtain and likely to be in poor condition. Therefore, it would be useful to have a convenient and readily available alternative to these models, i.e. a large animal model where the cellular composition and lung structure align more closely with those of human lung.

It has been demonstrated that bovine respiratory explants have almost identical epithelial histology compared to the human airway and these have already proven to be a good model in mechanistic studies of drug transport (Chemuturi et al., 2005). Schmidt et al. (2000) suggested that bovine respiratory explants are a good model to study the uptake of different peptides transport and metabolism. In this

regard, Schmidt et al. (2000) tested the stability of electrophysiological features and rates of metabolic turnover in bovine nasal tissue culture, and they reported that there was no difference in the aminopeptidase activities between human and bovine nasal culture. Thus, two approaches were used to attempt to tackle this issue. First, a preliminary trial aimed at developing a primary cell culture model using bovine bronchial cells was carried out. After this proved unsatisfactory a bovine bronchial tissue culture model was developed and used to investigate hyperoxia-induced cilia loss, and to evaluate the potential protective effects of supplemental vitamins E and C. To the best of this author's knowledge this is the first study to use such a model for this purpose. The reason for studying bronchus instead of trachea is not only that it is easier to handle during dissection, especially because of the presence of a large cartilage in the trachea, but also because the cilia are shorter than those on the trachea (Clarke, 1989), which makes it easier to assess ciliary coverage.

Little is known about the effect of hyperoxia on ciliary coverage in large mammalian airways, and no corresponding studies on the protective effects of antioxidant vitamins against hyperoxia-mediated cilia coverage loss have been conducted. Only preliminary trials (with vitamin E and C as antioxidants) were conducted in order to test or develop methods for estimating ciliary coverage; this will allow future research to more accurately develop potential therapeutic antioxidants and to help develop an increased understanding of the process of oxygen stress.

3.2 Materials and methods

3.2.1 Primary bovine bronchial cell culture

Primary bovine bronchial cell culture was carried out as described in Section 2.2.3. After counting the cells (see Section 2.2.4) using a haemocytometer, cells were plated at a density of 1×10^4 cells cm^{-2} on Thermanox cover slips (0.2 mm thickness) coated with type I collagen. The cover slips were placed in 30 mm diameter Petri dishes in a 1:1 mixture of LHC-9 and RPMI1640 media. Cultured cells were then incubated at 37 °C under humidified 5% CO_2. After 3 days of culture, cells were assessed using SEM, transmission electron microscopy (TEM) and confocal laser scanning microscopy (CLSM).

3.2.2 Bovine tissue sample collection, dissection and culture

Bronchi from fresh bovine lungs were dissected to produce matching pairs as described in detail in Section 2.2.1. These samples were randomly allocated to one of the treatment groups within cell culture inserts as described in Section 2.2.5.

3.2.3 Oxygen exposure and co-culture with vitamins

Bovine bronchial tissue samples were exposed to either normoxia (21% O_2) or hyperoxia (95% O_2) and supplemented with antioxidant vitamins as outlined in Sections 2.2.6 and 2.2.7.

3.2.4 SEM preparation

Both cell and tissue culture samples were analysed using SEM following standard protocols. Samples were fixed in 2.5% glutaraldehyde in 0.1 M sodium cacodylate buffer (Sigma Aldrich, Poole, UK), followed by dehydration with ascending ethanol concentrations and critical point drying using CO_2 as the transitional fluid. Observation was carried out using a Jeol JSM 5600 SEM (Jeol Ltd, Herts, UK) operated at 15 kV (Section 2.3). To obtain representative quantitative ciliary coverage data from the bronchial tissue samples, ten contiguous images were acquired at ×2500 magnification for each sample and ciliary coverage was analysed using ImageJ software as described in Section 2.3.

3.2.5 Transmission Electron Microscopy

Following standard protocols, cells cultured on collagen-coated cover slips (see Section 2.2.3) were fixed with 2.5% glutaraldeyhyde in 0.1 M sodium cacodylate

buffer, pH 7.2. Following three, five minute rinses in 0.1 M sodium cacodylate buffer, the samples were post-fixed in 1% osmium tetroxide in 0.1 M cacodylate buffer for 1-1.5 h. All samples were briefly rinsed in 0.1 M cacodylate buffer and dehydrated in an ascending ethanol series consisting of 30%, 50%, 70%, 90% (ethanol in water) and 100% for 15 min each with two absolute ethanol (100%) changes. Following dehydration, the samples were infiltrated with Spurr resin, being placing in ethanol/ Spurr resin mixes as follows: 3:1 for 2-3 h; 1:1 overnight; and 1:3 for 2-3 h. Once fully infiltrated, samples were placed into 100% resin in moulds and polymerised for 2-3 h at 70 °C. Samples were sectioned to 80 nm using a Reichert Ultracut E ultramicrotome and diamond knife, for examination using a Jeol 1200EX2 TEM (Jeol Ltd, Herts, UK).

3.2.6 Confocal laser scanning microscopy

Primary bronchial cell culture samples were analysed under confocal laser microscopy using an upright LSM510 Confocal laser scanning microscope (Carl Zeiss Ltd., Germany) to generate image stacks (Z-stacks), following a modified protocol described by Toskala et al. (2005). Cells in a collagen-coated Petri dish were fixed with Karnovsky's fixative (2% paraformaldehyde and 2.5% glutaraldehyde in 0.1 M sodium phosphate buffer, pH 7.5; SPI supplies, Cat. No. 02591-AB), for 1 h at room temperature. Following washing twice with PBS (5 min each wash), 20 µl ml^{-1} FITC-labelled tomato lectin (*Lycopersicon esculentum*; Vector Laboratories, CA) was added for 20 min at room temperature. It has been

suggested that this specifically binds to and has a high affinity for airway ciliated epithelial surfaces (Bankston et al., 1991). After washing the cells with PBS, they were visualised using a 40× water dipping objective (excitation wavelength was set at 488 nm and a 505-530 nm band pass filter was used).

3.2.7 Determination of cells in the medium

Epithelial cells in the culture medium sloughed from cultured bovine bronchial samples (Section 2.2.3) were collected and their number estimated as described in Section 2.2.4 using a light microscope (Olympus BH 2, Olympus, Japan) with a 40× objective. Triplicate samples of medium (1 ml each) were collected and centrifuged at 123 *g* for 5 min (Denley BR401 centrifuge). Cell pellets were then re-suspended in 1 ml of culture medium and carefully mixed by pipetting, before being applied to a haemocytometer for counting.

3.2.8 Validation of image analysis methods

For quantitative estimation of ciliary coverage in bovine bronchus a valid methodology was developed. This methodology was based on the use of a digitally-generated grid to facilitate the counting of cilia. The images were collected and digitally analysed using ImageJ software (http://rsb.info.nih.gov/ij/) as follows:

1- The images were first converted to 8-bit format, and the cropping tool was used to remove any microscope-generated text, e.g. the scale bar. This reproducible method was partly automated and saved as a macro to speed up quantification and to ensure that all the images were cropped in an identical manner (figure 3.1, below).

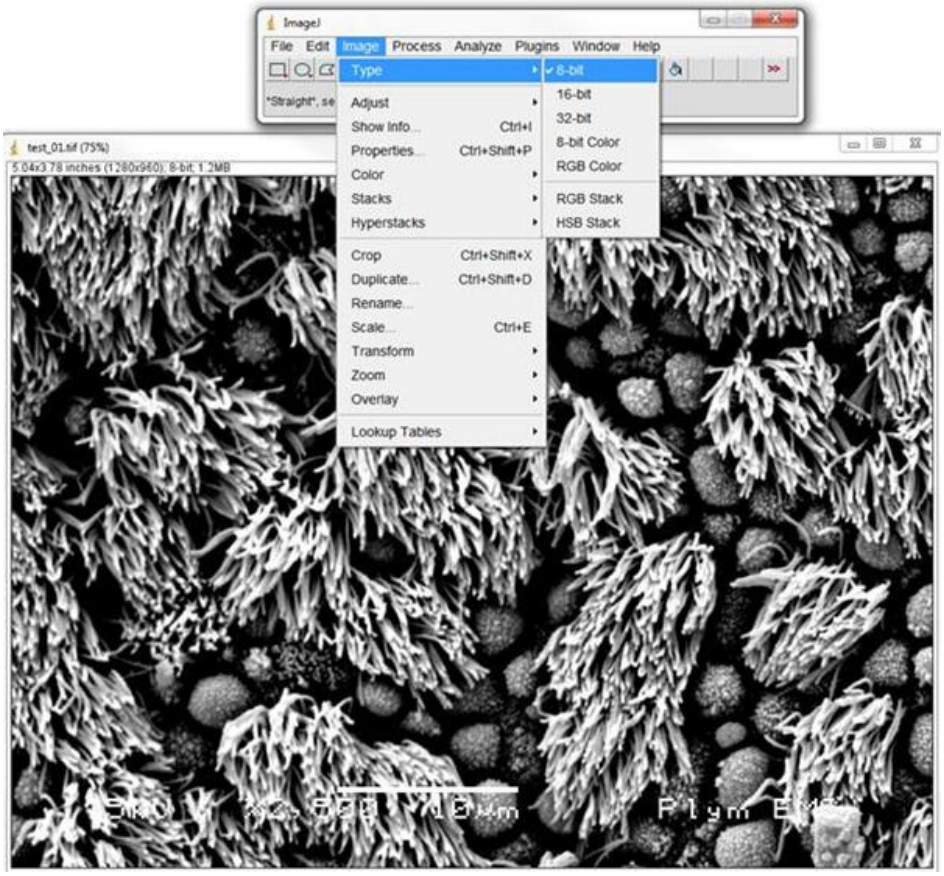

Figure 3.1 Screenshot of SEM image of bovine bronchial ciliated epithelium opened by using image J software and converted to 8 bit type.

2- The image analysis steps were then performed, starting with choosing the Plugins option from the main menu, selecting the Analyse option and applying the grid (settings: grid type, lines; area per point, 0.21 in^2) (Figure 3.2, below).

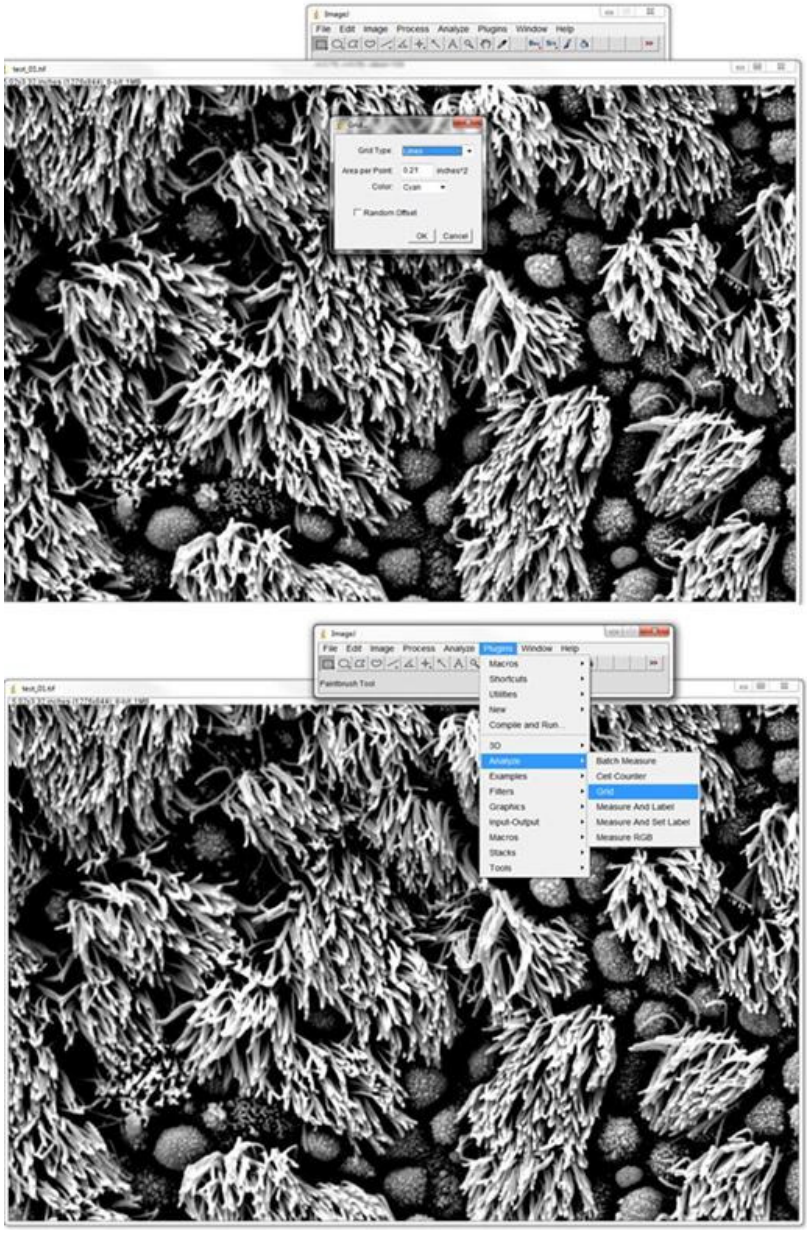

Figure 3.2 Screenshot of SEM image with the ImageJ grid option selected and the grid setting applied.

3- The cell counter tool (Plugins, Analyse, cell counter) was used to count squares containing cilia (Figure 3.3, below) in a manner similar to the method of counting cells using a haemocytometer (e.g. the cilia that appear on the upper and right side edges of squares were counted, whereas cilia that appear on the lower and left side edges of squares were not counted).

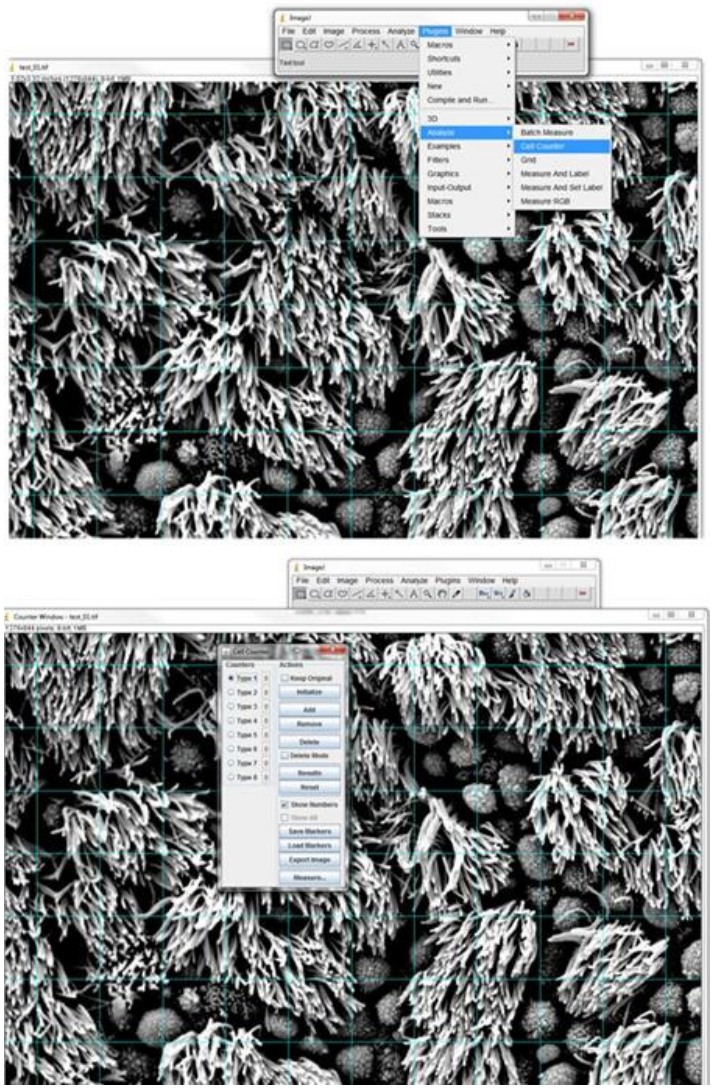

Figure 3.3 Screenshot of SEM image with image J. Following grid apply, cell counter plugin selected and initialize and type 1 cell option was used for counting cilia-containing squares.

4- Finally the percentage of ciliary coverage was calculated as:

$$\text{Cilia coverage } \% = (\text{number of ciliated squares})/(\text{totel number of squares }) * 100$$

There are two common methods usually used to estimate ciliary abundance from SEM images. The more traditional method is based on an observer estimate of the cilia and uses a scale that divides the cilia coverage of the surface into three categories: images with ciliated area more than 75%; those with coverage 50-75%; and those with coverage < 50% (Konrad et al., 1995), thus resulting in rough categorical results. The other is a computer-driven, image analysis-based method using commonly available software such as Adobe Photoshop™ (Adobe, USA) to convert grey scale SEM images into binary images followed by thresholding (known as the threshold method and developed by Rankin et al., 2007- see Figure 3.4, overleaf).

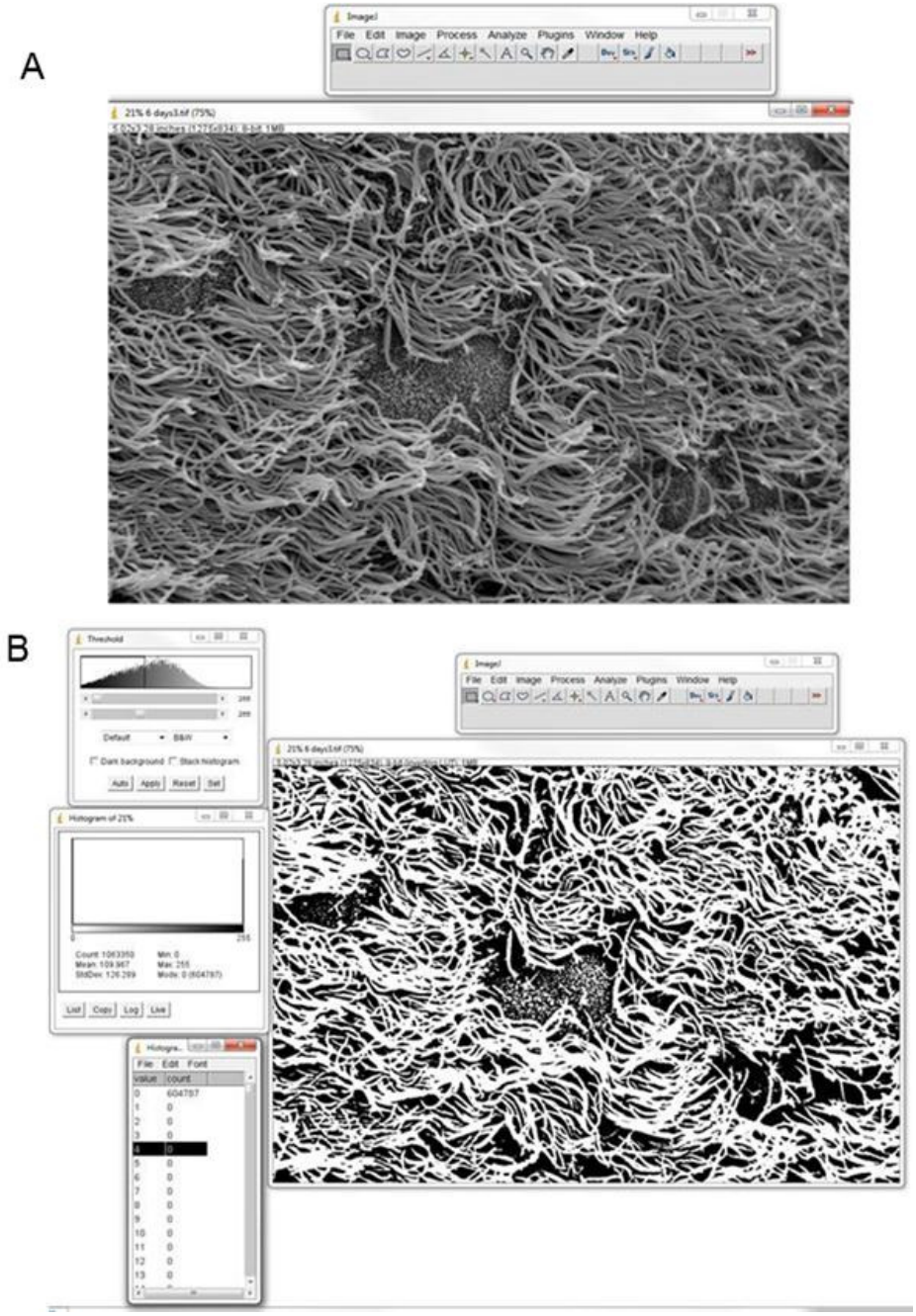

Figure 3.4 Estimation of the ciliary coverage from SEM images of bovine bronchial ciliated epithelium using the threshold method (A) the image before threshold apply, almost full of cilia coverage. (B) after thresholding the image histogram option was used to calculate the cilia cover percentage and found to be 57%, whereas estimated with grid scoring method gave 88% ciliary coverage.

3.2.9 Statistical Analysis

Statistical analysis was performed using Minitab 16 (Minitab Ltd, Coventry, UK). All results are presented as means ± SE. Significance was accepted at $P < 0.05$. Two-way ANOVA was used to analyse data for the effect of hyperoxia on ciliary coverage within time, whereas the antioxidant vitamins treatment data was analysed by one-way ANOVA. A follow up analysis using Fisher's Least Significant Difference (LSD) method was used. Unpaired Student's *t*-test was used to compare between hyperoxia and normoxia ciliary coverage data using two different methods (threshold and grid scoring methods).

3.3 Results

3.3.1 Attempts at producing monolayers of ciliated epithelial cells using culture of primary bovine bronchial cells

Primary bovine bronchial epithelial cells were cultured with the aim of estimating ciliary coverage using SEM and TEM. After three days of culturing on collagen-coated cover slips (see Section 3.2.1), both TEM and SEM images (Sections 3.2.4 and 3.2.5, respectively) showed the formation of an incomplete monolayer. Most of the cells had microvilli with some scattered ciliated cells (Figure 3.5, page 76). Cells could be maintained in culture up to 10 days. The challenge proved to be in

the estimation of the ciliary coverage (which was one of the main objectives of the study), because of the rounded shapes and disorganised interfacing of the cells.

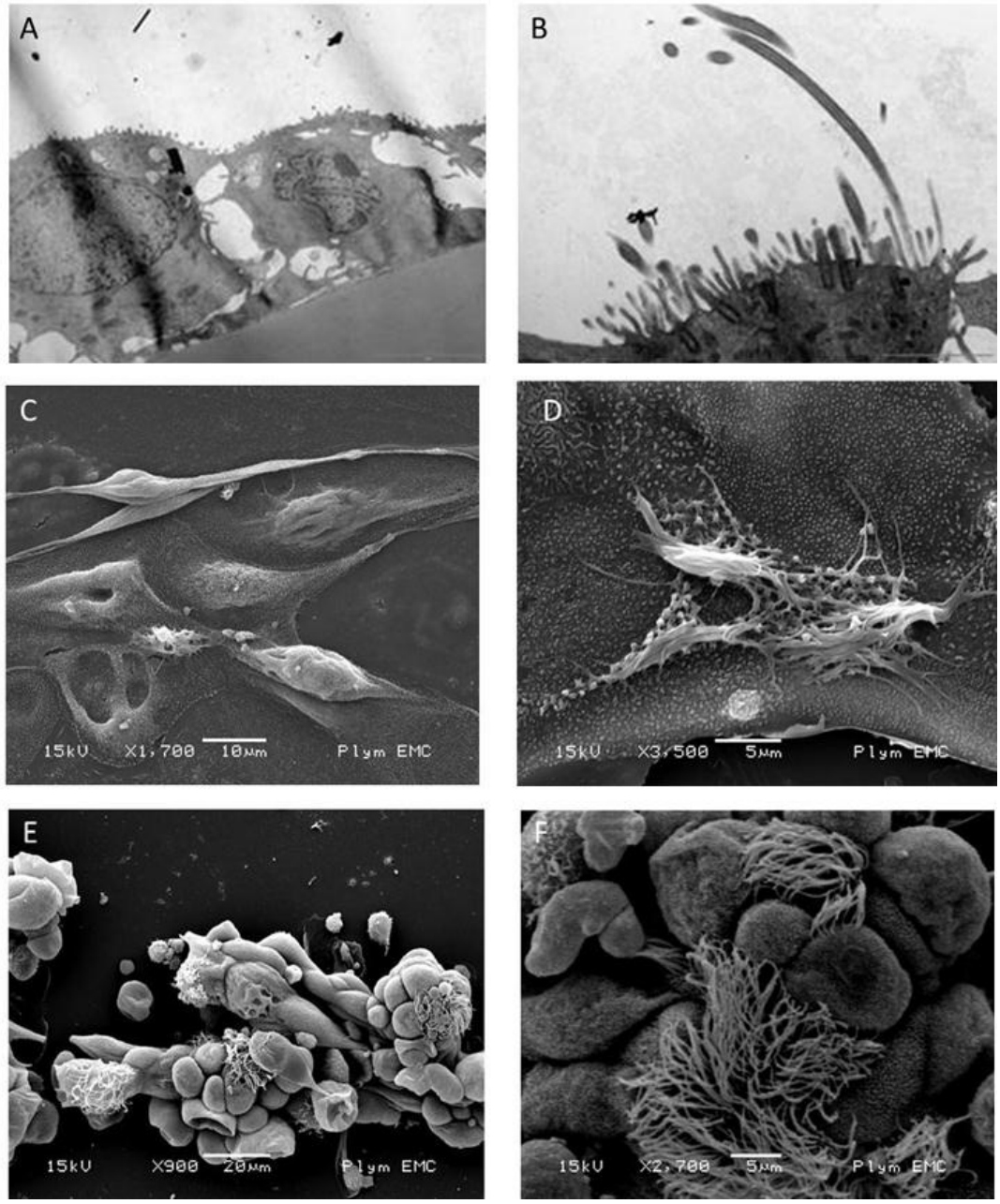

Figure 3.5 Primary bovine bronchial epithelial cells cultured on collagen-coated Thermonax coverslips. (A, B) TEM after 3 days of culture showing cells with growth of microvilli and a few cilia on the apical surface; (C, D) SEM after 3 days of culture; and (E, F) SEM after 10 days of culture (cells appear to be more aggregated); samples from two experiments were used.

3.3.2 Cilial surface identification used fluorescence-labelling/ CLSM

CLSM images for cells cultured for three days showed that although the tomato lectin has been shown to bind effectively to ciliated cells (Toskala et al., 2005), there appeared to be a great deal of non-specific binding i.e. binding of the lectin to other cell membrane components as well as the cilia. The aggregation of the cells tended to emphasise this effect (Figure 3.6, overleaf).

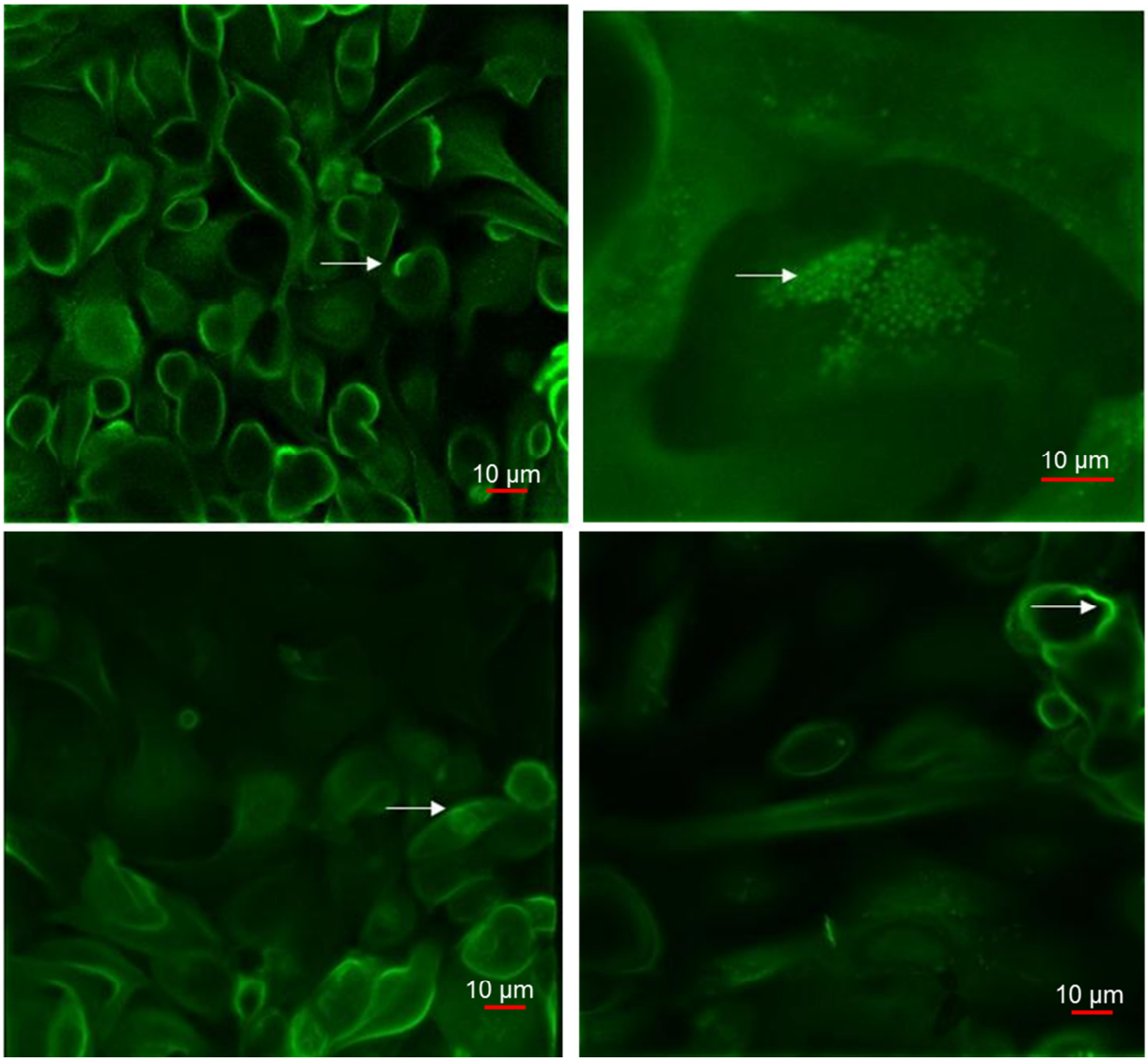

Figure 3.6 Fluorescence labelling of cultured primary bovine bronchial cells with FITC-labelled *Lycopersicon esculentum* lectin. Cells were cultured for 3 days on collagen-coated Petri dishes. Confocal scanning microscopy images (40×) showing cells with an apical ciliated surface (white arrows). Also note the aggregation of cells.

3.3.3. Validation of image analysis methods

The Culturing of bovine bronchial tissue was used to estimate ciliary coverage under hyperoxia. A comparison between the grid scoring method outlined in Figures 3.1-3.3 and the threshold method outlined in Figure 3.4 used in previous studies to estimated ciliary coverage was done to test the validity of the newly developed ciliary coverage estimated method. SEM images from samples exposed to 21% O_2 and 95% O_2 for 6 days were assessed. The measurements using both methods were done on the same images, with the threshold method being used as the standard. The relationships between the % coverage values obtained using the two methods for each set of data were tested using Pearson's correlation (Figure 3.7, overleaf). The results reflect a significant difference between the two methods. For the images of samples exposed to 21% O_2 there was a weak and non-significant positive correlation ($R = 0.060$, $P = 0.711$); a similar result was obtained from the images of samples exposed to 95% O_2 ($R = 0.172$, $P = 0.487$). The % coefficient of variance (%CV) was calculated for each set of data and found to be 3.5% and 10.08% for the 21% and 95% data sets, respectively, using the grid scoring method, while it was 7.6% and 15.9% for the 21% and 95% data sets, respectively using the threshold method.

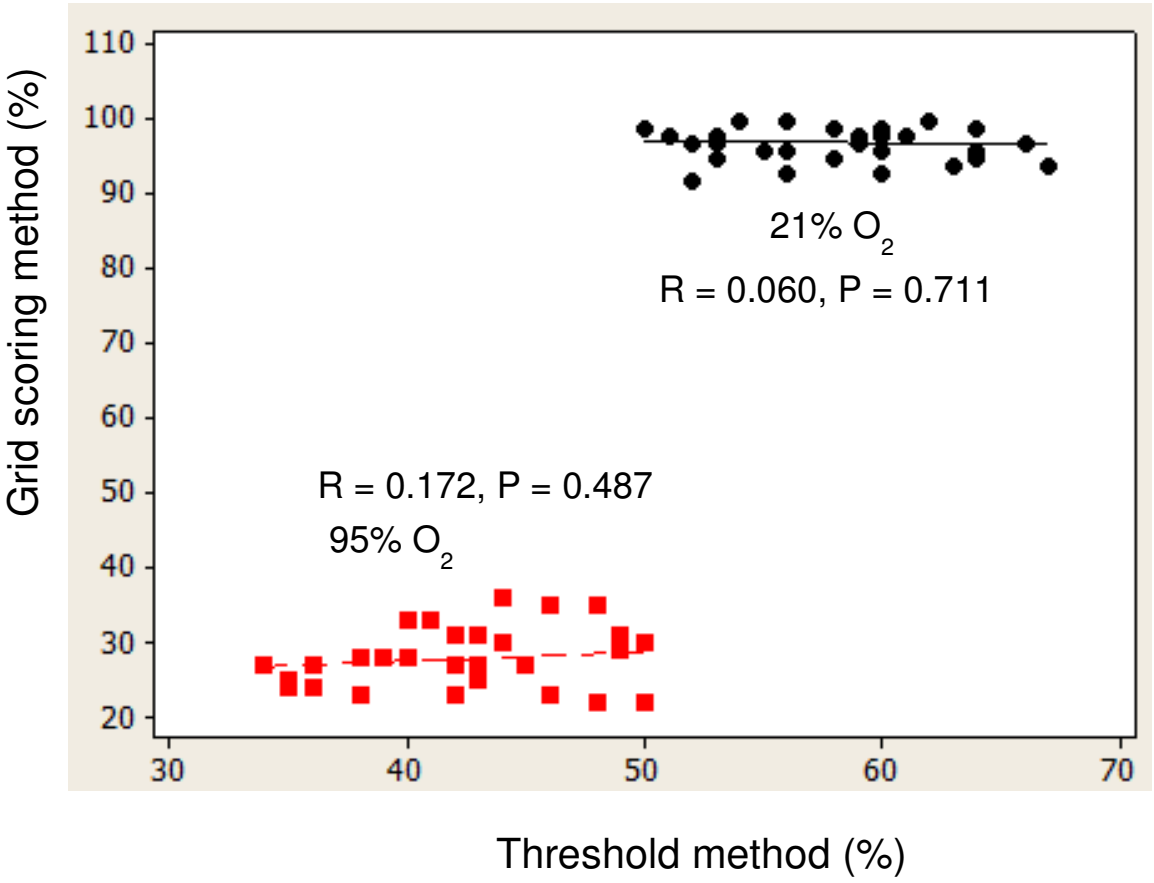

Figure 3.7 Comparisons between the % ciliary coverage obtained using the threshold and grid scoring methods. SEM images of bovine bronchus samples after 6 days of exposure to hyperoxia (red points) and normaxia (black points) as indicated were analysed for % ciliary coverage using both methods, after which Pearson's correlation coefficients were calculated. Samples from three different animals, 3 samples from each animal were used and ten images from each sample were visuals.

3.3.4 Determination of ciliary coverage of bovine bronchial tissue under hyperoxia and normoxia

The ciliary coverage of bovine bronchial tissue samples from three animals was examined using a grid method approach. Upon isolation of the bronchial tissue, ciliary coverage was 100% in all cases. A significant loss of ciliary coverage over time was found on exposure of tissue to 95% oxygen. Ciliary loss became apparent within 48 h of exposure and was progressive throughout the period studied. A highly significant difference ($P < 0.0001$) in ciliary coverage was found in bovine bronchial tissue within hyperoxia and normoxia concentrations and within days between hyperoxia and normoxia (e.g. after the first day of exposure the mean ciliary coverage was 91.10 ± 0.96% under 95% O_2 compared to 97.20 ± 0.62% under 21% O_2, whereas after six days of exposure the mean was 30.45 ± 1.37% under 95% O_2 compared to 90.63 ± 0.89% under 21% O_2) (Figure 3.8, overleaf). The relationship between time and hyperoxia and normoxia was also highly significant ($P < 0.0001$), i.e. there was little loss of ciliary coverage in tissue exposed to 21% O_2 over 6 days.

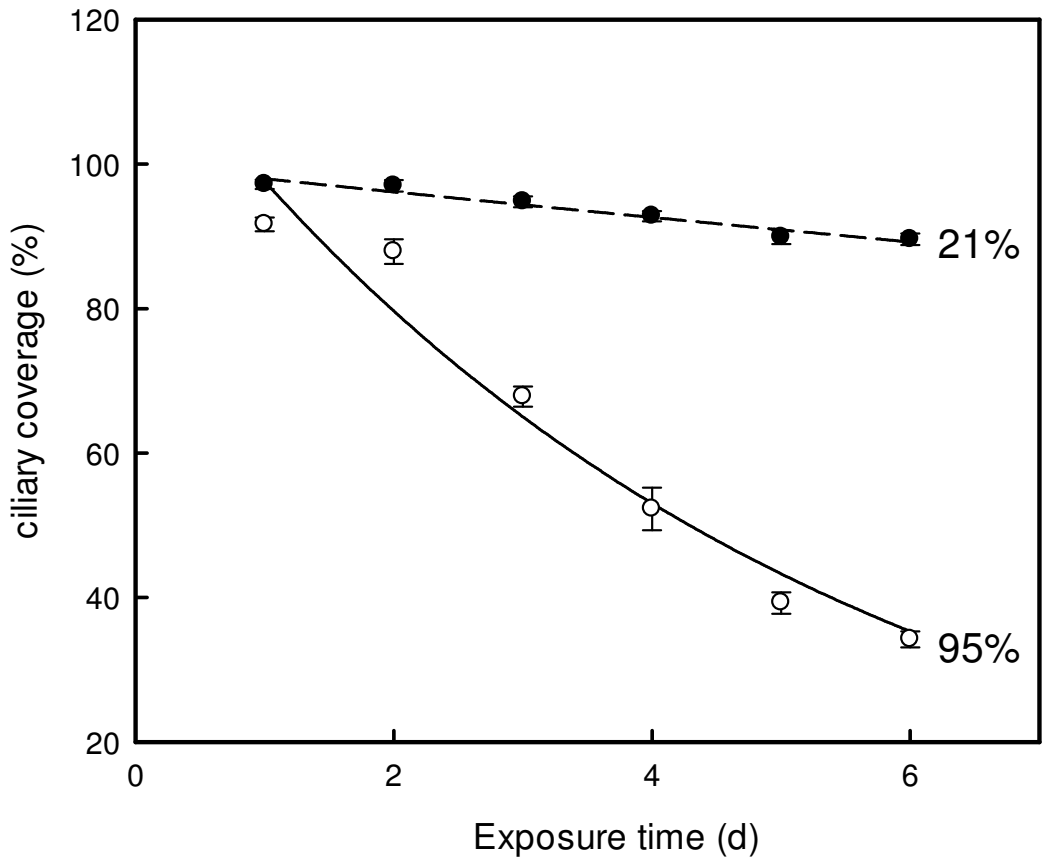

Figure 3.8 Ciliary coverage of cultured bovine bronchus tissue at an air-liquid interface exposed to normoxia (●, 21% O_2) and hyperoxia (○, 95% O_2) for up to 6 days. Data are means ± SE, n = 9; Samples from three different animals, three samples from each animal were used.

3.3.5 Histopathological changes

SEM images showed several histopathological changes induced by exposure to 95% O_2 accompanying cilia coverage loss over time. From the fourth day there was an increase in the appearance of blebs on the surface of the epithelium. Also, an increased number of sloughed cells and partially detached ciliated cells was observed over time (Figure 3.9, overleaf). Likewise the number of cells found in the medium (presumed to have been sloughed from the epithelium either in groups or individually) increased with time. Many of these cells were apparently intact ciliated cells. However, some clearly had abnormal morphology (Figure 3.10, page 85).

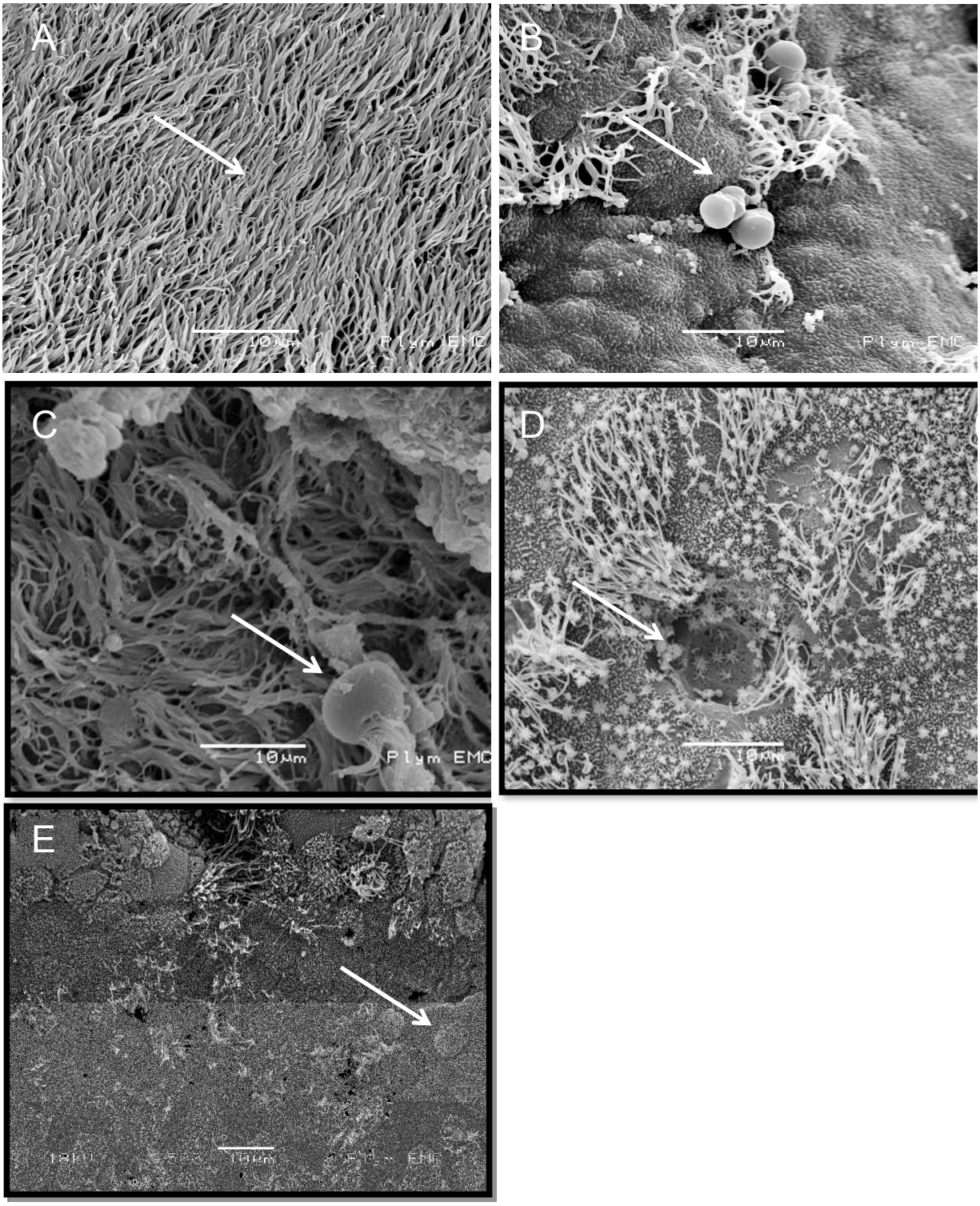

Figure 3.9 SEM images of cultured bovine bronchial tissue exposed to either (A) normoxia (21% O_2) or hyperoxia (95% O_2) for 4 days, where (B) cellular blebbing, (C) sloughing cells, (D) cavities left by sloughing cells and (E) detached cells have been observed. Samples from three different animals, 3 samples from each animal were used and ten images from each sample were visuals..

.

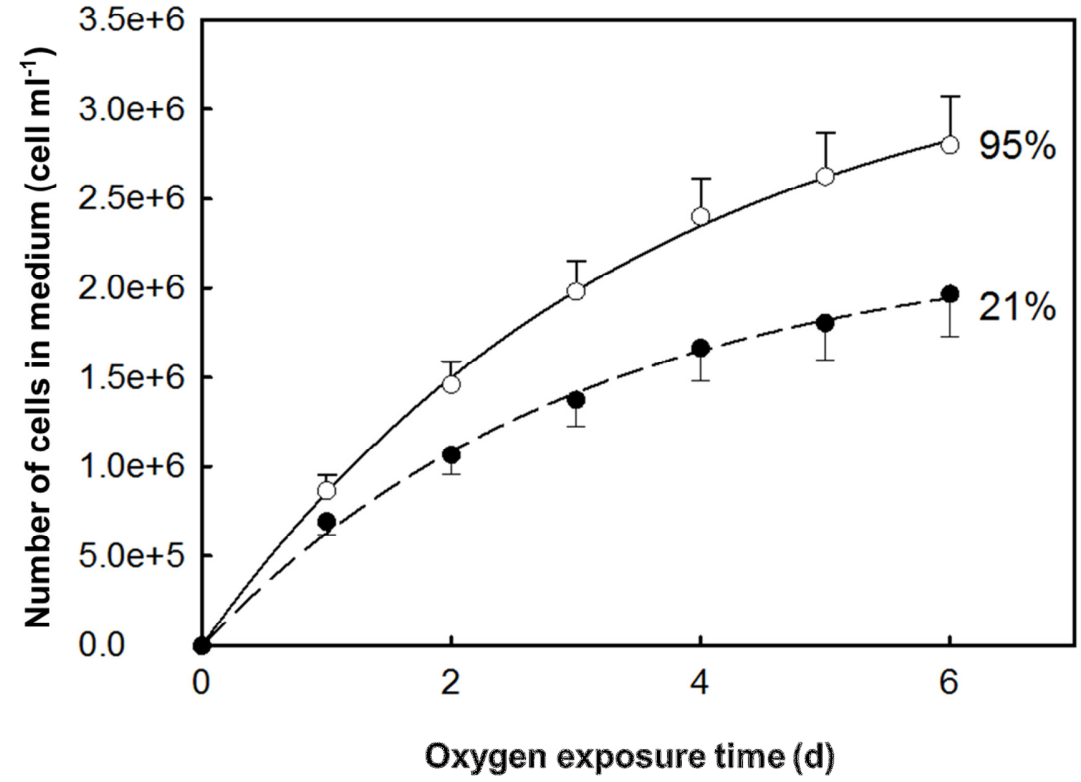

Figure 3.10 Cumulative cell number in the medium from bovine bronchial tissue samples that had been exposed to either normoxia (●, 21% O_2) or hyperoxia (○, 95% O_2). Light microscopy images (×40) showing (A) epithelial cells in groups, or (B) individually in the medium with (C) some abnormal ciliated cells. Data are means ± SEM from triplicate samples from a single animal.

3.3.6 Effects of antioxidant vitamins on the decline in ciliary coverage induced by hyperoxia

To assess the possible protective role of antioxidant vitamins against hyperoxia-induced ciliary coverage loss, the effects of ascorbate and α-tocopherol on bovine bronchial tissue samples exposed to normoxia and hyperoxia for 4 days were investigated. The antioxidant vitamins (ascorbate, 10^{-6} and 10^{-7} M, and α-tocopherol, 10^{-7} M individually or in combination of both antioxidant) provided some protection against hyperoxia. There was a significant difference between tissue samples treated with antioxidants during hyperoxia and those which were untreated (one-way ANOVA, $P < 0.05$) (Figure 3.11, overleaf). However, this protection was at a relatively low level, and there was still a highly significant difference ($P < 0.0001$) in the % ciliary coverage of bronchial tissue exposed to hyperoxia in the presence of the vitamins compared to the normoxia control.

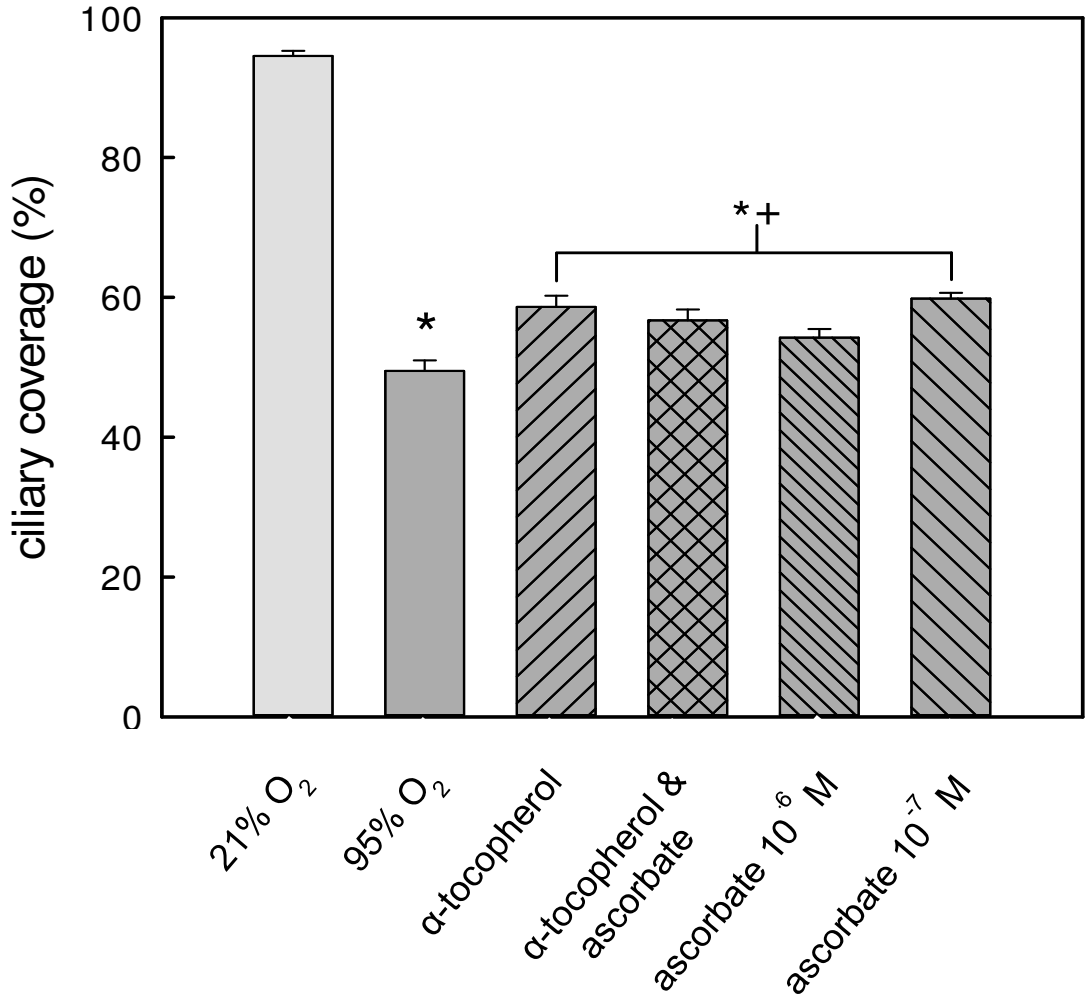

Figure 3.11 Ciliary coverage of cultured bovine bronchial tissue samples exposed to normoxia (21% oxygen) and hyperoxia (95% oxygen) for 4 days and supplemented with ascorbate or α-tocopherol alone, or a combination of both (α-tocopherol, 10^{-7} M and ascorbate, 10^{-6} M see Section 3.2.3). * = Significantly different relative to control ($p < 0.05$), += significantly different relative to 95% oxygen ($p < 0.05$). Data expressed as means ± SEM, $n = 9$**.** Samples from three different animals, three samples from each animal were used.

3.4 Discussion

It is well documented that cilia are crucial for mucociliary clearance (see Chapter one) - damage or loss of cilia and/or ciliated cells, and the consequent effects on mucociliary transport, play a vital role in a variety of pulmonary diseases. The main aim of this study was to establish a primary ciliated epithelial cell model to investigate ciliary coverage under hyperoxic conditions. Primary cell culture is the use of cells isolated freshly from tissue without being transformed to immortalise them. Therefore, they should have the same geno/phenotypes as the cells *in vivo* especially when grown at air-liquid interface (Pezzulo et al., 2011). As described in Chapter one the pseudostratified epithelium lining the airways consists of cells exhibiting mixed phenotypes. Thus primary airway tissue culture might be subject to a variation between individual preparations. For example, in primary tissue culture ciliated cells have been found to be differentially distributed, with a high ciliated cell density in ligament regions (Oliveira et al., 2003). Therefore, an approach using a primary cell line may potentially possess less inherent variability. Another objective of this study was to use fluorescence-labelling to quantify the density of ciliary coverage. It was hoped that this method would represent a simpler and quicker alternative to traditional SEM approaches, particularly, with the successful cultured and differentiated of ciliated cells overtime. Unfortunately, the disorganised manner in which the successfully differentiated cells grew (see Figure 3.5) made accurate optimization of the staining protocol highly challenging. Consequently, until it is possible to develop a suitable method for accurate staining

of cilia associated with differentiated cells, primary tissue culture represents the best option for continuing studies of this type.

An alternative was the use of tissue culture, and hence attempts were made to establish an effective tissue culture model. A bovine bronchus tissue culture model was developed as described in detail in Section 2.2.5 and used to study the effects of high oxygen concentrations on epithelial cells and ciliary coverage. Initially samples started with essentially 100% ciliary coverage and it was to culture the samples successfully for up to 10 d. Despite early issues with mucus and preparation artefacts, these problems were overcome and good quality SEM images were obtained.

The tissue culture method used here has been adapted from previous studies, which used rat trachea and human bronchus tissue culture for the same purpose (Kay et al. 2002, Rankin et al. 2007). the two common methods used to estimate ciliary abundance from SEM images (see Section 3.2.8) including the older of the two methods, which is based on an observer estimate of the cilia and the more recently developed computer-driven, image analysis-based method (threshold method). Both were found to be either difficult to adopt for the bovine tissue samples and somewhat inaccurate as it was difficult to obtain the full procedure used by Rankin and consequently it is possible that the procedure used here might have missed some crucial preparative steps. A simple method for quantifying ciliary coverage, based on blind scoring (blinding the laboratory researcher to sample identity) of images was used because a previously computer-aided method based on thresholding of images of human cilia (Rankin et al. 2007) was found not to be applicable to bovine tissue. This was due to the difference in length observed

between human and bovine cilia (Figure 3.12, page 90). The current method, although simple, provided more detailed information on loss of ciliary coverage compared to methods previously used where images were categorized into broad categories of coverage (such as the method described by Konrad et al. 1995).

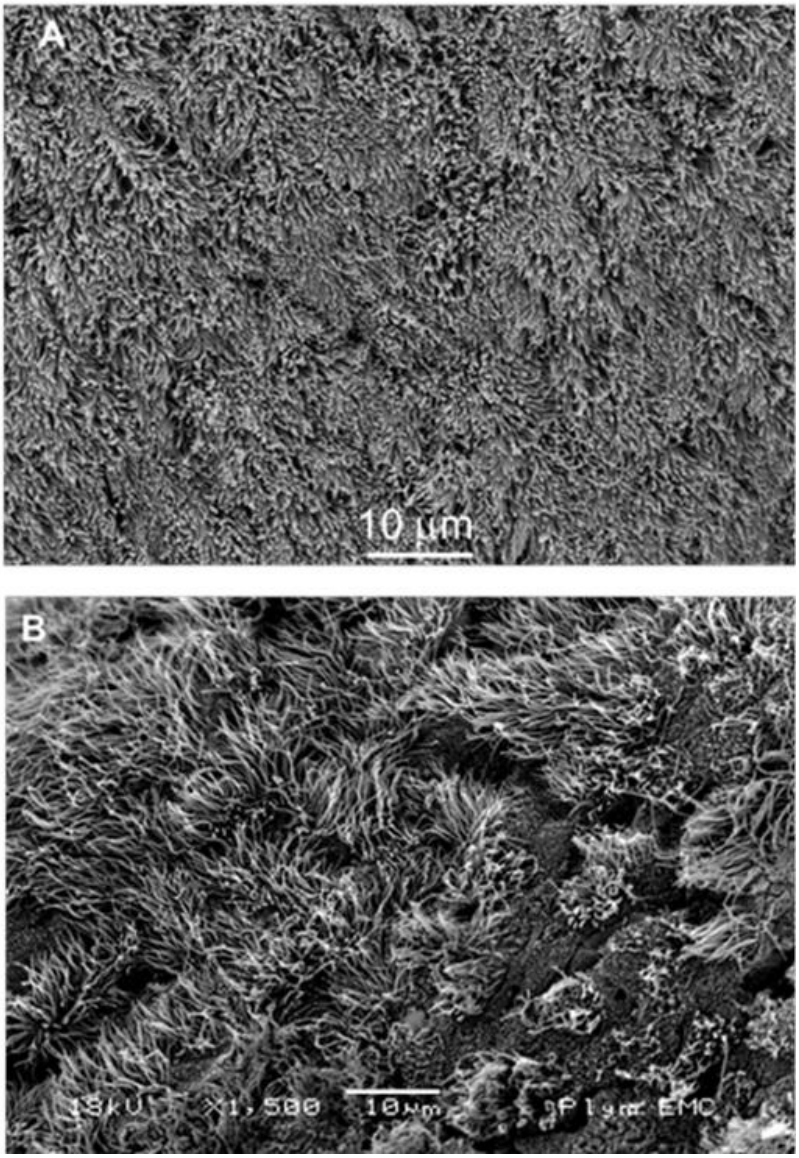

Figure 3.12 SEM images showing (A) bronchus tissue from human bronchus (from Rankin et al., 2007) and (B) bovine bronchus- note the cilia length in each case.

Significant progressive decline in ciliary coverage during exposure to hyperoxia (95% O_2) was found compared to normoxia (21% O_2) (Figure 3.8, page 82), with the observation of some histopathological changes (Figure 3.9, page 84). From the results of this study, (i) the number of cells in each sample used in experiments was estimated to be 8.1×10^5 (based on a surface area of 9 mm^2 for each sample and of 100 μm^2 for each cell); (ii) predicted calculation of the initial rate of cumulative number of cells sloughing to the medium was 9.8×10^5 cells d^{-1} in 95% O_2 and 7.2×10^5 cells d^{-1} in 21% O_2 (thus, the increase in rate of cells sloughing to medium with 95% O_2 was 35% compared to 21% O_2, with most of the cells looking intact); (iii) conversely, by estimated the % ciliary coverage loss d^{-1}, the net rate of ciliary loss was 24.3% d^{-1} with 95% O_2 and 1.9% d^{-1} with 21% O_2, which is equivalent to an initial net rate of cell loss of 1.9×10^5 cells d^{-1} with 95% O_2 and 1.5×10^4 d^{-1} with 21% O_2. From these estimates, the loss of ciliary coverage can be accounted for by modest increase in the rate of sloughing.

Although these results are consistent with others that show the deleterious effects of ROS generated by hyperoxia in the respiratory epithelium, in other studies the emphasis has been on cell death (either by necrosis and apoptosis) rather than sloughing, accounting for this. For example, a reduction in protein synthesis rate and suppression of DNA synthesis accompanied exposure of rats and mice to hyperoxia (Tierney and Hacker, 1989, Konsavage et al., 2010). Cell integrity could be disrupted as a consequence of oxidant injury by hyperoxia, in which apoptosis and/or necrosis and alteration in signal transduction pathway regulated cells death are present in the cells exposed to hyperoxia depending on cells type and density (Petrache et al., 1999, Mantell and Lee, 2000). Nevertheless, the increase in

sloughing cells observed in this study suggested that other mechanisms may be involved in airway epithelium barrier disruption (discussed in detail in Chapter five).

It is important to consider cell turnover during oxidative stress, which in the airway epithelium is estimated to occur at a low level under normal conditions. However, this rate has been found to be rapid, leading to effective restitution after injury (Yahaya, 2012). The regulation of the balance of cell turnover in airway epithelium has been found to be changed via oxidant stress resulting from hyperoxia-induced increase in ROS production (Jyonouchi et al. 1998). Shimizu et al. (1994) demonstrated that within 12 hours, cells from unwounded tissue, flattened and migrated into a wounded site and poorly differentiated cells formed within 24 h. However, the net rate of cell loss under normoxia seen in the present study is much lower than the rate of cell sloughing, which implies that there is a rapid turnover of cells since the majority of those sloughed have been replaced.

There are other mechanisms have been proposed as being involved in cilia damage by hyperoxia. Mitochondria are considered as a major source of ROS (Turrens, 2003), and the large numbers of mitochondria in the ciliated cells, especially near the basal bodies of the cilia, might make ciliated cells particularly prone to oxidative stress. Li et al. (2004) demonstrated that ρ^0 respiration-deficient HeLa cells have more resistance to the damaging effects of exposure to 80% O_2 for 5 days compared to the wild type cells. It has been found that generation of ROS from mitochondria increases linearly with increasing oxygen concentration. However, the release of ROS appears to be biphasic, with significant production occurring when cells are exposed to high oxygen concentration (> 60 %) and lower production when cells are exposed to concentrations below 50 % (Turrens, 2003).

These findings might explain the increase of cell resistance pre-exposed to hyperoxia, through an adaptive increase in antioxidants capacity to compensate for moderate hyperoxia (Haddad, 2002b).

One of the possible pathways that could be affected by oxidative stress and provides a biochemical basis for ciliary ultrastructure abnormality and dysfunction is the impairment of ciliary energetics. The ciliary stroke is determined by ATPases, one of the necessary requirements for ciliary motion. The activity of ATPases is altered by oxidative damage as a consequence of oxidative stress, for example, Ca^{2+}-ATPase inactivation is a result of exposure to H_2O_2 (Zaidi et al., 2003).

With the hypothesis that increase the antioxidant vitamins α-tocopherol and ascorbate supplementation might minimize epithelial cilia loss induced by hyperoxia, the *in vitro* bovine model was chosen as a first study to quantitatively evaluate the vitamin effects. The results indicated a significant difference in ciliary coverage loss between bronchial tissue samples exposed to hyperoxia and those exposed to hyperoxia in the presence of the vitamins. Extracellular oxidants oxidise ascorbate to dehydroascorbate (DHA) which is then able to penetrate cells via the glucose transport facility (Vera et al., 1994) and then be reduced to ascorbate (Nualart et al., 2003). The normal ascorbate plasma concentration is in the range 61.4-80 µM (Schorah et al., 1996). Increases in oxidative stress parameters (e.g. TBARS and carbonyl group formation) have been found to be associated with the low concentration of vitamin C in plasma (< 40 µM), and it has been shown that the raised of vitamin C concentration (> 50 µM) can prevent against oxidative damage (Gey et al., 1993, Panda et al., 2000). Ascorbate protects against oxidative damage in a dose dependent manner and the damage level. Guaiqui et al. (2001)

demonstrated that HL-60 cells preloaded with ascorbate in three different concentrations (25 µM-1mM) protect against H_2O_2, by which cell resistant to damage increased with increasing dose. However, the percentage of the survival cells decreased to the half with a high concentration of H_2O_2 (> 100 µM) and the protection of vitamin C was only modest.

The Recommended Dietary Allowance (RDA) for vitamin E is 15 mg d^{-1} and for vitamin C is 75-90 mg d^{-1}, with these values being raised twofold under oxidative conditions (e.g. smoking) and chronic diseases (Carr and Frei, 1999b). However, it has been shown that increasing the daily consumption of vitamin C to levels of 2000 mg d^{-1} conferred no further protection, suggesting cells were saturated by this point (Johnston and Sarah, 2001). A possible reason is that the plasma and tissue become saturated when the vitamin consumption above 100 mg d^{-1} (Carr and Frei, 1999b, Rumsey and Levine, 1998). There are two possible explanations as to why there were no significant differences in the parameters observed in this study between the various individual ascorbate concentrations or when ascorbate was used in combination with α-tocopherol. Firstly, the cells might be saturated and therefore increasing the vitamin concentration proffered no additional protection and secondly, given that the tissue is disconnected from a blood supply, it could already be deficient in these vitamins and supplementing cells with high vitamin concentrations was not sufficient to provide the protection. One of the limitations of this study is that the concentration of vitamins in the cells was not determined. It has been suggested that O_2^- and H_2O_2 injure cells through generation of more effective oxidizing species such as $OH^\bullet$, O_2^- reduces ferric to ferrous iron which in turn reacts with H_2O_2 to generate $OH^\bullet$ (Farber, 1994). Intracellularly, $OH^\bullet$ is

neutralized by ascorbate generating DHA, where α-tocopherol acts as scavenger of peroxyl radical.

Vitamin E and C have been shown to play a valuable role in reducing cell death due to oxidative injury (Jyonouchi et al., 1998, Perez-Cruz et al., 2003). In addition, vitamin E has been reported to significantly minimize the carbonyl content increase associated with hyperoxia in retinal pigmented epithelial cells (Lu et al., 2006). Moreover, Yamaok et al. (2008) found that exposed mice suffering from severe vitamin E deficiency in response to hyperoxia for 72 h showed significant histological damage and higher IL-6 mRNA expression in lung tissue with a decrease in survival. Thus, they suggested that lack of vitamin E may worsen oxidative damage and lung inflammation. Kc et al. (2005) demonstrated the protective role of vitamin C supplementation against human mitochondrial oxidative damage by which dehydroascorbic acid (the oxidized form of vitamin C) enters the mitochondria and accumulates inside as ascorbate, providing protection against mitochondrial membrane depolarization and DNA damage.α-tocopherol has been suggested as having anti-oxidative properties, through the signaling apoptotic lipid (Sylvester, 2007). Pedeboscq et al. (2012) show that α-tocopherol has inhibitory effect on cytotoxic response in the early steps of cell death by inhibited the staurosporine (PKC inhibitors) induced cell death in different cell line in a dose depend manner. They also found that other ROS scavenging antioxidants including trolox, NAC and propofol had no inhibition effects of staurosporine -induce cell death.

Chapter 4: Hyperoxia-induced oxidative damage in bovine bronchus tissue culture

4.1 Introduction

Several *in vivo* studies have shown that exposure to hyperoxia causes pulmonary failure, cell death and tissue damage, and inflammation within 48-72 h (Crapo et al., 1980, Olivera et al., 1995). The types of injury observed in animal lungs following exposure to hyperoxia are found to be similar to those in acute respiratory distress syndrome patients and are characterised by epithelial and endothelial cell apoptosis and necrosis (Zaher et al., 2007). Evidence for this comes from markers of oxidative stress e.g. protein oxidation, lipid peroxidation and DNA damage. The production of ROS during exposure to elevated oxygen fractions is believed to be responsible for the injury that appears in the lungs or in cultured cells (Freeman and Crapo, 1982, Mach et al., 2011). The increase in ROS production can stimulate other responses involved in cell pathogenesis e.g. the up-regulation of vascular adhesion molecules leading to the recruitment of phagocytic cells into the lung and consequent inflammation (Brueckl et al., 2006).

Studies have documented the effects of oxygen on the main antioxidant enzyme activity and regulation including the glutathione system (i.e. glutathione reductase, glutathione peroxidase and total glutathione level) in the respiratory tract epithelium (Freeman et al., 1986, Housset et al., 1991, Ho et al., 1996). A study by Pietarinen-Runtti et al. (1998) determined the effects of hyperoxia on the levels of several antioxidants in a BEAS-2B human bronchial cell and the results indicated significant cell injury after 72 h of exposure, with an increase in LDH release and

an increase of 55-58% in the total glutathione level in cells exposed to hyperoxia compared with the control cells.

Another effect of ROS exposure is lipid peroxidation, which has been studied in detail through epithelial cell behaviour *in vivo* and *in vitro*. Lipid peroxidation can lead to other cellular effects such as alteration in membrane receptors, impaired membrane permeability, increased membrane solidity and decreased activity of membrane-bound enzymes, all of which contribute to disruption of membrane function (Sarma et al., 2010). Studies have demonstrated that the elevation of lipid peroxidation contributes to airway epithelial diseases such as asthma and chronic obstructive pulmonary diseases (COPD) (Wood et al., 2003, Paredi et al., 2000).

Protein modification is another major effect of excess ROS generation. For example, an *in vivo* study conducted in this context showed that oxidative protein damage could affect the activities of the DNA repair enzymes in epithelial cells (Wiseman and Halliwell, 1996). Furthermore, *in vitro* studies have established that generation of ROS affects the function of redox-sensitive proteins that act as components of a large sub-membranous signaling complex, thus obstructing cellular signaling mechanisms (Cosentino-Gomes et al., 2012, Thannickal, 2003).

With regards to DNA damage, *in vitro* studies have shown that the frequency of mutation is greatly increased by exposure of DNA to ROS which can result in cancer development (Wiseman and Halliwell, 1996), possibly via mechanisms involving the loss of wild type oncogenes (alleles) which correspond to mutant normal cellular genes (proto-oncogenes) (Cerutti, 1994). Panayiotidis et al. (2004) have shown that hyperoxia increases single and double strand breaks and

decreases DNA methylation in the A549 lung cell line. In an *in vivo* study, it has been found that Type II alveolar epithelial cells showed DNA oxidation and fragmentation induced by hyperoxia that correlated with time even though the cells remained morphologically intact and viable (Roper et al., 2004).

Having established the bovine bronchial tissue culture model (see Chapter 3), the objective of this study was to further elucidate the mechanisms involved in oxygen toxicity to bovine bronchial tissue. Although many studies have focused on understanding the DNA damage caused by hyperoxia in alveolar endothelial and epithelial type cells, to our knowledge, this is the first study that shows hyperoxia-induced DNA strand breaks in bronchial epithelial tissue culture using single cell gel electrophoresis (comet assay).

4.2 Materials and Methods

4.2.1 Sample collection, dissection and culture

All samples of bovine bronchial tissue were collected, dissected and cultured as outlined in Section 2.2.1

4.2.2 Oxygen exposure

Samples of bovine bronchial tissue were cultured and exposed to normoxia or hyperoxia as described in Section 2.2.6

4.2.3 Determination of lactate dehydrogenase (LDH) activity

Lactate dehydrogenase (LDH) activity is widely used to determine levels of cell damage, by which LDH is released into the medium following cell membrane leakage or rupture. In this study, LDH that had been released into the culture medium was measured as described by Bergmeyer and Bernt (1974). Culture medium was collected in 1.5 ml Eppendorf tubes and placed in ice prior to processing. Reaction mixture (240 µl), containing 5 mg sodium pyruvate and 1.2 mg NADH (Melford Laboratories Ltd., Ipswich, UK) in 10 ml of 50 mM sodium phosphate buffer (pH 7.5), was added to 60 µl samples of medium in a 96 well plate. The oxidation of NADH was monitored by measuring the absorbance at 340 nm for 15 min in a plate reader (VersaMax^{TM}, Molecular Devices, Sunnyvale, CA). Measurements were carried out in triplicate. Enzyme activity was calculated using an extinction coefficient of 6.3 mM^{-1} cm^{-1} using the equation:

$$\text{Activity } (\mu mol^{-1}\ min^{-1}\ ml^{-1}) = \frac{A_{340}\ min^{-1}\ (sample) - A_{340}\ min^{-1}\ (blank)}{\sum \times Ve} \times Va \times DF$$

Where Va: total volume of assay (ml), DF: dilution factor, $\sum$: molar extinction coefficient of NADH at 340 nm (6.3 mM^{-1} cm^{-1}), Ve: volume of enzyme solution (ml)

4.2.4 Detection of lipid peroxidation

The thiobarbituric acid reactive substance (TBARS) assay has been used widely to assess levels of lipid peroxidation as a consequence of oxidative stress (Ohkawa et al., 1979). Tissue was chopped into small pieces (about 1-2 mm), and homogenized using a Potter homogenizer at a ratio of 1 g of tissue to 4 ml of RIPA buffer (50 mM Tris-chloride, pH 7.6, containing 150 mM NaCl, 0.1% SDS and 1% Triton X-100). The homogenates in 1.5 ml Eppendorf tubes were then centrifuged at 13,000 *g* for 10 min at 4 ℃. Ice-cold 10% TCA 1:1 was added to the supernatant and the mixture centrifuged at 13,000 *g* for 5 min at 4 ℃. Supernatant was then mixed 1:1 with of 0.67% (w/v) thiobarbituric acid in 1.5 ml Eppendorf tubes. The mixture was incubated at 80 ℃ for 30 min, and after cooling 290 µl was transferred to a 96-well plate. The absorbance was then measured at 532 nm using a plate reader (VersaMax^{TM}, Molecular Devices, Sunnyvale, CA). The concentration of malondialdehyde (MDA) was determined by reference to a standard curve produced using 0-50 µM 1,1,3,3-tetramethoxypropane (Figure 4.1, overleaf). Measurements were carried out in triplicate.

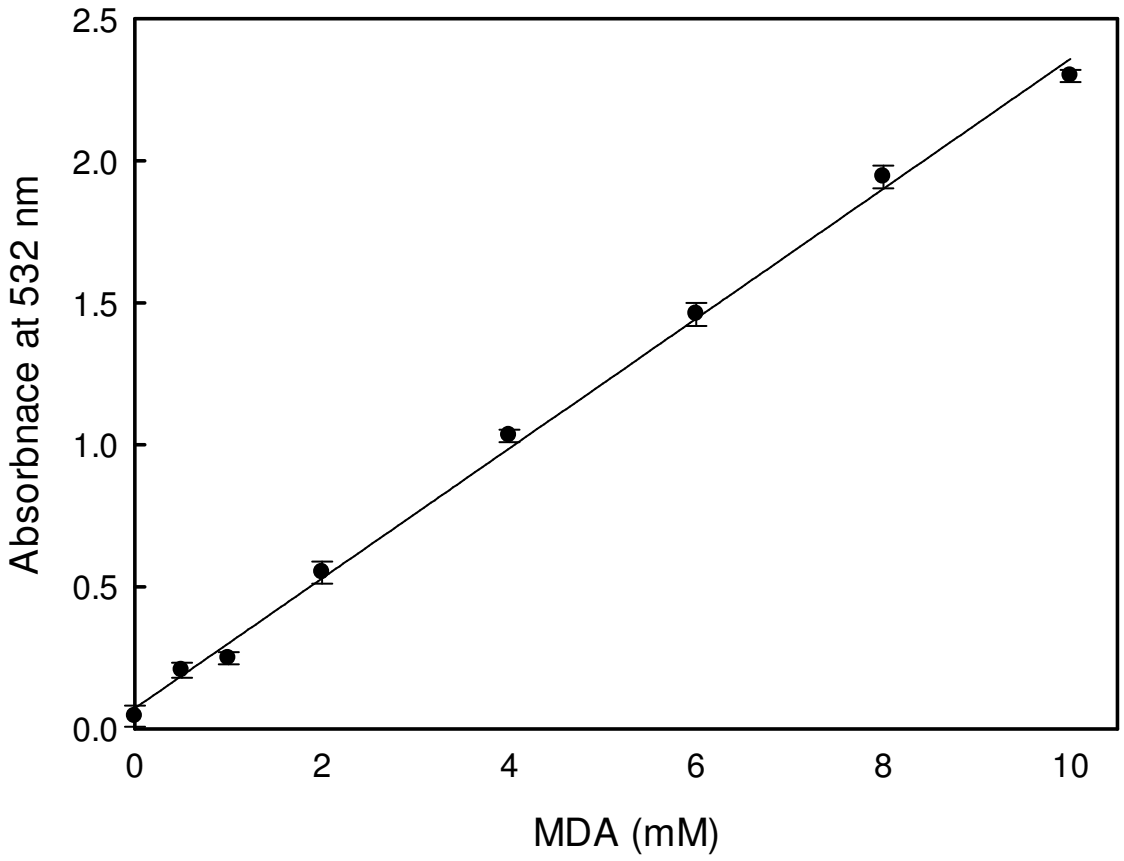

Figure 4.1 Standard curve for the thiobarbituric acid reactive substance (TBARS) assay, obtained using 1,1,3,3-tetramethoxypropane. Results are means ± SEM, *n* = 3. MDA = malondiadehyde.

4.2.5 Determination of total glutathione

Total glutathione was determined using a method based on that of Owens and Belcher (1965). Epithelial tissue was separated from the cartilage tissue below, weighed, chopped into small pieces (1-2 mm) and homogenized using a Potter homogenizer with a ratio of 1 g of tissue to 4 ml of homogenization buffer (250 mM Tris-chloride, pH 7.4, containing 1 mM EDTA). The homogenate was centrifuged in 1.5 ml Eppendorf tubes at 13,000 *g* for 10 min at 4 ℃, after which the supernatant was mixed 1:1 with DTNB solution (100 mM potassium phosphate, pH 7.4, containing 10 mM DTNB and 5 mM EDTA) and placed on ice until use. The assay mix was prepared by mixing 0.6 U of glutathione reductase (Sigma G-3664 from *Saccharomyces cerevisiae*) with the assay buffer. Samples (40 µl) were transferred to a 96-well plate, followed by addition of 210 µl assay mix. After equilibration for 1 min the reaction was started by adding 60 µl of 1 mM NADPH (Melford, Ipswich, UK) dissolved in assay buffer and the absorbance recorded at 412 nm over 5 min using a plate reader (VersaMax^{TM}, Molecular Devices, Sunnyvale, CA). In each run there was a blank (buffer) and a standard (20 µM reduced glutathione) to calibrate the results. Samples were measured in triplicate and total glutathione was calculated as:

$$\text{Total glutathione (µmol/g wet weight)} = \frac{\text{A412 (sample)} - \text{A412 (blank)}}{\text{A412 (standard)}} \times 20\ \mu M \times DF$$

where, DF = dilution factor and ΔA = the rate of change of absorbance.

4.2.6 Detection of DNA strand breaks using the comet assay

Single-cell gel electrophoresis (SCGE) or the 'Comet assay' is a technique used to detect DNA damage in individual cells, where the DNA is electrophoresed in an agarose gel. Damaged nuclear DNA appears with a comet-like tail while the undamaged nuclear DNA has a circular shape (Kumaravel et al., 2009).

4.2.6.1 Cell preparation

Epithelial cells lining the bronchial tissue were collected as a pellet in 50 ml centrifuge tube after digestion in MEM containing 0.1% bacterial protease (Sigma P8811, from *Streptomyces griseus*) as described in Section 2.2.3 for 30 min, and a small sample (50 µl) was placed in a 1.5 ml centrifuge tube containing 50 µl of 10% Trypan blue stain (Sigma, Poole, UK), gently mixed by pipetting and transferred to a Neubauer haemocytometer to assess cell viability and to count the cells as outlined in Section 2.2.4. Cell viability was > 90% throughout. The remaining cells were used to determine DNA damage using the comet assay as follows.

4.2.6.2 Preparation of slides

Superfrost™ microscope slides (Fisher Scientific, Loughborough, UK) were fully coated with a thin layer of 1% normal gelling temperature agarose, and left for 24 h to air dry before sample loading. Cells (10^5 slide^{-1}) were mixed with 180 µl of 0.5%

low-melting agarose (LMP) and two drops (75 µl each) applied to the pre-coated agarose slide, covered with a coverslip (20 mm^2) and placed at 4℃ for 10-15 min to allow the agarose to set.

4.2.6.3 Cell lysis, unwinding and electrophoresis

Immediately before use, 1% Triton X 100 and 10% Dimethyl Sulphoxide (DMSO) (were added to chilled (4 ℃) lysis buffer containing 2.5 M NaCl, 100 mM EDTA and 10 mM Tris base, pH 10. This was then poured into a pre-chilled staining (Coplin) jar. Coverslips were gently removed and the slides with embedded cells placed carefully in the jars, and immersed in the lysis buffer for at least 1 h at 4 ℃. Slides were then placed in a horizontal electrophoresis tank (Pharmacia Biotech, UK) and incubated with electrophoresis buffer (containing 0.3 M NaOH, 1 mM EDTA, pH ≥ 13) for 40 min to allow unwinding of DNA before electrophoresis at 25 V for 30 min at 4 ℃.

4.2.6.4 Neutralization, staining and visualisation

Following electrophoresis, the slides were carefully placed in a staining jar and washed with distilled water for 5 min at 4 ℃. Neutralization was carried out by immersing slides in 0.4 M Tris-chloride buffer, pH 7.5, (three times, 5 min each, at 4 ℃). Slides were left to air dry and 20 µl of 0.05 mg $ml^{-}1$ ethidium bromide was applied to stain the DNA, after which they were covered with coverslips (VWR Ltd., U.K.). The slides were visualized using fluorescence microscopy (Leica DMR,

excitation wavelength 510 nm/ emission wavelength 590 nm). Komet 5.0 image analysis software (Andor Technology plc, Belfast, UK) was used to score comets from individual cells for % tail DNA. For each slide, 100 nuclei slide^{-1} (50 in each agarose gel drop) were scored.

4.2.7 Determination of total protein oxidation

As a consequence of protein oxidation, carbonyl groups are formed on the side chains of some amino acid residues (Stadtman and Levine 2003). An OxyBlot kit from Chemicon International (Millipore S7150) was used to detect protein carbonyl content as a marker of oxidative stress. The assay is based on the generation of dinitrophenylhydrazones (DNP) from the derivatization of the carbonyl groups by 2,4-dinitrophenylhydrazine (DNPH), followed by detection of DNP-labelled proteins by western blotting.

4.2.7.1 Preparation of oxidised protein for use as a positive control

Bovine serum albumin (BSA) (10 mg ml^{-1}) was treated with $FeCl_3$/ascorbate buffer (25 mM HEPES, pH 7.2, containing 100 µM $FeCl_3$ and 25 mM ascorbate) for use as a positive control. The BSA was incubated in the buffer at 37 ℃ for 5 h before being dialyzed with 50 mM HEPES containing 1 mM EDTA. The oxidized protein was split into aliquots and stored at -20 ℃. Cellulose membrane dialysis tubing used was prepared following the manufacturer's instructions (Sigma aldrich, U.K.).

Briefly, the tubes were washed with water before being rinsed with 0.3% sodium sulphide solution at 80 ℃ for 1 h to remove sulphur compounds. Tubes were then washed for 2 min with hot water, and then washed with 0.2% sulphuric acid solution and finally rinsed with hot water before use.

4.2.7.2 Protein extraction and carbonyl group derivatization

After gently separating the epithelial tissue from the cartilage located beneath using sterile scissors, the epithelium was chopped into small pieces (1-2 mm) and homogenized using a Potter homogenizer (5 passes) in lysis buffer (50 mM Tris-chloride, pH 7.4, containing 1 mM EDTA, 1% Triton X100, 50 mM DTT and 20 µl ml^{-1} protease inhibitor cocktail (Roche 1836153; one tablet/10 ml of reconstituted inhibitor solution) The proteins (5 µl) were denatured by adding an equal volume of 12% sodium dodecyl sulphate (SDS) followed by derivatization of the carbonylated proteins with DNPH solution (solution containing 2,4-dinitrophenylhydrazine in 2 M hydrogen chloride) where the 2,4-dinitrophenyl (DNP) groups formed. For the negative control, the DNPH solution was substituted using derivatization-control solution containing hydrogen chloride (by which carbonyl groups in the proteins skip the derivatization step and hence no DNP groups are formed). Treated samples, and both positive (Section 4.2.7.1) and negative controls were incubated for 15 min at room temperature before adding the neutralization solution provided with the Oxyblot kit. Samples were stored at 4 ℃ before being subjected to sodium dodecyl sulphate-polyacrylamide gel electrophoresis (SDS-PAGE) and western blotting on the following day as described in Sections 4.2.7.3 and 4.2.7.4.

4.2.7.3 Preparation of SDS-PAGE

SDS-PAGE was performed according to Laemmli (1970). A 12% acrylamide solution was freshly prepared (3.5 ml of distilled water, 2.5 ml of 1.5 M Tris-chloride, pH 8.8, containing 0.4% SDS and 4 ml of 30% acrylamide/ bis-acrylamide) and 50 µl of 10% fresh ammonium persulphate (APS) and 5 µl of TEMED were immediately added before the mixture was poured into a mini gel kit glass plate assembly (Small mighty II, USA). The glass plates had been cleaned with 70% ethanol and allowed to dry before use. To give a flat top to the gel, a layer of water was carefully added on the gel surface. The mixture was incubated for 30 min at room temperature to allow time for to polymerization. The stacking gel mixture (2.3 ml of distilled water, 1 ml of 1 M Tris-HCl, pH 6.8, containing 10% SDS, and 0.67 ml of 30% acrylamide/ bis-acrylamide, followed by addition of 30 µl of 10% APS and 5 µl of TEMED as mentioned above) was then added after the water had been poured off and a comb placed carefully at the top of the stacking gel. The mixture was left for 30 min at room temperature to polymerize. After polymerization, the glass plate assembly was clamped tightly to the apparatus, which was then transferred to the electrophoresis tank. Electrophoresis running buffer (0.025 M Tris, 0.19 M glycine, 3.5 mM SDS, pH 8.3) was added to cover the top of the gel before the comb was removed and the wells rinsed out using a Pasteur pipette. The tank was then filled with the desired running buffer volume. Samples were thawed at room temperature and 50 µg of carbonyl proteins mixed with 20 µl of loading buffer (1 ml of 0.5 M Tris- chloride, pH 6.8, 0.8 ml glycerol, 16 ml of 10% SDS and 0.32 ml 0.05% bromophenol blue plus 4.18 ml distilled water). Samples

of the positive (Section 4.2.7.1) and negative controls were also prepared in the same way before loading into the gel. Standard DNP-labelled proteins (5 µl), provided with the kit, were mixed with 20 µl of loading buffer containing 50 mM DTT. Gels were run at 200 V for 45-50 min until the blue tracking dye reached the end of the gel. Gels were carefully removed from the glass plates and electroblotted as described in Section 4.2.7.4, below.

4.2.7.4 Western blotting

Polypeptides from SDS-PAGE gels prepared as described in Section 4.2.7.3 above were transferred to polyvinylidene difluoride (PVDF) membranes (Millipore Ltd, Watford, UK), following the manufacturer's procedure. Prior to blotting, the membrane was activated by immersion in methanol for 15 s, then double distilled water for 2 min and finally in blotting transfer buffer (12 mM Tris, 96 mM glycine, pH 8.3, and 20% methanol) for 5 min. Meanwhile, the blotting apparatus was placed on a tray and the sandwich prepared as follows. A foam pad soaked with transfer buffer was placed first, then a layer of soaked filter paper, followed by the gel which had been soaked in transfer buffer for 5 min. The PVDF membrane was then placed carefully on top of the gel and the bubbles removed. The membrane was covered with another piece of soaked filter paper and a second foam pad then laid over the filter. The apparatus containing the sandwich was clamped tightly together and transferred to the blotting tank filled with pre-cooled transfer buffer (4 ℃). An ice pack was used to keep the buffer cold and gels were blotted at 100 V for 35-40 min. Following blotting, the membrane was placed in blocking buffer

(containing PBS plus 0.05 Tween-20 (PBS-T) and 1% BSA, pH 7.4) for 1 h at room temperature (protein side up) with gentle shaking. The membrane was then incubated overnight with the first antibody, rabbit anti-DNP (1:150) (diluted in blocking buffer immediately before use) at 4 ℃. The membrane was then washed with PBS-T buffer three times (5 min each), and incubated with the second antibody, HRP-conjugated goat anti-rabbit IgG (1:300 dilution in blocking buffer), for 1 h at room temperature followed by washing three times with PBS-T. The membrane was carefully drained and immediately developed using enhanced chemiluminescence reagent (Geneflow, 20-500-120), which was prepared according to the manufacturer's instructions just before use. The membrane was incubated with the chemiluminescence reagent for 1 min at room temperature and placed on a plastic sheet where any underlying bubbles were removed before visualization under a UVP Bioimaging system. The intensity of the chemiluminescence relating to the levels of oxidised protein was analysed using ImageJ (http://rsbweb.nih.gov/ij/).

4.2.7.5 Estimation of total protein in tissue extracts

The total protein content was evaluated using a bicinchoninic acid (BCA) assay kit (Pierce, product NO. 2161297A), according to the manufacturer's microplate protocol. The working reagent (200 µl, prepared by mixing BCA reagent A with B at of 50:1 part respectively) was added to 25 µl samples. The plates were incubated at 37℃ for 30 min then plates were allowed to cool to room temperature. Samples protein concentrations were determined by calibration against standard curve were

2 mg ml^{-1} bovine serum albumin (BSA) stock was used to prepare serial dilution of 0.025-2 mg ml-^{1} (Figure 4.2, below). All samples and standards were used in triplicate in 96 well plates and the absorbance was measured at 562 nm using a plate reader (VersaMax^{TM}, Molecular Devices, Sunnyvale CA).

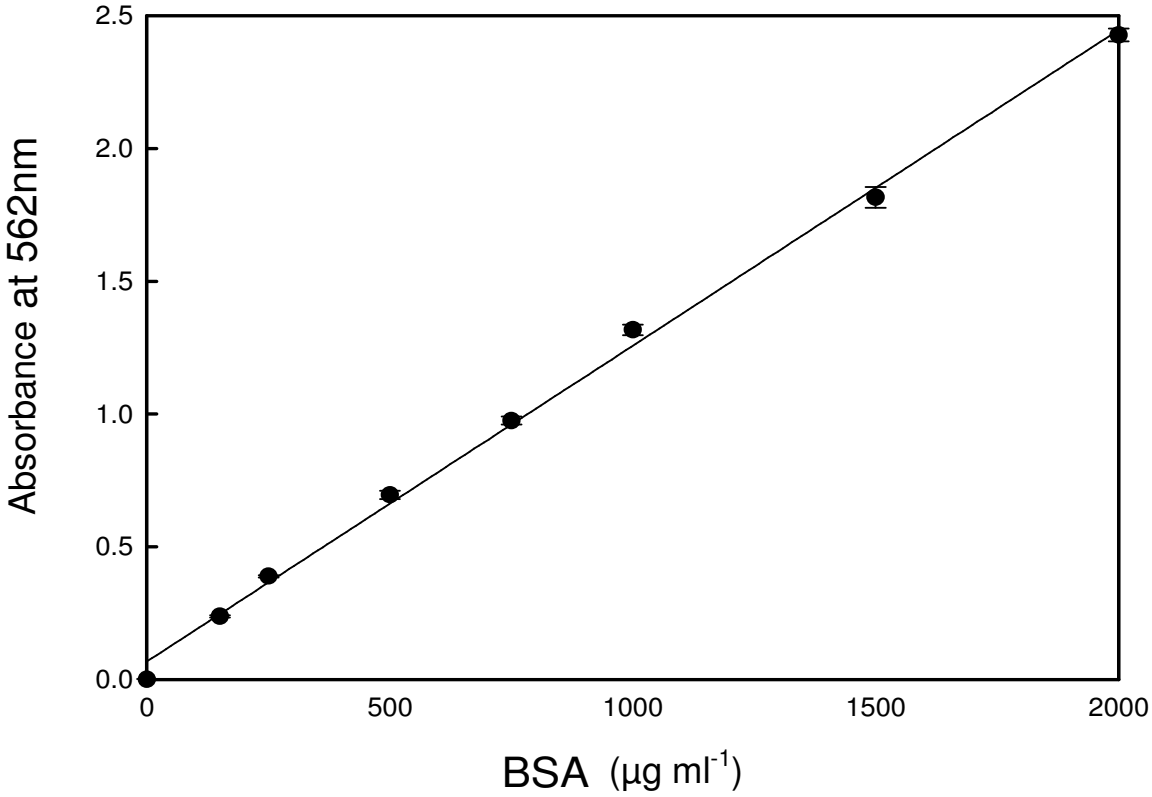

Figure 4.2 Calibration curve for the determination of protein using bicinchoninic acid (BCA) reagent. Results are means ± SE; measurements are in triplicate for each concentration used.

4.2.8 Statistical analyses

Statistical analyses were carried out using Minitab 16 (Minitab Ltd, Coventry, UK). Results are presented as means ± SEM and $P < 0.05$ was accepted as significant. Significant differences were determined between groups using two-way analysis of variance (ANOVA) following by Fisher's Least Significant Difference (LSD) method to analyse LDH data, whereas other data were analysed using unpaired Student's *t*-tests.

4.3 Results

4.3.1 Effect of hyperoxia on lactate dehydrogenase release from bovine bronchial tissue

During the exposure of bovine bronchial tissue, samples of culture medium were collected daily and assayed for lactate dehydrogenase (LDH) activity. In all cases the LDH activity in the medium decreased over time (Two-way ANOVA, $P < 0.001$ between days). However, the cumulative LDH release was much greater for tissue exposed to hyperoxia compared to tissue exposed to normoxia (Two-way ANOVA, $P < 0.01$ between treatments; Figure 4.3, overleaf). After exposure for one day, LDH activities were 0.24 ± 0.03 µmol min^{-1} ml^{-1} and 0.27 ± 0.02 µmol min^{-1} ml^{-1} in samples exposed to 95% and 21% O_2, respectively, whilst at the end of the sixth

day of exposure, LDH activity levels were 0.14 ± 0.01 µmol min^{-1} ml^{-1} and 0.05 ± 0.01 µmol min^{-1} ml^{-1}, respectively.

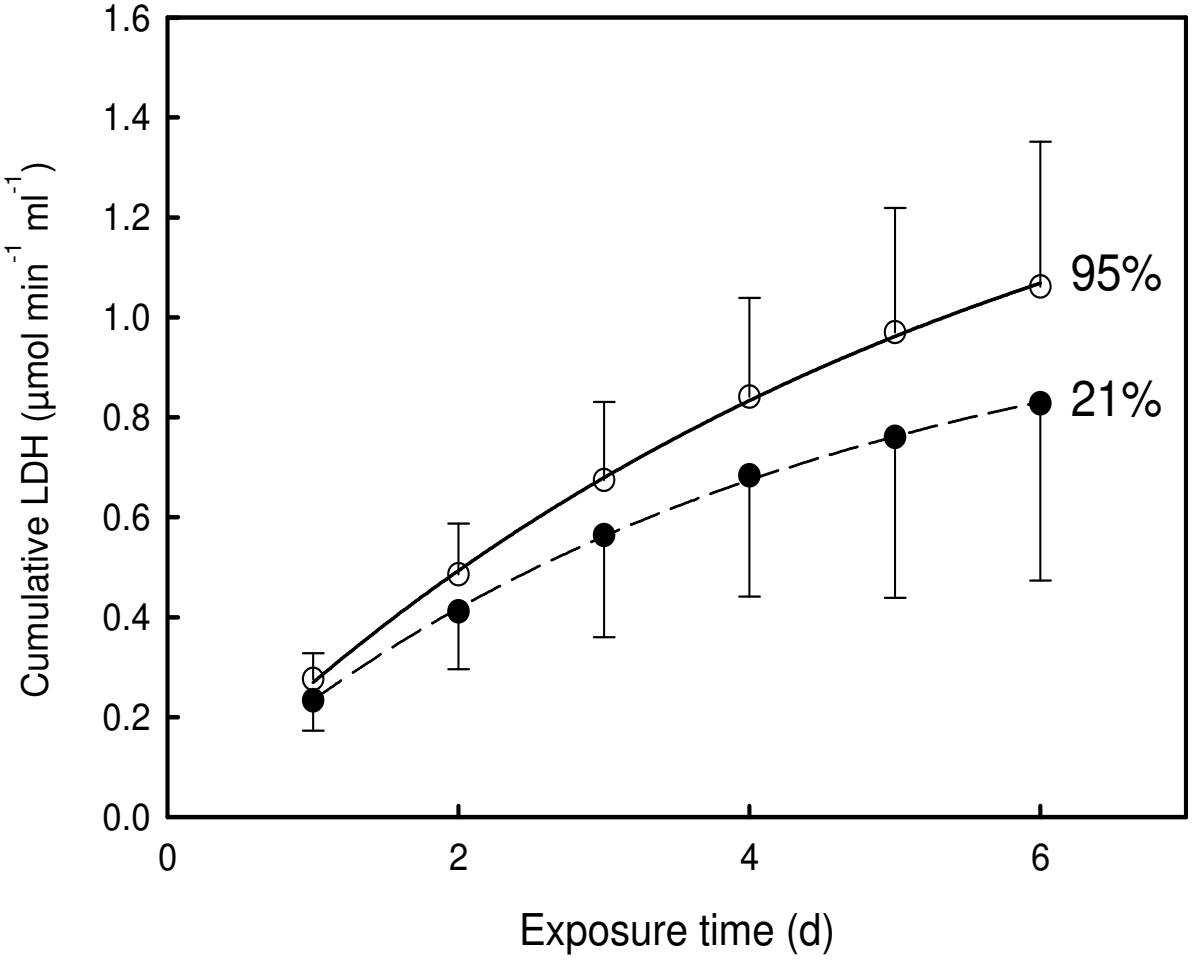

Figure 4.3 Cumulative LDH activity in the medium from bovine bronchial tissue samples exposed to either normoxia (●, 21% O_2) or hyperoxia (○, 95% O_2). Data are means ± SE, from triplicate samples from three different animals, *n* = 9. Samples from three different animals, three samples from each animal were used.

4.4.2 Detection of lipid peroxidation induced by hyperoxia

After four days of culture of the bovine bronchial tissue, samples were homogenised and after centrifugation extracts were used for the measurement of TBARS. There was a significant increase (*t*-test, $P < 0.05$) in MDA in bronchial tissue exposed to hyperoxia (351.9 ± 16.3 µmol g^{-1} wet weight tissue) compared to tissue cultured under normoxia (247.4 ± 10.8 µmol g^{-1} wet weight tissue) (Figure 4.4,below).

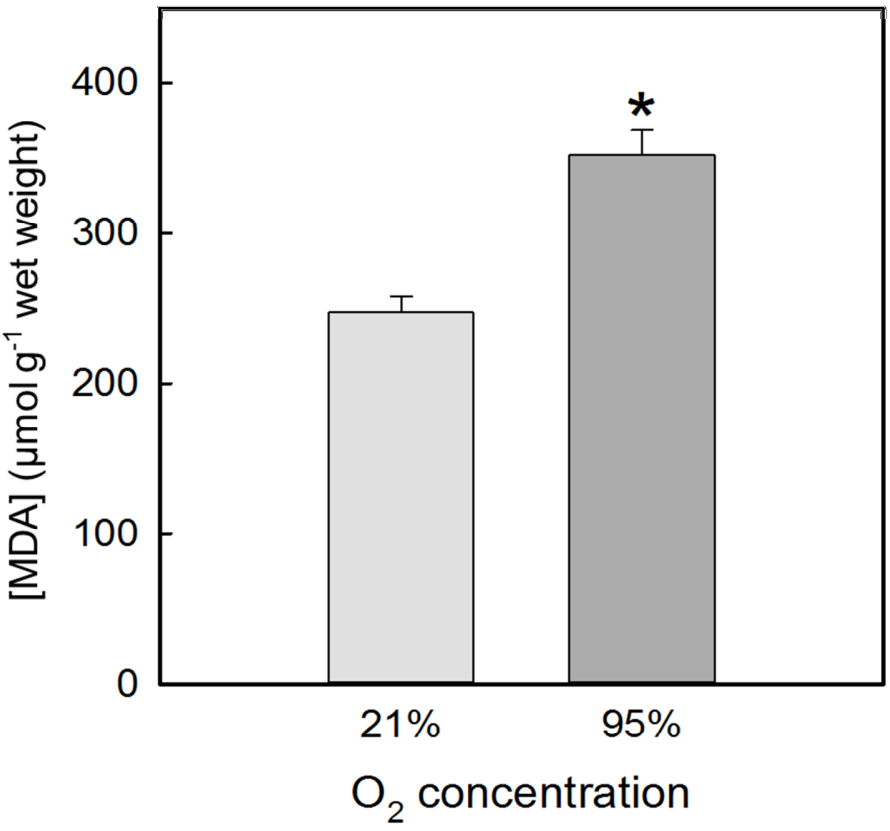

Figure 4.4 lipid peroxidation in extracts of homogenised bovine bronchus tissue cultured for four days under normoxic and hyperoxic conditions. Data are means ± SE, from triplicate samples from three different animals, *n* = 9. Samples from three different animals, three samples from each animal were used.

4.4.3 Detection of DNA damage using the comet assay

Alkaline Single-Cell Gel Electrophoresis (SCGE) or the comet assay was used to quantify hyperoxia-induced DNA oxidative damage after four days of culture. For each treatment 500 nuclei/ animal were analysed from five slides, i.e. 100 nuclei slide^{-1}. A marginally significant increase ($P = 0.048$) in DNA strand breaks was observed under hyperoxia (% tail DNA = 18.7 ± 2.2) compared to normoxia (11.1 ± 1.5) (Figure 4.5, overleaf).

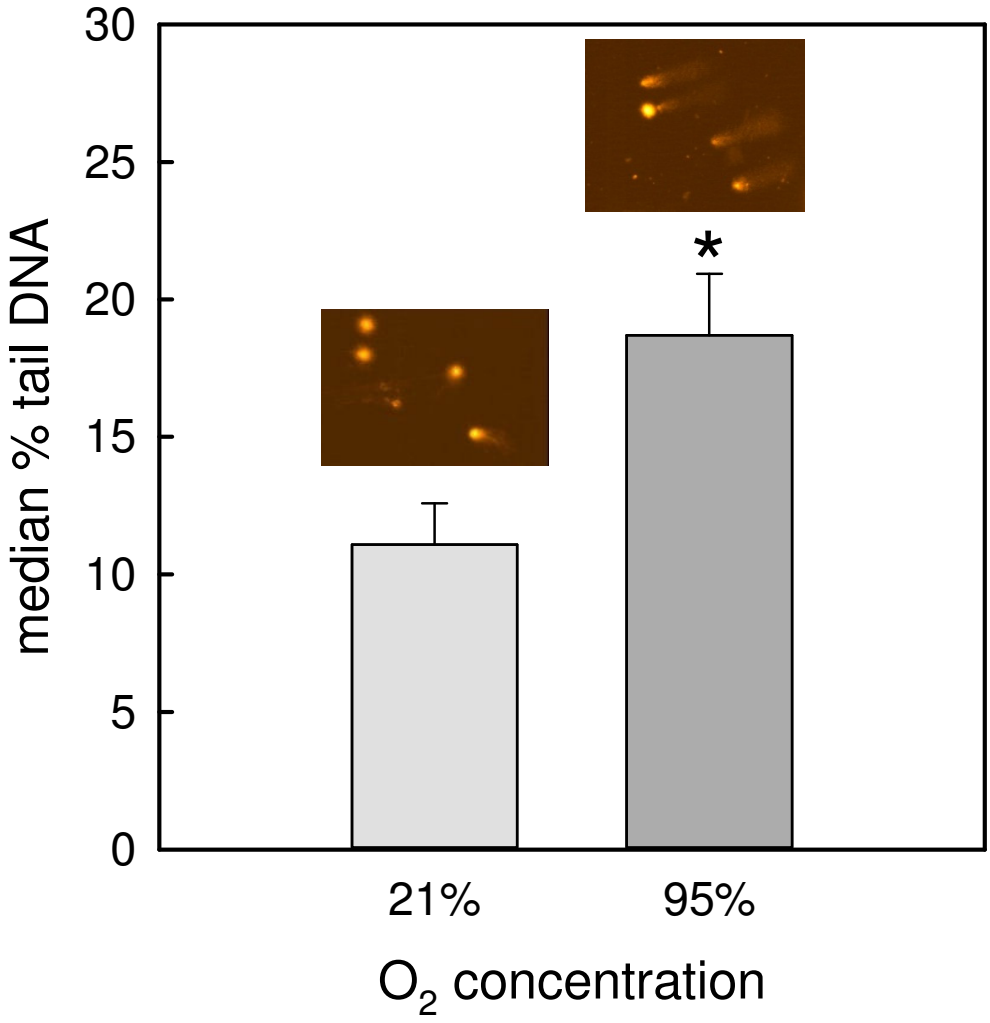

Figure 4.5 DNA damage (% tail DNA) in cells isolated from bronchus tissue exposed to hyperoxia and normoxia. Cells were released from the tissue by incubation with protease, and then the level of DNA damage was assessed using the comet assay. Data are means ± SE; samples from three different animals were used and 500 nuclei from each animal were scored. Inset: example comet images showing increased levels of comet DNA under hyperoxia (damaged) compared with undamaged DNA under normoxia. * = significant differences relative to control, ($p < 0.05$). $n = 9$.

4.4.4 Determination of protein oxidation

The levels of oxidized proteins were assessed in extracts from the bronchial epithelial tissue samples exposed to hyperoxia for four days, using the OxyBlot Protein Oxidation Detection Kit. In this assay, protein carbonyls are detected on immunoblot after derivatization. Oxidised protein bands were observed in the range 43-68 kDa (Figure 4.6A, below). There was a significantly higher level of protein carbonyls in samples exposed to hyperoxia ($P < 0.05$) compared to normoxia (Figure 4.6B, overleaf).

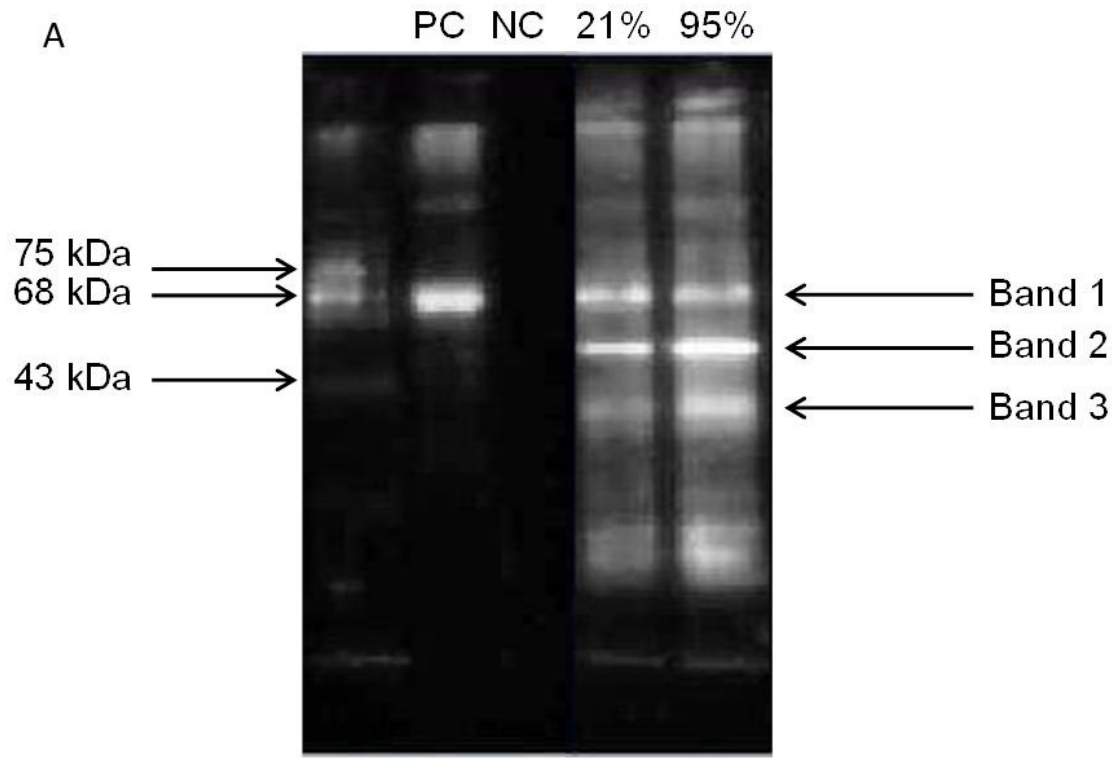

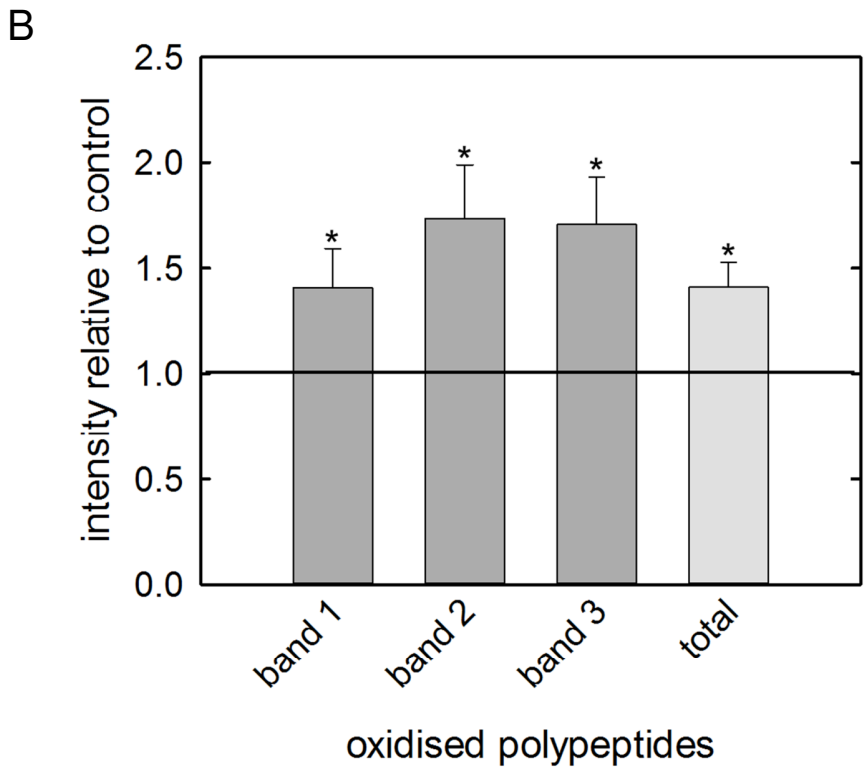

Figure 4.6 Immunoblotting assay of protein carbonyl groups as a marker of oxidative damage to polypeptides in extracts from bovine bronchial samples exposed to normoxia (21% O_2) or hyperoxia (95% O_2). (A) representative immunoblot of a 12% polyacrylamide gel, where PC = positive control and NC =negative control (see Materials and Methods, section 4.2.7.3), and concentration of O_2 is as indicated. (B) Fluorescence intensity relative to the control (black line at 1.0), quantified using ImageJ. Bands 1-3 refer to the prominent bands on the blot (labelled in A), whereas 'total' refers to the total fluorescence intensity from all bands. Data in B are means ± SE, *n* = 9. * = significant differences relative to control blots ($p < 0.05$). Samples from three different animals, three samples from each animal were used.

4.4.5 Effect of hyperoxia on total glutathione in bovine bronchial tissue

There was a significant increase (P< 0.05) in total glutathione in samples exposed to hyperoxia (228.9 ± 19.9 µmol g^{-1} wet weight tissue) compared to samples exposed to normoxia (188.6 ± 14.6 µmol g^{-1} wet weight tissue) (Figure 4.7, below).

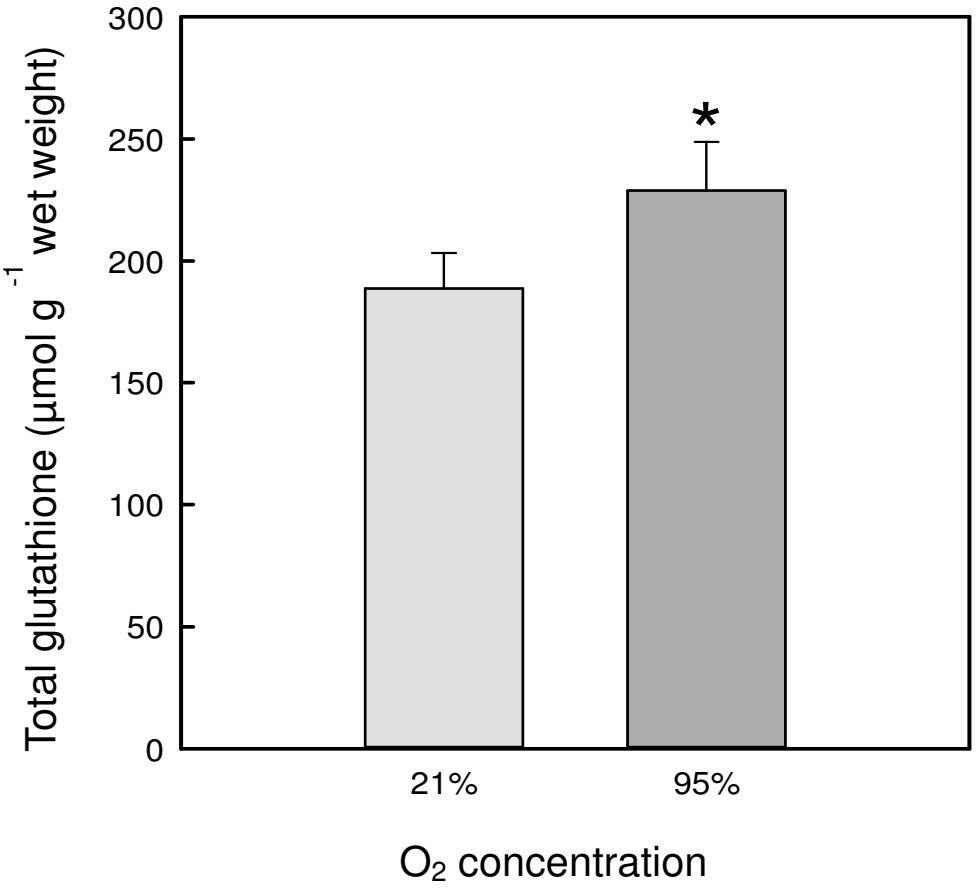

Figure 4.7 Total glutathione in extracts of homogenised bovine bronchus tissue. There is a significantly higher level of glutathione in tissue exposed to hyperoxia. Data are means ± SE, *n* = 9. Samples from three different animals, three samples from each animal were used. * = Significantly difference relative to control (p < 0.05).

4.5 Discussion

Increased levels of reactive oxygen species (ROS) including free radicals, and resultant oxidative stress and damage, have been implicated in many pulmonary diseases (Wright et al., 1994). Oxidants induce both biochemical and morphological alterations via oxidation of cellular components. Our results indicate that hyperoxia (95% O_2) induces bronchial epithelial tissue oxidative stress and consequent oxidative damage over time, as (i) the cumulative LDH level in the medium was significantly higher from the third day of exposure to hyperoxia (Figure 4.3, page 113), (ii) there was significant elevation in the level of lipid peroxidation in cultured bovine tissue exposed to 95% O_2 (Figure 4.4, page 114), (iii) a significant increase in tail DNA in epithelial cells was found after exposure of bovine tissue to hyperoxia (Figure 4.5, page 1116), (iv) a significant increase in protein oxidation under was seen under hyperoxic conditions (OxyBlot kit was used to determine the protein carbonyl levels; Figure 4.6, page 118) and (v) total glutathione levels were significantly higher after treatment of bovine tissue with hyperoxia compared to normoxia (Figure 4.7, page 119).

The findings of this study are in accordance with the study by Alttas and Al-Said (2010), who found that elevated ROS levels were associated with elevated extracellular LDH levels in rats after exposure to hyperoxia and that the antioxidant capacity was reduced. The higher level of LDH released from epithelial cells under hyperoxia confirms the cytotoxicity of prolonged exposure which may result in necrosis. Also, hyperoxia has been suggested to be pro-apoptotic and the

mechanism that leads to epithelial cell death is in part, apoptotic- these findings confirm the suggested concept that hyperoxia activates both necrosis and apoptosis cellular death pathways (Wang et al., 2003, De Paepe et al., 2005). Chambellan et al. (2005) demonstrated that hyperoxia-induced alveolar epithelial cell death was via a mitochondrial-dependent apoptotic pathway by the activation of Bax at the mitochondrial membrane site in response to increased ROS production, and that over expression of Bcl-x provided protection against cell death. Other studies have suggested that mitochondria increase the production of ROS during hyperoxia, for example, although respiration deficient Hela cells decreased the production level of ROS under hyperoxia compared with the wild-type; however, cell death can be observed (Li et al., 2004). Also, manganese-superoxide dismutase (MnSOD) over expression in animals has been shown to give mild protection against hyperoxia-induced lung injury, while CuZn-superoxide dismutase (CuZnSOD) over expression animals has been shown to give a higher level of protection (Ho et al., 1997). These results suggest that hyperoxia-induced cell death requires the generation of ROS from mitochondrial and cytosolic sources.

A time-dependent increase in the cholesterol/ fatty acid ratio in the cell membrane, as a result of oxidative stress, has previously been found in human U87 (glioblastoma) cells cultured under hyperoxia, and this in turn affected the properties of the membrane leading to the formation of membrane blebs (D'agostino et al., 2009). The ubiquity of lipids in cells and the ease of their peroxidation can lead to loss of cell function through changes in membrane fluidity and weakening of cellular compartmentation. These changes can lead to altered membrane receptor mobility, and could lead to leakage of intracellular enzymes

(Shapiro et al., 1989). Hence, the increase in lipid peroxidation seen here could account for the elevated LDH levels in the medium seen after exposure to 95% O_2.

It is commonly recognized that for significant DNA damage to occur, ROS have to overwhelm the intracellular antioxidant capacity (Halliwell and Aruoma, 1991). ROS-induced DNA damage can lead to either strand breaks or base modifications. There are two general mechanisms by which oxidative stress can lead to DNA damage, these being either (a) formation of $OH^{\bullet}$ from the reaction of H_2O_2 with metal (Fe and Cu) ions that are bound to the DNA (Halliwell and Aruoma, 1991) or (b) activation of nucleases that lead to DNA strand breaks (Birnboim, 1988). Both types of damage have been detected in lung cells as a consequence of exposure to hyperoxia. (Barker et al.2006, Roper et al. 2004). A study by Chambellan et al. (2006) suggested an inhibition of DNA transcription and replication resulting in a decline in cell phosphorylation status and subsequent protective growth factor detention in human bronchial epithelial cell line exposed to hyperoxia. Other studies have reported that cells exposed to hyperoxia may block the G1 to S phase checkpoint progression in the cell cycle via an increase in P21 cyclin-dependent kinase inhibitor (CDK), thus causing retardation of the cell cycle (Barazzone et al., 1998, Helt et al., 2004). Cell cycle retardation may give more time for repair from hyperoxia-induced damage, and therefore avoid the replication and possible mutation.

Oxidative damage in cells can also lead to protein modification (Wright et al., 1994), and this has been considered as one of the key mechanisms of hyperoxia-induced lung damage (Freeman et al., 1982). During oxidation the side chains of proline, arginine, lysine and threonine can be modified to incorporate aldehydes or ketones

(carbonyl groups). A series of papers by Davies (Davies, 1987a, Davies et al., 1987b, Davies et al., 1987c) has described the major oxidative modifications of proteins, and the cell damage that follows. Also, modification of tyrosine (carbon 3) by oxidative stress has been suggested as another explanation of protein modification (Narasaraju et al. 2003). There are two possible mechanisms of protein nitration: the formation of peroxynitrite ($ONOO^-$) or the oxidation of NO by myeloperoxidase and the formation of nitrite (NO_2^-) as a result, which is able to nitrate tyrosine residues in proteins (Radi, 2004). Lamb et al. (1999) have detected increased levels of nitrotyrosine in bronchial epithelial cells after 72 h of hyperoxia exposure. Nitration of several proteins in the 29-66 kDa range was observed, in particular, SP-A and t1α surfactant protein in hyperoxic rat lung tissue (Narasaraju et al., 2003).

Glutathione concentration in the airway epithelial fluid is about 100-fold higher than the concentration in extracellular fluid associated with other epithelial tissues (van Klaveren et al., 1997), clearly showing the importance of glutathione in antioxidant defence in lung tissue. The finding herein that glutathione level significantly increased under hyperoxia is in accordance with the study by Pietarinen-Runtti et al. (1998) in which glutathione levels significantly increased after 24-48 h of hyperoxia exposure in BEAS-2B bronchial epithelial cells. However, responses of the glutathione system and the enzymes involved in glutathione metabolism vary between different pulmonary diseases (Comhair and Erzurum, 2002). For instance, glutathione peroxidase (GPx) activity has been shown to be increased in chronic beryllium disease patients, whilst there was a contrasting decrease in smokers and no change in asthma patients (Comhair and Erzurum, 2002). Other studies also

show variations in cells and species in cysteine and cystine transport (Bannai, 1984, Bukowski et al., 1995). Several *in vitro* studies of human airway epithelial cell lines (e.g. A549, 16HBE14o-, NCI-$H_2$92) have demonstrated increased intracellular glutathione levels under hyperoxia. This increase may be due, at least in part, to increases in glutamylcysteine ligase (γ-glutamylcysteine synthetase) levels (Rahman et al., 2001). In contrast, other studies have suggested that increases in glutathione are not essential for defence against hyperoxia; Ho et al. (1997) reported that glutathione peroxidase deficient mice do not have increased sensitivity to hyperoxia.

One of the common features here is suggesting the mechanism of the involvement of H_2O_2, which is required for the lipid peroxidation and probably for the DNA damage detected by comet assay, and it is the ROS species that glutathione protects against. The rate of H_2O_2 generation has been reported to increase 10-fold with 100% O_2, with linear increase from 0-60% O2 followed with a more rapid rate of increase up to 100% O_2 (Turrens et al., 1982).

Chapter 5: Hyperoxia-induced barrier permeability dysfunction in 16HBE14o- cell line

5.1 Introduction

Tight junctions (TJ) are junctional protein complexes that help seal the spaces between cells to form a primary barrier to paracellular transport (Schneeberger and Lynch, 1992). TJs containing a number of proteins including occludins, claudins, junction adhesion molecules and membrane associated proteins (Balda and Matter, 2008). They segregate the apical and basolateral membrane domain surfaces to provide cell polarity, by which the movement of proteins and lipids from apical to basolateral cell surfaces are regulated (Mandel et al., 1993). It is important that these TJ proteins remain intact and selectively permeable in endothelial and epithelial cells, since the collapse of such structures allows the free passage of ions and molecules, as well as the entry of immune cells, and could lead to the eventual breakdown of the cellular layer and its barrier function (Boueiz and Hassoun, 2009, Anderson and Van Itallie, 2009).

Zona occludens-1 (ZO-1, 220 kDa) was first discovered in 1986 as an antigen for a monoclonal antibody raised against a junction fraction from the liver (Stevenson et al., 1986). It is considered to be the first intracellular protein component of the TJ that functionally links integral proteins (occludin and claudin) to the actin-myosin cytoskeleton (Fanning et al., 1998) (Figure 5.1, overleaf). It belongs to a family of membrane-associated guanylate kinases (MAGUK) involved in signal transduction during cell-cell contact (Gottardi et al., 1996). ZO-1 can be found in various types of epithelial and endothelial cells, where tight junctions have to be particularly efficient (Li and Poznansky, 1990). ZO-1 has been shown to interact with occludins

(Stevenson et al. 1986), in addition to its interactions with different membrane-associated proteins including catenin, paxillin, talin and actin (González-Mariscal et al., 2003). Actin plays an important role in barrier function; the cell shape can be deformed by the contraction of the actin filaments, and the disruption of these filaments (for example by cytochalasin) results in an increase in intercellular permeability (Madara et al., 1986).

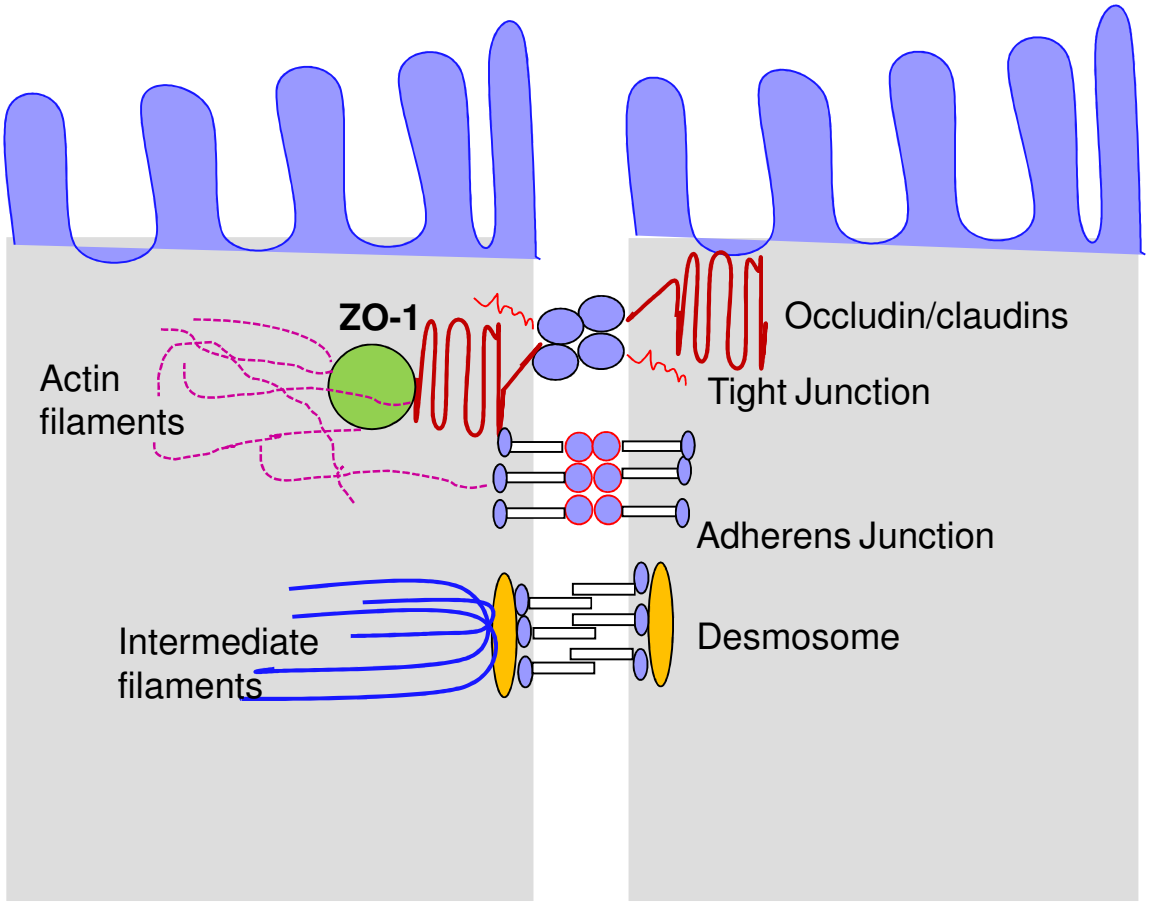

Figure 5.1 The tight junction protein complex between two adjacent epithelial cells.

16HBE14o- is a well-characterized human bronchial epithelial cell line, derived from a one-year-old male heart-lung transplant patient, which forms a resistant polarized monolayer under appropriate culture conditions (Forbes et al., 2003). This cell line has also been used to evaluate drug delivery to respiratory epithelium and epithelial permeability, as well as oxidant damage and stress during lung injury in an *in vitro* model (Rahman et al., 2001). Cozens et al., (1994) and Forbes (2000) have reported that these cells preserve the properties of bronchial epithelium such as differentiation, the structure of microvilli and cilia, ion transport regulation, and tight junction formation. This ability is important in any cell line that is to be used as a drug transport model.

It is known that a variety of both exogenous and endogenous factors can affect the permeability of epithelial and endothelial tight junctions (Walsh et al., 2000). For example, Ohtake et al. (2003) demonstrated that the impairment of paracellular permeability in rabbit nasal epithelium by poly-L-arginine induced ZO-1 serine/threonine phosphorylation and occludin dephosphorylation. Similarly, Zhang et al. (2007) reported a decrease in ZO-1 and integral protein mRNA expression accompanying TJ permeability increase in rat alveolar epithelium, but glutamine supplementation provided protection against TJ alteration and barrier impairment. An *in vivo* study of neonatal mice by You et al. (2012) demonstrated the alteration of TJ function and structure, focusing on the TJ proteins occludin and ZO-1, leading to an increase in airway epithelial permeability after exposure to hyperoxia. These results are accordance with those of McCarthy et al. (1996) who demonstrated that oxidative stress enhances monolayer permeability in caco-2 cells without affecting cell viability. Furthermore, other studies show that

histopathological changes such as oedema and cell infiltration accompany hyperoxia exposure (Altemeier and Sinclair, 2007, Auten and Davis, 2009).

The role of inflammation in affecting TJs and increasing their permeability is suggested by various studies. Mazzon and Cuzzocrea (2007) elucidated the possible role of TNF-α in pulmonary barrier dysfunction and structural alteration that caused acute lung inflammation in mice. In addition, Walsh et al. (2000) postulated in a review, based on evidence from several studies, that IFN-γ alters paracellular permeability via several mechanisms, including possibly direct effects on ZO-1 and/or via changes in the perijunctional actin cytoskeleton. This, however, has not been validated by subsequent studies. Bruewer et al. (2003) found that the cytokines IFN-γ and TNF-α affected the epithelial barrier by causing internalization of the transmembrane proteins junction adhesion molecule 1, occludin, and claudin. However, their effects on ZO-1 were minimal.

The protective roles of vitamins E and C as antioxidants are well known. Both are capable of reducing, and thereby eliminating, ROS and thus preventing interactions between ROS and cells (Carr et al., 2000). There are also reports regarding the improvement or maintenance of lung function among smokers when given vitamin E and C supplements, in which the adhesion of platelets and leukocytes to lung endothelial cells are prevented (Lehr et al., 1997).

It is known that vitamin C is an important cofactor for hydroxylase and oxygenase enzymes involved in the formation of collagen, one of the main components of structural and connective tissue (e.g. bone and cartilage). It is also involved in the formation of carnitine, which is essential for fatty acids transport from cytosol into

mitochondria; and in the synthesis of neurotransmitters (signal from neurons to target cells) (Carr and Frei, 1999). Vitamin C accelerates hydroxylation to ensure ideal activity of hydroxylase and oxygenase enzymes via preserving the active centre of metal ions such as iron and copper in a reduced state (Naidu, 2003). Vitamin C, in addition, helps in the regeneration of the active forms of other antioxidants from their radicals (e.g. urate, β-carotene and α-tocopherol) (Halliwell and Gutteridge, 1986), and helps to prevent lipid peroxidation through the conversion of α-tocopheroxyl to α-tocopherol (Neuzil et al., 1997).

Vitamin E acts as a chain-breaking antioxidant, important in the prevention of the oxidation of the lipid component of low density lipoprotein (LDL) and the eventual release of free radicals into the epithelial and endothelial cells (Faruqi et al., 1994). vitamin E react with lipid peroxyl radical to form α-tocopheroxyl, the latter then react with vitamin C or other hydrogen donor to form the reduced active form of vitamin E. Vitamin E supplementation has been found to increase LDL resistance to oxidation resulting in decreased risk of atherosclerosis and heart disease (Meydani, 2001). Vitamin E also acts as a surfactant on the surface of the alveolar cells, which is actively secreted by Type II cells (Kolleck et al., 2002). Insufficient vitamin E in lung tissue is also reported to cause the adhesion of leukocytes to the endothelium, which in turn results in inflammation (Faruqi et al. 1994).

The aims of the study were (1) to elucidate the impact of 24 h exposure to hyperoxia on the TJ protein ZO-1 in the16 HBE14o- cell line; (2) to evaluate the effects of antioxidants in maintaining the cell monolayer integrity; and (3) to test the

potential connection between pro-inflammatory cytokines and the tightness of bronchial cells.

5.2 Materials and Methods

5.2.1 16HBE14o- cell culturing and harvesting

The 16HBE14o- human bronchial epithelial cell line was obtained from Dr Dieter Gruenert (University of California, San Francisco, USA). Cells were received as a fully confluent monolayer in tissue culture flasks (25 cm^2), immediately seeded into a new flask and assigned as Passage 2.65. Cells were grown in vented culture flasks (BD Falcon, Oxford, UK) or Transwell insert membranes pre-coated with 1% Type 1 bovine collagen. Cells were cultured for several passages (2.65-2.69) before experimentation, in minimum essential medium eagle (MEM) medium containing 10% fetal bovine serum (FBS) , 1% antibiotic (containing 10,000 U ml^{-1} penicillin G, 10 mg ml^{-1}streptomycin and 25 µg ml^{-1}amphotericin B) and 1% L-glutamine. Medium was prepared aseptically and stored at 4 ℃; before use it was warmed to 37 ℃. When the cells were 80-90% confluent, they were passaged by trypsinization; firstly, the monolayer of cells was washed twice with Hank's Balanced Salt Solution (HBSS). To release the cells, 0.25% trypsin containing 0.5 mM EDTA (at a dilution of 1:5) was as then added for 5 min at 37 ℃ with gentle agitation to help the cells detach. Following this 5 ml of medium containing FBS

was added to neutralize the trypsin and the mixture was centrifuged at 130 *g* for 5 min. The cell pellet was then re-suspended in fresh medium at a density of 5×10^5 (split ratio of 1:5 and 1:10 for 25 and 75 cm^2 flasks respectively) and cultured at the required cell density in vented tissue culture flasks under in 5% CO_2 at 37 ℃. Cells were counted using a Neubauer haemocytometer. After 24 h of culturing the medium was changed to remove dead cells. After this the medium was changed every 2-3 days.

5.2.2 Cryopreservation of cells

Cells were routinely frozen as stocks for further use in experiments. Cell pellets were harvested as described in Section 2.5.1 (1×10^6 cells ml^{-1}) and re-suspended in a freezing solution containing 40% MEM medium, 50% FBS and 10% dimethyl sulphoxide (DMSO). One ml of suspension was placed in a 2 ml cryovial and stored immediately at -80 ℃.

5.2.3 Maintenance of cells for experiments

For the following experiments 200 µl of re-suspended cells (Section 5.2.1) in fresh medium at a concentration of 2.5×10^5 cells ml^{-1} were cultured in 12-well Transwell membrane inserts (pore size 0.4 µm and 1.13 cm^2 surface area). The cells were maintained in culture for 3 days in 37 ℃ in an incubator before the medium was removed from the inner membranes and the cells were cultured with an air-liquid

interface for up to 6 days (after which a maximum mean transepithelial resistance (TER) of 251 $\Omega.cm^2$ was reached, see Section 5.2.4); in which only medium (1 ml) on the basolateral side in the lower compartment of the wells was retained. The cells were then co-cultured with vitamins and exposed to oxygen as described in Sections 2.2.6 and 2.2.7 for 24 h. The effect of solvents used for dissolving α-tocopherol were verified by evaluating cell viability using Trypan blue as described in Section 2.2.4 in cells exposed to normoxia for 24 h and received equal volume of solvent as the antioxidant treatment cells, no toxic effects was detected as seen in Figure 5.2 below.

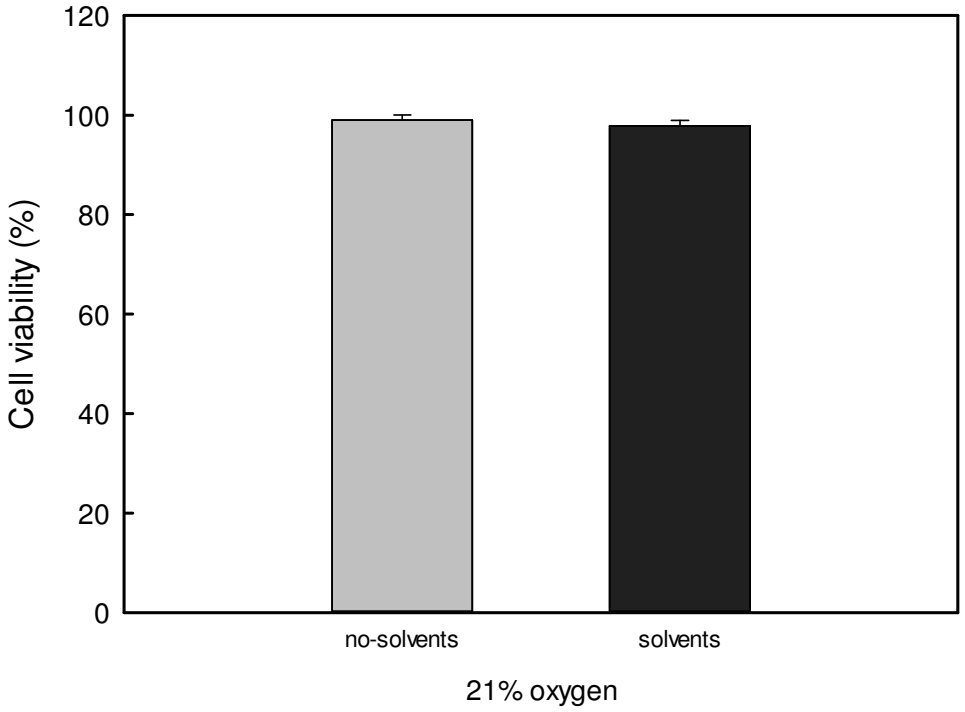

Figure 5.2 Cell viability in 16HBE14o- cells cultured for 24 h with and without α-tocopherol solvents under normoxia. Data are means ± SE from triplicate samples for one experiment.

5.2.4 Measurement of transepithelial resistance (TER)

TER is widely used as an indicator of tight junction integrity (Pohl et al., 2009). TER was measured using an EVON^{TM} voltohmmeter (World Precision Instruments, Sarasota, FL) and the voltage resistance through monolayer cells was recorded as $\Omega.cm^2$. A Transwell insert with no cultured cells was used as a blank, where the resistance reading was subtracted from sample readings and then multiplied by the insert membrane surface area (1.13 cm^2). Monolayers of cells were incubated with PBS for 10 min at room temperature to equilibrate before the reading (Pohl et al., 2009).

5.2.5 Immunofluorescence detection of ZO-1 tight junction protein

The intercellular linkage protein ZO-1 was determined by fluorescence labelling as described by Wan et al. (2000). Control and treated cells were washed first with CSK buffer (10 mM PIPES; pH 6.8, containing 50 mM NaCl, 0.5% Triton X-100 and 3 mM $MgCl_2$), and then fixed using 3.7% formaldehyde in CSK buffer for 20 min at room temperature. Fixed samples were washed with PBS (3 times, 5 min each) and permeabilized by incubation with 0.5% Triton X-100 in CSK buffer for 10 min followed by blocking with 1% bovine serum albumin (BSA) in PBS for 1 h at room temperature to avoid any non-specific binding by the selective antibody. Cells on the membrane insert were then incubated with the primary antibody, polyclonal rabbit anti-ZO-1 (final concentration of 5 µg ml^{-1}, 1:100 dilution in blocking buffer;

Invitrogen, UK) at 4 ℃ overnight. Next day, after three five minute washes with PBS, samples were incubated with Alexa Fluor 488-labelled goat anti-rabbit secondary antibody (final concentration of 10 mg ml^{-1}, 1:200 dilution in blocking buffer; Invitrogen, UK) for 1 h at room temperature (samples were wrapped with aluminium foil and kept in the dark). After three, five minute washes, the membrane (membrane insert base) with the monolayer of cells was cut gently from the insert wall with a scalpel blade and placed on a glass microscope slide with the cultured surface up. The cells were then mounted with DPX and covered with a 22 × 22 mm glass coverslip. The slides were left overnight in the dark at room temperature to allow the mounting to set. CLSM was carried out, pinhole, detector gain and laser transmission were adjusted to produce a stack of images (Z-stack) using an upright LSM510 CLSM (Carl Zeiss Ltd., Germany) equipped with a 40× water dippingobjective (excitation wavelength was set at 488 nm and a 505-530 nm band pass filter was used). The original images were subject to blinded analysis; by which all the images were relabelled and image processing was carried out with assistance from colleagues. A negative control was used where the cultured cells were subjected to same procedure without addition of the primary ZO-1 antibody. The ZO-1-associated fluorescence was calculated using ImageJ software (http://rsbweb.nih.gov/ij/) equipped with the Neuron J tracing tool plugin (Iden et al., 2012) as follows:

1- The Ism image files were opened in ImageJ and converted to 8-bit grayscale images and re-saved (Figure 5.3, overleaf).

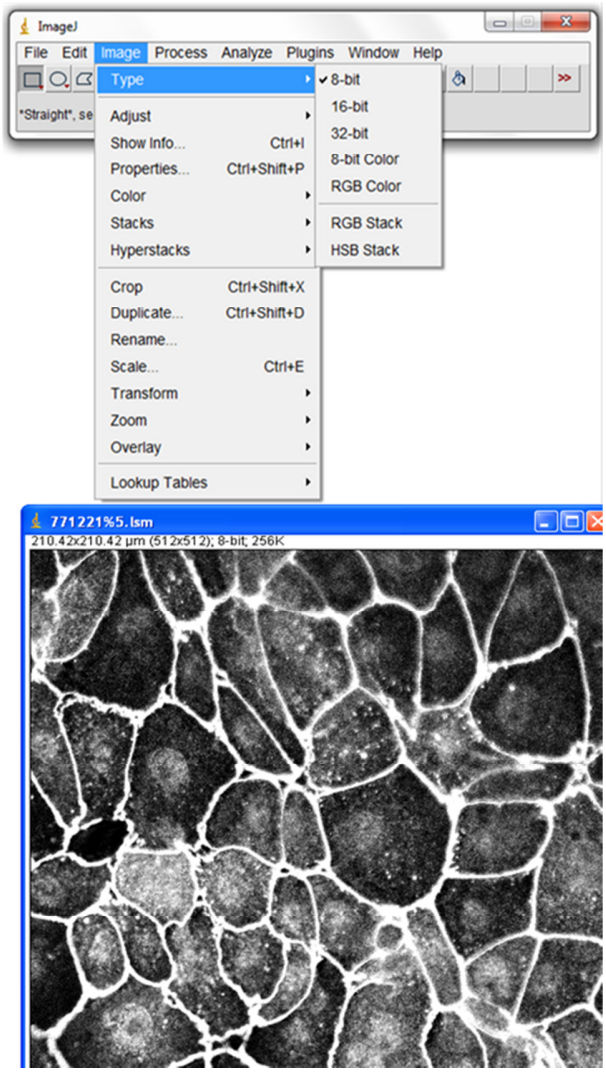

Figure 5.3 Screenshot of human bronchial 16HBE140o- cell line obtained by confocal laser scanning microscopy and converted to 8 bit type with image J.

2- Neuron J was then run from plugins where the Neuron J tool appeared instead of image J tool (Figure 5.4, below).

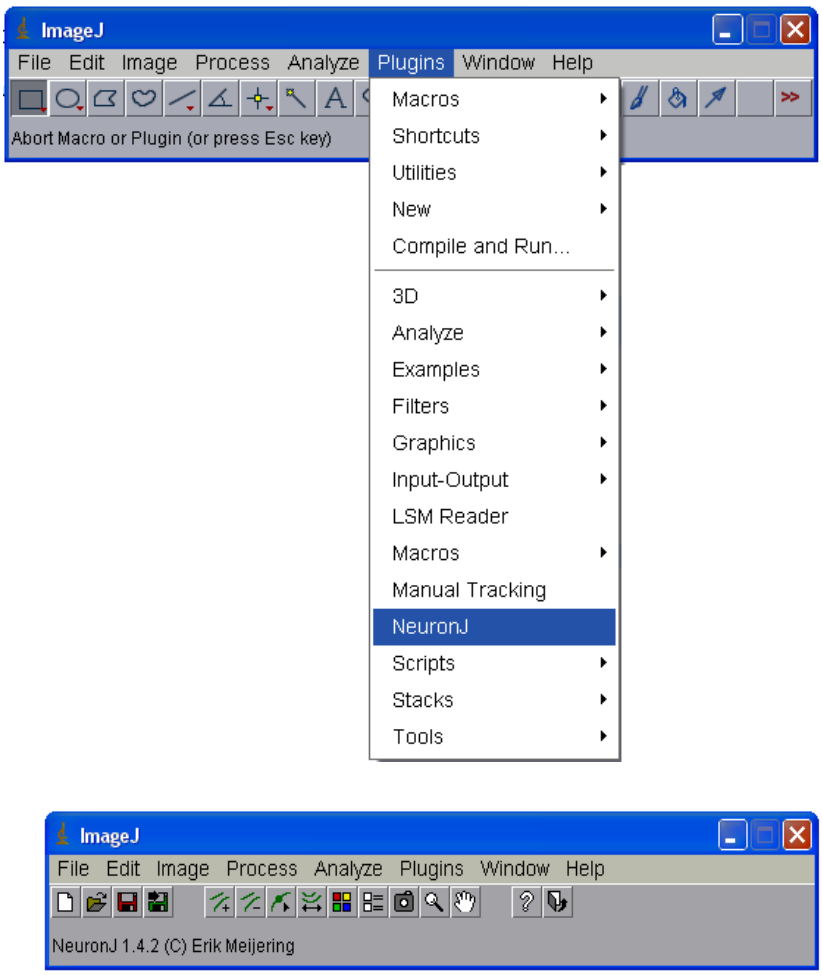

Figure 5.4 Screenshot of Neuron J command box run from ImageJ plugins.

3- The lsm 8-bit image re-opened using the Neuron J open file icon as shown in Figure 5.5 below.

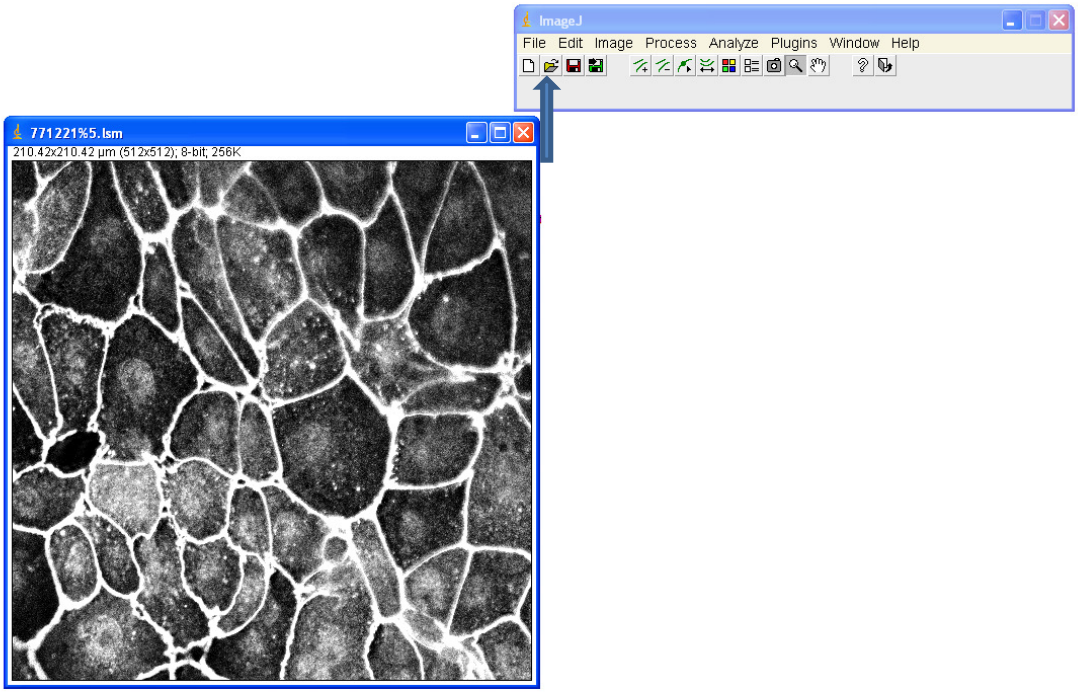

Figure 5.5 Screenshot of lsm 8-bit image re-opened by Neuron J open.

4- The add tracings tool was the run to trace 10-12 cells in plan view of lsm image as shown in figure 5.6 below.

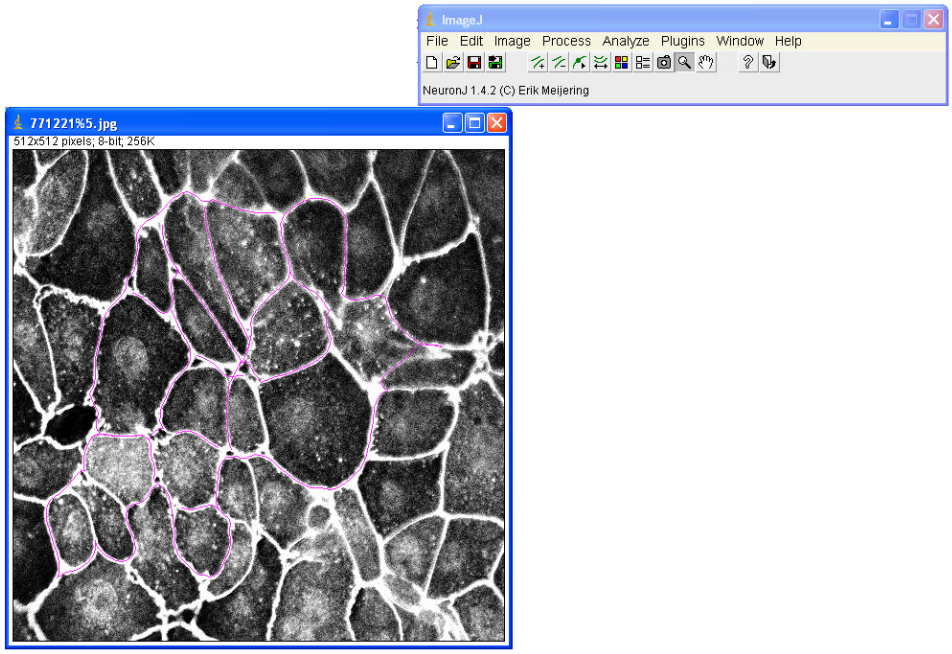

Figure 5.6 Screenshot of lsm image with the tracing tool added.

5- The ‘Measure tracings’ function was then run followed step 4, and the sum length and mean value information that appeared in the Groups window (Figure 5.7) was then transferred to an Excel sheet to complete the final calculation.

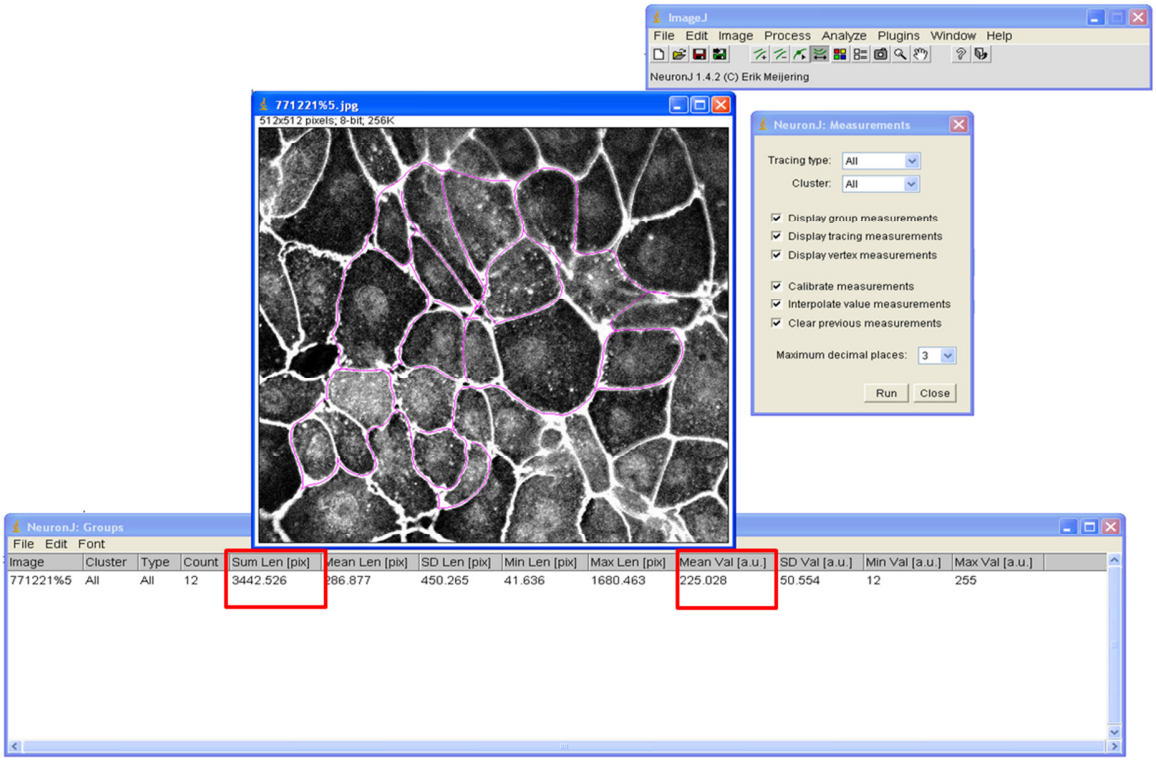

Figure 5.7 Screenshot of the information results produced by measure tracings command box where the sum length and mean value (red box) were transfer to Excel sheet for further analysis.

6- Finally, the ZO-1-associated mean fluorescence intensity per cell was calculated as follows:

$$\text{ZO} - 1 \ \text{flourescence intensity} = (\text{mean value of } 10 - 12 \text{ cells} * \text{total length}) / (\text{number of cells})$$

5.2.6 Detection of pro-inflammatory cytokines by Enzyme-Linked Immunosorbent Assay (ELISA)

After 24 h of culture as described in Section 5.2.3, samples (1ml) of medium were collected and stored at -80 ℃ until required. Samples were thawed and centrifuged at 130 *g* for 5 min. The supernatants were used to determine levels of cytokines IL-6, IL-8 and TNF-α.

Sandwich ELISA is a specific quantitative assay based on the binding of antigen to a specific antibody. Four main steps are involved: the antigen of interest (cytokines in this case) is bound to the capture antibody; primary antibody (biotin detection antibody) is then bound to the antigen (cytokines); the conjugate streptavidin-horseradish peroxidase (HRP) is bound to the primary antibody; and finally the HRP substrate solution (TMB) is added resulting in detectable colour development (Figure 5.8, page 143).

The assay was carried out over three days. On the first day, 96-well polystyrene microtitre plates were coated with the (50 µl well^{-1}) capture antibody dissolved in (1 µg ml^{-1}) PBS for the target cytokines (BD-Pharmingen, Oxford, UK) and kept overnight at 4 ℃. On the second day, plates were washed three times with washing buffer (PBS, containing 0.05% Triton X-100) before blocking with 2% BSA dissolved in PBS (150 µl well^{-1}) for 4 h at room temperature, followed by a washing step as above. The samples of medium containing the cytokines of interest were then added (50 µl well^{-1}) and the plates kept overnight at 4 ℃. On the third day, the plates were washed with the washing buffer to remove all unbound cytokines. The

detection antibodies (BD-Pharmingen, Oxford, UK) (0.5 µg ml^{-1}) were dissolved in 2% BSA (in PBS) then added to the plates before incubation for 4 h at room temperature. Following washing, 50 µl of conjugate streptavidin-HRP dissolved in 2% BSA (in PBS) (1:250) was added to each well. After washing, 100 µl of chromogenic substrate tetramethylbenzidine (TMB) was added to each well before incubation for 15 min at room temperature to allow colour development (the TMB peroxidase substrate contains 3,3',5,5'-tetramethylbenzidine at a concentration of 0.4 g l^{-1}; peroxidase substrate solution contains H_2O_2 at a concentration of 0.02% in citric acid buffer). The conjugate catalyses the oxidation of the chromogenic substrate (TMB) by H_2O_2 leading to development of a blue colour. To stop the reaction the HRP was denatured by adding 1 M sulphuric acid (50 µl $well^{-1}$) resulting in a colour change to yellow, the absorbance of which was read at 450 nm using a plate reader (VersaMax™, Molecular Devices, Sunnyvale, CA) equipped with SoftMax Pro software version 5.4.

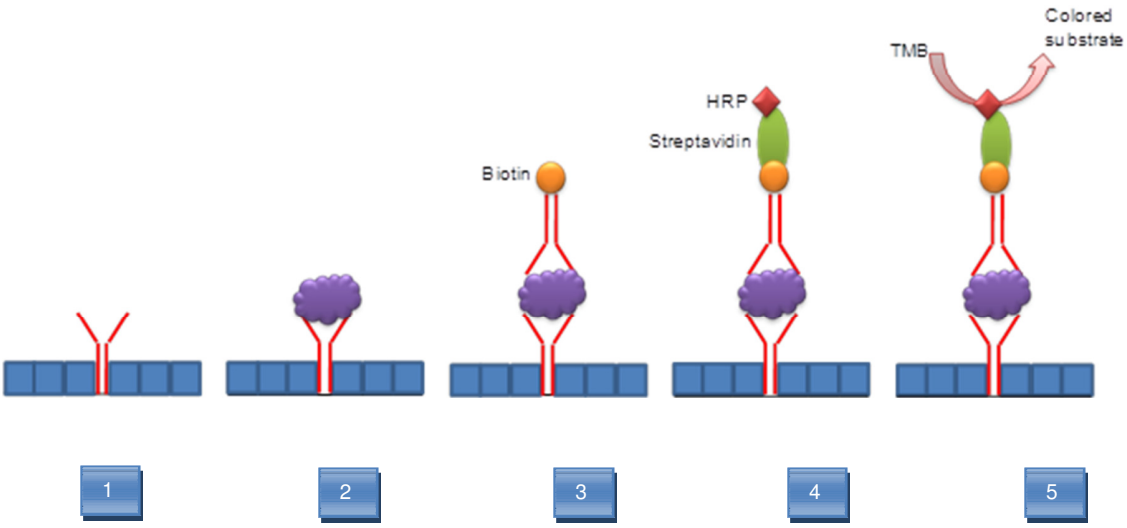

1 Plate coated with capture antibody for 24 h at 4 ℃ followed by addition of blocking buffer

2 Addition of samples containing specific antigen (cytokine)

3 Biotin detection antibody binds to antigen

4 Secondary antibody conjugate streptavidin-HRP binds to biotin

5 Chromogenic substrate TMB converted to coloured product by the conjugate

Figure 5.8 Diagrammatic illustration of the sandwich ELISA protocol.

5.2.7 Reverse transcription- real time quantitative polymerase chain reaction (RT-PCR)

To investigate the expression of gene ZO-1 and specific pro-inflammatory cytokines in 16HBE14o- cells, reverse transcription with qRT-PCR were used as follows:

5.2.7.1 Total RNA extraction

A mammalian RNeasy miniprep kit (Sigma Aldrich, UK) was used to extract total RNA. All steps were carried out according to the manufacturer's protocol; briefly, cultured cells on membrane inserts at a density 2.5 × 10^5 cells ml^{-1} were trypsinised (as described in Section 5.2.3) and collected as pellets in 1 ml microcentrifuge tubes by centrifugation at 130 *g* for 5 min. The pellets were then lysed by adding 250 µl of lysis solution containing 1% 2-mercaptoethanol with gentle pipetting to improve the extraction. The cell lysate was transferred to a filtration column and centrifuged for 2 min at 21,000 *g* (Heraeus Fresco 21 microcentrifuge, Thermo Scientific). An equal volume of 70% ethanol was added to the flow-through liquid, mixed gently and centrifuged for 15 s at 13,000 *g* before transfer onto a new binding column. Following washing with 500 µl of wash solution 1, DNA digestion was performed using DNase I column enzyme (Sigma Aldrich, UK) where 80 µl of digest RDD buffer/ DNase I (70:10) was added prior to 15 min incubation at room temperature, followed by washing with 250 µl of solution 1 and centrifugation for 15 s at 6,600 *g*. After placing the RNeasy column into a new collection tube, 500 µl of wash solution 2 was added and the assembly centrifuged

for 2 min at 13,000 *g* to remove the residual ethanol. The RNeasy column was again transferred to a new collection tube and 50 µl of elution solution was added followed by centrifugation for 1 min at 6,600 *g*. Samples were stored at -80 ℃ until use.

5.2.7.2 Assessment of the quantity of the total RNA

A NanoVue Plus spectrophotometer (GE Healthcare, Little Chalfont, UK) was used to measure the RNA concentration and purity. Samples (2 µl) were placed onto the NanoVue after blanking with an equal volume of elution solution. The A_{260}/A_{280} and A_{260}/A_{230} ratios were used as an indicator for the RNA purity. These should be in the ranges 1.8-2.1 and 1.8-2.2, respectively, if the RNA is sufficiently pure as recommended by the manufacture.

5.2.7.3 Reverse transcription

Reverse transcription (RT) was used to synthesise complementary DNA (cDNA) from a single-stranded RNA template. An Applied Biosystems kit was used to prepare the cDNA in which the reverse transcriptase was obtained from Moloney Murine Leukaemia Virus (M-MLV). Following the manufacturer's protocol, 11 µl of master mix (containing RT buffer, dNTP mix and RNase inhibitor) was added to 1 µg of total RNA with volume up to 20 µl with water. The RT-PCR conditions are summarized in Table 5.1 below and RT reaction was performed in Veriti 96-well

Thermal cycler (Applied Biosystems, Grand Island, USA). Samples were kept at 4 ℃ for a short time (2 weeks) or at -20 ℃ for longer periods (up to 6 months).

Table 5.1 Reverse transcription thermal cycling conditions

37 °C	1 h
95 °C	5 min
4 °C	to hold

5.2.7.4 PCR

5.2.7.4.1 Primer design and list of primers

Primers were designed using Primer Express Software (Applied Biosystem, UK). All primers were synthesized by Eurofin MWG/Operon (Germany, http://www.eurofinsgenomics.eu). The following criteria were considered when the primers were designed: primer length should be between 18 and 30 base pairs (bp) (where higher annealing temperatures required for longer primer); G/C content (50%), maintain annealing temperatures of primers 50-65 ℃ (the difference between forward and reverse temperature +/- 2 ℃); and the specificity of the primer sets were verified using the Basic Local Alignment Search Tool (BLAST) (Altschul et al., 1997). (http://blast.ncbi.nlm.nih.gov/Blast.cgi). Primers used are listed in Table 5.2 (overleaf).

Table 5.2 Primers used for gene expression measurement via RT-PCR (F: forward, R: reverse)

Primer name	Primer sequence	Primer length (bp)
IL-6 F	AGTCCAGCCTGAGGGCTCTT	20
IL-6 R	GCCCAGTGGACAGGTTTCTG	20
IL-8 F	TCAGAGACAGCAGAGCACACAA	22
IL-8 R	GGCCAGCTTGGAAGTCATGT	20
TNF-α F	TGAGGCCAAGCCCTGGTAT	19
TNF-α R	GAGATAGTCGGGCCGATTGA	20
ZO-1 F	GCAATGGAGGAAACAGCTATATGG	24
ZO-1 R	TGAGGATTATCTCGTCCACCAGAT	23
GAPDH F	CTGCTCCTCCTGTTCGACAGT	21
GAPDH R	CCGTTGACTCCGACCTTCAC	20
B-actin F	GCGCGGCTACAGCTTCA	18
B-actin R	TGGCCGTCAGGCAGCTCGTA	20

5.2.7.4.2 Explanation of real time PCR

Three main steps are involved in the polymerase chain reaction (PCR): denaturation, annealing and extension. qPCR is based on monitoring DNA amplification in real time, where the PCR product is detected by the increase in fluorescence signal through each cycle. SYBR Green gives a strong fluorescence signal (excitation at 494 nm and emission at 521 nm) when associated with double-stranded DNA (Figure 5.9, overleaf).

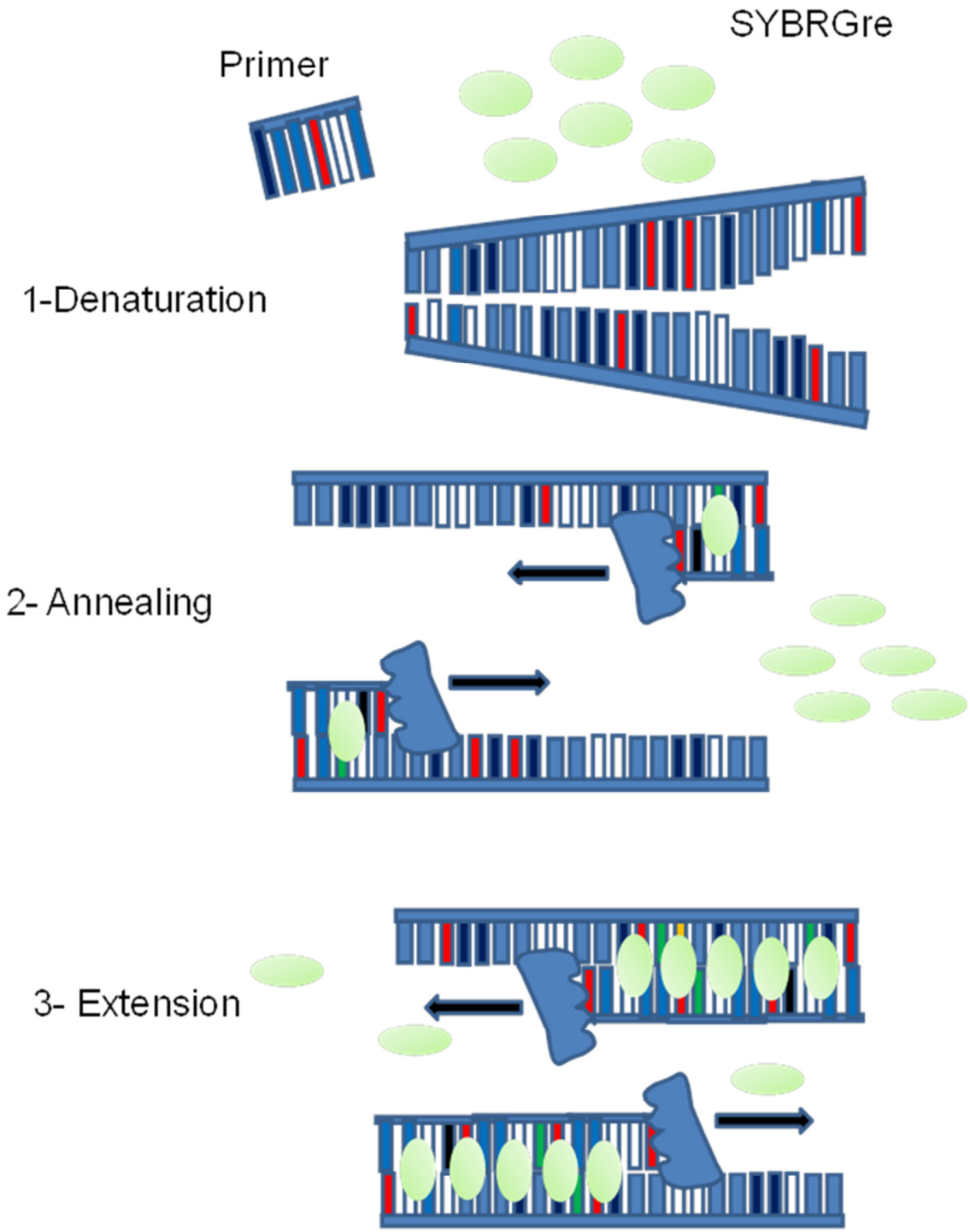

Figure 5.9 The main three steps of qPCR and the SYBR Green dye binding to the double-stranded DNA. The binding results in production of fluorescence emission signals light which can be viewed in real time, the more dye bound the more copies of gene.

5.2.7.4.3 Selection of suitable reference gene (Housekeeping gene).

To allow for inter sample variability, a normalisation with suitable housekeeping gene where the relative not changes under experimental conditions usually used with qRT-PCR (Dheda et al., 2004). Two common housekeeping genes widely used with samples undergoing oxidative stress, glyceraldehyde-3-phosphate dehydrogenase (GAPDH) and β-actin, were tested with cultured cells exposed to normoxia, hyperoxia, and normoxia plus 10 ng ml^{-1} TNF-α (as a positive control) for 12 h and 24 h. The levels of expression of genes for IL-8, IL-6 and TNF-α were calculated as described in Section 5.2.7.4 below. Both internal expression genes did not vary under oxidative stress. Evaluation of the endogenous chosen reference gene with experimental conditions was carried out (see Figure 5.10 for an example).

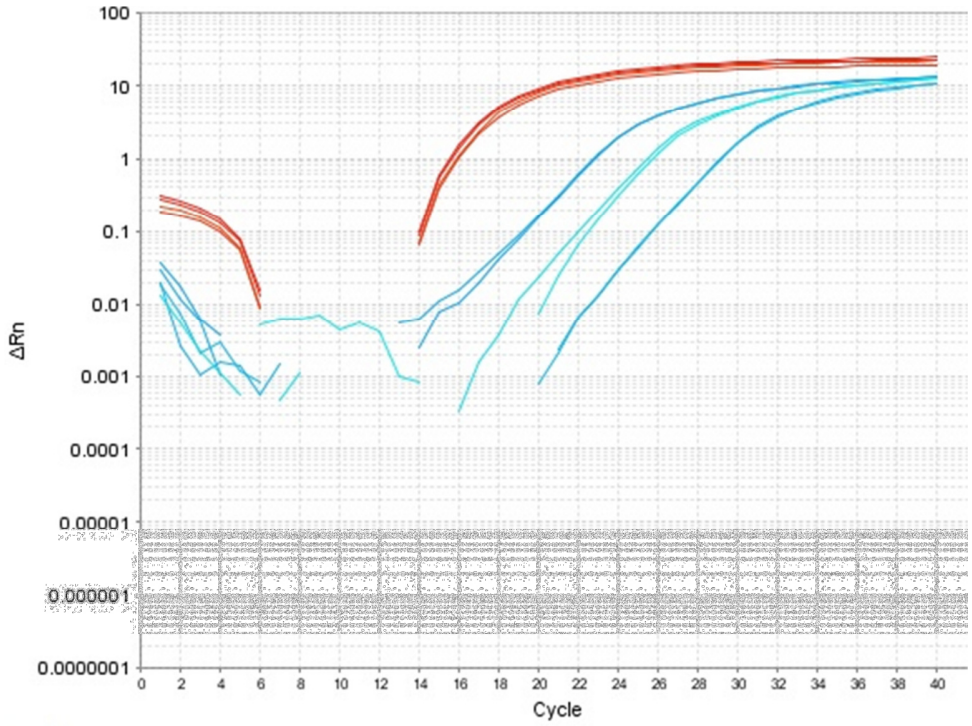

Figure 5.10 Amplification plot for comparison between GAPDH (red lines) and TNF-α (blue line). 16HBE14o- cells were cultured at air-liquid interface under normoxia, hyperoxia and stimulated with TNF-α (positive control) and subjected to qRT-PCR. Sample runs in duplicate for each gene and treatment.

5.2.7.4.5 Quantitative real time PCR (qPCR)

Quantitative real time PCR was performed using a StepOnePlus thermal cycler and Power SYBR Green® kit (Applied Biosysterms, UK) according to the manufacturer's instructions, using 500 pmol of the forward and reverse primers for each target. Melting-curve analysis was used to identify non-specific product and adjusted at 60-90 ºC (see Figure 5.11, page 152 for an example). Briefly, cDNA

samples were prepared as described in section 5.2.7.3 and run in 96-well plates in triplicate with a final volume of 20 µl (5 µl of a five-fold dilution (in molecular grade water) of cDNA, plus 15 µl master mix). Master mix preparation is described in Tables 5.3. The amplification of the template was carried out under the following conditions; pre-heating for 95 ℃ for 10mins, followed by 40 cycles at 95 ℃ for 30 seconds, 60 ℃ for 1 minute and 72 ℃ for 1 minute The real time quantitative PCR data was analysed following the $2^{-\Delta\Delta Ct}$ method as described by Livak and Schmittgen (2001), using GAPDH as an endogenous control and resting cells as a reference sample. Thus, the relative quantity of the target transcript is described as the fold increase relative to the reference sample and GAPDH.

Table 5.3 preparation of qPCR master mix (final volume 20 µl)

component	volume (µl)
SYBRGreen	10
Forward primer	1.25
Reverse primer	1.25
Molecular grade water	2.5

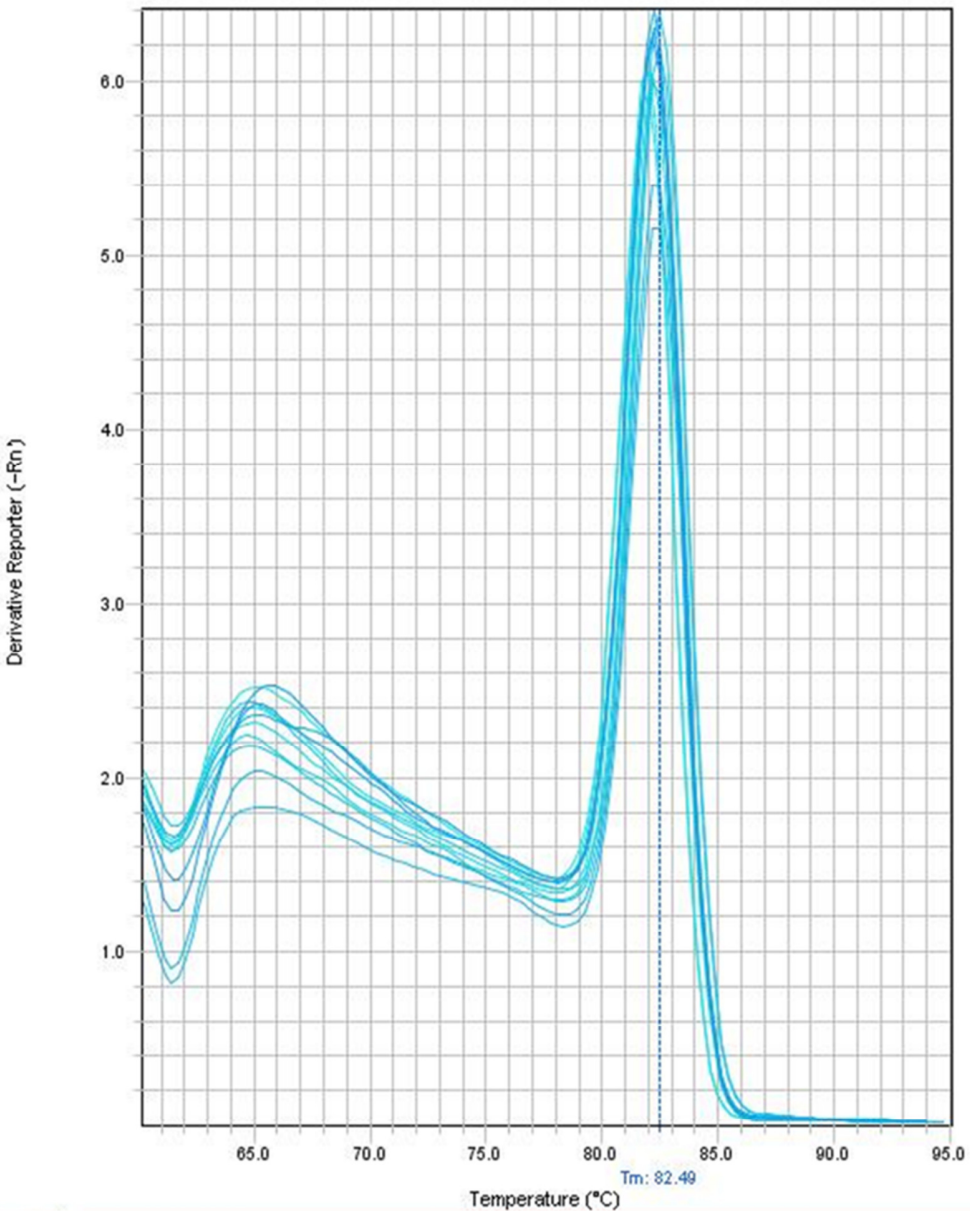

5.11 Melt Curve for TNF-α. The derivative melting peak is the highest at the melting temperature 82.49 ℃ representing a specific melting curve with no primer or unwanted products.

5.3 Statistical analysis

The statistical analysis was performed using Minitab 16 (Minitab Ltd, Coventry, UK). Differences among groups were determined by one-way analysis of variance ANOVA followed by Fisher's LSD test. All results are presented as means ± SEM and significance is accepted at $P \leq 0.05$.

5.3 Results

5.3.1 Effects of hyperoxia on the integrity of 16HBE14o- cell monolayers

When 16HBE14o- cells were grown as monolayers at an air-liquid interface, tight junctions developed in 6 days (Figure 5.12, overleaf), with a TER value of 251.2 ± 4.1 $\Omega.cm^2$ (mean ± SE). Exposure to normoxia, hyperoxia, and treatment with different concentrations of α-tocopherol and ascorbate followed. Loss of monolayer integrity was indicated by a significant decrease in TER value after 24 h of exposure to hyperoxia compared to normoxia (168.5 ± 6.3 $\Omega.cm^2$ with 95% O_2 versus 251.2 ± 4.1 $\Omega.cm^2$ with 21% O_2, Figure 5.13, page 155). Co-culture of the cells with antioxidant vitamins did not reduce the impact of hyperoxia significantly; the mean values increased to 182.7 ± 6.0 $\Omega.cm^2$ with α-tocopherol (10^{-7} M), 171.5

± 5.9 Ω.cm^2 with α-tocopherol and ascorbate (10^{-7} M and 10^{-6} M respectively), 177.2 ± 4.7 Ω.cm^2 with 10^{-6} M ascorbate; and 176.7 ± 5.5 Ω.cm^2 with 10^{-7} M ascorbate compared to hyperoxia only (168.5 ± 6.3 Ω.cm^2). However, a significant decline in TER value was still seen in cells co-cultured with antioxidant vitamins under hyperoxia compared to normoxia.

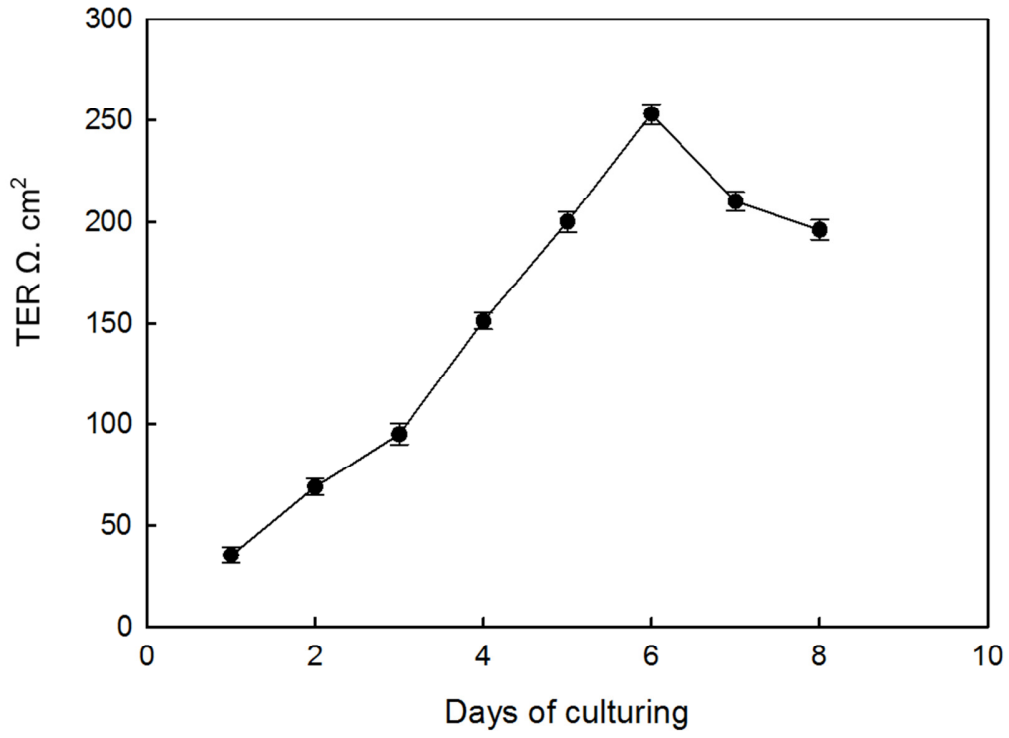

Figure 5.12 Changes in transepithelial electrical resistance (TER) in 16HBE14o- epithelial cell monolayers over time after culture on Transwell inserts. Data are means ± SE from three samples from one experiment.

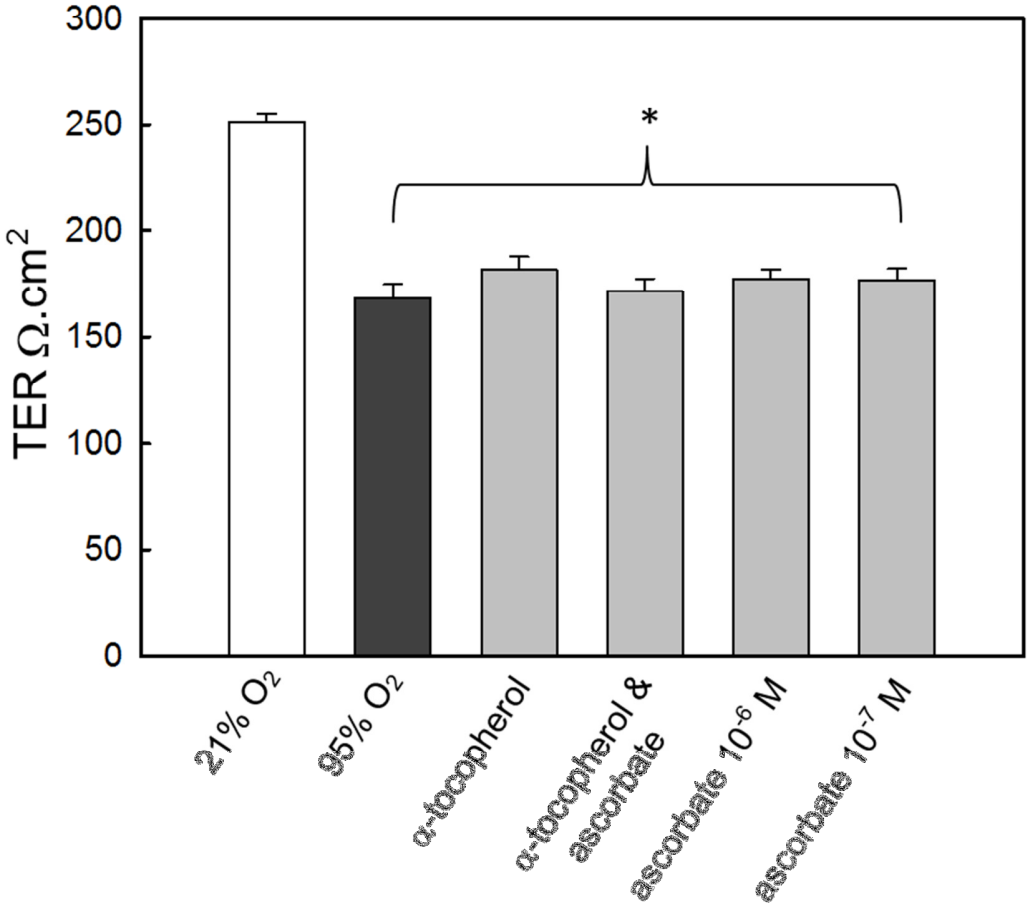

Figure 5.13 Changes in transepithelial electrical resistance (TER) in 16HBE14o- epithelial cell monolayers after 6 days culture on Transwell inserts followed by 24 h of exposure to normoxia and hyperoxia, and treatment with antioxidant vitamins. Data are means ± SE, Three different experiments with triplicate samples for each was used, *n* = 3. * = significant difference versus normoxia (Fisher's LSD, $p < 0.001$).

5.3.2 Effects of hyperoxia on ZO-1 localization in human bronchial cells

The localization of the ZO-1 linkage protein in the tight junction complex was examined using immunofluorescence staining images obtained by CLSM. ZO-1-associated fluorescence appeared as continuous lines along the margins of the control cells, whereas fragmentary staining was observed in cells exposed to hyperoxia (Figure 5.14, overleaf). The ZO-1-associated staining intensity level, measured using the Neuron J tool showed a significant decline in hyperoxic cells compared to control cells ($P < 0.01$). Co-culture with antioxidants significantly increased the intensity level ($P < 0.05$), though this increase was not sufficient to prevent entirely the hyperoxia-induced decrease in ZO-1; the intensity was significantly decreased in the co-cultured cells compared to normoxia (Figure 5.15, page 158).

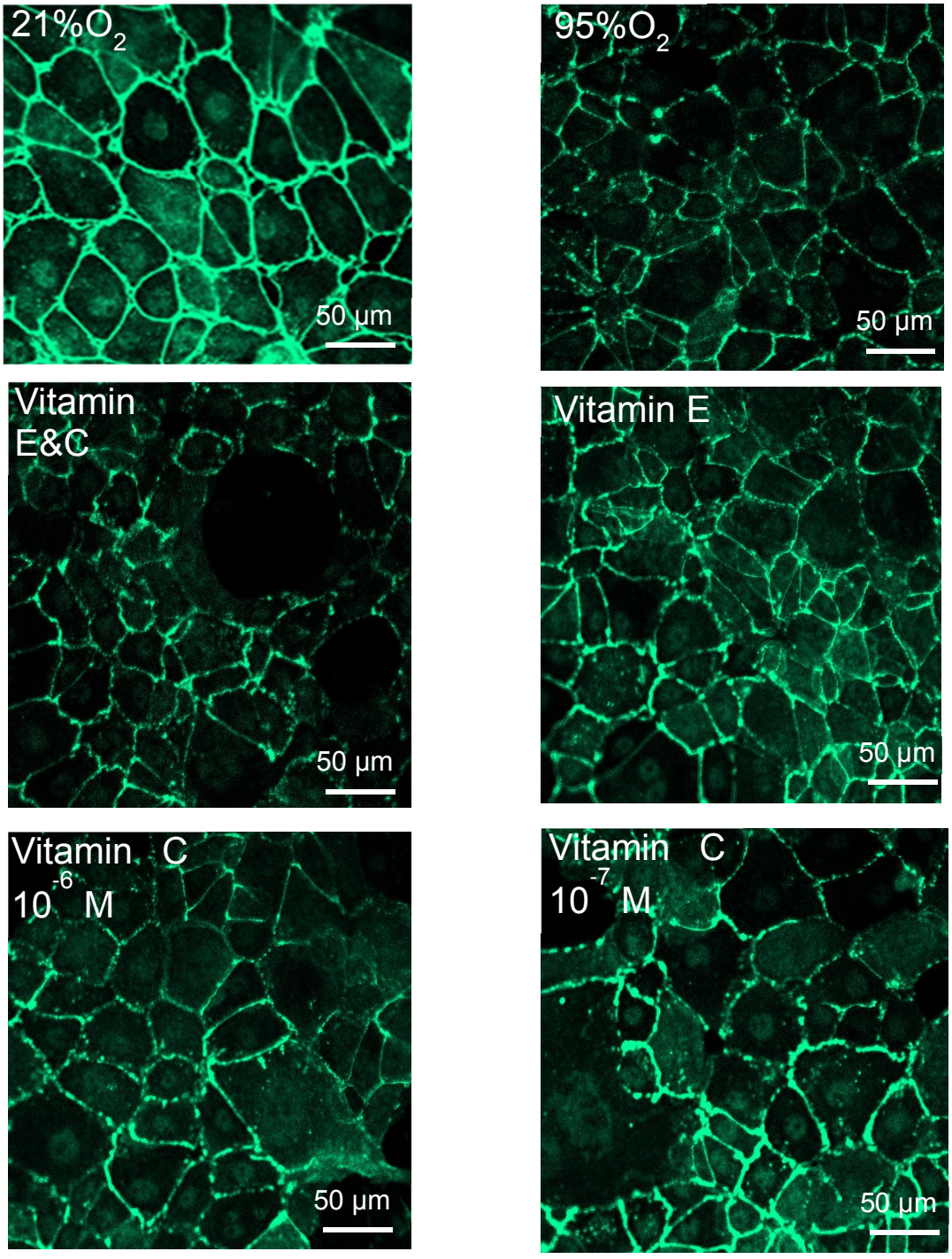

Figure 5.14 Immunofluorescence staining was performed to determine the location of ZO-1 protein in human bronchial cell monolayers. Confocal microscopy images showed continuous lines of the ZO-1 protein in control cells (21% O_2), whereas reduced intensity signals and discontinuous lines were seen in cells exposed to 95% O_2 and in monolayers exposed to hyperoxia and supplement with antioxidant vitamins.

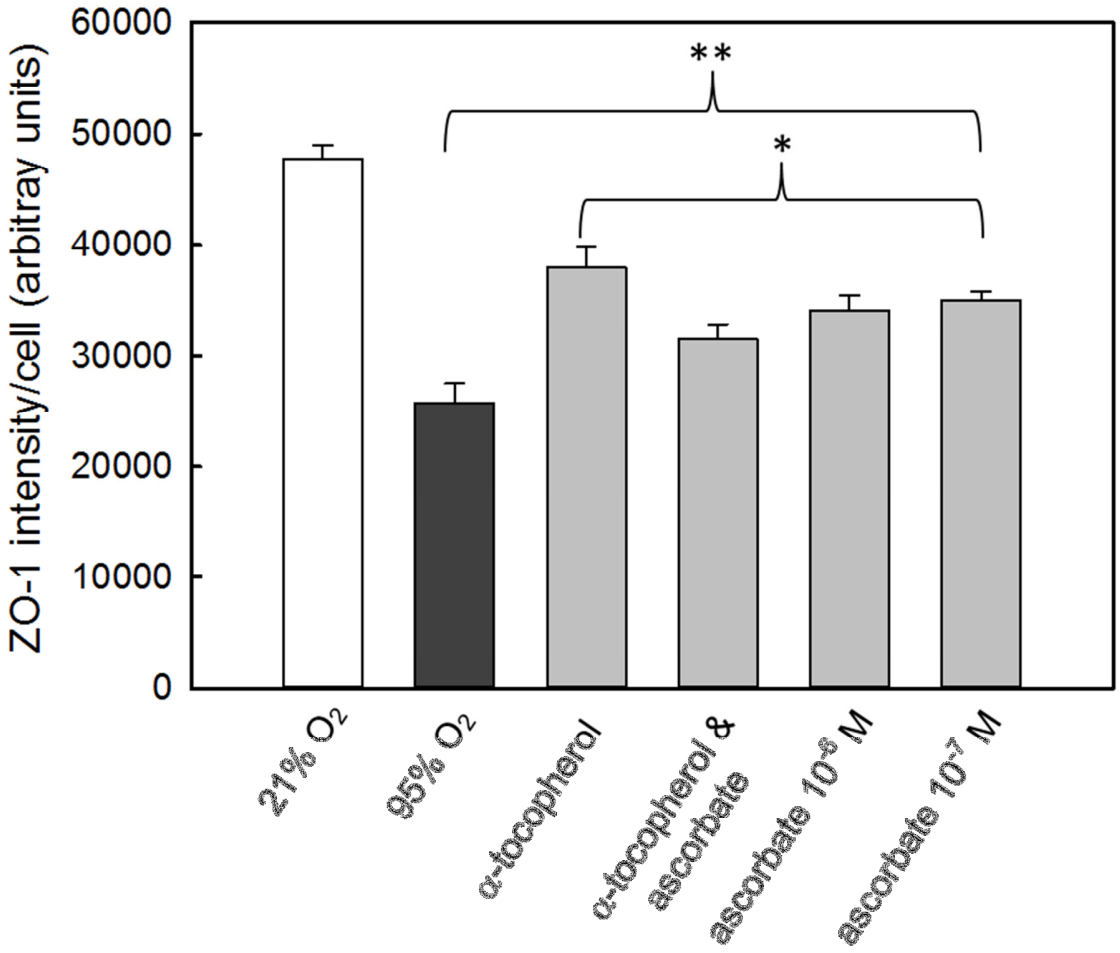

Figure 5.15 Immunofluorescence staining was performed to determine the intensity of ZO-1 protein in human bronchial cell monolayers using confocal microscopy. The ZO-1 staining intensity assessed using the Neuron J tracing tool. Data are means ± SE, *n* = 3. **significant difference compared to control ($P < 0.01$), *significant difference compared to hyperoxia (Fisher's SD, $P < 0.05$). Three different experiments with triplicate samples for each were used.

5.3.3 ZO-1 mRNA expression in bronchial cells by hyperoxia

Hyperoxia significantly reduced the expression of ZO-1 gene in both hyperoxic cells and hyperoxic cells treated with antioxidant vitamins compared to the control cells ($P < 0.001$, Figure 5.16, overleaf). A statistically significant increase in expression levels was seen in cells co-cultured with antioxidant vitamins under hyperoxia compared to cells exposed to hyperoxia only (0.51 ± 0.03 95% O_2, 0.64 ± 0.01 with α-tocopherol, 0.69 ± 0.03 with α-tocopherol and ascorbate, 0.72 ± 0.02 with 10^{-6} M ascorbate and 0.76 ± 0.02 with 10^{-7} M ascorbate, $P < 0.05$).

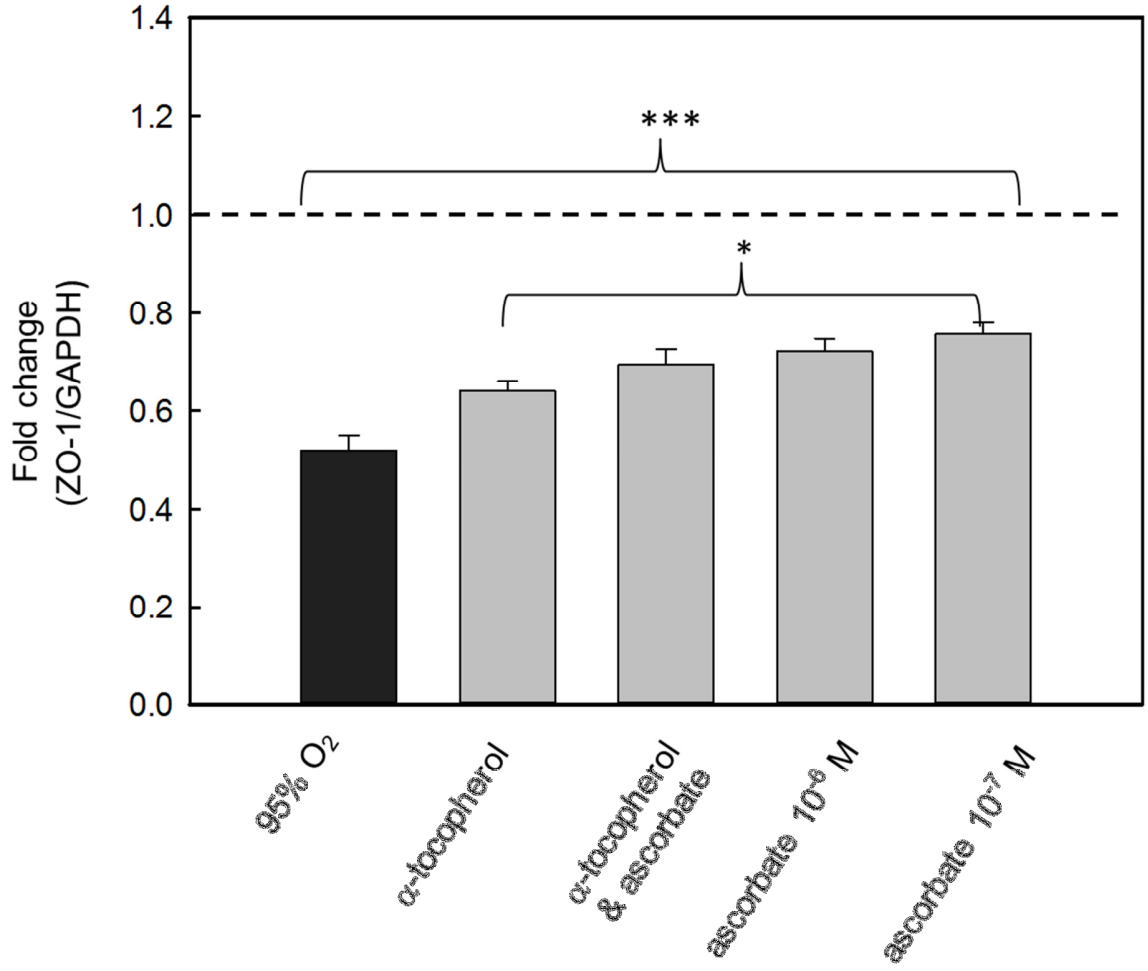

Figure 5.16 ZO-1 gene expression in 16HBE14o- cells, in response to hyperoxia and hyperoxia plus antioxidant vitamins after 24 h of treatment. The gene expression was assessed by qRT-PCR. Data are means ± SEM, *n* = 3. *significant difference P < 0.05 compared to hyperoxia, ***significant difference P < 0.001 compared to normoxia (express as dotted line at 1.0). Three different experiments with triplicate samples for each were used.

5.3.4 Determination by ELISA of pro-inflammatory cytokines released into the medium in response to hyperoxia

The levels of IL-6, IL-8 and TNF-α released into the medium were measured using ELISA. The mean concentration for the three cytokines was significantly higher in hyperoxic cells (IL-8, 1247.9 ± 5.1; IL-6 1884.41 ± 6.6; and TNF-α, 124 ± 6.2 pg ml^{-1}) compared to normoxic cells (IL-8 590.8 ± 3.7; IL-6, 549.3 ± 4; and TNF-α, 27.1± 2.8 pg ml^{-1}, $P < 0001$ in all cases), as shown in Figure 5.17, overleaf. The results also showed that the introduction of antioxidant vitamins significantly reduced the levels of inflammatory cytokines in the culture medium induced by hyperoxia ($P<0.05$). The mean concentrations were: 10^{-7} M α-tocopherol IL-8, 984.7 ± 5.1; IL-6, 1337.8 ± 5.3; and TNF-α, 87.4 ± 3.2 pg ml^{-1}; α-tocopherol and ascorbate IL-8, 953.7 ± 3.6; IL-6, 1291.6 ± 4.2; and TNF-α, 82.3 ± 2.9 pg ml^{-1}; 10^{-6} M ascorbate IL-8, 1036.8 ± 3.8; IL-6, 1435.7 ± 4.1; and TNF-α. 92.1 ± 3.5 pg ml^{-1} and 10^{-7} M ascorbate IL-8, 911.2 ± 4.7; IL-6, 1317.9 ± 5.3, and TNF-α, 81 ± 3.2 pg ml^{-1} compared to hyperoxia alone. Despite this significant reduction, treatment with antioxidant vitamins still had only modest effect, and a significant increase in the cytokine level in medium from cells co-cultured with antioxidant vitamins compared to the normoxia control was again observed (Figure 5.17).

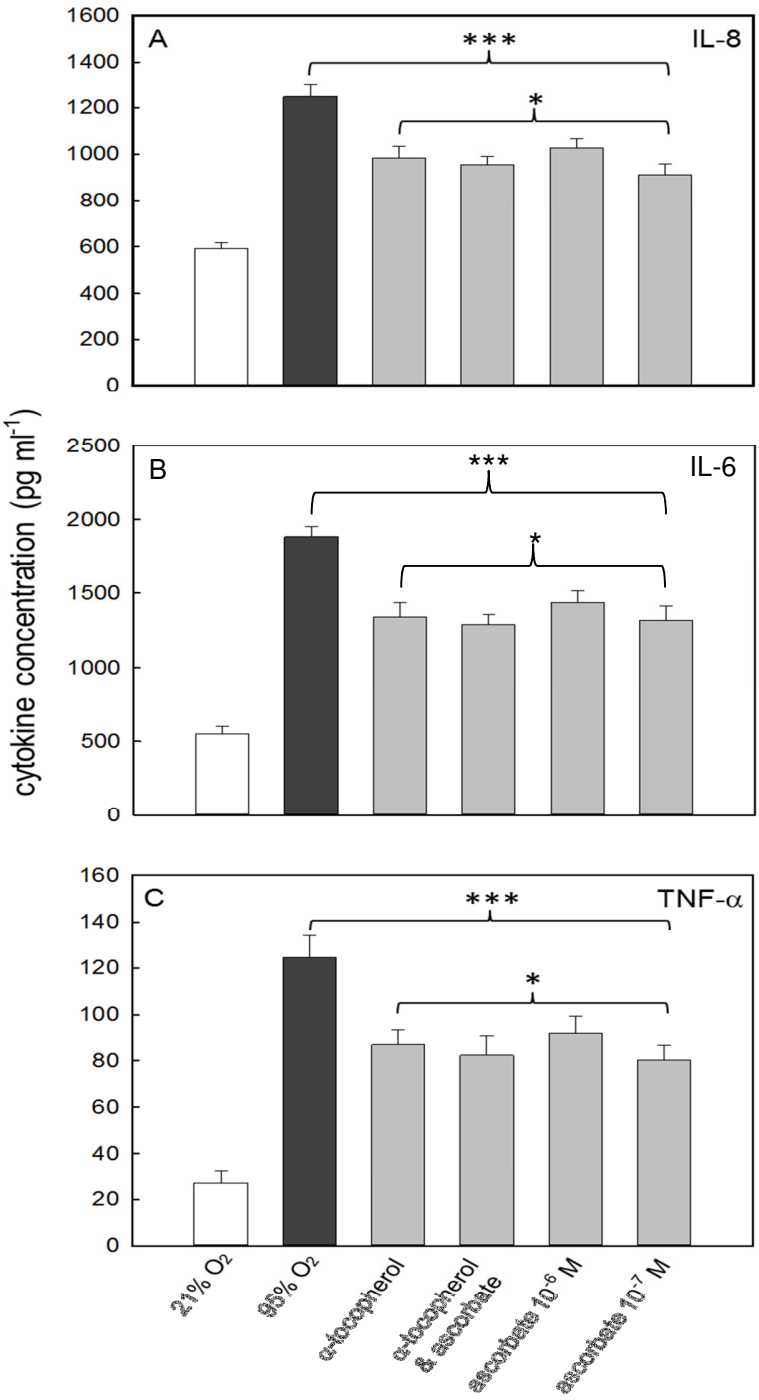

Figure 5.17 Concentrations of the pro-inflammatory cytokines IL-8 (A), IL-6 (B) and TNF-α (C), determined by ELISA, released into the medium by 16HBE14o- cells, in response to hyperoxia treatment for 24 h in the presence or absence of antioxidant vitamins C (ascorbate) and E (α-tocopherol). Data are means ± SE, n = 3. * significant difference ($P < 0.05$) compared to hyperoxia. *** significant difference ($P < 0.001$) compared to control (normoxia). Three different experiments with triplicate samples for each were used.

5.3.5 pro-inflammatory cytokines mRNA expression of in 16HBE14o- cells by hyperoxia

Exposure of cells to hyperoxia for 24 h significantly upregulated the expression of the genes of IL-8, IL-6 and TNF-α cytokines (2.10 ± 0.06 with IL-8; 1.93 ± 0.05 with IL-6 and 2.05 ± 0.06 with TNF-α, $P < 0.001$) compared to normoxia (Figure 5.18, page 164). This hyperoxia-induced increase in cytokine gene expression was significantly decreased by antioxidant vitamins (IL-8, 1.50 ± 0.03 with α-tocopherol; 1.32 ± 0.05 with α-tocopherol and ascorbate; 1.48 ± 0.03 with ascorbate at 10^{-6} M; and 1.55 ± 0.05 with ascorbate at 10^{-7} M; for IL-6, 1.38 ± 0.05 with α-tocopherol; 1.54 ± 0.02 with α-tocopherol and ascorbate; 1.44 ± 0.03 with ascorbate at 10^{-6} M; and 1.69 ± 0.02 with ascorbate at 10^{-7} M; for TNF-α 1.65 ± 0.02 with α-tocopherol; 1.54 ± 0.04 with α-tocopherol and ascorbate; 1.43 ± 0.04 with ascorbate at 10^{-6} M; and 1.50 ± 0.02 with ascorbate at 10^{-7} M; $P < 0.01$ in all cases). Although, this reduction in expression by antioxidant vitamins was significant) compared with hyperoxia, there was a highly significant difference ($P < 0.001$) in the cytokine gene expression compared to normoxia (Figure 5.18, overleaf).

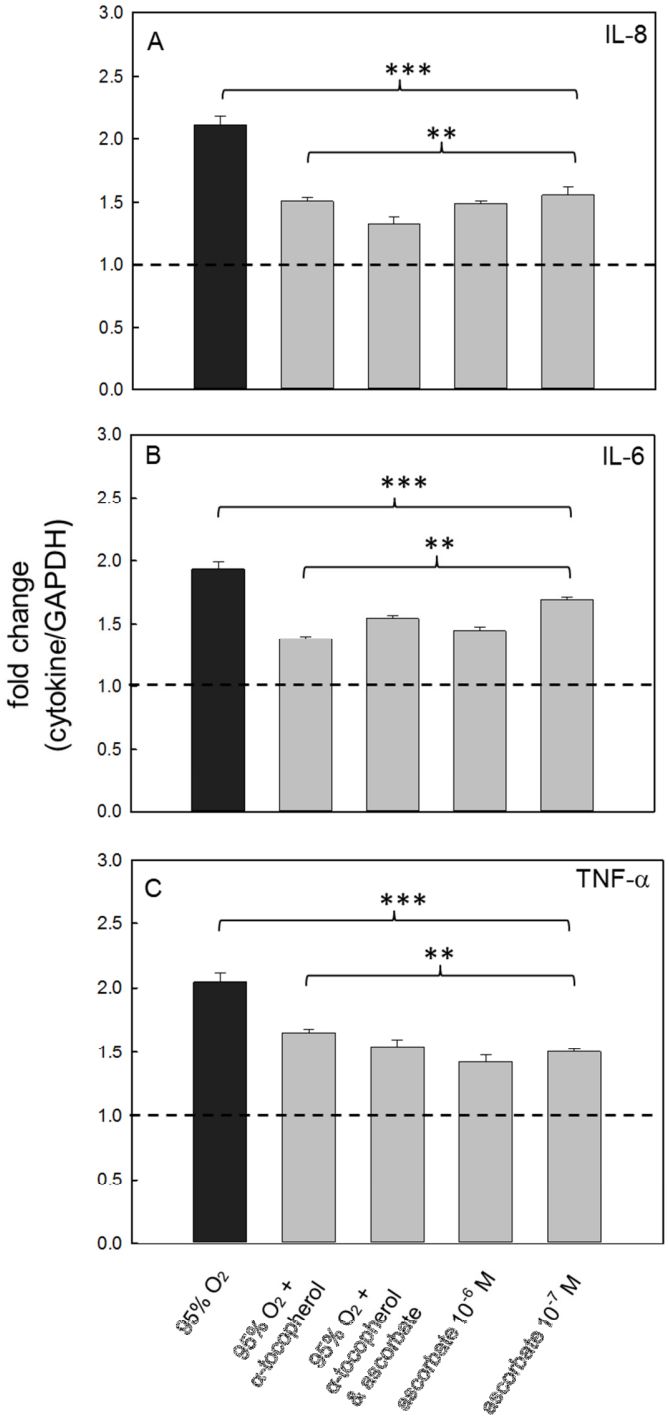

Figure 5.18 IL-8 (A), IL-6 (B) and TNF-α (C) gene expression in 16HBE14o- cells, in response to hyperoxia and antioxidant vitamin supplementation after 24 h of exposure. Gene expression was assessed by qRT-PCR. Data are means ± SEM, *n* = 3. * significant difference ($P < 0.01$) compared to hyperoxia. ** significant difference ($P < 0.001$) compared to normoxia (expressed as dotted line at 1.0). Three different experiments with triplicate samples for each were used.

5.4 Discussion

Hyperoxia has been identified as a contributor to acute and chronic lung injury, and there is a body of research that has been undertaken towards understanding the mechanisms behind its deleterious effects (Barazzone et al., 1998, Allen et al., 2000). However, the molecular aspect mechanisms involved in the pulmonary epithelial barrier disruption and treatment are still deficient. Therefore, this study was carried out to evaluate some aspects of the molecular mechanisms that contribute to hyperoxia-induced disruption of ciliated epithelium integrity. In addition, to examine the effects of antioxidant vitamins (α-tocopherol and ascorbate) in protecting against hyperoxia-induced paracellular permeability one of the key tight junction linkage proteins ZO-1 and the pro-inflammatory mediators IL-8, IL-6 and TNF-α were investigated. The 16HBE14o- cell line was employed because it exhibits important characteristics of bronchial epithelial cells such as the formation of tight junctions (TJ) when grown at an air liquid interface. Furthermore, it is known that the junction integrity can be modified under physiological and pathophysiological conditions resulting in changes in monolayer permeability (Forbes, 2000).

The results indicated that hyperoxia (i) weakened the 16HBE14o- cell line leading to increased monolayer permeability as indicated by a significant decrease in transepithelial electrical resistance; (ii) down-regulated ZO-1 gene expression consistent with (iii) a decline in ZO-1-associated fluorescence, which was estimated, using the Neuron J tracing tool in the ImageJ image analysis package

(the first time to the author's knowledge that this approach has been used) and (iv) resulted in increased pro-inflammatory cytokine production accompanied by (v) up regulation of cytokine gene expression, suggesting that inflammatory mediators might play a role in the hyperoxia-induced bronchial epithelial cell disruption. Furthermore, (vi) the antioxidant vitamins α-tocopherol and ascorbate, individually or in combination, partially protected against the impact of hyperoxia, i.e. improved levels of ZO-1 expression, increased ZO-1 associated fluorescence, decreased cytokine secretion and gene expression. However, the protective effect of the vitamins was not enough to significantly reduce the epithelial permeability.

Epithelial barrier function depends on cellular TJ integrity. Structural alterations in TJs that may result in the diffuse infiltration of inflammatory cells, and increased pulmonary oedema have been reported in *in vivo* studies (Warner et al., 1998, Altemeier and Sinclair, 2007). Several mechanisms have been proposed to be involved in the rapid disruption of TJ integrity, one of which is an involvement of ROS, particularly H_2O_2 (Rao, 2008). H_2O_2 is known to disrupt the association between ZO-1 and occludin in the TJ complex (Yu et al., 2012). For example, exposure of airway epithelial (Calu-3) cells to H_2O_2 resulted in remodelling of the actin cytoskeleton and redistribution of ZO-1 and occludin in TJs (Boardman et al., 2004). Since hyperoxia has been shown to stimulate ROS production (Altemeier and Sinclair, 2007), it has been suggested that ROS might be involved hyperoxia-induced TJ disruption by alteration of the structure and function of the junctions, either by causing direct modification of the structure and function of TJ proteins or indirectly by modulating signaling pathways. For example, the decreased expression of ZO-1 seen in this work suggests a role of signaling in the regulation

of TJ permeability. It has been shown that oxidative stress moderated protein tyrosine phosphatase and tyrosine kinase activities resulting in an increased cellular protein tyrosine phosphorylation (Rao et al., 2000). TJ and adherens junction (AJ) proteins are possible targets for tyrosine phosphorlation (Collares-Buzato et al., 1998). H_2O_2 has been found to be the ROS species involved in Caco-2 monolayer permeability by the oxidation of protein thiol and glutathione (Rao et al., 2000). Moreover, oxidative stress increases epithelial permeability accompanied by tyrosine phosphorylation and disruption of TJ proteins, and tyrosine kinase inhibitors can provide protection against oxidation (González-Mariscal et al., 2003). Rao et al. (2002) demonstrated that oxidative stress induced redistribution of occludin-ZO-1 and E-cadherin-β-actin complexes, dissociation of occludin and ZO-1, and dissociation of the actin cytoskeleton and TJ/AJ complexes. Protection by genistein (a tyrosine kinase inhibitor) suggested the role of tyrosine kinase in the reassembly of junctional complexes in a MDCK kidney cell line (Meyer et al., 2001). In addition, the disruption of cytoskeletal elements and actin microfilaments by cytochalasin-b (cell permeable mycotoxin) causes disruption of TJs and desmosomes, increasing paracellular permeability and restructuring of junctional complexes in intestinal Caco-2 monolayers (Ma et al., 1995). The findings of these studies are supported by this study, the results of which results included the increase of intact sloughing cells into the medium (Chapter 3) and the reduction of ZO-1 protein-associated fluorescence. The decrease in the level of expression of ZO-1 observed here suggests a role of signaling molecules in the regulation of TJ permeability. You et al. (2012) suggested that the decline in ZO-1 and occludin mRNA expression, accompanied

by an increase in restructuring of TJ observed over time in hyperoxia-exposed neonate rats was due to the effect of hyperoxia on synthesis of these proteins at the transcriptional level.

Also, another mechanism that may be involved in the oxidant-mediated TJ structure/function alteration is increasing levels of intracellular calcium (Welsh et al., 1985).It has been shown that membrane lipid peroxidation leads to phospholipids acting as an ionophores, resulting in an increase in intracellular calcium (Serhan et al., 1981) . The accumulation of calcium in hepatocytes, for example, makes the cells more vulnerable to oxidative damage (Thor et al., 1984). Martinez-Palomo et al. (1980) have shown that Madin-Darby canine kidney (MDCK) monolayer permeability increases when the calcium concentration rises via the action of ionophores; suggesting the role of calcium in sealing and stabilize the structure of the occludin junction.

Cytokine-mediated inflammation also plays a crucial role in many types of lung injury (Goodman et al., 2003). The increase in secretion of pro-inflammatory cytokines (TNF-α, IL-6 and IL-8) in the medium and expression of these cytokines indicated in this study supports the idea that inflammation is one of the factors that affects the epithelial barrier. It has been shown that TNF-α decreases expression of the genes for occludin and ZO-1 as well as other TJ proteins, alters the localisation of these proteins in TJs and leads to the functional opening of TJs, suggesting a role of TNF-α in lung barrier dysfunction (Coyne et al., 2002). For example, Mazzon and Cuzzocrea (2007) showed that inhibition of TNF-α, either pharmacologically (using etanercept) or genetically (using TNF-α R1 knockout

mice), in carrageenan-induced lung inflammation in mice, protected against the loss of TJ proteins and reduced inflammatory cell infiltration. Moreover, an increase in the pro-apoptotic protein, Bax, and a decrease in the anti-apoptotic protein, Bcl-2, were shown to be mediated by TNF-α (Mazzon and Cuzzocrea 2007). Another signaling pathway that has been found to be associated with an increase in IL-8 and cell apoptosis is the activation of Fas ligand in primary human bronchiolar epithelial cells (Hagimoto et al., 1999). Thus, the pulmonary epithelial cell response to inflammatory stimuli involves the activation of apoptotic pathways and inflammatory cascades (Hu et al., 1999).

It is important to distinguish between the two functional roles of TJs- gate functions (permeability) and fence functions (polarity). It has been found that actin depolymeriser cytochalasin D caused a significant decrease in gate function in the Caco-2 cell line, characterized by a rapid decline in TER, but the change in ZO-1 level and occludin localization was modest to the effect of NH_4Cl on these protiens (Musch et al., 2006). These finding should be taken with interest in future studies as the actin filaments associated with ZO-1 and other proteins junctional complex responsible on the cytoskeleton structure.

One of the approaches used to reduce lung injury by oxidants is to restore the antioxidant/oxidant pool by supplementing with antioxidants. As glutathione is considered to be a major antioxidant in epithelial lung fluid where the level is about 40 fold more than in the plasma, several studies have attempted to restore the glutathione level in the airway tract. For example, aerosolized glutathione has been found to increase the glutathione level in the pulmonary epithelial fluid (Buhl et al.,

1990). Additionally, transport of glutathione against a concentration gradient has been observed in alveoli cell type II (Hagen et al., 1986).

To assess the protective role of antioxidant vitamins on bronchial cell integrity, α-tocopherol (vitamin E, lipid-soluble) and ascorbate (vitamin C, water-soluble) were chosen in this study to provide protection against lipid peroxidation and aqueous free radicals, respectively. The results of this study show for the first time that these antioxidant vitamins attenuate the effects of hyperoxia on the production of inflammatory mediators and ZO-1 expression in the 16HBE14o- cell line. However, this attenuation was partial, as there were still significant effects of hyperoxia compared to normoxia even in the presence of a combination of these antioxidants. Vitamin E can also exert other effects in cells because of its other biological functions. For example, it exhibits inhibitory effects on cell proliferative and protein kinase C activity in vascular smooth muscular cells, where the proliferation of these particular cells has been associated with arteriosclerosis and hypertension (Tasinato et al., 1995). Similarly, Boscoboinik et al. (1991) have demonstrated the non-antioxidant protective actions of vitamin E through the inhibition of protein kinase C, which is involved in several pro-inflammatory signaling pathways.

Vitamin C has been found to protect against free radical damage in the lung and central nervous system (Iqbal et al., 2004). The xanthine oxidoreductase has been found to be involved in different respiratory and cardiovascular diseases associated with oxidative stress such as acute lung injury enzyme (Boueiz et al., 2008); and implicated in the disruption of integrity of barrier endothelial cells in lung (Boueiz et al., 2008). Pretreatment with ascorbic acid significantly diminishes the lung damage caused by superoxide anion in guinea pig trachea instillation with

xanthine oxidase/ xanthine solution (Becher and Winsel, 1989). Furthermore, ascorbate might act as an anti-inflammatory agent *in vivo*- a cross sectional study of 3258 men suggested an inverse association of vitamin C and dietary intakes with inflammation biomarkers (Wannamethee et al., 2006). In addition, there may be a synergistic effect of vitamin C in combination with vitamin E because of its ability to regenerate the active form of vitamin E. Kagan et al. (1992) reported that vitamin C recycles endogenous vitamin E by its ability to reduce chromanoxyl radicals to chromanol in low density lipoproteins. Moreover, vitamin E in combination with vitamin C has been found to markedly reduce pro-inflammatory activity and oxidative damage, as well as protect cell viability and integrity induced by exposure to tobacco smoking in a human brain endothelial cell line, (Hossain et al., 2011). Caco-2 cells incubated with H_2O_2 showed increase in monolayer permeability and treatment with vitamin E and A ($OH^{\bullet}$ scavenger) had no reducing effect in this regard (Rao et al., 2000). The effect of vitamins in this study with the increase of total glutathione in homogenate tissue (Chapter 4), suggested that it is likely that H_2O_2 mediated the oxidative damage by hyperoxia. Therefore, using a catalase mimetic or treatment with thiol compounds such as GSH might provide protection through the inhibition of thiol oxidation and tyrosine phosphorylation. Further studies are therefore needed to elucidate the role of each hyperoxia-generated ROS involved in epithelial monolayer disruption in order that a suitable antioxidant can be suggested.

Chapter 6: General discussion and future work

6.1 General discussion

The airway epithelium is in direct contact with the outer environment, particularly the bronchial epithelial tissue, which is vulnerable to damage as a consequence of oxidative stress (Narasaraju et al., 2003). Hyperoxia leads to pathophysiological consequences and inflammation, and several researchers have described the excess production of ROS in response to hyperoxia exposure leading to alteration in signaling and cell death. Respiratory epithelial tissue has specific functions that maintain pulmonary homeostasis under normal and disease conditions. Mucociliary clearance is one of these functions, and is dependent on good ciliary function.

Quantitative analysis of ciliary coverage under hyperoxic conditions was the first major aim of this work. It is difficult to extrapolate results taken from small animal studies to larger ones, and it is only possible to obtain human bronchial epithelium through invasive techniques such as bronchoscopy (see Chapter 3 for more details). Researchers have described similar anatomy and physiology of bovine upper respiratory tract epithelium in comparison to humans. Therefore, the first objective of this study was to develop a primary tissue culture model, using bovine bronchial tissue. Despite the successful use of the model in this study, there were some challenges such as the cartilage thickness, which is not only hard to deal with during preparation of the tissue for culture, but also is believed to affect the diffusion of nutrients from the medium into the samples. Another disadvantage was the length and the tendency of cilia to ‘fold over’. These problems could be avoided in future by using smaller airway (bronchiole) samples. However, that cell

phenotypes differ between large and small airways should be considered, and so a systematic survey of the smaller bovine airways would be necessary in order to establish the limit where cilial coverage is still as close to 100% as possible. As an alternative, the approach of using bovine primary epithelial cell culture, which it was hoped would show less variability, was tried (Chapter 3). The submerged cell culture method was used; although this maintains epithelial cells for culture periods of several weeks, ciliated cell morphological differentiation and function has been described to be suppressed under these conditions (Clark et al., 1995). This method could be further developed in future studies by culturing isolated bovine bronchial cells at an air-liquid interface using collagen coated Transwell inserts. Also a comparative study between primary bovine cell and human cell line used in this work (16HBE14o-) in generating ciliated epithelial cells and tight junction might lead to the development of an appropriate cell culture model for such studies in future.

A method to quantitatively estimate ciliary coverage was developed that was applicable for use with a large animal model. This aim was achieved with some success, using readily available ImageJ software to quantitatively measure cilia coverage surface, instead of more complex image analysis methods or observational estimation used in methods applied in the literature (see Chapter 3). Culturing bovine bronchial tissue under elevated oxygen fraction led to a decline in the ciliary coverage over time. The culture model and the image analysis technique demonstrated an adverse effect of elevated oxygen on ciliary coverage. The fluorescence labeling used in this study with primary cell culture raised some issues with non-specific binding (see chapter 3 for more details); it would be

interesting to alternatively estimated ciliary coverage by using fluorescence labeling with tissue culture; this technique has been used previously in ciliogenesis studies using tissue and cell (Ostrowsk and Nettesheim, 1995, Toskala et al., 2005). Also possibly furture optimization of method might reduce this problems.

The second objective in this study was to investigate the possible association between non–enzymatic antioxidant supplementation, particularly α-tocopherol and ascorbate, and acquired tolerance of ciliated bronchial epithelial cells to hyperoxia (Chapter 3 and 5). The naturally occurring antioxidant content in the tissue should be considered; a point of interest is that the samples used for the experiments here were isolated from blood supply and *in vivo* physiological antioxidant nutrition and thus the level of vitamins in cells might have been affected. The deficiency of these vitamins in the tissue might be one of the explanations of the slight loss of ciliary coverage over time noted when tissue samples were cultured under normoxia. Vitamin C is produced in most animals from glucose, but primates, guinea pigs and humans lack this ability (Pollock and Mullin, 1987), due to the gene (*Gulo*) for gulonolactone oxidase, the enzyme that catalyzes the last step of ascorbate synthesis, being missing (Nishikimi et al., 1988). Although, vitamin C significantly decreased in plasma and tissue after one week in $Gulo^{-/-}$ mice, where the gulonolactone oxidase is not expressed and dietary vitamin C is required, however, some tissue including the lungs maintained the vitamin C concentration at 25% of wild type level upon vitamin C withdrawal (Kim et al., 2012), suggesting that there may be an uncharacterized pathway to produce ascorbate in small amount.

To gain more understanding of the mechanism of oxidative stress involvement in cilia loss, studies of biochemical markers (LDH, total glutathione, lipid peroxidation,

damage to DNA, protein oxidation) to indicate oxidative damage in the bovine bronchus tissue were carried out (Chapter 4). One of the questions that requires further investigation is whether the damage of epithelial cells by ROS (i.e. lipid peroxidation resulting in cell membrane disruption and intracellular enzyme leakage), promotes cell sloughing (tight junction weakness) as seen in results presented in this work. Detection of specific intracellular ROS generated by hyperoxia would enable more effective antioxidants to be used. For example, using fluorescence probes that allow the measurement of specific fluorescent products produced from the reaction of ROS with that probe (Kalyanaraman et al., 2012). For example, dichlorofluorescein is used to detect H_2O_2 and diydroethidium to detect $O_2^{\bullet}$, with the probes fluorescing when oxidized by a specific ROS (Zhang et al., 2003).

The interruption of cell death pathways is an approach used in recent studies investigating protective or therapeutic schemes against oxidative stress. Mitogen activation of protein kinase (MAPK) and caspase (e.g. 3, 8 and 9) has been associated with cell death caused by oxidative stress. Hyperoxia activates the generation of ROS by mitochondrial and NAPDH oxidases. Blocking these pathways with a flavoprotein inhibitor (diphenylene iodonium) can reduce the activation of MAPK including extracellular signal regulated kinase 1/2 (ERK1/2) in murine epithelial cells resulting in decrease the activation of caspase-9 and 3 and the release of cytochrome *c*; this results suggested ERK1/2 as a vital signalling molecule for cellular death by ROS (Zhang et al., 2003). It is suggested that the association of these factors is investigated in future studies.

Results from this work demonstrated an increase in cell numbers in the medium (see Chapter 3), this is particularly important given the idea that the cell junctions, cell-cell or cell-membrane junction, are seen to be subject to oxidative stress resulting in sloughing cells. The objective of this part of the study was to detect the effects of hyperoxia on the predominant tight junction protein ZO-1 in human bronchus cell line 16HBE14o-; the possible role of pro-inflammatory cytokines in weakening tight junctions was also discussed in this work (Chapter 5). There was increase in IL-6, IL-8 and TNF-α secretion in cells exposed to hyperoxia and hyperoxia plus vitamin supplementation. However, there was a significant decrease in the levels of cytokines between antioxidant vitamin supplemented cells and normoxia. This was reflected in the mRNA expression level of cytokines. Oxygen toxicity occurred through direct ROS effects or indirectly by the inflammatory response activation, the subsequent effects of which include increased pulmonary permeability and propagation of various inflammatory cells (Altemeier and Sinclair 2007). The damage to the epithelial cell barrier results in alteration the permeability and fluid accumulation within the lungs. Increase in the permeability has been reported as a consequence of inflammation; primary human bronchial epithelial cells incubated with a combination of TNF-α and IFN-γ resulted in alteration in TJs with a decrease in TJ strand numbers and depth. These changes have been shown to be regulated through the upregulation of protein kinase C PKC (Coyne et al., 2002).

It is believed that this is the first study that subjected a human bronchi cell line to an investigation of the effect of cytokine induction by hyperoxia on cell tight junction proteins. Previous studies attempted to evaluate the effect of cytokines on protein

junctions were based on an intestinal cell line- only one study by Coyne et al. (2002) used primary human bronchial epithelial cells from the airway of a cystic fibrosis patient to detect the effect of cytokines on several TJ properties. *In vivo* an inflammatory cycle can be started from the increase production of IL-8 by epithelial cells leading to the attraction of neutrophils, and secretion of neutrophil elastase by these neutrophils, which in turn enhances the expression of IL-8 by epithelial cells (Nakamura et al., 1992). IL-6 has also been found to be secreted by epithelial cells, and is increased in sputum from COPD patients (Bhowmik et al., 2000). As the cultured cell are disconnected from blood, More broadly, research is also needed to mimic the *in vivo* environment, by co-culture with immune cells isolated from blood such as neutrophils and monocytes, or alternatively by using a human cell line, will provide a better idea about inflammatory mediator effects. For example, HL-60 (promyelocytic leukemia cells) can be differentiated into granulocytes such as neutrophils, monocytes, macrophages and eosinophils depending on the using of different compounds used to stimulate differentiation (Collins, 1987).

The results of this research supported the hypothesis that administration of antioxidant vitamins (α-tocopherol and ascorbate) reduced the loss of cilia (or ciliated cells) and enhanced integrity cells in response to hyperoxia-induced oxidative stress, and are consistent with other studies which demonstrated the protective role of antioxidant vitamins on cell integrity and function (see Chapters 1 and 5).

It has been found that of vitamin C not only has a protective role as a reducing agent (antioxidant), and in addition there are a few studies that suggest it acts as anti-inflammatory, in which a decrease in C-reactive protein concentration (as a

marker of inflammation) and fibrinogen associated with endothelial dysfunction has been reported in patients with different pulmonary diseases (Block et al. 2004, Wannamethee et al. 2006). Moreover, vitamin C has been reported to increase neutrophil chemotaxis via the enhancement of detoxification of the histamine in blood (Johnston et al. 1992). This is mean that ascorbate can also act as a pro-oxidant leading to production of hydroxyl radicals ($OH^{\bullet}$) in the presence of iron or copper ions, so perhaps this contributes to the incomplete protection offered by ascorbate seen here. In addition, it has been postulated that vitamin C is involved in the production and modulation of pro-inflammatory cytokines and leukocyte activities. Elevated pro-inflammatory cytokines production, IL-1 beta, IL-6 and TNF-α, in response to oxidative stress evoked by smoking exposure and the pro-inflammatory monocyte properties were decreased after treatment with the antioxidant vitamins C and E (Hossain et al., 2011). However there is a limitation with respect to the dose and time response, and more studies are needed to confirm the anti-inflammatory role of vitamin C, particularly in epithelial tissue.

The reason for the incomplete protection found here with the combination of ascorbate and α-tocopherol is uncertain, although one possibility is that H_2O_2 was responsible for some of the effects of hyperoxia on monolayer integrity, since the main activity of α-tocopherol is against lipid peroxyl radicals and ascorbate is not noted for an ability to directly detoxify H_2O_2. Nevertheless, there is clearly a relationship between ascorbate and glutathione, which certainly would be involved in detoxification of H_2O_2, and which we have shown previously is elevated in ciliated epithelium when bovine bronchial tissue is cultured under 95% O_2.

6.2 Conclusion and suggestions for future work

The following conclusions can be drawn from the present study:

1- The unique bovine culture model used in this study has proved to be promising model for the investigation of mechanisms by which hyperoxia leads to ciliary loss. This method is not only accurate to apply for estimated ciliary coverage from large animal SEM images but also easy to apply. The biochemical results confirmed previous findings of the deleterious effects of hyperoxia used with small animal or cell line and contributes additional evidence to gain a better understanding of the underlying mechanisms. This model may serve as a basis for future studies regarding oxidative damage and possible treatment in pulmonary ciliated epithelium.

2- This work provided new evidence in the mechanisms of hyperoxia-induced monolayer permeability in human bronchial cell line. The results indicated that hyperoxia targets ZO-1 protein localization and synthesis accompanied by the potential role of pro-inflammatory mediators

3- This work provided the first insight into the protective role of antioxidant vitamins α-tocopherol (vitamin E) and ascorbate (vitamin C) against ciliary loss and increase monolayer permeability by hyperoxia. However, the partially protection of these antioxidant found in this study suggested that rather a combination of events mediated the ciliated epithelial loss and disruption of the epithelial barrier under hyperoxic conditions. Also the

results support the idea that H_2O_2 may be the major ROS species that might be involved in cell damage.

Many complicated signalling pathways are involved in hyperoxia-induced cell death, which is regulated by redox-sensitive transcription factors and MAPKs transduction pathways. NF-κB plays a crucial role in mediated cell death and in inflammatory responses. Therefore one possibility for further work may be the inhibition of NF-κB activity a particular points during exposure hyperoxia. NF-κB/luc transgenic mice, for example, could be used for this purpose, where these animals have been used before as an indicator for NF-κB activity under hyperoxia. A better understanding of the signalling pathways behind epithelial cell death and the inflammation might help to identify new strategies to reduce oxidative lung injury.

A further interesting future topic is investigation of the association between hyperoxia and the inhibition of cellular repair mechanisms; the alteration of which may contribute to the structural and functional disruption of airway epithelium. Activating repair pathways may be lead to the development of therapeutic approaches for lung oxidative treatment.

In future investigations it might be possible to use the bovine bronchial tissue model used in this study to investigate the recovery stage after hyperoxia exposure; this research could be done with or without antioxidants.

Studies show that antioxidants are upregulated at lower levels of hyperoxia (< 60%) which can then protect against following exposure to high levels of oxygen (Comhair and Erzurum 2002), however, direct exposure to high levels of oxygen (>

95%) means that antioxidant expression is not rapid enough to mitigate lung injury (Yoo et al. 1994, Comhair et al.2000). Therefore, measuring the antioxidant levels in the bronchus tissue during the exposure and after in the recovery stage should be considered.

One of the mechanisms that have been suggested as being involved in hyperoxia-induced tight junction disruption is tyrosine phosphorylation. Therefore in the future, immunofluorescence assays using appropriate anti-phosphotyrosine antibodies could be used to detect tyrosine phosphorylation in hyperoxia exposed cells.

Overall, this work provided evidence, at least in part, of how hyperoxia can modulate cellular responses, and also of how antioxidants can reduce hyperoxia-induced monolayer permeability, and therefore perhaps reduce the risk of lung injury in critically ill patients. However, this research has thrown up many questions in need of further investigation before the association between ciliated cell loss and cell damage/death and hyperoxia more clearly understood.

References

Ahmed, M. N., Suliman, H. B., Floz, R. J., Grayck, E. N., Golson, M. L., Mason, N. & Auten, R. L. 2003. Extracellular superoxide dismutase protects lung development in hyperoxia.exposet newborn mice. *American Journal of Respiraory and Critical Care Medicine*, 16, 400-405.

Alberts, B., Johnson, A., Walter, P., Lewis, J., Raff, M. & Roberts, K. 2002. Molecular Biology of the Cell. 4 ed. Garland Publishing Inc,US.

Aldred, S. & Griffiths, H. R. 2004. Oxidation of protein in human low-density lipoprotein exposed to peroxyl radicals facilitates uptake by monocytes; protection by antioxidants *in vitro*. *Environmental Toxicology and Pharmacology*, 15, 111–117.

Allen, G., Menendezi, I., Ryan, M., Mazor, R., Wispe, J., Fiedler, M. & Wong, H. 2000. Hyperoxia synergistically increases TNF-a-induced interleukin-8 gene expression in A549 cells. *American Journal of Physiology,Lung Cellular and Moleucular Physiology*, 278, L253-L260.

Altemeier, W. A. & Sinclair, S. E. 2007. Hyperoxia in the intensive care unit: why more is not always better. *Current Opinion in Critical Care*, 13, 73-78.

Alttas, O. & H., A.-S. 2010. Effects of hyperoxia periodic training on free radicals production, biological antioxidants potential and lactate dehydrogenase activity in the lungs of rats, Rattus norvigicus. *Saudi Journal of Biological Sciences*, 17, 65-71.

Anderson, J. M. & Van Itallie, C. M. 2009. Physiology and Function of the Tight Junction. *Cold Spring Harb Perspectives in Biology*, 1, 002584.

Andreeva, A. V., Kutuzov, M. A. & Voyno-Yasenetskaya, T. A. 2007. Regulation of surfactant secretion in alveolar type II cells. *American Journal of Physiology. Lung Cellular and Molecural Physiology*, 293, L259-L271.

Auten, R. L. & Davis, J. M. 2009. Oxygen toxicity and reactive oxygen species: the devil is in the details. *Pediatric Research,* 66, 121-127.

Bakan, N., Taysi, S., Yilmaz, O., Bakan, E., Kuşkay, S., Uzun, N. & Gündoğdu, M. 2003. Glutathione peroxidase, glutathione reductase, Cu-Zn superoxide dismutase activities, glutathione, nitric oxide, and malondialdehyde concentrations in serum of patients with chronic lymphocytic leukemia.

Clinica Chimica Acta, International Journal of Clinical Chemistry, 338, 143-149.

Balda, M. S. & Matter, K. 2008. Tight junctions at aglance. *Journal of Cell Science* 121, 3677-3682.

Bankston, P. W., Porter, G. A., Milici, A. J. & Palade, G. E. 1991. Differential and specific labeling of epithelial and vascular endothelial cells of the rat lung by Lycopersicon esculentum and Griffonia simplicifolia I lectins. *European Journal of Cell Biology,* 54, 187-195.

Bannai, S. 1984. Induction of cystine and glutamate transport activity in human fibroblasts by diethyl maleate and other electrophilic agents. *The Journal of Biological Chemistry*, 259, 2435-2440.

Barazzone, C., Horowitz, S., Donati, Y. R., Rodriguez, I. & Piguet, P. 1998. Oxygen Toxicity in mouse lung: pathways to cell death. *American Journal of Respiratory Cell and Molecular Biology*, 19, 573-581.

Barazzone, C. & White, W. 2000. Mechanisms of cell injury and death in hyperoxia. *American Journal of Respiratory Cell and Molecular Biology*, 22, 517-519.

Barker, G. F., Manzo, N. D., Cotich, K. L., Shone, R. K. & Waxman, A. B. 2006. DNA Damage Induced by Hyperoxia: Quantitation and Correlation with Lung Injury. *American Jouranl of Respiratory Cell and Molecular Biology*, 35, 277-288.

Barnes, S. D., Agee, C. C., Peace, R. J. & Leffler, C. W. 1983. Effects of elevated Po2 upon tracheal explants. *Respiration Physiology*, 53, Pages 285–293.

Bellomo, R., Bailey, M., Eastwood, G. M., Nichol, A., Pilcher, D., Hart, G. K., Reade, M. C., Egi, M. & Cooper, D. J. 2011. The dangers of oxygen therapy – hyperoxia and mortality. *Critical Care*, 15, R90.

Bergen, Y. V. & Phillips, K. 2005. Size Matters. *The Journal of Experimental Biology*, 208, 1-3.

Bergmeyer, H. U. & Bernt, E. 1974. Lactate dehydrogenase. In: BERGMEYER, H. U. (ed.) *Methods in Enzymatic Analysis.*

Berlett, B. S. & Stadtman, E. R. 1997. Protein Oxidation in Aging, Disease, and Oxidative Stress. *The Journal of Biological Chemistry* ,15, 20313-20316.

Berthiaume, Y., Voisin, G. & Dagenais, A. 2006. The alveolar type I cells: the new knight of the alveolus?. *The Journal of Physiology*, 572, 609-610.

Betteridge, D. J. 2000. What is oxidative stress?. *Metabolism*, 49, 3-8.

Bhowmik, A., Seemungal, T. A., Sapsford, R. J. & Wedzicha, J. A. 2000. Relation of sputum inflammatory markers to symptoms and lung function changes in COPD exacerbations. *Thorax,* 55, 114-120.

Birnboim, H. C. 1988. A superoxide anion induced DNA strand-break metabolic pathway in human leukocytes: effects of vanadate. *Biochimestry and Cell Biology*, 66, 374-381.

Blanchard, B., Vena, M. M., Cavalier, A., Le Lannic, J., Gouranton, J. & Kobisch, M. 1992. Electron microscopic observation of the respiratory tract of SPF piglets inoculated with Mycoplasma hyopneumoniae. *Veterinary Microbiology*, 30, 329-341.

Block, G., Jensen, C., Dietrich, M., Norkus, E. P., Hudes, M. & Packer, L. 2004. Plasma C-reactive protein concentrations in active and passive smokers: influence of antioxidant supplementation. *Journal of the American Collage of Nutrition*, 23, 141-147.

Boardman, K. C., Aryal, A. M., Miller, W., M. & Waters, C. M. 2004. Actin re-distribution in response to hydrogen peroxide in airway epithelial cells. *Journal of Cellular Physiology* ,199, 57-66.

Boscoboinik, D., Szewczyk, A., Hensey, C. & Azzi, A. 1991. Inhibition of cell proliferation by alpha-tocopherol. Role of protein kinase C. *The Journal of Biological Chemistry*, 266, 6188-6194.

Boueiz, A. & Hassoun, P. M. 2009. Regulation of endothelial barrier function by reactive oxygen and nitrogen species. *Microvascular Research*, 77, 26-34.

Brash, D. E. & Havre, P. A. 2002. New careers for antioxidants. *PNAS USA*, 99, 13969-13971.

Brechot, J.-M., Hurbain, I., Fajac, A., Daty, N. & Bernaudin, J.-F. 1998. Different pattern of MRP localization in ciliated and basal cells from human bronchial epithelium. *Journal of Histochemistry and Cytochemistry*, 46, 513-517.

Breen, A. P. & Murphy, J. A. 1995. Reactions of oxyl radicals with DNA. *Free Radical Biology and Medicine*, 18, 1033–1077.

Brigelius-Flohe, R. & Traber, M. G. 1999. Vitamin E: function and metabolism. *FASEB Journal*, 13, 1145-1155.

Bruewer, M., Luegering, A., Kucharzik, T., Parkos, C. A., Madara, J. L., Hopkins, A. M. & Nusrat, A. 2003. Proinflammatory cytokines disrupt epithelial barrier function by apoptosis-independent mechanisms. *The Journal of Immunology*, 171, 6164-6172.

Buckley, S., Driscoll, B., Barsky, L., Weinberg, K., Anderson, K. & Warburton, D. 1999. ERK activation protects against DNA damage and apoptosis in hyperoxic rat AEC. *Amercan Journal of Physiology. Lung Cellular and Molecular Physiology*, 277, L159-L166.

Buhl, R., Vogelmeier, C., Critenden, M., Hubbard, R. C., Hoyt, R. F. J., Wilson, E. M., Cantin, A. M. & Crystal, R. G. 1990. Augmentation of glutathione in the fluid lining the epithelium of the lower respiratory tract by directly administering glutathione aerosol. *PNAS USA*, 87, 4063-4067.

Bukowski, D. M., Deneke, S. M., Lawrence, R. A. & Jenkinson, S. G. 1995. A noninducible cystine transport system in rat alveolar type II cells. *The American Jouranl of Physiology*, 268, L21-L26.

Carr, A. & Frei, B. 1999a. Does vitamin C act as a pro-oxidant under physiological conditions?. *FASEB Journal*, 13, 1007-1024.

Carr, A. C. & Frei, B. 1999b. Toward a new recommended dietary allowance for vitamin C based on antioxidant and health effects in humans. *The American Journal of Clinical Nutrition,* 69, 1086-1107.

Cerutti, P. A. 1994. Oxy-radicals and cancer. *The Lancet*, 344, 862-863.

Chambellan, A., Cruickshank, P. J., Mckenzie, P., Cannady, S. B., Szabo, K., Comhair, S. a. A. & Erzurum, S. C. 2006. Gene expression profile of human airway epithelium induced by hyperoxia *in vivo*. *American Journal of Respiratory and Molecular Biology*, 35, 424–435.

Chemuturi, N. V., Hayden, P., Klausner, M. & Donovan, M. D. 2005. Comparison of human tracheal/bronchial epithelial cell culture and bovine nasal respiratory explants for nasal drug transport studies. *Journal of Pharmaceutical Sciences*, 94, 1976-1985.

Chetty, A., Cao, G. J., Severgnini, M., Simon, A., Warburton, R. & Nielsen, H. C. 2008. Role of matrix metalloprotease-9 in hyperoxic injury in developing lung. *American Jouranl of Physiology Lung Cellular and Molecular Physiology*, 295, L584-L592.

Clark, A. B., Randell, S. H., Nettesheim, P., Gray, T. E., Bagnell, B. & Ostrowski, L. E. 1995. Regulation of ciliated cell differentiation in cultures of rat tracheal epithelial cells. *American Jouranl of Respiratory Cell and Molecular Biology*, 12, 329-338.

Clerch, L. B. & Massaro, D. 1993. Tolerance of rats to hyperoxia. Lung antioxidant enzyme gene expression. *The Journal of Clinical Investigation*, 91, 499-508.

Collins, S. J. 1987. The HL-60 promyelocytic leukemia cell line: proliferation, differentiation, and cellular oncogene expression. *Blood*, 70, 1233-1244.

Comhair, S. A., Thomassen, M. J. & Erzurum, S. C. 2000. Differential induction of extracellular glutathione peroxidase and nitric oxide synthase 2 in airways of healthy individuals exposed to 100% O(2) or cigarette smoke*. American Journal of Respiratory Cell and molecular Biology*, 23, 350-354.

Comhair, S. a. A. & Erzurum, S. C. 2002. Antioxidant responses to oxidant-mediated lung diseases. *American Jouranl of Physiology. Lung Cellular and Molecular Physiology*, 283, L246-L255.

Coraux, C., Martinella-Catusse, C., Nawrocki-Raby, B., Hajj, R. B., H., Escotte, S., Laplace, V., Birembaut , P. & Puchelle, E. 2005. Differential expression of matrix metalloproteinases and interleukin-8 during regeneration of human airway epithelium *in vivo*. *Journal of Pathology*, 206, 160-196.

Coraux, C., Roux, J., Jolly, T. & Birembaut, P. 2008. Epithelial cell–extracellular matrix interactions and stem cells in airway epithelial regeneration. *Proceeding of the American Thoracic Society*, 5, 689-694.

Cormack, D. H. 1998. Lungs. *Clinically integrated histology.* Philadelphia: Lippincott-Raven Publishers.

Cosentino-Gomes, D., Rocco-Machado, N. & Meyer-Fernandes, J. R. 2012. Cell signalling through protein kinase C oxidation and activation. *International Journal of Molecular Sciences*, 13, 10697–10721.

Coyne, B. C., Vanhook, M. K., Gambling, T. M., Carson, J. L., Boucher, R. C. & Johnson, L. G. 2002. Regulation of Airway Tight Junctions by Proinflammatory Cytokines. *Molecular Biology of the Cell*, 13, 3218-3234.

Cozens, A. L., Yezzi, M. J., Kunzelmann, K., Ohrui, T., Chin, L., Eng, K., Finkbeiner, W. E., Widdicombe, J. H. & Gruenert, D. C. 1994. CFTR expression and chloride secretion in polarized immortal human bronchial epithelial cells*. American Jouranl of Respiratory Cell and Molecular Biology*, 10, 38-47.

Crapo, J. D., Barry, B. E., Foscue, H. A. & Shelburne, J. 1980. Structural and biochemical changes in rat lungs occurring during exposures to lethal and adaptive doses of oxygen. *The American Revieew of Respiratory Disease*, 122, 123-143.

Crosby, L. M. & Waters, C. M. 2010. Epithelial repair mechanisms in the lung. *American Journal of Physiology Lung Cellular and Molecular Physiology*, 298, L715-L731.

Cross, C. E., Van Der Vliet, A., O'neill, C. A., Louie, S. & Halliwell, B. 1994. Oxidants, antioxidants, and respiratory tract lining fluids. *Environmental Health Perspectives*, 102, 185-191.

D'agostino, D. P., Olson, J. E. & Dean, J. B. 2009. Acute Hyperoxia Increases Lipid Peroxidation and Induces Plasma Membrane Blebbing in Human U87 Glioblastoma Cells. *Neuroscience*, 159, 1011-1022.

D'angio, C. T. & Finkelstein, J. N. 2000. Oxygen regulation of gene expression: a study in opposites. *Molecular Genetics and Metabolism*, 71, 371-380.

Davies, K. J. A. 1987a. Protein Damage and Degradation by Oxygen Radicals 1. General Aspects. *The Jurnal of Biological Chemistry*, 262, 9895-9901.

Davies, K. J. A., Lin, S. W. & Pacifici, R. E. 1987c. Protein Damage and Degradation by Oxygen Radicals IV Degrdation of Denatured Protein. *The Journal of Biological Chemistry*, 262, 9914-9920.

Davies, K. J. A., M.E., D. & Lin, S. W. 1987b. Protein Damage and Degrdation by Oxygen Radical II Modification of amino acids. *The Journal of Biological Chemistry*, 262, 9902-9907.

De Paepe, M. E., Mao, Q., Chao, Y., Powell, J. L., Rubin, L. P. & Sharma, S. 2005. Hyperoxia-induced apoptosis and Fas/FasL expression in lung epithelial cells. *American Journal of Physiology. Lung Cellular and Mollecular Biology*, 289, L647-L659.

De Water, R., Willems, L. N., Van Muijen, G. N., Franken, C., Fransen, J. A., Dijkman, J. H. & Kramps, J. A. 1986. Ultrastructural localization of bronchial antileukoprotease in central and peripheral human airways by a gold-labeling technique using monoclonal antibodies. *The American Review of Respiratory Disease*, 133, 882-890.

Dean, J. B., Mulkey, D. K., Henderson, R. A., Potter, S. J. & Putnam, R. W. 2004. Hyperoxia, reactive oxygen species, and hyperventilation: oxygen sensitivity of brain stem neurons. *Journal of Applied Physiology*, 96, 784-791.

Dedhia, H. V. & Banks, D. E. 1994. Pulmonary response to hyperoxia: Effects of magnesium. *Environmental Health Perspectives*, 102, 101-105.

Dimitrov, N. V., Meyer, C., Gilliland, D., Ruppenthal, M., Chenoweth, W. & Malone, W. 1991. Plasma tocopherol concentrations in response to supplemental vitamin E. *The American Journal of Clinical Nutrition*, 53, 723-729.

Dodane, V. & Kachar, B. 1996. Identification of isoforms of G proteins and PKC that colocalize with tight junctions. *The Journal of Membrane Biology*, 149, 199-209.

Erlandsen, S. L. & Magney, J. E. 1992. Respiratory System. *Colour Atlas of Histology.* St Louis: Mosby-Year Book, Inc.

Evans, M. J., Shami, S. G., Cabral-Anderson, L. J. & Dekker, N. P. 1986. Role of nonciliated cells in renewal of the bronchial epithelium of rats exposed to NO2. *American Journal of Pathology*, 123, 126-133.

Evans, M. J., Van Winkle, L. S., Fanucchi, M. V. & Plopper, C. G. 2001. Cellular and molecular characteristics of basal cells in airway epithelium. *Experimental Lung Research*, 27, 401-415.

Fanning, A. S., Jameson, B. J., Jesaitis, L. A. & Anderson, J. M. 1998. The tight junction protein ZO-1 establishes a link between the transmembrane protein occludin and the actin cytoskeleton. *The Journal of Biological Chemistry*, 273, 29745-29753.

Farber, J. L. 1994. Mechanisms of cell injury by activated oxygen species. *Environmental Health Perspectives,* 10**,** 17-24.

Faruqi, R., De La Motte, C. & Dicorleto, P. E. 1994. Alpha-tocopherol inhibits agonist-induced monocytic cell adhesion to cultured human endothelial cells. *The Journal of Clinical Investigation*, 94, 592-600.

Fehrenbach, H. 2001. Alveolar epithelial type II cell: defender of the alveolus revisited. *Respiratory Research*, 2, 33–46.

Fiedler, M. A., Kaetzel, C. S. & Davis, P. B. 1991. Sustained production of secretory component by human tracheal epithelial cells in primary culture. *Amercan Journal of Physiology. Lung Cellular and Molecular Physiology*, 261, L255-L261.

Flamme, S. E. & Kowalczyk, A. P. 2008. *Cell junctions: Adhesion,development, and disease.* Wiley,John & Sons,Incorporated.

Flieder, D. B. & Vazquez, M. F. 2000. Lung tumors with neuroendocrine morphology:A perspective for the new millennium. *Radiologic Clinics of North America,* 38, 563-577.

Forbes, B. 2000. Human airway epithelial cell lines for *in vitro* drug transport and metabolism studies. *Pharmaceutical Science & Technology Today*, 3, 18-27.

Forbes, B., Shah, A., Martin, G. P. & Lansley, A. B. 2003. The human bronchial epithelial cell line 16HBE140: as a model system of the airways for studying drug transport. *International Journal of Pharmaceutics,* 257, 161-167.

Freeman, B. A., Mason, R. J., Williams, M. C. & Crapo, J. D. 1986. Antioxidant enzyme activity in alveolar type II cells after exposure of rats to hyperoxia. *Experimental Lung Research*, 10, 203-222.

Freeman, B. A., Topolosky, M. K. & Crapo, J. D. 1982. Hyperoxia increases oxygen radical production in rat lung homogenates. *Archives of Biochemistry and Biophysics*, 216, 477-484.

Gey, K. F., Moser, U. K., Jordan, P., Stahelin, H. B., Eichholzer, M. & Ludin, E. 1993. Increased risk of cardiovascular disease at suboptimal plasma concentrations of essential antioxidants: an epidemiological update with special attention to carotene and vitamin C. *American Journal of Clinical Nutrition*, 57, 787S-797S.

Godfrey, R. W. A., Severs, N. J. & Jeffery, P. K. 1994. A comparison between the epithelial tight junction morphology of human extrapulmonary bronchi and rat trachea. *European Respiratory Journals*, 7, 1409–1415.

González-Mariscal, L., Betanzos, A., Nava, P. & Jaramillo, B. E. 2003. Tight junction proteins*. Progres in Biophysics Molecular Biology*, 81, 1-44.

Goodman, R., Pugin, J., Lee, J. & Matthay, M. 2003 Cytokine-mediated inflammation in acute lung injury. *Cytokine & Growth Factor Reviews*, 14, 523-535.

Gottardi, C. J., Arpin, M., Fanning, A. S. & Louvard, D. 1996. The junction-associated protein, zonula occludens-1, localizes to the nucleus before the maturation and during the remodeling of cell-cell contacts. *PNAS USA*, 93, 10779-10784.

Green, K. J. & Jones, J. C. 1996. Desmosomes and hemidesmosomes: structure and function of molecular components. *FASEB Journal*, 10, 871-881.

Guaiqui, V. H., Vera, J. C. & Golde, D. W. 2001. Mechanism of vitamin C inhibition of cell death induced by oxidative stress in glutathione-depleted HL-60 cells. *The Journal of Biological Chemistry*, 276, 40955-40961.

Gurtner, G. H., Michael, J. R., Farrukh, I. S., Sciuto, A. M. & Adkinson, N. F. 1985. Mechanism of hyperoxia-induced pulmonary vascular paralysis: effect of antioxidant pretreatment. *Journal of Applied Physiology*, 59, 953-958.

Gushima, Y., Ichikado, K., Suga, M., Okamoto, T., Lyonaga, K., Miyakawa, H. & Ando, M. 2001. Expression of matrix metalloproteinases in pigs with hyperoxia- induced acute lung injury. *European Respiratory Journal*, 18, 827-837.

Gutteridge, J. M. & Halliwell, B. 1990. The measurement and mechanism of lipid peroxidation in biological systems. *Trends in Biochemical Sciences*, 15, 129-35.

Haddad, J. J. 2002a. Oxygen-sensing mechanisms and the regulation of redox-responsive transcription factors in development and pathophysiology. *Respiratory Research*, 3, 1-26.

Haddad, J. J. 2002b. Science review: Redox and oxygen-sensitive transcription factors in the regulation of oxidant-mediated lung injury: role for nuclear factor-κB. *Critical Care*, 6, 481-490.

Hagimoto, N., Kuwano, K., Kawasaki, M., Yoshimi, M., Kaneko, Y., Kunitake, R., Maeyama, T., Tanaka, T. & Hara, N. 1999. Induction of interleukin-8 secretion and apoptosis in bronchiolar epithelial cells by Fas ligation. *American Journal of Respiratory Cell and Molecular Biology*, 21, 436-45.

Halliwell, B. & Aruoma, O. I. 1991. DNA damage by oxygen-derived species Its mechanism and measurement in mammalian systems. *FEBS Letters*, 281, 9-19.

Halliwell, B. & Chirico, S. 1993. Lipid peroxidation:its mechanism, measurement, and significance. *American Journal of Clinical Nutrition*, 57, 715S-725S.

Halliwell, B. & Gutteridge, J. M. 1999. *Free Radicals in Biology and Medicine,* Oxford, U.K, Clarendon Press (Oxford and New York).

Hamid, A. A., Aiyelaagbe, O. O., Usman, L. A., Ameen, O. M. & Lawal, A. 2010. Antioxidants: Its medicinal and pharmacological applications. *African Journal of Pure and Applied Chemistry*, 4, 142-151.

Hancock, J. T., Desikan, R. & Neill, S. J. 2001. Role of reactive oxygen species in cell signalling pathways. *Biochemical Society Transactions*, 29, 345-349.

Hazinski, T. A. 2002. The Respiratory System. *Rudolph's Pediatrics.* 21-illustrated ed.: McGraw-Hill Professional.

Helt, C. E., Staversky, R. J., Lee, Y. J., Bambara, R. A., Keng, P. C. & O'reilly, M. A. 2004. The CDK and PCNA domains on p21 Cip1 both function to inhibit G1/S progression during hyperoxia. *American Journal of Physiology. Lung Cellular and Molecular Physiology*, 286, L506-L513.

Hildebrandt, F., Benzing, T. & Katsanis, N. 2011. Ciliopathies. *The New England Journal of Medicine*, 364, 1533-1543.

Ho, Y. S., Magnenat, J. L., Bronson, R. T., Cao, J., Gargano, M., Sugawara, M. & Funk, C. D. 1997. Mice deficient in cellular glutathione peroxidase develop normally and show no increased sensitivity to hyperoxia. *The Journal of Biological Chemistry*, 272, 16644-16651.

Holley, M. C. & Afzelius, B. A. 1986. Alignment of cilia in the immotile cilia syndrome. *Tissue & Cell*, 18, 521-529.

Hossain, M., Mazzone, P., Tierney, W. & Cucullo, L. 2011. *In vitro* assessment of tobacco smoke toxicity at the BBB: Do Antioxidant Supplements Have a Protective Role?. *BMC Neuroscience*, 12, 92.

Housset, B., Hurbain, I., Masliah, J., Laghsal, A., Chaumette-Demaugre, M. T., Karam, H. & Derenne, J. 1991. Toxic effects of oxygen on cultivated alveolar epithelial cells, lung fibroblasts and alveolar macrophages. *The European Respiratory Journal*, 4, 1066-1075.

Howat, W. J., Holmes, J. A., Holgate, S. T. & Lackie, P. M. 2001. Basement Membrane Pores in Human Bronchial Epithelium. *The American Journal of Pathology*, 158, 673–680.

Hu, W., Johnson, H. H. & Shu, H. B. 1999. Tumor necrosis factor-related apoptosis-inducing ligand receptors signal NF-kB and JNK activation and apoptosis through distinct pathways. *The Journal of Biological Chemistry*, 274, 30603–30610.

Iqbal, K., Khan, A. & Khattak, M. A. 2004. Biological Significance of Ascorbic Acid (Vitamin C) in Human Health – A Review. *Pakistan Journal of Nutrition,* 35-13.

Jackson, A. D., Rayner, C. F., Dewar, A., Cole, P. J. & Wilson, R. 1996. A human respiratory-tissue organ culture incorporating an air interface*. American Journal of Respiratory and Critical Care Medicine*, 153, 1130-1135.

Jacobson, J. M., Michael, J. R., Jafri, M. H. & Gurtner, G. H. 1990. Antioxidants and antioxidant enzymes protect against pulmonary oxygen toxicity in the rabbit. *Journal of Applied Physiology*, 68, 1252-1259.

Janero, D. 1990. Malondialdehyde and thiobarbituric acid-reactivity as diagnostic indices of lipid peroxidation and peroxidative tissue injury. *Free Radical Biology and Medicine*, 9, 515-540.

Jean, J.-C., George, E., Kaestner, K. H., Brown, L. a. S., Spira, A. & Joyce-Brady, M. 2013. Transcription Factor Klf4, Induced in the Lung by Oxygen at Birth, Regulates Perinatal Fibroblast and Myofibroblast Differentiation. *PLoS ONE*, 8, e54806.

Johnston, C. S., Martin, L. J. & Cai, X. 1992. Antihistamine effect of supplemental ascorbic acid and neutrophil chemotaxis*. Journal of the American Collage of Nutrition*, 11, 172-176.

Johnston, C. S. & Sarah, K. 2001. Plasma-saturating intakes of vitamin C confer maximal antioxidant protection to plasma. *Journal of the American Collage of Nutrition*, 20, 623-627.

Junqueira, L. C. & Carneiro, J. 2005. Basic histology:Text & Atlas. 11 ed.: McGraw-Hill Companies.

Junqueira, L. C., Carneiro, J. & Kelley, R. O. 1989. Respiratory system. *Basic Histology. A Lange medical book.* Connecticut: Appleton & Lange.

Jyonouchi, H., Sun, S., Abiru, T., Chareancholvanich, S. & Ingbar, D. H. 1998. The effects of hyperoxic Injury and antioxidant vitamins on death and proliferation of human small airway epithelial cells. *American Journal of Respiratory Cell and Molecula Biology*, 19, 426–436.

Kagan, V. E., Serbinova, E. A., Forte, T., Scita, G. & Packer, L. 1992. Recycling of vitamin E in human low density lipoproteins. *Journal of Lipid Research*, 33, 385-397.

Kalyanaraman, B., Darley-Usmar, V., Davies, K. J., Dennery, P. A., Forman, H. J., Grisham, M. B., Mann, G. E., Moore, K., Roberts, L. J. & Ischiropoulos, H. 2012. Measuring reactive oxygen and nitrogen species with fluorescent probes: challenges and limitations. *Free radical Biology and Medicine*, 52, 1-6.

Kay, R. J., Moate, R. M., Bray, I., Sneyd, J. R. & Langton, J. A. 2002. Cultured rat trachea as model for the study of ciliary abundance-the effect of oxygen. *Anesthesiology*, 97, 275-277.

Kazzaz, J. A., Xu, J., Palaia, T. A., Mantell, L., Fein, A. M. & Horowitz, S. 1996. Cellular oxygen toxicity. Oxidant injury without apoptosis. *The Journal of Biological Chemistry*, 271, 15182-15186.

Kc, S., Cárcamo , J. M. & Golde, D. W. 2005. Vitamin C enters mitochondria via facilitative glucose transporter 1 (Glut1) and confers mitochondrial protection against oxidative injury*. Federation of American Societies for Experimental Biology Journal*, 19, 1657-1667.

Kelly, F. J. 1993. Free radical disorders of preterm infants. *British Medical Bulletin*, 49, 668-678.

Kim, H., Bae, S., Yu, Y., Kim, Y., Kim, H. R., Hwang, Y. I., Kang, J. S. & Lee, W. J. 2012. The Analysis of Vitamin C Concentration in Organs of Gulo-/- Mice Upon Vitamin C Withdrawal. *Immune Network*, 12, 18-26.

Kim, V., Benditt, J. O., Wise, R. A. & Sharafkhaneh, A. 2008. Oxygen Therapy in Chronic Obstructive Pulmonary Disease. *Proceeding of American Thoracic Societ*, 5, 513-518.

Knight, D. A. & Holgate, S. T. 2003. The airway epithelium: structural and functional properties in health and disease. *Respirology,* 8**,** 432-46.

Kolleck, I., Schlame, M., Fechner, H., Looman, A. C., Wissel, H. & Rustow, B. 1999. HDL is the major source of vitamin E for type II pneumocytes. *Free Radical Biology and Medicine*, 27, 882–890.

Kolleck, I., Sinha, P. & Rüstow, B. 2002. Vitamin E as an antioxidant of the lung: mechanisms of vitamin E delivery to alveolar type II cells. *American Journal of Respiratory and Critical Care Medicine* 166, S62-S66.

Konrad, F., Schiener;R., Marx;, T. & Georgieff, M. 1995. Ultrastructure and mucociliary transport of bronchial respiratory epithelium in intubated patients. *Intensive Care Medicine*, 21, 482-489.

Konradova, V., Janota, J., Sulova, J. & Sukova, B. 1988. Effect of 90% oxygen exposure on the ultrastructure of the tracheal epithelium in rabbits. *Respiration*, 54, 24-32.

Konradova, V., Uhlik, J., Vajner, L., Herget, J. & Adaskova, J. 2003. Mild hyperoxia induces moderate pathological alteration in airway epithelium (ultrastructural study). *Veterinary Medicine– Czech***,** 48, 313-320.

Konsavage, W., Zhang, L., Vary, T. & Shenberger, J. S. 2010. Hyperoxia inhibits protein synthesis and increases eIF2α phosphorylation in the newborn rat lung. *American Jouranl of Physiology. lung Cellular and Molecular Physiology*, 298, L678-L686.

Kubo, A., Kubo-Yuba, A., Tsukita, S., Tsukita, S. & Amagai, M. 2008. A novel specific component of the apical structure of vertebrate motile cilia. *Molecular Biology of the Cell*, 19, 5338-5346.

Kumaravel, T. S. & Jha, A. N. 2006. Reliable Comet assay measurements for detecting DNA damage induced by ionising radiation and chemicals. *Mutation Research*, 605, 7-16.

Laemmli, U. K. 1970. Cleavage of structural proteins during the assembly of the head of bacteriophage T4. *Nature*, 227, 680-685.

Lamb, N. J., Gutteridge, J. M., Baker, C., Evans, T. W. & Quinlan, G. J. 1999. Oxidative damage to proteins of bronchoalveolar lavage fluid in patients with acute respiratory distress syndrome: evidence for neutrophil-mediated hydroxylation, nitration, and chlorination. *Critical Care Medicine*, 27, 1738-1744.

Lawson, G. W., Winkle, L. S. V., Toskala, E., Senior, R. M., Parks, W. C. & Plopper, C. G. 2002. Mouse strain modulates the role of the ciliated cell in acute tracheobronchial airway injury-distal airways. *The American Journal of Pathology*, 160, 315–327.

Lebleu, V. S., Macdonald, B. & Kalluri, R. 2007. Structure and function of basement membranes. *Experimental Biology and Medicine (Maywood, N.J.)*, 232, 1121-1129.

Lechapt-Zalcman, E., Prulière-Escabasse, V., Advenier, D., Galiacy, S., Charrière-Bertrand, C., Coste, A., Harf, A., D'ortho, M. P. & Escudier, E. 2006. Transforming growth factor-beta1 increases airway wound repair via MMP-2 upregulation: a new pathway for epithelial wound repair*?. American Journal of Physiology Lung Cellular and Molecular Physiology*, 290, L1277-L1282.

Lechner, J. F. & Laveck, M. A. 1985. A serum-free method for culturing normal human bronchial epithelial cells at clonal density. *Methods in Cell Science*, 9, 43-48.

Lee, P. J., Alam, J., Wiegand, G. W. & Choi, A. M. 1996. Overexpression of heme oxygenase-1 in human pulmonary epithelial cells results in cell growth arrest and increased resistance to hyperoxia. *PNAS USA*, 93, 10393-10398.

Lee, P. J. & Choi, A. M. 2003. Pathways of cell signalling in hyperoxia. *Free Radical Biology and Medicine,* 35, 341-350.

Lehr, H. A., Weyrich, A. S., Saetzler, R. K., Jurek, A., Arfors, K. E., Zimmerman, G. A., Prescott, S. M. & Mcintyre, T. M. 1997. Vitamin C blocks inflammatory platelet-activating factor mimetics created by cigarette smoking. *The Journal of Clinical Investigation*, 99, 2358-2364.

Lenton, K. J., Therriault, H., Cantin, A. M., Fulop, T., Payette, H. & Wagner, J. R. 2000. Direct correlation of glutathione and ascorbate and their dependence on age and season in human lymphocytes. *The American Journal of Clinical Nutrition*, 71, 1194-1200.

Levine, R. L., Wehr, N., Williams, J. A., Stadtman, E. R. & Shacter, E. 2000. Determination of carbonyl groups in oxidized proteins. *Methods in Molecular Biology*, 99, 15-24.

Li, C. X. & Poznansky, M. J. 1990. Characterization of the ZO-1 protein in endothelial and other cell lines. *Journal of Cell Science,* 97, 231-237.

Li, J., Gao, X., Qian, M. & Eaton, J. W. 2004. Mitochondrial metabolism underlies hyperoxic cell damage. *Free Radical Biology and Medicine*, 36, 1460-1470.

Lodish, H., Berk, A., Zipursky, S., Matsudaira, P., Bltimore, D. & Darnell, J. 2000. *Molecular Cell Biology.* New york: W.H.Free man and Company.

Lounge, T. N. B. 2009. How the Lung Work, The Respiratory System. *http://www.nhlbi.nih.gov/health/dci/Diseases/hlw/hlw_respsys.html*.

Lu, L., Hackett, S. F., Mincey, A., Lai, H. & Campochiaro, P. A. 2006. Effects of different types of oxidative stress in RPE cells. *Journal of Cellular Physiology*, 206, 119-125.

Lua, Y., Parkyna, L., Otterbeina, L. E., Kureishib, Y., Walshb, K., Raya, A. & Raya, P. 2001. Activated Akt protects the lung from oxidant-induced injury and delays death of mice. *The Journal of Experimental Medicine*, 193, 545-550.

Ma, T. Y., Hollander, D., Tran, L. T., Nguyen, D., Hoa, N. & Bhalla, D. 1995. Cytoskeletal regulation of Caco-2 intestinal monolayer paracellular permeability. *Journal of Cellular Physiology*, 164, 533-545.

Mach, W. J., Thimmesch, A. R., Pierce, J. T. & Pierce, J. D. 2011. Consequences of hyperoxia and the toxicity of oxygen in the lung. *Nursing Research and Practice*, 260482, 7.

Madara, J. L., Barenberg, D. & Carlson, S. 1986. Effects of cytochalasin D on occluding junctions of intestinal absorptive cells: further evidence that the cytoskeleton may influence paracellular permeability and junctional charge selectivity. *The Journal of Cell Biology*, 102, 2125-2136

Mantell, L. L. & Lee, P. J. 2000. Signal transduction pathways in hyperoxia-induced lung cell death. *Molecular and Metabolism*, 71, 359-370.

Marnett, L. J. 2002. Oxy radicals, lipid peroxidation and DNA damage. *Toxicology*, 27, 219-222.

Martensson, J., Han, J., Griffith, O. W. & Meister, A. 1993. Glutathione ester delays the onset of scurvy in ascorbate-deficient guinea pigs. *PNAS USA*, 90, 317–321.

Martinez-Palomo, A., Meza, I., Beaty, G. & Cereijido, M. 1980. Experimental modulation of occluding junctions in a cultured transporting epithelium. *The Journal of Cell Biology*, 87, 736-745.

Matsui, H., Randell, S. H., Peretti, S. W., Davis, C. W. & Boucher, R. C. 1998. Coordinated clearance of periciliary liquid and mucus from airway surfaces. *Journal of Clinical Investigation*, 102, 1125-1131.

Matsumura, H. & Setoguti, T. 1989. Freeze-fracture replica studies of tight junctions in normal human bronchial epithelium. *Acta Anatomica (Basel)*, 13, 219-226.

Mazzon, E. & Cuzzocrea, S. 2007. Role of TNF-α in lung tight junction alteration in mouse model of acute lung inflammation. *Respiratory Research*, 8, 75-94.

Mccarthy, K. M., Skare, I. B., Stankewich, M. C., Furuse, M., Tsukita, S., Rogers, R. A., Lynch, R. D. & Schneeberger, E. E. 1996. Occludin is a functional component of the tight junction. *Journal of Cell Science*, 109, 2287-2298.

Meister, A. 1981. Metabolism and functions of glutathione. *Trends in Biochemical Sciences*, 6, 231–234.

Meister, A. 1994. Glutathione-ascorbic acid antioxidant system in animals. *The Journal of Biological Chemistry*, 269, 9397-9400.

Meydani, M. 2001. Vitamin E and atherosclerosis: beyond prevention of LDL oxidation. *The Journal of Nutrition*, 131, 366S-368S.

Meyer, T. N., Schwesinger, C., Ye, J., Denker, B. M. & Nigam, S. K. 2001. Reassembly of the tight junction after oxidative stress depends on tyrosine kinase activity. *The journal of Biological Chemistry*, 276, 22048-22055.

Min, J. H., Codipilly, C. N., Nasim, S., Miller, E. J. & Ahmed, M. N. 2012. Synergistic protection against hyperoxia-induced lung injury by neutrophils blockade and EC-SOD overexpression. *Respiratory Research*, 13, 53.

Mojon, D., Boscoboinik, D., Haas, A., Bohnke, M. & Azzi, A. 1994. Vitamin E inhibits retinal pigment epithelium cell proliferation *in vitro*. *Ophthalmic Research*, 26, 304–309.

Moran, D. T. & Rowley, J. C. 1988. Respiratory System. *Visual Histology.* Lippincott Williams and Wilkins.

Morin, P. J. 2005. Claudin Proteins in Human Cancer: Promising New Targets for Diagnosis and Therapy. *Cancer Research*, 65, 9603-9606.

Musch, M. W., Walsh-Reitz, M. M. & Chang, E. B. 2006. Roles of ZO-1, occludin,and actin in oxidant-induced barrier disruption. *American Journal of Physiology -Gasrointestinal and Liver Physiology*, 290, 222-231.

Nagase, H., Visse, R. & Murphy, G. 2006. Structure and function of matrix metalloproteinases and TIMPs. *Cardiovascular Research*, 69, 562-573.

Naidu, K. A. 2003. Vitamin C in human health and disease is still a mystery ? An overview. *Nutrition Journal*, 2, 7.

Nakamura, H., Yoshimura, K., Mcelvaney, N. G. & Crystal, R. G. 1992. Neutrophil elastase in respiratory epithelial lining fluid of individuals with cystic fibrosis induces interleukin-8 gene expression in a human bronchial epithelial cell line. *The Journal of Clinical Investigation*, 89, 1478-1484.

Narasaraju, T. A., Jin, N., Narendranath, C. R., Chen, Z., Gou, D. & Liu, L. 2003. Protein nitration in rat lungs during hyperoxia exposure: a possible role of

myeloperoxidase. *Amercan Journal of Physiology. Lung Cellular and Molecular Physiology*, 285, L1037-L1045.

Neuzil, J., Thomas, S. & Stocker, R. 1997. Requirement for, promotion, or inhibition by alpha-tocopherol of radical-induced initiation of plasma lipoprotein lipid peroxidation. *Free Radical and Biological Medicin*, 22, 57-71.

Nishikimi, M., Koshizaka, T., Ozawa, T. & Yagi, K. 1988. Occurrence in humans and guinea pigs of the gene related to their missing enzyme L-gulono-gamma-lactone oxidase. *Archive of Biochemsitry and Biophysics*, 267, 842-846.

Nualart, F. J., Rivas, C. I., Montecinos, V. P., Godoy, A. S., Guaiquil, V. H., Golde, D. W. & Vera, J. C. 2003. Recycling of vitamin C by a bystander effect. *The Jjournal of Biological Chemistry*, 278, 10128-10133.

Ochoa, J. J., Ramirez-Tortosa, M. C., Quiles, J. L., Palomino, N., Robles, R., Mataix, J. & Huertas, J. R. 2003. Oxidative stress in erythrocytes from premature and full-term infants during their first 72 h of life. *Free Radical Research*, 37, 317-322.

Ohkawa, H., Ohishi, N. & Yagi, K. 1979. Assay for lipid peroxides in animal tissues by thiobarbituric acid reaction. *Analytical Biochemistry*, 95, 351-358.

Ohtake, K., Maeno, T., Ueda, H., Ogihara, M., Natsume, H. & Morimoto, Y. 2003. Poly-L-arginine enhances paracellular permeability via serine/threonine phosphorylation of ZO-1 and tyrosine dephosphorylation of occludin in rabbit nasal epithelium. *Pharmaceutical Research*, 20, 1838-1845.

Olive, P. L. 1998. The role of DNA single- and double-strand breaks in cell killing by ionizing radiation. *Radiation Research*, 150, S42-S51.

Oliveira, M. J., Pereira, A. S., Guimarães, L., Grande, N. R., De Sa, C. M. & Aguas, A. P. 2003. Zonation of ciliated cells on the epithelium of the rat trachea. *Lung*, 18, 275-282.

Olivera, W. G., Ridge, K. M. & Sznajder, J. I. 1995. Lung liquid clearance and Na,K-ATPase during acute hyperoxia and recovery in rats. *American Journal of Respiratory and Critical Care Medicine*, 152, 1229-1234.

Ostrowsk, L. E. & Nettesheim, P. 1995. Inhibition of Ciliated Cell Differentiation by Fluid Submersion. *Experimental Lung Research*, 21, 957-970.

Owens, C. W. I. & Belcher, R. V. 1965. colorimetric micro-method for the determination of glutathione. *Biochemistry Journal*, 94, 705-711.

Padayatty, S. J., Katz, A., Wang, Y., Eck, P., Kwon, O., Lee, J. H., Chen, S., Corpe, C., Dutta, A., Dutta, S. K. & Levine, M. 2003. Vitamin C as an antioxidant:

evaluation of its role in disease prevention. *Journal of the American College of Nutrition*, 22, 18-35.

Palmieri, B. & Sblendorio, V. 2007. Oxidative stress tests: overview on reliability and use. *European Review for Medical and Pharmacological Sciences*, 11, 383-399.

Panayiotidis, M. I., Rancourt, R. C., Allen, C. B., Riddle, S. R., Schneider, B. K., Ahmad, S. & White, C. W. 2004. Hyperoxia-induced DNA damage causes decreased DNA methylation in human lung epithelial-like A549 cells. *Antioxidants and Redox Signalling*, 6, 129-136.

Panda, K., Chattopadhyay, R., Chattopadhyay, D. J. & Chatterjee, I. B. 2000. Vitamin C prevents cigarette smoke-induced oxidative damage *in vivo*. *Free Radical Biology and* Medicine, 29, 115-124.

Paredi, P., Kharitonov, S. A., Leak, D., Ward, S., Cramer, D. & Barnes, P. J. 2000. Exhaled ethane, a marker of lipid peroxidation, is elevated in chronic obstructive pulmonary disease. *American Journal of Critical Care Medicine*, 162, 369-373.

Park, K. S., Wells, J. M., Zorn, A. M., Wert, S. E., Laubach, V. E., Fernandez, L. G. & Whitsett, J. A. 2006. Transdifferentiation of ciliated cells during repair of the respiratory epithelium. *American Journal of Respiraory Cell and Molecular Biology*, 34, 151-157.

Patton, J. S. & Byron, P. R. 2007. Inhaling medicines: delivering drugs to the body through the lungs. *Nature Reviews Drug Discovery*, 6**,** 67-74.

Pedeboscq, S., Rey, C., Petit, M., Harpey, C., De Giorgi, F., Ichas, F. & Lartigue, L. 2012. Non-antioxidant properties of α-tocopherol reduce the anticancer activity of several protein kinase inhibitors *in vitro. PLoS ONE*, 7, e36811.

Perez-Cruz, I., Carcamo, J. M. & Golde, D. W. 2003. Vitamin C inhibits FAS-induced apoptosis in monocytes and U937 cells. *Blood*, 102, 336-343.

Petrache, I., Choi, M. E., Otterbein, L. E., Chin, B. Y., Mantell, L. L., Horowitz, S. & Choi, A. M. 1999. Mitogen-activated protein kinase pathway mediates hyperoxia-induced apoptosis in cultured macrophage cells. *American Jouranl of Physiology. Lung Cellular and Molecular Physiology,* 277, L589-L595.

Pezzulo, A. A., Starner, T. D., Scheetz, T. E., Traver, G. L., Tilley, A. E., Harvey, B.-G., Crystal, R. G., Mccray Jr., P. B. & Zabner, J. 2011. The air-liquid interface and use of primary cell cultures are important to recapitulate the transcriptional profile of *in vivo* airway epithelia. *American Journal of Physiology. Lung Cellular and Molecular Physiology*, 300, L25–L31.

Pietarinen-Runtti, P., Raivio, K. O., Saksela, M., Asikainen, T. M. & Kinnula, V. L. 1998. Antioxidant Enzyme Regulation and Resistance to Oxidants of Human Bronchial Epithelial Cells Cultured under Hyperoxic Conditions. *American Jouranl of Respiratory Cell and Molecular Biology*, 19, 286-292.

Plopper, C. G. & Hyde, D. M. 2008. The non-human primate as a model for studying COPD and asthma. *Pulmonary Pharmacology and Therapeutics*., 21, 755-766.

Pohl, C., Hermanns, M. I., Uboldi, C., Bock, M., Fuchs, S., Dei-Anang, J., Mayer, E., Kehe, K., Kummer, W. & Kirkpatrick, C. J. 2009. Barrier functions and paracellular integrity in human cell culture models of the proximal respiratory unit. *European Journal of Pharmaceutics and Biopharmaceutics*, 72, 339-349.

Pollock, J. I. & Mullin, R. J. 1987. Vitamin C biosynthesis in prosimians: evidence for the anthropoid affinity of Tarsius. *American Journal of Physical Anthropology*, 73, 65-70.

Powell, C. L., Swenberg, J. A. & Rusyn, I. 2005. Expression of base excision DNA repair genes as a biomarker of oxidative DNA damage. *Cancer Letters*, 229**,** 1-11.

Puchelle, E., Zahm, J., Tournier, J. & Coraux, C. 2006. Airway epithelial repair, regeneration, and remodeling after injury in chronic obstructive pulmonary disease. *The Proceedings of American Thoracic Society*, 3, 726-733.

Radi, R. 2004. Nitric oxide, oxidants, and protein tyrosine nitration. *PNAS USA*, 101, 4003–4008.

Rahman, I., Mulier, B., Gilmour, P. S., Watchorn, T., Donaldson, K., Jeffery, P. K. & Macnee, W. 2001. Oxidant-mediated lung epithelial cell tolerance: the role of intracellular glutathione and nuclear factor-kappaB. *Biochemical Pharmacology*, 62, 787-794.

Ranek, M. J., Cotten, S. W. & Willis, M. S. 2011. Albert Szent-Györgyi, MD, PhD discoverer of vitamin C and a pioneer of cellular respiration, muscle physiology, and cancer development. *LabMedicine*, 42, 694-698.

Rankin, H. V., Moody, A. J., Moate, R. M., Macnaughton, P. D., Rahamim, J., Smith, M. E. & J.R., S. 2007. Elevated oxygen fraction reduces cilial abundance in explanted human bronchial tissue. *Ultrastructural Pathology*, 31, 339-46.

Rao, R. 2008. Oxidative stress-induced disruption of epithelial and endothelial tight junctions. *Frontiers and Bioscience*, 1, 7210-7226.

Rao, R., Baker, R. D. & Baker, S. S. 1999. Inhibition of oxidant-induced barrier disruption and protein tyrosine phosphorylation in Caco-2 cell monolayers by epidermal growth factor. *Biochemical Pharmacology*, 57, 685-695.

Rao, R. K., Basuroy, S., Rao, V. U., Karnaky, J. K. J. & Gupta, A. 2002. Tyrosine phosphorylation and dissociation of occludin-ZO-1 and E-cadherin-beta-catenin complexes from the cytoskeleton by oxidative stress. *The Biochemical Journal*, 368, 471-481.

Rao, R. K., Li, L., Baker, R. D., Baker, S. S. & Gupta, A. 2000. Glutathione oxidation and PTPase inhibition by hydrogen peroxide in Caco-2 cell monolayer. American Journal of Physiology. *Gastrointestinal and Liver Physiology*, 279, G332-G340.

Rautiainen, M., Collan, Y., Nuutinen, J. & Afzelius, B. A. 1990. Ciliary Orientation in the Immotile Cilia Syndrome. *European Archives of Oto-Rhino-Laryngology*, 247, 100-103.

Rautiainen, M., Matsune, S., Shima, S., Sakamoto, K., Hanamure, Y. & Ohyama, M. 1992. Ciliary Beat of Cultured Human Respiratory Cells Studied with Differential Interference Microscope and High-Speed Video System. *Acta Oto-Laryngologica*, 112, 845-851.

Rautiainen, N., Collan, Y. & Nutinen, J. 1986. Amethod for measuring the orientation (beat direction) of respiratory cilia. *Arch Ortorhinolaryngol*, 243, 265-268.

Rawlins, E. L. & Hogan, B. L. 2008. Ciliated epithelial cell lifespan in the mouse trachea and lung. *Amercan Journal of Physiology. Lung Cellular and Molecular Physiology*, 295, L231-L234.

Rayner, C. F. J., Rutman, A., Dewar, A., Cole, P. J. & Wilson, R. 1995. Ciliary disorientation in patients with chronic upper respiratory tract inflammation. *American Journal of Respiraory and Critical Care* Medicine, 151**,** 800-804.

Reed, W., Carson, J. L., Moats-Staats, B. M., Lucier, T., Hu, P., Brighton, L., Gambling, T. M., Huang, C. H., Leigh, M. W. & Collier, A. M. 2000. Characterization of an axonemal dynein heavy chain expressed early in airway epithelial ciliogenesis. *American Journal of Respiratory Cell and Molecular Biology*, 23, 734-741.

Rock, J. R. & Hogan, B. L. M. 2011. Epithelial Progenitor Cells in Lung Development, Maintenance, Repair, and Disease. *The Annual Review of Cell and Developmental Biology*, 27, 493–512.

Rogers, A. V., Dewar, A., Corrin, B. & Jeffery, P. K. 1993. Identification of serous-like cells in the surface epithelium of human bronchioles. *The European Respiratory Journal*, 6, 498-504.

Romer, L. H., Birukov, K. G. & Garcia, J. G. N. 2006. Focal Adhesions. *Circulation Research*, 98, 606-616.

Romieu, I. 2005. Nutrition and lung health. *The International Journal of Tuberculosis and Lung Disease*, 9, 362-374.

Roper, J. M., Mazzatti, D. J., Watkins, R. H., Maniscalco, W. M., Keng, P. C. & O'reilly, M. A. 2004. In vivo exposure to hyperoxia induces DNA damage in a population of alveolar type II epithelial cells. *American Jouranl of Physiology Lung Cellular and Molecular Physiology*, 286**,** L1045- L1054.

Rose, R. C. 1988. Transport of ascorbic acid and other water-soluble vitamins. *International Journal of Biochemistry and Biophysics*, 947, 335-366.

Rumsey, S. C. & Levine, M. 1998. Absorption, transport, and disposition of ascorbic acid in humans. *The Journal of Nutritional Biochemistry*, 9**,** 116–130.

Rutland, J., Cox, T., Dewar, A. & Cole, P. 1983. Screening for ciliary dyskinesia - a spectrum of defects of motility and structure. *European Journal of Respiratory Diseases*, 64, 71-77.

Rutman, A., Cullinan, P., Woodhead, M., Cole, P. J. & Wilson, R. 1993. Ciliary disorientation - A possible variant of primary ciliary dyskinesia, *Thorax*, 48, 770-771.

Sarma, A. D., Mallick, A. R. & Ghosh, A. K. 2010. Free Radicals and Their Role in Different Clinical Conditions: An Overview. International Journal of *Pharma Sciences and Research*, 1, 185-192.

Schafer, F. Q. & Buettner, G. R. 2001. Redox environment of the cell as viewed through the redox state of the glutathione disulfide/glutathione couple. *Free Radical Biology and Medicine*, 30, 1191-212.

Schmidt, M. C., Simmen, D., Hilbe, M., Boderke, P., Ditzinger, G., Sandow, J., Lang, S., Rubas, W. & Merkle, H. P. 2000. Validation of excised bovine nasal mucosa as *in vitro* model to study drug transport and metabolic pathways in nasal epithelium. *Journal of Pharmaceutical Sciences*, 89, 396-407.

Schneeberger, E. E. & Lynch, R. D. 1992. Structure, function, and regulation of cellular tight junctions. *The American Journal of Physiology*, 262, L647-L661.

Schorah, C. J., Downing, C., Piripitsi, A., Gallivan, L., Al-Hazaa, A. H., Sanderson, M. J. & Bodenham, A. 1996. Total vitamin C, ascorbic acid, and dehydroascorbic acid concentrations in plasma of critically ill patients. *American journal of Clinical Nutrition*, 63**,** 760-765.

Shapiro, A. B., Maturen, A., Herman, G., Hryhorczuk, D. O. & Leikin, J. B. 1989. Carbon monoxide and myonecrosis: a prospective study. *Veterinary and Human Toxicology*, 31**,** 136-137.

Serhan, C., Anderson, P., Goodman, E., Dunham, P. & Weissmann, G. 1981. Phosphatidate and oxidized fatty acids are calcium ionophores. Studies employing arsenazo III in liposomes. *The Journal of Biological Chemistry*, 256, 2736-2741.

Sharma, B., Bhattacharya, A., Gandhi, R., Sood, J. & Rao, B. K. 2008. Pharmacovigilance in Intensive Care Unit - An Overview. *Indian Journal of Anaesthesia*, 52, 373.

Shasby, D. M. 2007. Cell-cell adhesion in lung endothelium. *American Jouranl of Physiology Lung Cellular and Molecular Physiology*, 292**,** L593-L607.

Sherwood, L. 2005. *Fundamentals of physiology:A human perspective.* 3 ed.: Cengage Learning.

Shimizu, T., Nishihara, M., Kawaguchi, S. & Sakakura, Y. 1994. Expression of phenotypic markers during regeneration of rat tracheal epithelium following mechanical injury. *American Journal of Respiratory Cell Molecular Biology,* 11**,** 85-94.

Shull, S., Heintz, N. H., Periasamy, M., Manohar, M., Janssen, Y. M., Marsh, J. P. & Mossman, B. T. 1991. Differential regulation of antioxidant enzymes in response to oxidants. *The Journal of Biological Chemistry*, 266**,** 24398-24403.

Sleigh, M. A., Blake, J. R. & Liron, N. 1988. The propulsion of mucus by cilia. *American Review of Respiratory Disease*, 137**,** 726-741.

Sleigh, M. A. & Silvester, N. R. 1983. Anchorage functions of the basal apparaus of cilia. *Journal of Submicroscopic Cytology,* 15**,** 101-104.

Slutsky, A. S. 1999. Lung injury caused by mechanical ventilation. *Chest*, 116**,** 9S-15S.

Snider, G. L. & Rinaldo, J. E. 1980. Oxygen therapy, oxygen therapy in medical patients hospitalized outside of the intensive care unit. *Tthe American Review of Respiratory Disease*, 122**,** 29-36.

Stadtman, E. R. & Levine, R. L. 2003. Free radical-mediated oxidation of free amino acids and amino acid residues in proteins. *Amino Acids*, *25*, 207-218.

Stannard, W. & O'callaghan, C. 2006. Ciliary function and the role of cilia in clearance. *Journal of Aerrsol Medicine*, 19**,** 110-115.

Stevenson, B. R., Siliciano, J. D., Mooseker, M. S. & Goodenough, D. A. 1986. Identification of ZO-1: a high molecular weight polypeptide associated with the tight junction (zonula occludens) in a variety of epithelia. *The Journal of Cell Biology*, 103, 755-766.

Stohs, S. J. & Bagchi, D. 1995. Oxidative mechanisms in the toxicity of metal ions. *Free Radical and Biological Medicin.,* 18**,** 321-336.

Sun, Y. & Oberley, L. W. 1996. Redox regulation of transcriptional activators. *Free Radical Biology and Medicine,* 21**,** 335-348.

Sussana, T. E., Rangasamya, T., Blakea, D. J., Malhotraa, D., El-Haddadb, H., Bedjac, D., Yatesa, M. S., Kombairajua, P., Yamamotod, M., Libye, K. T., Sporne, M. B., Gabrielsonc, K. L., Championb, H. C., Tuderf, R. M. & Kenslera, T. W. 2009. Targeting Nrf2 with the triterpenoid CDDO-imidazolide attenuates cigarette smoke-induced emphysema and cardiac dysfunction in mice. *PNAS USA*,106**,** 250–255.

Suzuki, Y., Aoki, T., Takeuchi, O., Nishio, K., Suzuki, K., Miyata, A., Oyamada, Y., Takasugi, T., Mori, M., Fujita, H. & Yamaguchi, K. 1997. Effect of hyperoxia on adhesion molecule expression in human endothelial cells and neutrophils. *The American Journal of Physiology,* 272**,** L418-L425.

Sylvester, P. W. 2007. Vitamin E and apoptosis. *Vitamins and Hormones*, 76, 329-356.

Tasinato, A., Boscoboinik, D., Bartoli, G. M., Maroni, P. & Azzi, A. 1995. d-Alpha-tocopherol inhibition of vascular smooth muscle cell proliferation occurs at physiological concentrations, correlates with protein kinase C inhibition, and is independent of its antioxidant properties. *PNAS USA,* 92**,** 12190–12194.

Thannickal, V. J. 2003. The paradox of reactive oxygen species: injury, signalling, or both?. *American Jouranl of Physiology Lung Cellular and Molecular Physiology*, 284, L24-L25.

Thor, H., Hartzell, P. & Orrenius, S. 1984. Potentiation of oxidative cell injury in hepatocytes which have accumulated Ca2+. *The Journal of Biological Chemsitry, 259, 6612-6615.*

Thorley, A. J. & Tetley, T. D. 2007. Pulmonary epithelium, cigarette smoke, and chronic obstructive pulmonary disease. *International Journal of Chronic Obstructive Pulmonary Disease,* 2**,** 409–428.

Tice, R. R., Agurell, E., Anderson, D., Burlinson, B., Hartmann, A., Kobayashi, H., Miyamae, Y., Rojas, E., Ryu, J. C. & Sasaki, Y. F. 2000. Single Cell Gel/Comet Assay: Guidelines for In Vitro and In Vivo Genetic Toxicology Testing. *Environmental and Molecular Mutagenesis,* 35**,** 206-221.

Tierney, D. F. & Hacker, A. D. 1989. Polyamines, DNA Synthesis, and Tolerance to Hyperoxia of Mice and Rats*. American Journal of Respiraory and Critical Care Medicine*, 139, 387-392.

Tompkins, D. H., Besnard, V., Lange, A. W., Wert, S. E., Keiser, A. R., Smith, A. N., Lang, R. & Whitsett, J. A. 2009. Sox2 Is Required for Maintenance and Differentiation of Bronchiolar Clara, Ciliated, and Goblet Cells. *PLos ONE*, 4**,** e8248.

Toskala, E., Smiley-Jewell, S. M., Wong, V. J., King, D. & Plopper, C. G. 2005. Temporal and spatial distribution of ciliogenesis in the tracheobronchial airways of mice. *American Jouranl of Physiology Lung Cellular and Molecular Physiology,* 289**,** L454-L459.

Townsend, D. M. & Tew, K. D. 2003. The role of glutathione-S-transferase in anti-cancer drug resistance. *Oncogene,* 22**,** 7369-7375.

Traber, M. G. & Sies, H. 1996. Vitamin E in humans: demand and delivery. *Annual Review of Nutrition,* 16**,** 321-347.

Trachootham, D., Lu, W., Ogasawara, M. A., Nilsa, R. D. & Huang, P. 2008. Redox regulation of cell survival. *Antioxidants and Redox Signalling* 10**,** 1343-1374.

Trautmann, A., Krüger, K., Akdis, M., Müller-Wening, D., Akkaya, A., Bröcker, E. B., Blaser, K. & Akdis, C. A. 2005. Apoptosis and loss of adhesion of bronchial epithelial cells in asthma. *International Archives of Ailergy and Immunology,* 138**,** 142-150.

Tsukaguchi, H., Tokui, T., Mackenzie, B., Berger, U. V., Chen, X. Z., Wang, Y., Brubaker, R. F. & Hediger, M. A. 1999. A family of mammalian Na+-dependent L-ascorbic acid transporters. *Nature,* 399**,** 70-75.

Turi, J. L., Jaspers, I., Dailey, L. A., Madden, M. C., Brighton, L. E., Carter, J. D., Nozik-Grayck, E., Piantoadosi, C. A. & Ghio, A. J. 2002. Oxidative stress activates anion exchange protein 2 and AP-1 in airway epithelial cells. *American Jouranl of Physiology Lung Cellular and Molecular Physiology,* 283**,** L791-L798.

Turrens, J. F. 2003. Mitochondrial formation of reactive oxygen species. *The Journal of Physiology,* 552**,** 335-344.

Turrens, J. F., Freeman, B. A., Levitt, J. G. & Crapo, J. D. 1982. The effect of hyperoxia on superoxide production by lung submitochondrial particles. *Archives of Biochemistry and Biophysics,* 217**,** 401-410.

Van Der Velden, V. H. J., Savelkoul, H. F. J. & Versnel, M. A. 1998. Bronchial epithelium: morphology, function and pathophysiology in asthma. *European Cytokine Network,* 9**,** 585-598.

Van Der Vliet, A. & Cross, C. E. 2000. Oxidants, nitrosants, and the lung. *The American Journal of Medicine,* 109**,** 398-421.

Van Der Vliet, A., O'neill, C. A., Cross, C. E., Koostra, J. M., Volz, W. G., Halliwell, B. & Louie, S. 1999. Determination of low-molecular-mass antioxidant concentrations in human respiratory tract lining fluids. *The American Journal of Physiology. Lung Cellular and Molecular Biology,* 276**,** L289-L296.

Van Klaveren, R. J., Demedts, M. & Nemery, B. 1997. Cellular glutathione turnover in vitro, with emphasis on type II pneumocytes. *European Respratory Journal,* 10**,** 1392-1400.

Vera, J. C., Rivas, C. I., Zhang, R. H., Farber, C. M. & Golde, D. W. 1994. Human HL-60 myeloid leukemia cells transport dehydroascorbic acid via the glucose transporters and accumulate reduced ascorbic acid. *Blood,* 84**,** 1628-1634.

Vermeer, P. D., Denker, J., Estin, M., Moninger, T. O., Keshavjee, S., Karp, P., Kline, J. N. & Zabner, J. 2009. MMP9 modulates tight junction integrity and cell viability in human airway epithelia. *American Journal of Physiology. Lung cellular and molecular physiology,* 296**,** L751–L762.

Walsh, S. V., Hopkins, A. M. & Nusrat, A. 2000. Modulation of tight junction structure and function by cytokines. *Advanced Drug Delivery Reviews*, 41, 303-313.

Wang, F., Daugherty, B., Keise, L. L., Wei, Z., Foley, J. P., Savani, R. C. & Koval, M. 2003. Heterogeneity of claudin expression by alveolar epithelial cells. *American Journal of Respiraory Cell and Molecular Biology,* 29.

Wannamethee, S. G., Lowe, G. D., Rumley, A., Bruckdorfer, K. R. & Whincup, P. H. 2006. Associations of vitamin C status, fruit and vegetable intakes, and markers of inflammation and hemostasis. *The American Journal of Clinical Nutrition*, 83, 567-574

Wanner, A., Salathe, M. & Riordan, O. 1996. Mucociliary clearance in the airways. *American Jouranl of Respiratory and Critical Care Medicine,* 154**,** 868-902.

Warner, B. B., Stuart, L. A., Papes, R. A. & Wispe, J. R. 1998. Functional and pathological effects of prolonged hyperoxia in neonatal mice. *American Journal of Physiology. Lung Cellular and Moleucular Physiology,* 275**,** L110-L117.

Weichselbaum, M., Sparrow, M. P., Hamilton, E. J., Thompson, P. J. & Knight, D. A. 2005. A confocal microscopic study of solitary pulmonary neuroendocrine cells in human airway epithelium. *Respiratory Research,* 10**,** 115.

Welsh, M. J., Shasby, D. M. & Husted, R. M. 1985. Oxidants increase paracellular permeability in a cultured epithelial cell line. *The Journal of Clinical Investigation*, 76, 1155-1168.

White, C. W., Avraham, K. B., Shanley, P. F. & Groner, Y. 1991. Transgenic mice with expression of elevated levels of copper-zinc superoxide dismutase in the lungs are resistant to pulmonary oxygen toxicity. *The Journal of Clinical Investigation,* 87**,** 2162-2168.

Wilson, R., Alton, E., Rutman, A., Higgins, P., Al Nakib, W., Geddes, D. M., Tyrrell, D. A. & Cole, P. J. 1987. Upper respiratory tract viral infection and mucociliary clearance. *European Journal of Respiratory Diseases,* 70**,** 272-279.

Wiseman, M. & Halliwell, B. 1996. Damage to DNA by reactive oxygen and nitrogen species: role in inflammatory disease and progression to cancer. *The Biochemical Journal*, 313, 17-29.

Wispe, J. R., Warner, B. B., Clark, J. C., Dey, C. R., Neuman, J., Glasser, S. W., Crapo, J. D., Chang, L. Y. & Whitsett, J. A. 1992. Human Mn-superoxide dismutase in pulmonary epithelial cells of transgenic mice confers protection from oxygen injury. *The Journal of Biological Chemistry,* 267**,** 23937-23937.

Wisseman, C. L., Simel, D. L., Spock, A. & Shelburne, J. D. 1981. The prevalence of abnormal cilia in normal pediatric lungs. *Archives of Pathology and Laboratory Medicine.,* 105**,** 552-555.

Wood, L. G., Gibson, P. G. & Garg, M. L. 2003. Biomarkers of lipid peroxidation, airway inflammation and asthma. *The European Respiratory Journal*, 21, 177-186.

Wright, D. T., Cohn, L. A., Li, H., Fischer, B., Li, M. & Adler, K. B. 1994. Interactions of oxygen radicals with airvvay epithelium. *Enviromental health perspectives,* 102**,** 85-90.

Wu, M., He, Y. H., Kobune, M., Xu, Y., Kelley, M. R. & Martin Ii, W. J. 2002. Protection of Human Lung Cells against Hyperoxia Using the DNA Base Excision Repair Genes hOgg1 and Fpg. *American Journal of Respiratory and critical care medicine*, 166, 192-199.

Wyatt, T. A., Sisson, J. H., Allen-Gipson, D. S., Mccaskill, M. L., Boten, J. A., Devasure, J. M., Bailey, K. L. & Poole, J. A. 2012. Co-exposure to cigarette smoke and alcohol decreases airway epithelial cell cilia beating in a protein kinase Cε-dependent manner. *The American Journal of Pathology*, 181, 431-440.

Xu, D., Guthrie, J. R., Mabry, S., Sack, T. M. & Truog, W. E. 2006. Mitochondrial aldehyde dehydrogenase attenuates hyperoxia-induced cell death through activation of ERK/MAPK and PI3K-Akt pathways in lung epithelial cells. *American Journal of Physiology. Lung Cellular and Molecular Physiology.,* 291**,** L966-L975.

Yahaya, B. 2012. Understanding Cellular Mechanisms Underlying Airway Epithelial Repair: Selecting the Most Appropriate Animal Models. *The Scientific World Journal,* 961684**,** 12 pages.

Yamaoka, S., Kim, H. S., Ogihara , T., Oue, S., Takitani, K., Yoshida, Y. & Tamai, H. 2008. Severe Vitamin E deficiency exacerbates acute hyperoxic lung injury associated with increased oxidative stress and inflammation. *Free Radical Research*, 42, 602-612.

Yang, G., Abate, A., George, A. G., Weng, Y. H. & Dennery, P. A. 2004. Maturational differences in lung NF-kappaB activation and their role in tolerance to hyperoxia. *The Journal of Cinical Investigation*, 114, 669-678.

Yee, M., Vitiello, P. F., Roper, J. M., Staversky, R. J., Wright, D. T., Mcgrath-Morrow, S. A., Maniscalco, W. M., Finkelstein, J. N. & O'reilly, M. A. 2006. Type II epithelial cells are critical target for hyperoxia-mediated impairment of postnatal lung development. *American Jouranl of Physiology Lung Cellular and Molecular Physiology,* 291**,** L1101-L1111.

Yoo, J. H., Erzurum, S. C., Hay, J. G., Lemarchand, P. & Crystal, R. G. 1994. Vulnerability of the human airway epithelium to hyperoxia. Constitutive expression of the catalase gene in human bronchial epithelial cells despite oxidant stress. *The Journal of Clinical Investigation*, 93, 297-302.

You, K., Xu, X., Fu, J., Xu, S., Yue, X., Yu, Z. & Xue, X. 2012. Hyperoxia disrupts pulmonary epithelial barrier in newborn rats via the deterioration of occludin and ZO-1. *Respiratory Research*, 13, 36

Yu, W., Beaudry, S., Negoro, H., Boucher, I., Tran, M., Kong, T. & Denker, B. M. 2012. H2O2 activates G protein, α 12 to disrupt the junctional complex and enhance ischemia reperfusion injury. *PNAS USA,* 109**,** 6680-6685.

Zaher, T. E., Miller, E. J., Morrow, D. M. P., Javdan, M. & Mantell, L. L. 2007. Hyperoxia-induced signal transduction pathways in pulmonary epithelial cells. *Free Radical Biology and Medicine,* 42**,** 897-908.

Zahm, J. M., Kaplan, H., He´ Rard, A. L., Doriot, F., Pierrot, D., Somelette, P. & Puchelle, E. 1997. Cell migration and proliferation during the In vitro wound repair of the respiratory epithelium. *Cell Motility and the Cytoskeleton,* 37**,** 33-43.

Zaidi, A., Barron, L., Sharov, V. S., Schoneich, C., Michaelis, K. & Michaelis, M. L. 2003. Oxidative Inactivation of Purified Plasma Membrane Ca2+-ATPase by Hydrogen Peroxide and Protection by Calmodulin. *Biochemistry*, 42, 12001–12010.

Zhang, X., Shan, P., Sasidhar, M., Chupp, G. L., Flavell, R. A., Choi, A. M. & Lee, P. J. 2003. Reactive oxygen species and extracellular signal-regulated kinase 1/2 mitogen-activated protein kinase mediate hyperoxia-induced cell death in lung epithelium. *American Journal of Respiratory Cell and Molecular Biology,* 28**,** 305-315.

Zhou, H., Saidel, G. M. & Cabrera, M. E. 2007. Multi-organ system model of O2 and CO2 transport during isocapnic and poikilocapnic hypoxia. *Respiratory Physiology and Neurobiology,* 156**,** 320-330.